Formulation Development and Optimization via In Vivo Predictive In Vitro and In Silico Tools

Dissertation

zur

Erlangung des Doktorgrades (Dr. rer. nat.)

der

Mathematisch-Naturwissenschaftlichen Fakultät

der

Rheinischen Friedrich-Wilhelms-Universität Bonn

vorgelegt von

Tim Becker

aus

Köln

Bonn 2024

Angefertigt mit Genehmigung der Mathematisch-Naturwissenschaftlichen Fakultät
der Rheinischen Friedrich-Wilhelms-Universität Bonn

Erstgutachter: Prof. Dr. Karl G. Wagner
Zweitgutachter: Prof. Dr. Marc Hübner

Tag der Promotion: 10.06.2024
Erscheinungsjahr: 2024

I. Danksagung

Die vorliegende Arbeit entstand unter der Leitung von Professor Dr. Karl Gerhard Wagner am Institut für Pharmazeutische Technologie and Biopharmazie der Rheinischen Friedrich-Wilhelms-Universität Bonn.

Besonders danken möchte ich meinem Doktorvater, Professor Dr. Karl Gerhard Wagner für das entgegengebrachte Vertrauen, dieses Projekt bearbeiten zu dürfen. Dies ermöglichte mir, einen umfangreichen Einblick in die Formulierungsentwicklung zu erhalten und durch Deine große Unterstützung Die Möglichkeit meine eigene Expertise in diesem Feld aufzubauen. Ebenfalls danke ich Dir, dass Du stets ein offenes Ohr für mich hattest und mich bei jeglichen Fragestellungen mit einem wertvollen Rat in die richtige Richtung gelenkt hast.

Professor Dr. Marc Hübner danke ich für die Übernahme des Zweitgutachtens. Ich danke Professor Dr. Ulrich Jaehde und Professor Dr. Achim Hörauf für die Bereitschaft Teil der Prüfungskommission zu sein.

Ich bedanke mich herzlich beim IMMIP-Team, Professor. Dr. Achim Hörauf, Professor Dr. Marc Hübner, Dr. Ken Pfarr, Dr. Andrea Schiefer, Dr. Alexandra Ehrens und Tilman Aden für die wertvolle Zusammenarbeit. Den Kolleginnen und Kollegen des Helmholtz-Zentrums für Infektionsforschung, Professor Dr. Marc Stadler, Dr. Miriam Große und Dr. Katharina Rox danke ich ebenfalls für die produktive Zusammenarbeit. Ganz besonders möchte ich mich bei Dr. Anna Krome, Jan Heitkötter und Dr. Stefan Kehraus bedanken mit denen ich viel gemeinsame Zeit im Labor und anschließenden Gesprächen verbringen durfte. Vielen Dank an das gesamte CorA-Projekt für die großartige Kooperation und Unterstützung meiner Arbeit. Hierdurch konnte ich viele wertvolle Erfahrungen sammeln und neue Bereiche kennenlernen.

I thank the Simulations-Plus team, especially Dr. Xavier Pepin, for the fruitful collaboration and evaluations and discussions on the *in silico* modelling. Your great expertise and support were a valuable part for the preclinical development of corallopyronin A.

Herzlich bedanken möchte ich mich bei Thilo Faber für die Erstellung der mikroskopischen Aufnahmen und bei Sahel Vahdati für die Durchführung und Unterstützung bei den Zellkulturexperimenten.

Meinen Kolleginnen und Kollegen der Pharmazeutischen Technologie danke ich für die schöne Zeit am Institut, die kooperative Zusammenarbeit im Labor und die schönen gemeinsamen Ausflüge und Grillabende.

Vielen Dank an meine Bürokollegen, Dr. Katharina Dauer, Florian Pöstges und Karla Viehmeister, die immer für konstruktive Gespräche zur Verfügung standen, einen stets aufgebaut haben und schlechte Laune durch eine Runde Tischtennis oder Basketball vergessen haben lassen. Es war eine einmalige Zeit mich euch. Weiterhin möchte ich Euch, sowie Tobias Siefen, Thilo Faber und Bernadette Riemann für die tollen Erlebnisse danken, die ich abseits des Instituts mit Euch erleben durfte. Katharina Dauer, Karla Viehmeister, Annika Rautenberg, Florian Pöstges und Roman Groß danke ich für den unvergesslichen Trip nach New York und Boston.

Herzlichen Dank an Jürgen Hohmann, Alexander Ramich, Martina Gerlitz und Petra Zitzmann, die bei technischen und bürokratischen Schwierigkeiten stets unterstützend zur Seite standen.

Der größte Dank gilt meinen Eltern und meiner Schwester Pia für Ihren bedingungslosen Rückhalt. Eure aufmunternden Worte und Euer Vertrauen in mich haben mich immer motiviert. Ohne Euch wäre mein Lebensweg und diese Arbeit unmöglich gewesen.

II. Abbreviations

ACAT	Advanced compartmental absorption and transit
ADMET	Absorption, Distribution, Metabolism, Elimination and Toxicology
AP	ADMET Predictor software
ANOVA	Analysis of Variance
API	Active Pharmaceutical Ingredient
ASD	Amorphous Solid Dispersions
AU	Arbitrary Unit
AUC	Area Under the Plasma Concentration Curve
BA	Bioavailability
BCRP	Breast Cancer Resistance Protein
BCS	The Biopharmaceutics Classification System
BID	Bis in die; two administrations per day
C_{max}	Maximum Observed Plasma Concentration
CorA	Corallopyronin A
CorA’	Corallopyronin A’
CorC	Corallopyronin C
CYP	Cytochrome P450
DSC	Differential Scanning Calorimetry
Eq.	Equation
FaSSIF	Fasted State Simulating Intestinal Fluid
FeSSIF	Fed State Simulating Intestinal Fluid
GIT	Gastrointestinal tract
GLP	Good Laboratory Practice
HPLC	High-performance Liquid Chromatography
HPMC	Hydroxypropylmethyl cellulose
HPMC-AS	Hydroxypropylmethyl cellulose acetate succinate
HZI	Helmholtz Centre for Infection Research
IC50	Half maximal inhibitory concentration

IV	Intravenous
IVIVR	*in vitro in vivo* Relationship
MIC	Minimal Inhibitory Concentration
MRI	Magnetic resonance imaging
MTD	Maximum Tolerated Dose
NTD	Neglected Tropical Diseases
PAMPA	Parallel Artificial Membrane Permeability Assay
PBBM	Physiologically based Biopharmaceutic Model
PBPK	Physiologically based pharmacokinetic
PBS	Phosphate Buffered Saline
PD	Pharmacodynamic
P_{eff}	Human effective jejunal permeability
PE	Prediction errors
PEG	Polyethylene glycol
P-gp	P-glycoprotein
PK	Pharmacokinetic
PO	Per os
PVP	Polyvinylpyrrolidone
PVPVA	Polyvinylpyrrolidone-co-vinylacetate
RGM	Rat gastric medium
RIM	Rat intestinal medium
SD	Standard Deviation
SEEDS	Self-emulsifying drug delivery system
SEM	Scanning electron micrographs
SLN	Solid Lipid Nanoparticles
$t_{1/2}$	Half-life
T_g	Glass Transition Temperature
t_{max}	Time of Maximum Observed Plasma Concentration
USP	United States Pharmacopeia
WHO	World Health Organization

III. Table of Content

1. General Introduction

1.1 Need for Novel Anti-infectives

The history of infectious diseases is as long as the human history itself [1]. Indeed, infectious diseases are still an immense burden, which has come into focus with novel threats such as the COVID-19 pandemic in 2019 [2,3]. With the help of global efforts and the provision of public funding the research in this field has been enormously advanced. Despite raising attention to infectious diseases, further challenges have continued to intensify. The massive use of antibiotics, e.g. as a COVID-19 (co-)treatment, forces the ongoing emergence of antimicrobial resistance [4]. According to the World Health Organization (WHO), drug resistance could prospectively cause 10 million deaths each year by 2050. Apart from the expected mortality rate, antimicrobial resistance could push up to 24 million people into extreme poverty by 2030, if no action is taken [5]. To overcome drug resistance it is essential to find new compound classes or compounds with new modes of action [6,7].

Although attention to infection diseases has increased, there is a lack of global interest in some areas. Neglected tropical diseases (NTD) play a rather minor role in Europe and North America. As an unfortunate consequence, investments in combating NTDs are disproportionate compared to the amount of people affected because there are limited financial incentives for industrial companies [8]. The cost-intensive research and development process of a novel active pharmaceutical ingredient (API) contrasts with the low revenue potential of an anti-infective [9,10]. Accordingly, the drug pipelines of pharmaceutical companies are underrepresented in anti-infectives, particularly for NTDs. Currently, the most promising NTD related drug candidates are funded by public and private sponsors and driven forward in collaboration of universities and research centers providing essential basic research and development [11].

1.2 Preclinical Drug Development

To date, the need for novel treatment options in almost all disease area continues unabated. Reasons for this include the high risk for termination due to potentially insufficient efficacy, safety or even commercial issues resulting from a cost-intensive and time-consuming drug development process [12,13]. Several years pass from drug

discovery over drug characterization in preclinical and clinical studies to the final approval of the drug product with a subsequent market entry. Prior first clinical trials in human, various preclinical experiments are required to ensure efficacy and safety of the drug candidate. In addition, the examination of physicochemical characteristics gives insights about *in vitro* and *in vivo* experiment limitations. Typical challenges may arise, namely, limited compound availability or unfavorable drug properties, especially poor solubility and/or poor permeability, which further complicate the development process [14]. Beside the provision of service formulations for *in vitro* and preclinical tests, such as *in vitro* investigations regarding absorption, distribution, metabolism, elimination and toxicology (ADMET) characteristics or efficacy assessments in various animal models, it is also desirable to develop and test formulation principles and related drug product prototypes which could be a representative for a final commercial formulation [7,15]. Implementation of reliable analytics as well as providing appropriate vehicles are essential for successful *in vitro* and *in vivo* experiments. As a first step, solutions allow to carry out important *in vitro* and *in vivo* pharmacokinetic (PK) and pharmacodynamic (PD) evaluations. Despite representing seemingly simple formulations, the development process is often hampered by the limited drug availability and poor solubility [14]. As oral administration is mostly the favored route of administration for reasons of simplicity and patient compliance, the development of an enabling formulation for poorly soluble drugs even in preclinical phase supports a positive outcome of preclinical studies and a promising formulation approach for human use [14,16]. In addition, finding appropriate vehicles for intravenous (IV) administration allows the determination of biopharmaceutical relevant parameters regarding distribution, elimination, fraction absorbed and bioavailability (BA) of oral formulations. The difficulty with poorly soluble drug candidates is to provide a vehicle that is capable to dissolve a sufficient amount of drug without the risk of precipitation, while maintaining high tolerability. A further aspect of preclinical drug development is the toxicological investigation comprising *in vitro* setups as well as *in vivo* evaluations in rodent and non-rodent species. In contrast to PK and PD studies, the dose levels required for a toxicology study exceed the therapeutically relevant ones many times. Subsequently, appropriate vehicles are required, that provide sufficient drug exposure after oral administration as well as adequate tolerability of the vehicle itself [17]. Even though, intestinal precipitation must not be excluded in principle

due to the present oral administration, providing a vehicle with appropriate solubility potentially results in a higher exposure especially at higher dose levels. The latter is crucial for the toxicological assessment. Once the drug candidate is completely characterized and safety and efficacy demonstrated in preclinical experiments, first-in-human (FIH) clinical studies will follow to examine safety, tolerability and the ADME-profile [18]. Later clinical trials focus on sick patients. In case of success, the drug product can be submitted for approval, which is required for the first market entry.

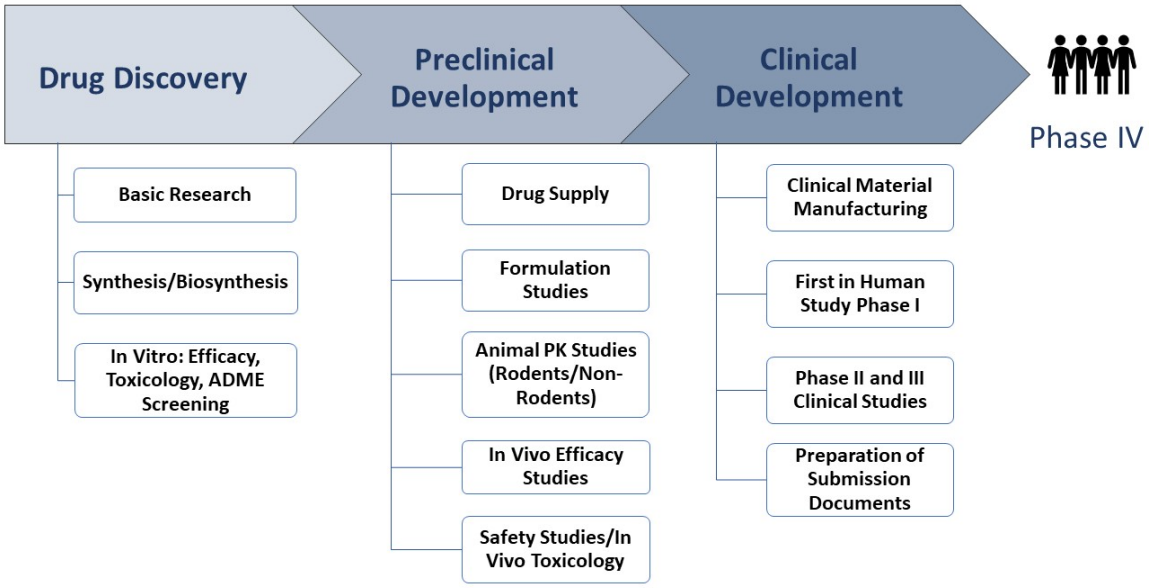

Figure 1. Schematic overview of the drug development process comprising discovery, preclinical and clinical development.

1.3 Enabling Formulations

Oral BA of drugs depends on several factors. The biopharmaceutics classification system (BCS) categorizes drugs on the basis of their solubility and permeability properties [19]. Drugs of BCS class I show both good solubility and permeability, whereas BCS class III show good solubility and poor permeability. Poorly soluble drugs with high permeability are classified with BCS II and drugs with poor solubility and poor permeability are classified with BCS IV. High-throughput screenings in drug discovery led to highly effective drug candidates, but this was accompanied by an increasing number of poorly water-soluble drugs as the enhanced target affinity is often associated with higher overall lipophilicity, e.g. due to higher molecular weights and/or molecular structures [20,21]. These drug specific characteristics influence the development process. Typically, poorly soluble BCS

II compounds exhibit a dissolution rate-limited absorption, which has a direct impact on the BA [22]. The dissolution represents the rate limiting step for absorption. One approach addressing insufficient drug availability is to increase the dose. Beside potential toxic side effects, this leads to an uneconomical drug substance consumption, so that more innovative approaches are needed [20,23,24]. To date, a wide range of solubility-enabling formulations have been developed with the goal to enhance the dissolution and solubility of poorly soluble drugs, and thus, improving absorption and BA [25,26]. Various principles have been established over the past decades, such as particle size reduction, self-emulsifying drug delivery systems, cyclodextrins, lipid-based formulations, usage of cosolvents, addition of surface-active agents, mesoporous inorganic carriers, building of soluble complexes and amorphous solid dispersions (ASD) [25,27,28]. The choice for the most promising development path depends on numerous factors, so that a general formulation recommendation is impossible. The physicochemical properties, drug substance supply and the individual equipment often limit the opportunity for high throughput screenings. However, addressing solubility issues even in early phases of drug product development prevents time-consuming and cost-intensive readjustments and benefits due to reducing of experimental (animal) studies by selecting formulations with sufficient exposure [14].

One of the most common strategies to improve oral BA is the particle size reduction in micro- or even nanoscale. Indeed, the enhancement in solubility is negligible and the dissolution rate is rather the driving force. According to the Noyes-Whitney equation (**Eq. 1**) which was extended by Nernst and Brunner (**Eq. 2**), a reduction of the particle size leads to an increasing dissolution rate, while the saturation concentration is limited by the given solubility:

$$\frac{dc}{dt} = k \cdot (c_s - c_t) \quad \textbf{(1)}$$

$$\frac{dc}{dt} = \frac{D \cdot A}{h \cdot V} \cdot (c_s - c_t) \quad \textbf{(2)}$$

where *dc/dt* is the dissolution rate, *k* is the diffusion coefficient, c_s is the saturation concentration, c_t is the amount of dissolved drug at time point *t*, *D* is the diffusion coefficient of the drug in the respective solvent, *A* is the particle surface of the undissolved drug amount, *h* is the thickness of the diffusion layer and *V* is the volume of the dissolution

media [29,30]. The compound specific c_s cannot directly be impacted. However, for substances that tend to supersaturate, rapid dissolution could result in a high kinetic solubility. Thus, particle surface reduction is one principle to improve the oral BA as the dissolution rate is directly proportional to the particle surface area. For particle size reduction several techniques enable micronization or even nanoization. Micronization via jet milling, ball milling, wet milling or the use of a high-pressure homogenizer is widely used, depending on product properties and the targeted final particle size [31]. Moreover, building solid particles via spray drying or freeze drying is able to provide particles with a particle size < 10 µm [32,33]. Particles in the nano range are producible using media milling or nanoprecipitation, as well as, nanocarrier systems like liposomes, solid lipid nano particles (SLN), polymeric micelles or self-emulsifying drug delivery systems [31].

Another approach to improve the solubility is to include the drug molecule into complex cyclodextrin carriers which are composed of a lipophilic inner surface and a hydrophilic outer surface [34]. Depending on its number of glucose units cyclodextrins are classified as α-, β- and ϒ-cyclodextrin (α: 6; β: 7; ϒ: 8). For oral drug delivery β-cyclodextrins have been commonly used because they are readily available and the cavity size is suitable for a wide range of drugs [35].

Chemical adjustments as salt formation or using prodrugs can improve aqueous solubility. However, successful identification of a suitable counterion remains uncertain and feasible for only a few candidates depending on ionizable structures [36]. If possible, the development of a soluble prodrug can overcome BA limitations caused by poor solubility [37].

The addition of suitable excipients is a common strategy to improve the solubility behavior of poorly soluble drug candidates. Using cosolvents, e.g., ethanol, polyethylene glycol (PEG) 400 or N-methyl pyrrolidone is a promising approach, but often fail due to toxicology limitations of the solvent, instability or potential drug precipitation [28,38]. Moreover, cosolvents are primarily intended for liquid drug products. Likewise, lipid or surfactant based delivery strategies covering solution based formulation principles comprising emulsions, oil solutions or self-emulsifying drug delivery systems (SEDDS) [39]. In contrast to the liquid based SEDDS, the SLNs display a principle for a solid lipid based option applicable for oral drug delivery with potential controlled release and stability

enhancement [40,41]. SLNs consist of solid lipids and emulsifiers which are typically suspended in water. Further processing into tablets, pellets or capsules is conceivable. In general, SLNs are accompanied with low toxicological spectra, easy availability and low costs [42]. Drying techniques as lyophilization or spray drying can be used to convert an aqueous SLN dispersion into a dry product [40].

Mesoporous silica represents a further enabling formulation strategy for poorly soluble drugs. The focus of this carrier-based system is the oral drug delivery. Due to its inert and stable character, mesoporous silica is considered to be nontoxic. The principle behind is the adsorption of the drug into the small pores (pore size: 2 – 50 nm) of the insoluble carrier leading to an increased dissolution rate according to **Eq. 2.** [43]. In addition, the drug can be introduced to the pores in its metastable amorphous form leading to an enhanced dissolution rate compared to the crystalline state where higher energy is required to overcome the crystalline lattice energy [44]. Furthermore, the small pore size may prevent from crystal growth of amorphous drug because of its finite-size resulting in immobilization effects [45–48]. Beside faster dissolution rates the amorphous form potentially leads to a supersaturated solution that may offer higher absorption and BA, depending on the maintenance of the supersaturated state [49–51]. However, further downstream processing of the mesoporous silica intermediate into a final drug product remains challenging due to poor compressibility behavior and reaching a sufficient drug load [52].

The principle of formulating a solid dispersion has become increasingly important in recent decades. By that, the drug is molecularly dispersed in an inert carrier or matrix [53]. Polymers are used as amorphous carriers in which the drug can be dissolved and the drug dissolution is controlled by the dissolution of the polymer [54]. A further advantage of this approach is to overcome limited aqueous solubility, to transfer a formerly crystalline drug into its amorphous form. Despite the crystalline lattice provide a thermodynamical more stable state, this may be contrary to the dissolution process, necessary for intestinal drug absorption [55]. However, by converting the drug into the thermodynamical unfavored amorphous state it is able to increase the dissolution rate due to the less required energy to break up the crystal lattice [53,56,57]. In addition, the performance of an ASD is affected by the potential of supersaturation of the dissolved drug [54,58,59]. By

maintaining the supersaturated state for a biorelevant time drug absorption increases despite actual poor solubility [60]. Appropriate excipients have the potential to stabilize and prolong the supersaturated state and therefore, prevent precipitation [61]. For the selection of a suitable carrier in order to form an ASD several aspects should be considered: Formation of a long-term stable ASD in terms of recrystallisation, improved dissolution rates and the possibility of supersaturation by considering its stabilization. In general, amorphous polymers are commonly used as carrier systems where the drug is completely soluble forming a monophasic “glass solution” [53,62]. Typical representatives are polyvinylpyrrolidone (PVP), polyvinylpyrrolidone-co-vinylacetate (PVPVA), PEG, polymethacrylates or cellulose based derivates such as hydroxypropylmethyl cellulose (HPMC) and hydroxypropylmethyl cellulose acetate succinate (HPMCAS). The molecular weights differ in terms of their respective polymer chain length, resulting in different polymer properties like viscosity, glass transition temperature (T_g) or molecular mobility, which in turn potentially affect the stability of the ASD [63]. Physical stability of drug products, e.g., the maintenance of the amorphous state during the shelf life of a pharmaceutical product, is of great interest from an industrial and regulatory point of view and needs to be evaluated [64]. For preparation, several manufacturing techniques are used covering melting-based and solvent-based methods [53]. One of the most common methods for melting-based methods is the hot melt extrusion, where the polymer-drug mixture is simultaneously melted and homogenized via rotating screws. Thereby, the drug dissolves in the polymer. However, polymer dependent high temperatures are required. For thermolabile drugs the high temperatures are not feasible and exclude this technique for such drug candidates. Instead, solvent based techniques represent an alternative strategy using the rapid solvent evaporation principle. Spray drying is the most common technique to form ASDs via solvent evaporation [65]. Even though, the drying process possibly requires high temperatures, extent and duration differ in comparison to hot melt extrusion. In sum, this process needs high energies and the use of organic solvents, but enables the thermally more gentle production of ASDs [65]. In addition, this technique allows the generation of nano- to micro-sized particles.

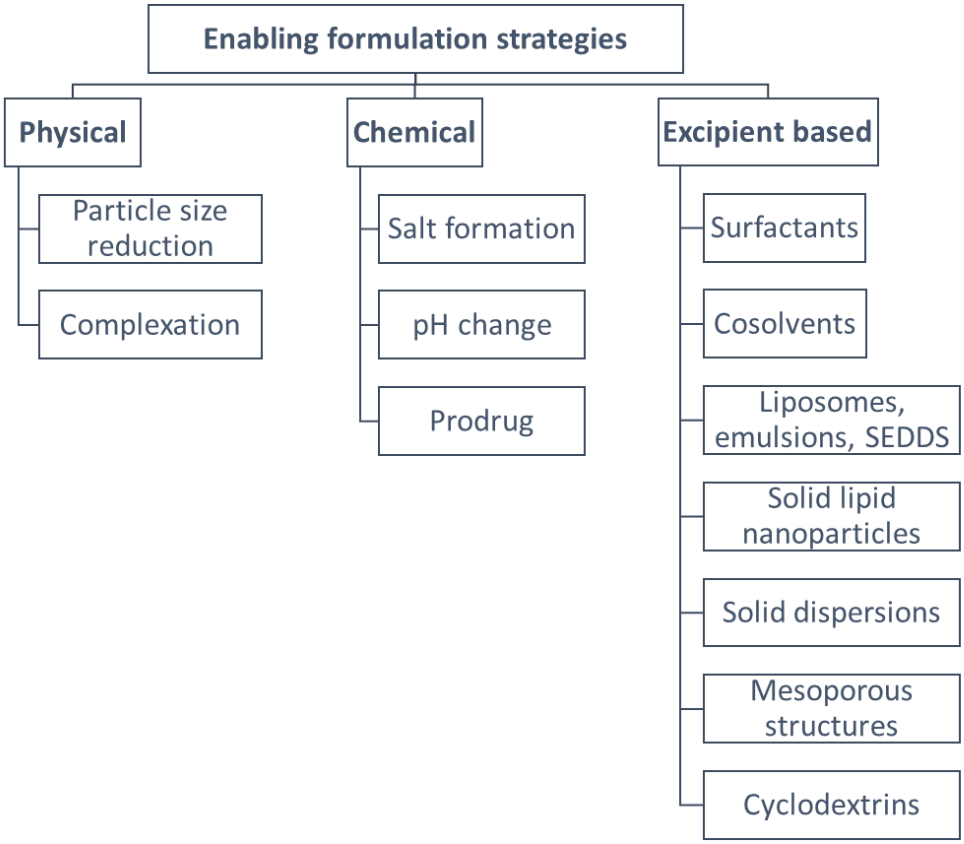

Figure 2. Overview of formulation principles for poorly water-soluble drugs.

1.4 Dissolution

In vitro drug dissolution tests are used under certain perspectives. From a regulatory point of view, dissolution experiments are intended either as a routine control test to guarantee consistent quality or as an opportunity for bioequivalence evaluations [66,67]. In principle, dissolution describes the amount of the drug which is dissolved from the dosage form in a specified time. It can be expressed as percentage based on the overall tested drug amount or mass concentration (W/V) displayed as cumulative amount. The speed at which the drug is dissolved can be described as dissolution rate in accordance to **Eq. 2** [68]. Another important aspect for dissolution studies is the presence of sink or non-sink conditions which are directly related to the dissolution rate [69]. Sink conditions are dependent on physicochemical drug properties and the experimental setup. In case the maximum achievable concentration during the dissolution experiment is close to the saturation solubility of the drug the dissolution rate would decrease. To overcome this problem, providing a setup where the dissolution rate is independent due to a high gap between saturation and maximum achievable concentration is required. It is reported that in case the volume of the test media exceeds 3-10 times the volume that causes

saturation of the drug, in accordance to Ph. Eur., sink conditions are present [70]. Although, sink conditions should be achieved by selecting optimal dissolution medium and volume, for poorly soluble drugs limitations occur due to experimental based volume restrictions. However, from a development point of view, sink conditions are not mandatory. In contrast, the focus at early drug development stages is on the performance evaluation of formulation candidates to select the most promising representatives for the next steps of the development process. In particular, poorly soluble drugs may require enabling formulations as described in **Chapter 1.3**. At this point the commonly used and well-known dissolution apparatuses (defined by the United States Pharmacopeia (USP); I: basket and II: paddle) are reaching their limits in terms of predictability of *in vivo* performance [71]. The value of the dissolution results improves by adapting the experimental setup to the conditions in the respective physiological environment [72]. This has given rise to the term biorelevant which describes an approach to approximate the conditions prevailing *in vivo*. Examples for important experimental settings are medium composition, volume, hydrodynamics and investigated dose [73]. After oral intake of a solid dosage form such as an immediate-release tablet, the formulation must disintegrate followed by drug dissolution prior intestinal absorption [22]. Dynamic processes such as supersaturation, precipitation or forming of colloidal reservoir systems may occur, especially for enabling formulations of poorly soluble drugs [74]. By adapting the *in vitro* dissolution setup, it is strived to display these dynamic processes to predict the *in vivo* behavior, whereby several dissolution approaches have been raised to date to support preclinical and clinical drug product development.

The artificial stomach duodenum model is based on two chambers where one is representing the stomach and a second the duodenum. After introducing the sample into the stomach chamber, the fluid is transferred after the respective stomach emptying time into the duodenum chamber. Both chambers are constantly quantified [75]. This method facilitates to investigate the influence of a pH-shift and gastric emptying rate. However, the experimental setup is not suitable for predicting *in vivo* absorption due to an absent absorption compartment [76].

A similar approach is the Biorelevant Gastrointestinal Transfer model that is based on a three-compartment system. Beside stomach and duodenum, a reservoir chamber serves

as a pool for bile salts and buffer to provide unaltered conditions [77]. Advantageous here is that it is implementable by using commercially available equipment. Similar to the artificial stomach duodenum model, this approach is not suitable for absorption simulations.

Further strategies have been evolved to approximate intestinal drug absorption within the dissolution experiment. Intestinal permeation can be investigated by cell-based systems using Caco-2 or Madin Darby canine kidney cell lines [76,78]. Complexity and effort of such membranes led to the cell-free alternative of artificial membrane systems comprising of cellulose based membranes [79]. Further advancements resulted in the parallel artificial membrane permeability assay (PAMPA) where the membrane is comprising of a hydrophobic polyvinylidene fluoride-filter impregnated with gastrointestinal lipids [80]. The membrane represents a barrier between donor and acceptor chamber. Commercially available dissolution setups such as the MicroDISS Profiler™ (Pion Inc., Billerica, MA, USA), take advantage of this approach by providing a mini-scale setup for dissolution-permeation studies. Side by side chambers are segregated by a PAMPA membrane and both chambers are filled with buffer media [81]. The sample is introduced to the donor chamber and dissolution of the drug is followed by permeation through the membrane, which serves as a surrogate for intestinal absorption. This is expected to approximate supersaturation and precipitation as it might occur *in vivo*. However, permeation is limited to the surface of the membrane and thus, insufficient permeation might not be able to prevent precipitation. As supersaturation is influenced by *in vivo* intestinal absorption, insufficient flux limits the predictability for poorly soluble drugs.

Another approach providing an absorption sink is the biphasic dissolution. The principle behind is that a water-immiscible organic solvent displays an absorptive compartment. In contrast to the membrane-based experiments, where the drug penetrates the membrane, in the biphasic dissolution approach the dissolved drug partitions from the aqueous to the organic layer according to its lipophilicity [82]. Various strategies have been developed for this purpose to mimic *in vivo* conditions and to improve the robustness of the system. In general, aspects like volume and type of aqueous and organic phase, introduced dose, vessel geometrics, hydrodynamics, running time and

quantification methods are important parameters. Denninger et al. recently introduced the biphasic dissolution assay BiPHa+ [83–85]. This fully automated apparatus aims to forecast oral absorption in human. Thus, biorelevant pH-shifts and media are integrated and the predictive power was demonstrated by an *in vitro in vivo* relationship (IVIVR) based on five commercial drug products [84]. Moreover, the partitioning profiles of the investigated drug products were integrated to *in silico* physiologically based pharmacokinetic (PBPK) models to successfully predict human PK profiles [85]. The investigation of the aqueous phase allows insights into potential supersaturation and precipitation, whereas the sum of partitioning into the organic phase serves as a surrogate for *in vivo* intestinal absorption. So far, the composition and concentration of biorelevant media mimic the gastrointestinal environment present in fasted state associated to the established medium of fasted state simulating intestinal fluid (FaSSIF) [86]. In sum, the biphasic dissolution serves as a promising approach to assess the *in vivo* performance of poorly soluble drugs and enabling formulations thereof. The BiPHa+ assay was able to simplify the experimental effort via automation of relevant steps. Although, this model is not suitable for regularity relevant investigations, it is one of the simplest models mimicking the *in vivo* absorptive sink and thus, supporting formulation selection during development processes [82].

1.5 Physiologically based Pharmacokinetic Modeling

PBPK models intend to depict concentration profiles of a drug in the blood and various tissues. The models base on input parameters which are related to the drug characteristics, site and means of administration and physiological conditions and processes [87]. Through this, comprehensive predictions regarding absorption, distribution, metabolism and elimination are enabled and can be used to assess the exposure in a target organ tissue [88]. Especially, for the oral administration of neat drugs or drug products, the physicochemical properties and physiological conditions in the gut determine intestinal absorption. In 1998, GastroPlus™, as the first commercially available software, introduced a mixing-tanks-in-series approach to describe intestinal drug movement combined with dissolution based on aqueous solubility and absorption rate constants referring to existing PK data [89]. In general, the software must be fed with several input parameters including physiochemical properties or *in vitro* determined

surrogates for drug absorption (e.g., transporter), metabolism (e.g., cytochrome P450 (CYP)) or elimination (renal and/or hepatic). Due to expanding opportunities and improvements of *in vitro* experiments and *in silico* software, the predictive power of the PBPK models increased over the last years [85]. However, time- and cost-effective drug development processes are in conflict of a holistic investigation of all conceivable *in vitro* experiments. Respective parameters can be estimated by utilizing *in silico* predictions based on the chemical structure. Thus, PBPK modeling is applicable even in early drug development processes. Beside human physiology, various animal physiologies are provided by the software. These differ in e.g., pH, fluid volume and transit times influencing drug release from the formulation and absorption. Nevertheless, building models of preclinical species is useful to gain confidence in the input parameters for a subsequent human PBPK model [87]. Later applications could be population simulations in terms of various ethnic groups, ages or disease stages [88]. Beside drug development, PBPK modeling also plays an increasingly important role for regulatory submissions by estimations such as FIH dose predictions or potential drug-drug interactions [88,90,91]. Overall, PBPK modeling has emerged to be a valuable tool to support drug development, clinical study design and regulatory applications.

2. Project Introduction

2.1 Corallopyronin A

NTDs include many chronic infection diseases concerning the poorest people world-wide [8,92]. Despite high prevalence (in sum one billion people) of several NTDs according to estimated 35,000 deaths per day, the pharmaceutical industry is hesitant in terms of research and development investments [93,94]. Despite high prevalence, it is in particular challenging to be profitable as high development costs meet financially weak environments, especially for poverty burden countries, resulting in a high risk to the return on investment [95]. Fortunately, several investment partners like governments and non-governmental organizations were convinced to invest in preventing and controlling these diseases [93]. Two representatives of NTDs are the onchocerciasis (global prevalence: 37 Mio.) and the lymphatic filariasis (global prevalence: 120 Mio.) [92,96,97]. Both are caused by parasitic helminths, specifically nematodes, threatening public health in tropical regions [98]. The helminths are transmitted by blood-feeding insects (mosquitos) and result in a long-term infection due to the long life of the worms (5-8 years). Dead worms trigger host inflammation leading to skin disease and blindness in the case of onchocerciasis and lymphoedema and elephantiasis in the case of lymphatic filariasis follow [98]. At lymphatic filariasis the adult worms, located in the lymphatic vessels, produce microfilariae that migrate into the blood allowing further transmission via mosquitos. At onchocerciasis the adult worms are located in subcutaneous tissue, visible as nodules. The released microfilariae migrate to the skin and the eyes. Transmission occurs via black flies, which are typically found along rivers, giving rise to the term “river blindness” [98]. An important pharmaceutical target are the *Wolbachia*-bacteria that are living in an endosymbiosis with the nematodes. A successful anti-*Wolbachia* therapy is able to sterilize and kill the adult worm to avoid further reproduction and rebound effects [99]. Although, with doxycycline an opportunity was found to be efficient against both, onchocerciasis and lymphatic filariasis, the extended treatment duration of 4-5 weeks is not in accordance to the mass drug administration which aims to interrupt the transmission cycle of these diseases [100]. In essence, identifying novel drug treatment strategies is one key to tackle the increasing drug resistance and decrease the risk for cross-resistance of existing antibiotics [101]. A promising anti-*Wolbachia*

candidate is corallopyronin A (CorA), a natural product of the myxobacteria *Corallococcus corraloides* [99,100,102,103]. In 1985, the CorA structure was elucidated and *in vitro* efficacy against Gram-positive pathogens has been demonstrated [104]. Meanwhile, the spectrum of action also includes Gram-negative bacteria with CorA representing a promising treatment option against *Chlamydia trachomatis, Orientia tsutsugamushi, Staphylococcus aureus,* and *Wolbachia* [102,105]. The pharmacological target of CorA is the DNA-dependent RNA-polymerase, in that CorA acts as a non-competitive inhibitor of the switch region [106]. Hence, the transcription of the RNA-polymerase is inhibited, inducing the death of the bacteria. This mode of action is not widely addressed by other antibiotics, which makes it advantageous against the bacterial resistance threat. In contrast to rifampicin, another inhibitor of the DNA-dependent RNA-polymerase, the binding site is at a different location preventing cross-resistance of the these two antibiotic candidates [102]. By using heterologous expression with the help of the production platform in the myxobacterium *Myxococcus xanthus* it was possible to increase the CorA production yield during the fermentation process [107]. The following isolation process via reversed-phase medium pressure liquid chromatography enabled a CorA purity of 90-99% [102]. Successful initial *in vitro* efficacy experiments, establishment of the analytics and a production providing sufficient drug purity paved the way into the preclinical development stage. Investigations revealed several pitfalls that need to be addressed with particular attention during the preclinical development process. As for CorA an undesired intramolecular isomerization leads to a loss of efficacy, one goal of the CorA-projects was to improve the storage stability. Moreover, an amorphous state accompanying with a low T_g of 5 °C provokes a waxy and sticky drug mass with ambitious handling properties [108]. Regarding its physicochemical properties, the lipophilic character (logP of 5.4) indicates good permeability, but rather poor aqueous solubility (pH 1: 0.11 µg/mL; pH 6.5: 91.13 µg/mL) [108]. Accordingly, appropriate formulation strategies were required to enable various preclinical investigations. This includes liquid formulations, valuable for *in vitro* and first rodent *in vivo* evaluations, and solid formulation for subsequent rodent and non-rodent *in vivo* trials. The formulation strategies were investigated with emphasis on stability, solubility and handling enhancement [108].

3. Scope and Objectives

Prior to a successful approval and market entry of a novel drug product, each project has to pass several steps. Especially during the preclinical drug development stage many potential hurdles need to be evaluated and addressed. During the development process it is essential to implement a rational drug development process to save valuable resources, costs and animal trials. To do so, *in vitro* tests and *in silico* tools were established to provide estimates regarding respective *in vivo* behavior. The need for appropriate CorA formulations was indicated due to its susceptibility to isomerize, poor solubility and waxy consistency. However, common technologies regarding manufacturing and characterization of drug products need a minimum of drug amount which in turn is often not feasible during preclinical phases.

The objective of this thesis was to introduce approaches regarding a resource saving drug product development and biorelevant *in vitro* and *in silico* setups to support the preclinical assessment of the anti-infective CorA. Thus, the biorelevant biphasic dissolution was used and adjusted to mimic intestinal conditions of preclinical species to support the formulation screening for these species and to improve confidence for human estimates. It was aimed to combine these results with PBPK modeling and make an initial prediction of FIH performances to provide a safe and rational entry into clinical phase I trials. To achieve these goals the following work packages were carried out:

1. Establishment of a down-stream process for the production of the solid drug products, a capsule or tablet containing the respected spray dried CorA-ASD intermediate.
2. Characterization of CorA and CorA formulations with a special attention towards the stability and dissolution enhancement.
3. Investigation of dissolution performances under preclinical biorelevant conditions.
4. Preclinical PK characterization of CorA and CorA-formulations in mice, jirds, rats and dogs.
5. Investigation of potential transport mechanisms that influences BA.
6. Establishment of PBPK models for cross species evaluations and FIH predictions.
7. Toxicological investigations of CorA in rats and dogs.

4. Materials and Methods

4.1 Materials

A)

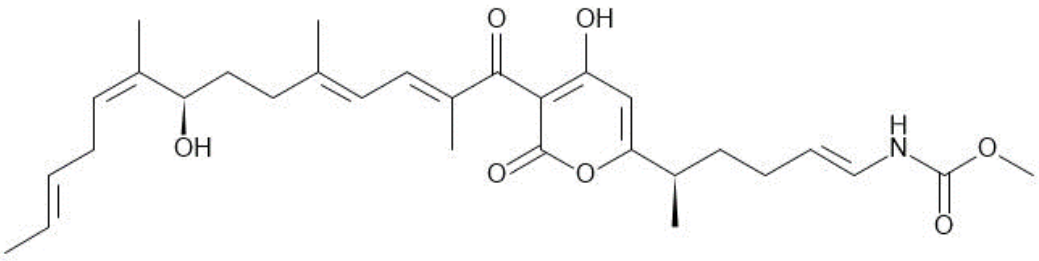

B)

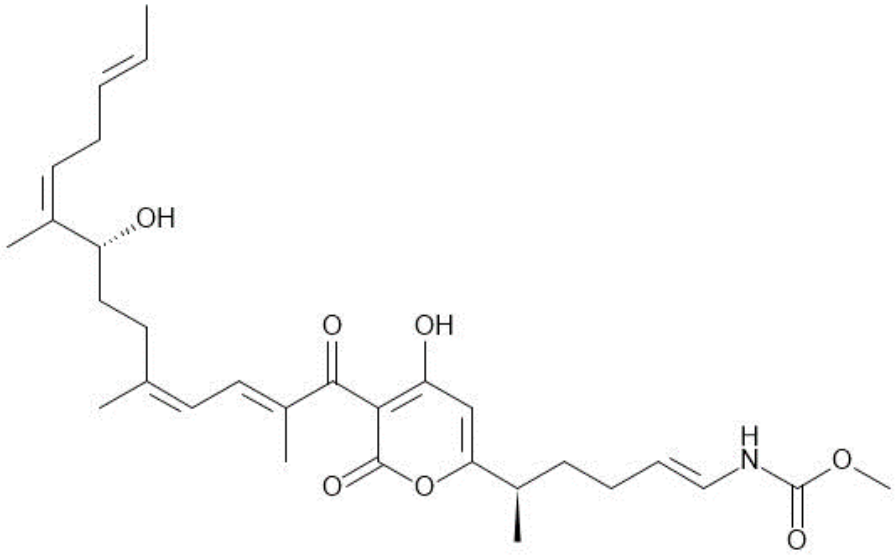

C)

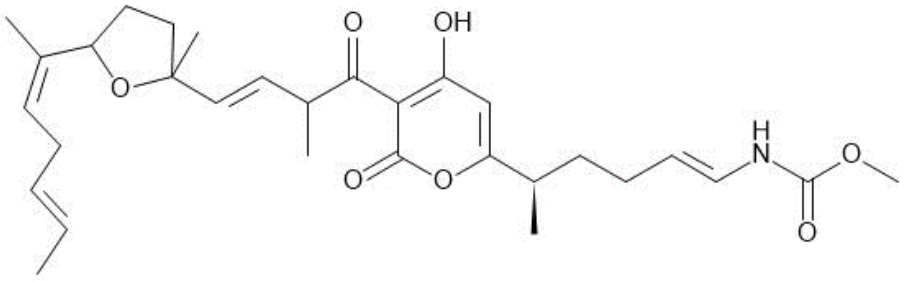

Figure 3. Chemical structure of CorA (A) and its main isomers CorA' (B) and CorC (C).

Figure 3 shows the chemical structure of CorA and its most relevant isomers corallopyronin A' (CorA') and corallopyronin C (CorC). The production of the drug substance by fermentation and subsequent isolation processes were carried out by the Helmholtz Centre for Infection Research (HZI) in Braunschweig. For the following *in vitro*

and *in vivo* experiments different CorA batches were used. To guarantee comparability, a CorA content of 90-95% was ensured for each batch.

Table 1. Overview of the used materials in this work.

Material	Tradename	Supplier
Acetonitrile (LC-MS grade)		Bernd Kraft GmbH (Duisburg, Germany)
Ammonium acetate (LC-MS grade)		Merck KGaA (Darmstadt, Germany)
Methanol (LC-MS grade)		Bernd Kraft GmbH (Duisburg, Germany)
Water (LC-MS grade)		Bernd Kraft GmbH (Duisburg, Germany)
Abs. ethanol (99.8%)		Carl Roth GmbH +. Co. KG (Karlsruhe, Germany)
Polyvinylpyrrolidone (Povidone)	Kollidon® 30 LP	BASF SE (Ludwigshafen, Germany)
Vinypyrrolidone-vinyl acetate copolymer (Copovidone)	Kollidon® VA 64	BASF SE (Ludwigshafen, Germany)
Acetaminophen		Caesar & Loretz GmbH (Hilden, Germany)
Hydroxypropyl methylcellulose 4000 (Hypromellose 4000)		Shin-Etsu (Venlo, Netherlands)
Mesoporous silica	Syloid® XDP 3050	GRACE (Worms, Germany)
Polyethylene glycol 200 and 400 (PEG 200; PEG 400)		Carl Roth GmbH + Co. KG (Karlsruhe, Germany)
Propylene glycol		VWR Chemicals (Darmstadt, Germany)
Macrogol 15 hydroxy stearate	Kolliphor® HS 15	BASF SE (Ludwigshafen, Germany)
Gibco™ Phosphate buffered saline (PBS) (pH 7.4; 1x)	DPBS (1X)	Thermo Fischer Scientific, Life Technologies Europe BV, (Bleiswijk, Netherlands)
n-Hexane		VWR Chemicals (Darmstadt, Germany)
Sorbitan monooleate	Span® 80	Croda GmbH (Nettetal, Germany)
Sodium tartrate		Merck KGaA (Darmstadt, Germany)
Di-sodium hydrogen phosphate monohydrate		Th. Geyer GmbH & Co. KG (Renningen, Germany)
Sodium dihydrogen phosphate mono hydrate		Th. Geyer GmbH & Co. KG (Renningen, Germany)
Lecithin		Alfa Aesar (Kandel, Germany)

Material	Tradename	Supplier
Sodium taurocholate hydrate, 96%		Alfa Aesar (Kandel, Germany)
Hydrochloric acid, 0.1 N		Sigma-Aldrich Chemie GmbH (Steinheim, Germany)
1-Decanol		Alfa Aesar (Kandel, Germany)
Sodium hydroxide		VWR Chemicals (Darmstadt, Germany)
Tri-potassium citrate		Carl Roth GmbH + Co. KG (Karlsruhe, Germany)
Tri-potassium phosphate		Alfa Aesar (Kandel, Germany)
Sodium phosphate monobasic anhydrous		VWR Chemicals (Darmstadt, Germany)
Glyceryl monooleate	Peceol	Gattefossé (Rheinfelden, Switzerland)
Sodium oleate		Sigma Aldrich (Taufkirchen, Germany)
Hydroxyethyl piperazineethanesulfonic acid	HEPES	Carl Roth GmbH + Co. KG (Karlsruhe, Germany)
Sodium chloride		Sigma-Aldrich Chemie GmbH (Steinheim, Germany)
Lysophosphatidyl-choline	Lipoid P LPC 80	Lipoid (Ludwigshafen, Germany)
Maleic acid		Merck KGaA (Darmstadt, Germany)
Dog FaSSIF		Biorelevant (London, United Kingdom)
Silica gel		Carl Roth GmbH + Co. KG (Karlsruhe, Germany)
Enteric Capsules, size 0	Vcaps® Enteric Capsules	Capsugel® (Morristown, NJ, USA)
Sterile water for injection	Ampuwa®	Fresenius Kabi Deutschland GmbH (Bad Homburg, Germany)
Hydroxyethyl cellulose	NATROSOL®	Caesar & Loretz GmbH (Hilden, Germany)
Reagents for cell culture experiments		Sigma Aldrich (Taufkirchen, Germany)
Trypsin-EDTA solution 10%		Sigma Aldrich (Taufkirchen, Germany)
Dulbecco's Modified Eagle's Medium		Sigma Aldrich (Taufkirchen, Germany)

4.2 Quantification of CorA by HPLC DAD

A quantification method via high-performance liquid chromatography (HPLC) was comprehensively described by Krome [109]. As CorA tends to isomerization and tautomerization, it was crucial to establish a method that allows a clear separation of all isomers, especially for *in vitro* stability assessments and CorA quantifications in plasma samples obtained from *in vivo* PK studies. The following method meets these requirements [108,109]. CorA samples were quantified by HPLC with an Alliance e2695 separation module and a 2998 PDA detector (Waters, Eschborn, Germany). HPLC conditions were set as follows: column: Waters XBridge® Shield RP18 column (3.5 µm, 2.1 x 100 mm, 130 A); temperature: 30 °C, injection volume: 5 µL; flow rate: 0.3 mL/min; wave length for quantification: 300 nm. The mobile phase A was comprised of acetonitrile and water (5:95, (V/V)) with 5 mM ammonium acetate and 40 µL acetic acid per liter and the mobile phase B was comprised of acetonitrile and water (95:5, (V/V)) with 5 mM ammonium acetate and 40 µL acetic acid per liter. The gradient was used as follows: 70%A/30%B to 20%A/80%B, stepwise within 30 min. Data were analyzed using the Empower 3 software (Waters, Eschborn, Germany) and quantified using an external reference standard. *In vitro* samples were diluted until reaching a maximum concentration of 0.1 mg/mL to ensure clear separation. Plasma samples were prepared as follows: Plasma was mixed with ice-cold acetonitrile (1:3, (V/V)), vortexed for 10 s and centrifuged at 11,000 G at 4 °C for 25 min. The supernatants were transferred to HPLC vials and maintained at 5 °C in an autosampler before injection. No major matrix effects were observed when mixing CorA-containing acetonitrile with plasma.

4.3 Manufacturing

4.3.1 Manufacture of the Spray-Dried CorA-ASD Formulations in a small-scale spray dryer

The used polymers were dried at 40 °C for 24 h under vacuum conditions using a vacuum oven chamber (Binder GmbH, Tuttlingen, Germany) to remove residual water. CorA and the respective polymer were dissolved in ethanol, targeting a solid concentration of 10% (w/v). The ratio between polymer and CorA was 80:20 resulting in a drug load of 20% for the produced ASDs (**Table 2**). The ethanolic solution was dried using a Büchi B-290 mini spray dryer, coupled to an Inert Loop-B295, Dehumidifier B-296 (Büchi, Flawil,

Switzerland) and an anemometer (model AF89-AD1AA13C0AA, Fluid components Intl. San Marcos, CA, USA). The spray dryer was further equipped with a two fluid nozzle (0.7 mm nozzle tip, 1.5 mm screw cap) and a 90 ° drying chamber. The manufacturing process was set with the inert gas nitrogen as drying gas and an aspirator rate of 100% (corresponding to 35 m^3/h). The inlet temperature of 85 °C resulted in an outlet temperature of 59 °C. The nitrogen spray gas flow was set at 473 L/h (corresponding to 40 mm height of the rotameter) and a solution feed rate of 5 mL/min was chosen. After the spray drying process, the collected spray dried powder (process yields of 60-65%) was dried at 25 °C for 24 h under vacuum conditions using the vacuum oven chamber to remove residual solvent.

Table 2. Composition of CorA-ASDs.

Formulation	Excipient	Composition	Drug load
ASD 1	Povidone (polyvinyl-pyrrolidone)	CorA 20% Povidone 80%	20%
ASD 2	Copovidone (vinylpyrrolidone-vinyl acetate copolymer))	CorA 20% Copovidone 80%	20%

4.3.2 Briquetting of the Spray-Dried CorA-ASDs

Spray dried products typically show small particle sizes accompanying with poor powder flowability properties [65]. For further processing into solid oral drug products, such as capsules or tablets, it is necessary to increase the particle size to enable tableting or easy capsule filling. Dry granulation was chosen as a solvent-free technique to reduce the risk for moisture induced physical instability. Roller compaction is a well-known granulation technique and has been used in the pharmaceutical industry for more than 50 years [110]. However, this technology requires a minimal quantity to be processed and the limited drug substance of CorA (batch sizes of 10-20 g) during preclinical development excluded this technology. Instead, briquetting was used as a small-scale alternative. Similar to roller compaction, the powder was exposed to high force which leads to the formation of a compact. In essence, the compaction is a process to alter powders or granules into a coherent specimen (e.g., tablets) [110,111]. The briquetting was performed using a pneumatic hydraulic tablet press (FlexiTab®, Röltgen GmbH & Co KG, Solingen, Germany).

For this purpose, an 18 mm round flat-face tooling with a compaction force of 197 MPa was used. After the briquetting process, the compacted material was manually granulated/crushed with a mortar and pestle and divided into sieve fractions.

4.3.3 Encapsulation of the CorA-ASD Granules

Capsules represent a very suitable option for initial human trials due to their ease of use and flexibility in dose adjustments. For *in vitro* and *in vivo* investigations, 75 mg of ASD granules were individually weighed into size 0 enteric hard capsules. The chosen dose level based on interspecies efficacy dose conversion from mouse to dog, provided by the FDA guideline [112]. The identified efficacious dose of 36 mg/kg in BALB/c mice resulted in an estimation of 7.3 mg/kg for dogs resulting in an absolute dose of 75 mg, based on an approximate body weight of 10 kg [113]. Hence, a dose level of 75 mg CorA (corresponding to 375 mg ASD) was targeted using enteric capsules, size 0, (Vcaps® Enteric Capsules, Capsugel®, Morristown, NJ, USA).

4.3.4 Tableting of the CorA-ASD Formulations

Tableting processes were performed using a pneumatic hydraulic tablet press (FlexiTab®, Röltgen GmbH & Co KG, Solingen, Germany). For sustained release matrix tablets, the 12x8 mm biconcave tooling with a cup radius of 10.4° was used. The ASD-granules were manually mixed with HPMC 4000 using a spatula and manually introduced to the die with the targeted tablet mass. **Table 3** summarizes the tablet compositions. Due to limited drug substance preliminary studies without CorA were conducted to find a compaction pressure resulting in a sufficient crushing strength (approx. 100-150 N). These preliminary studies revealed a compaction pressure of 97.2 MPa. After tableting, the tablets were stored at room temperature under nitrogen in air-tight vials.

Table 3. Composition of CorA-ASD tablets.

Formulation	Composition	Tablet weight (mg ± SD)	CorA dose (mg)
CorA-povidone-ASD HPMC 4000	CorA-povidone-ASD 80% HPMC 4000 20%	314.9 ± 2.3	50.4
CorA-copovidone-ASD HPMC 4000	CorA-copovidone-ASD 90% HPMC 4000 10%	281.2 ± 2.2	50.6

4.3.5 Preparation of Mesoporous Silica Formulation of CorA

The solid mesoporous silica formulation was prepared by the incipient wetness impregnation process [43,114]. A highly concentrated ethanolic solution of CorA (1 g/mL) was prepared using an ice-cooled ultrasonic bath. The solution was added dropwise to mesoporous silica in a 1:2 weight ratio. Simultaneously, the mesoporous silica was constantly manually mixed in a plastic mortar and pestle. After reaching a ratio of 2:1 (silica/CorA, (W/W)), the powder was dried at 25 °C for 24 h. A second loading cycle was performed similarly to achieve a final ratio of 1:1 of CorA-silica (W/W). The drying step was conducted at 25 °C for approx. 24 h to remove the residual solvent. Higher drying temperatures were impossible due to the thermal lability of CorA. As the maximum liquid to Syloid® XPD/silica ratio of 1.65:1 reported by the manufacturer, would have been below the required ratio of 2:1 liquid (CorA solution in ethanol 1g/ml) to solid ratio (W/W), the loading was performed in a twostep process well below this value in order to enable the liquid load in the dry state [115]. However, the maximum liquid load was tested empirically by testing ascending ratios between liquid and silica. The final amount of added liquid was determined to the extent that a free-flowing powder was still present after the loading steps.

For the toxicological studies in dogs the first loading was performed on a 0.97:1 liquid (CorA solution in ethanol 1 g/ml) to solid ratio (W/W). After an intermediate drying step (evaporation of ethanol) a second loading step was performed, subsequently. To determine the loading efficiency, 10 mg of CorA-mesoporous-silica were added to 10 mL

acetonitrile and continuous ultrasound was used for 1 h to induce drug release (ultrasound water bath Sonorex TK 52 H, Bandelin, Berlin, Germany). The withdrawn samples (1.0 mL) were centrifuged (5 min, 21,000 G, 37 °C) and the supernatant was diluted 10-fold with acetonitrile and quantified by HPLC (**Chapter 4.2**). After the final drying step an overall loading efficiency of 89% ± 3% resulted based on the extractable CorA amount from the loaded silica. Loading efficiency was defined as the extractable drug fraction out of the mesoporous silica.

4.3.6 Liquid Formulations of CorA for *In Vivo* Studies

During preclinical investigations of CorA several *in vivo* PK, as well as, PD studies required liquid formulations. Providing stable solution principles was essential for a successful and safe CorA administration. For PK studies in animals, vehicles for IV administration enable determination of oral BA and insights to elimination and distribution behavior of the drug candidate. Thus, a co-solvent based liquid formulation was developed by Krome et al. [108]. Good tolerability and applicability were demonstrated for preclinical studies in mice. However, preclinical studies include investigations in different species showing different tolerability. For dogs, e.g., the high amount of the non-ionic surfactant Kolliphor HS 15 was reported to cause histamine induced allergic reaction and excluded this composition for studies in dogs [116]. Likewise, when administered to rats, intolerance was observed, which led to animal deaths. Thus, alternatives were developed that involved either a proportion adjustment or a change in composition. Further liquid formulations for toxicological investigations were investigated, that are typically carried out with solutions due to easy dosing and ease of handling. **Table 4** summarizes the liquid formulations with corresponding maximum concentrations and the studies in which they were intended for.

Table 4. Composition of CorA liquid formulations.

Formulation	Excipients	Maximum tested concentrations resulting in a CorA-Solution	Study for which the vehicle was used
Liquid Formulation 1	20% Propylene glycol 20% Kolliphor HS 15 60% PBS, pH 7.4	20 mg/mL	PK study in mice PK study in rats
Liquid Formulation 2	20% Propylene glycol 4% Kolliphor HS 15 76% PBS, pH 7.4	7.5 mg/mL	PK study in dogs
Liquid-Formulation 3	60% PEG400 40% PBS, pH 7.4	3.6 mg/mL	PK study in rats
Liquid Formulation 4	100% PEG 200	100 mg/mL	Toxicology study in rats PK study in dogs

4.4 Characterization of CorA Formulations

4.4.1 Particle Size Distribution of Spray-Dried Products

Determination of particle size distributions based on the laser diffraction measuring principle. A Horiba LA-960 laser diffractometer (Horiba, Kyoto, Japan) equipped with a red laser diode (650 nm; 5 mW) and a blue light emitting diode (405 nm; 3 mW) was used. The device provides two different laser diffraction techniques: (1) Measurement in the natural dry powder state; (2) measurement of the powder which is dispersed in a liquid. To avoid a great material loss, option (2) was chosen for CorA-formulations. N-hexane was used as a dispersion medium that is not able to dissolve or swell the formulations or components thereof and has an appropriate low viscosity. The addition of 0.1% SPAN 80 reduced the surface tension and improved the wettability. Approx. 15 mL of this suspension was filled into a beaker and a small quantity of CorA-formulation was added. Ultrasonic sound was used for 30 s to break up residual agglomerates. Afterwards the suspension was introduced to the quartz cuvette of the laser diffractometer. Sustained

mixing by a magnetic stirrer in the cuvette prevented re-aggregation and sedimentation. At least 3 independent measurements were conducted.

4.4.2 Scanning Electron Microscopy for Particle Morphology

Samples were sputtered with platinum. A Helios™ G4 CX Dualbeam™ (Thermo Scientific™ Inc, Waltham, MA, USA) microscope, equipped with a secondary electron detector, was used at 2 kV and 4 mm working distance.

4.4.3 Karl Fischer Titration for Water Content Determination

To determine the water content during the stability study of the CorA drug products the Volumetric KF Titrator equipped with a Stromboli autosampler (Mettler Toledo, Columbus, Ohio, USA) was used. The samples were dried at 150°C and the evaporated water was absorbed in methanol and quantified via titration with CombiTitrant 2 (Supelco, Darmstadt, Germany). Sodium tartrate was used as a standard for a correction factor based on titrant potency.

4.4.4 Gas Chromatography for Residual Solvent Determination

Gas chromatography measurements were carried out to determine residual solvent after the spray drying process and after the preparation of the mesoporous silica formulations for toxicology studies. In both cases, the amount of ethanol was determined using a Focus GC Gas Chromatograph, equipped with a flame ionization detector and TriPlus RHS Autosampler (ThermoFisher Scientific, Dreieich, Germany). Experiments were conducted under the following setup: Column: FS_CS_624 quartz capillary with 30 m length and an inner diameter of 0.32 mm; column surface: 6% poly-(cyanopropyl) phenylsiloxane and 94% poly-(dimethyl) siloxane. Samples of approx. 30-40 mg, accurately weighed, were transferred to 1.0 mL of phosphate buffer pH 6.8. After incubation at 80 °C for 10 min in the headspace oven, 1.0 mL gas volume was injected. The starting temperature of the column oven was set to 60 °C and gradually heated to 80 °C with a rate of 2 K/min following a 10 K/min up to 150 °C. Compressed air (2.0 mL/min) was used as carrier gas and nitrogen for a 1/5 split flow during injection. A calibration curve with five concentrations covering the range of the quantified samples were used for quantification.

4.4.5 Biorelevant Solubility of CorA and CorA-ASD Formulations

Neat CorA, CorA-povidone-ASD, CorA-copovidone-ASD and CorA-silica were investigated regarding kinetic solubility using the shake flask method. Two different setups, monitoring CorA concentrations between 2 min and 4 h in case of neat CorA and CorA-ASDs and 4 h to 24 h in case of CorA-silica were carried out. FaSSIF-V2- and fed state simulating intestinal fluid (FeSSIF)-V2-media were used based on species-specific pH values. Setup 1 represents the pH values mimicking the human gut condition comprising FaSSIF-V2 (pH 6.5) and FeSSIF-V2 (pH 5.8) [86]. Setup 2 matched the mouse gut pH, resulting in FaSSIF-V2-mouse (pH 5.2) and FeSSIF-V2-mouse (pH 4.8) media [117]. Neat CorA and CorA-ASD-formulations were investigated in both setups, while CorA-silica was evaluated exclusively in experimental setup 1. An excess of sample was introduced in each case into 10 mL of the respective biorelevant media (**Table 5**) and incubated for 4 h (setup 1) and 1 h (setup 2) in a GFL 1083 shaking incubator (Gesellschaft für Labortechnik GmbH, Burgwedel, Germany) at 37 °C. The endpoints after 4 h (setup 1) and 1 h (setup 2) represent the intestinal transit times of humans (4 h) and mice (1 h) [118,119]. Samples (0.5 mL) were withdrawn and centrifuged for 5 min at 21,000 g and 37 °C. The supernatant was diluted 10-fold with methanol to avoid precipitation and quantified by HPLC (**Chapter 4.2**). Kinetic solubility profiles were established in triplicates.

Table 5. Composition and physicochemical characteristics of biorelevant media simulating the small intestine environment in human and mouse in fasted and fed state.

	FaSSIF-V2-human	FeSSIF-V2-human	FaSSIF-V2-mouse	FeSSIF-V2-mouse
Lecithin (mM)	3.0	10	3.0	10
Sodium taurocholate (mM)	0.2	2	0.2	2
Glyceryl monooleate (mM)		5		5
Sodium monooleate (mM)		0.8		0.8
Sodium chloride (mM)	68.6	125.5	68.6	125.5
Sodium hydroxide (mM)	34.8	102.4	34.8	102.4
Maleic acid (mM)	19.1	71.9	19.1	71.9
Sodium hydroxide 1 N	q.s.; pH 6.5	q.s.; pH 5.8		
Hydrochloric acid 1 N			q.s.; pH 5.2	q.s.; pH 4.8
Buffer capacity (mM/ΔpH)	10	25	10	25
Osmolality (mOsm/kg)	180	390	180	390
pH	6.5	5.8	5.2	4.8

4.5.6 Differential Scanning Calorimetry for T_g Determination

Differential Scanning Calorimetry (DSC) measurements were performed as part of the stability study to identify potential phase separation of CorA and polymer of the CorA-ASDs. The DSC analyses were conducted using the DSC 2 instrument (Mettler-Toledo GmbH, Gießen, Germany), equipped with a nitrogen cooling system. Samples were prepared as follows: Approx. 6-10 mg of the sample was weighted into a 40 µL aluminum crucible with a pierced lid. A temperature-modulated program (TOPEM-mode) with a constant temperature rising profile (2 K/min) starting at 0 °C was used. The end temperatures were set high enough to exceed the expected T_g by at least 50 °C (endpoint CorA-povidone: 170°C; CorA-copovidone: 130 °C). Measured data were analyzed with the STARe software DB V13.00 (Mettler-GmbH, Gießen, Germany).

4.5 Dissolution

4.5.1 USP II Dissolution for the CorA Drug Products Capsule and Tablet

Dissolution studies of acetaminophen-capsules, CorA-capsules (CorA dose: 75 mg) and CorA-tablets (CorA dose: 50 mg) were performed using the AT7 dissolution tester (Sotax

AG, Aesch, Switzerland). The test medium was 0.05 M phosphate buffer (pH 6.8) with a volume of 900 mL for acetaminophen and 500 mL for CorA samples. The paddle speed was set to 75 RPM and the temperature to 37 °C. Both, the capsules and the tablets, were placed in a sinker to avoid floating. Online quantification was conducted using an 8453 UV/VIS spectrophotometer (Agilent, Waldbronn, Germany). Absorption was determined at a fixed wavelength of 307 nm and the dissolution test duration was set to 3 h (capsules) and 7.5 h (sustained release tablets). The measuring interval was 3 min and light scattering correction was integrated by the 3-point drop line method (450 - 550 nm). The dissolution was calculated as the percentage of dissolved drug referred to the tested dose. All experiments were carried out at least in triplicates.

4.5.2 Mini-scale Dissolution for Small Formulation Quantities

Following the USP II dissolution a miniaturized apparatus was established by Zecevic et al. [120]. By using only 20 mL of dissolution media, this approach represents a valuable tool in early drug product development since small quantities of drug substance and formulation can be tested. The paddle speed was set to 75 RPM and the temperature to 37 °C. Similar to the original USP II dissolution setup (**Chapter 4.5.1**), quantification was performed via an UV/VIS spectrophotometer in a 3 min interval. The test medium varied for different settings including 0.05 M phosphate buffer (pH 6.8), 0.1 N HCl (pH 1), FaSSIF medium or FeSSIF medium. Depending on the requirements of the formulations, different dose levels were used. Medium and dose level are depicted in corresponding Figures. The dissolution was calculated as the percentage of dissolved drug referred to the tested dose. All experiments were performed in triplicates.

4.5.3 Monophasic Biorelevant pH Shift Dissolution

Non-sink dissolution of CorA-ASD formulations were performed under biorelevant mouse conditions. Thus, the experimental design was adapted concerning the pH profile and transit time in the mouse gut [117,121]. Fed state was assumed to be the most appropriate condition due to free food access for the mice during PK studies. As no appropriate test media mimicking the gastrointestinal conditions of mice are described in literature, human FeSSIF-V2 was adjusted to the reported mouse pH in a fed state similar to the procedure suggested by the GastroPlus PBPK software (versions 9.8.3, Simulations Plus, Inc., Lancaster, CA, USA). Dissolution during the stomach passage was simulated by

50 mL of aqueous dissolution media, set to pH 3.0 using a buffer concentrate based on McIlvaine buffer [122]. A sample size of 10 mg neat CorA and 50 mg of CorA-ASDs corresponding to 10 mg CorA were tested, respectively. After 20 min, the approximate stomach transit time in mice, FeSSIF-V2-like concentrate was added to shift the pH from pH 3.0 to 4.8, simulating the small intestine pH of mice [123]. Dissolution duration was set to 80 min in accordance to the stomach and small intestine transit time in mice [119]. Quantification was conducted using an Agilent 8454 UV/Vis spectrophotometer (Waldbronn, Germany), similar to the procedure described in **Chapter 4.5.1 and 4.5.2**. In contrast, the first derivative at 394 nm was used in order to eliminate scattering artefacts. A 1-micron full-flow filter prevented further scattering constraints due to undissolved or precipitated particles. Three independent dissolution tests were performed for each sample. For mouse PBPK simulations, dissolution results were incorporated to the model via Weibull parameters calculated from the monophasic dissolution setup. The percentage of released dose is described in **Eq. 3** [124].

$$\%Dose\ Released\ = Max\left(1 - e^{\left(1-\frac{-(t-T)^b}{A}\right)}\right) \quad \textbf{(3)}$$

where Max = maximum of released API, T = time lag, b = shape factor of the curve and A = time scale.

4.5.4 Species Specific Biphasic Dissolution

During the preclinical drug development of CorA *in vivo* PK studies were performed in different species. As the most common dissolution setups focus on the conditions present in human, estimations of potential formulation candidates in preclinical species remains difficult. The biphasic dissolution was chosen as a biorelevant approach that has been demonstrated to be predictive for human [84]. Respective adjustments were applied to the BiPHa+ model resulting in three different setups representing mouse, rat and dog. In general, for all tested setups, a sample size of 10 mg neat CorA or 50 mg of CorA-ASDs corresponding to 10 mg CorA were tested, respectively. The volume of the aqueous phase was 50 mL. Sufficient hydrodynamic was achieved by a prism shaped magnetic stirrer placed in the aqueous phase with a rotation speed of 170 RPM. The absorption-sink was generated by an organic phase comprised of 50 mL 1-decanole that was automatically

added during the dissolution after the respective stomach transit time. Potential required pH-shifts or bile salts were realized by a manual addition of buffer-concentrate and FaSSIF or FeSSIF components. The temperature during the dissolution experiments was kept at 37 °C. The run times followed the respective gastrointestinal transit time similar to the settings of the PBPK modeling software GastroPlus™. Quantification was conducted using an Agilent 8454 UV/Vis spectrophotometer (Waldbronn, Germany), similar to the procedure described in **Chapter 4.5.1 and 4.5.2**. The first derivative at 394 nm was used for both phases to eliminate scattering artefacts and biased quantification due to biorelevant media. A 1-micron full-flow filter prevented further scattering constraints due to undissolved or precipitated particles. Three independent dissolution tests were performed for each sample.

Mouse-setup: The experimental design was adapted concerning the pH profile and transit time in the mouse gut [117,121]. Fed state was assumed to be the most appropriate condition due to free food access for the mice during PK studies. As no appropriate test media mimicking the gastrointestinal conditions of mice are described in literature, human FeSSIF-V2 was adjusted to the reported mouse pH in a fed state similar to the procedure applied by the GastroPlus™ PBPK software. Dissolution during the stomach passage was simulated via 50 mL of aqueous dissolution media, set to pH 3.0 using a buffer concentrate based on McIlvaine buffer [122]. After 20 min, the approximate stomach transit time in mice, FeSSIF-V2-like concentrate was added to shift the pH from pH 3.0 to 4.8, simulating the small intestine pH of mice [123]. Dissolution duration was set to 80 min in accordance to the stomach and small intestine transit time in mice [119]. **Table 6** depicts the medium composition and **Figure 4** schematically illustrates the experimental setup for the species mouse. In accordance to available *in vivo* PK studies, neat CorA and CorA-ASDs (spray dried CorA-povidone and CorA-copovidone) were tested using this setup.

Table 6. Composition and characteristics of biorelevant mouse medium.

	FeSSIF-V2 like
Lecithin (mM)	2
Sodium taurocholate (mM)	10
Glyceryl monooleate (mM)	5
Sodium monooleate (mM)	0.8
Sodium chloride (mM)	25.0
Potassium citrate (mM)	10
Potassium phosphate (mM)	4.3
Sodium hydroxide (mM)	10
pH	**4.8**

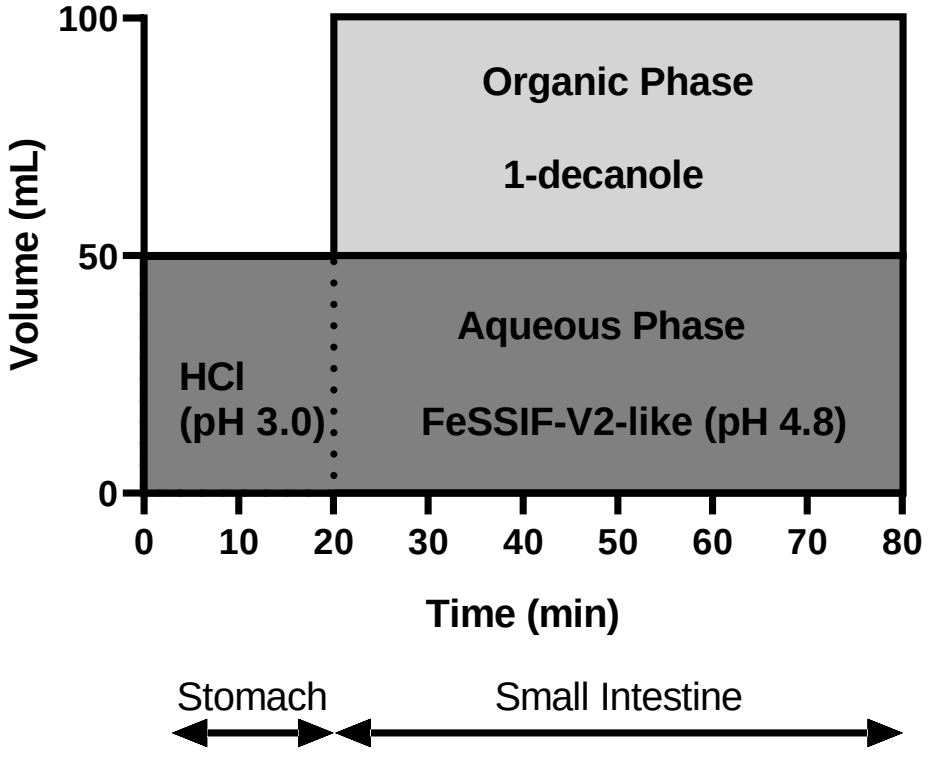

Figure 4. Biphasic dissolution setup for the mouse model.

Rat-setup: The composition and procedure based on Christfort et al. where gastrointestinal fluids were characterized and an *in vitro* model was developed [125]. This procedure was adapted to the BiPHa+-assay. Stomach and gut transit times were adjusted to 30 min for stomach and 108 min for the intestine, consistent with the transit times used by the PBPK modeling software GastroPlus™. The stomach part was mimicked by 33 mL rat gastric medium (RGM), while the intestinal part was induced by the addition of 16.7 mL concentrate comprising buffer components and bile salts resulting in rat intestinal medium (RIM). The buffer system based on HEPES (2-(4-(2-Hydroxyethyl)-1-piperazinyl)-ethansulfonsäure) resulting in a buffer capacity of 25.2 mM/ΔpH and an osmolality of 230 mOsm/kg for the RGM and 312 mOsm/kg for the RIM. **Table 7** depicts the medium composition and **Figure 5** schematically illustrates the experimental setup for the species rat. Spray dried CorA-povidone and CorA-copovidone were examined with this setup, according to the rat PK study.

Table 7. Composition and characteristics of the biorelevant rat media [125].

	RGM	**RIM**
Sodium taurocholate	1.3	24.1
Lysophosphatidyl-choline	0.8	3.7
Sodium chloride (mM)	111.7	119.6
HEPES (mM)		100
pH	**2.4**	**7.5**

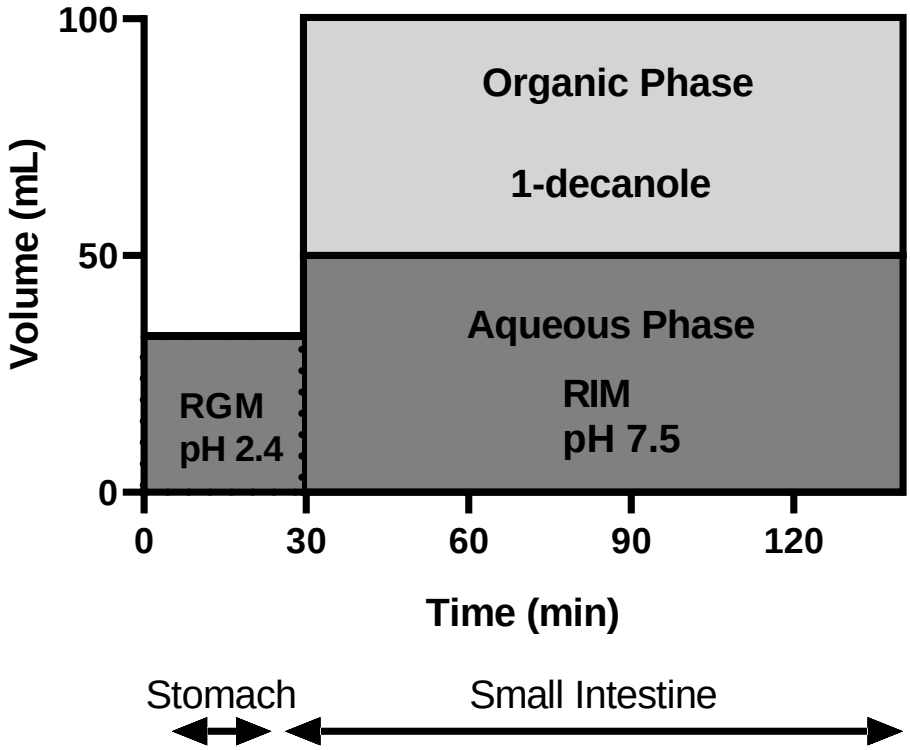

Figure 5. Biphasic dissolution setup for the rat model.

Dog-setup: As dogs represent an important part in terms of preclinical PK investigations of solid oral drug products, a commercial medium for *in vitro* dissolution tests is available [126]. It was used for the biphasic setup. The first 30 min, representing the stomach transit, 50 mL of 0.1 N HCl was used as dissolution medium since the dogs of the PK study were treated with pentagastrin prior the CorA administration. This was carried out to decrease the stomach pH to pH 1, similar to the pH present in fasted humans. Approx. 50 mg of the drug product, granulated CorA-povidone ASD, were filled into enteric capsules and placed in the aqueous phase (pH 1) with the help of a sinker. After 30 min the medium was replaced by 50 mL of the dog FaSSIF (FaSSIFc) medium. CorA amount that may have been removed was considered in the calculation. Simultaneously, the organic layer was introduced. The dissolution time was 138 min representing the gastrointestinal transit time in fasted dogs. **Table 8** shows the medium composition and **Figure 6** schematically illustrates the experimental setup for the species dog.

Table 8. Composition and characteristics of biorelevant dog medium.

	FaSSIFc
Lecithin (mM)	1.25
Sodium taurocholate (mM)	5
Sodium taurodeoxycholate (mM)	5
Lysophosphatidyl-choline (mM)	1.25
Sodium monooleate (mM)	1.25
Sodium chloride (mM)	59.63
Sodium hydroxide (mM)	21.66
NaH2PO4 x H2O	28.65
pH	**7.5**

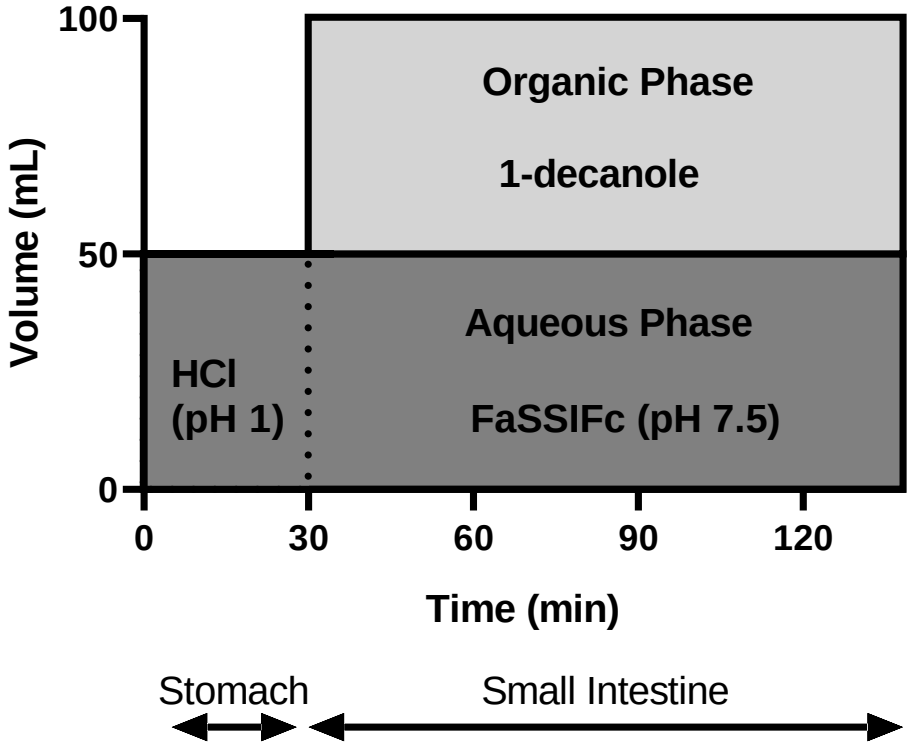

Figure 6. Biphasic dissolution setup for the dog model.

4.6 Stability Study Setup of the Solid Oral Drug Product Capsule

The stability of solid drug products of CorA were analyzed at different storage conditions that were selected in accordance to the ICH guideline Q1 A (R2) for stability testing of drug products [127]. A total of 375 mg granulated material of the ASD formulations CorA-povidone and CorA-copovidone, respectively, were filled into enteric capsules, size 0 (Vcaps® Enteric Capsules, Capsugel®, Morristown, NJ, USA). The dose of each capsule was 75 mg. Each capsule was stored in a closed 50 mL TWIST-OFF vial, containing silica desiccant and nitrogen as inert gas. Storage temperatures were set at 5 °C, 25 °C and 30 °C. Measurement time points were set at: immediately after manufacturing (T_0), 3 months and 6 months. Physical stability was assessed by DSC, water content and dissolution (USP II) after 3 and 6 months. Chemical stability was investigated via HPLC (**Chapter 4.2**) after 3, 6 and 12 months to determine the potential extent of isomerization and/or degradation. For sample preparation of chemical stability samples, the entire content of the capsule (375 mg, corresponding to 75 mg CorA) was dissolved in acetonitrile equivalent to 1 mg/mL of CorA. Afterwards, 100 µL of the solution was transferred into a HPLC glass vial and filled with 900 µL to obtain a 10-fold dilution. The vials were vortexed for 10 s and maintained at 5 °C in an autosampler before injection.

4.7 Preclinical PK Characterization of CorA

The PK parameter, obtained from the following PK studies, were examined using the received plasma concentrations. The extrapolated area under the plasma concentration curve (AUC_{0-inf}) was calculated using the PKPlus™ Version 9.7/2.5 (Simulations Plus, Inc., Lancaster, CA, USA) applying a non-compartmental approach. The maximum observed plasma concentration (C_{max}) and the associated time (t_{max}) were directly deduced from the corresponding plasma concentration time profiles. For the absolute BA calculation of the oral administrations **Eq. 4** was used.

$$\mathrm{BA}\ (\%) = \frac{AUC_{0-\infty}PO}{AUC_{0-\infty}IV} \cdot 100 \qquad \textbf{(4)}$$

During the preclinical development of CorA, PK studies were performed in several species that have individual experimental requirements. The following chapters describe the corresponding experimental study setups for each investigated species.

4.7.1 Studies for the Species Mouse

The PK evaluations in mice were performed at the University Hospital Bonn, Germany, according to the European Union Directive 2010/63/EU and was approved by the State Agency for Nature, Environment, and Consumer Protection North Rhine-Westphalia, Germany, (AZ 84-02.04.2015.A507). Female BALB/c mice (6–8 weeks old) were obtained from Janvier (Le Genest-Saint-Isle, France) distributed to four animals per treatment group. The animals were housed at the animal facility of the Institute for Medical Microbiology, Immunology and Parasitology at the University Hospital Bonn, Germany. The mice had free access to food and water throughout the experiment. Neat CorA and the solid spray dried CorA-povidone- and CorA-copovidone-ASD formulations were suspended in water, PBS pH 7.4 and corn oil, respectively, immediately prior to administration (CorA 36 mg/kg, volume 10 mL/kg). The results of the CorA-povidone ASD and CorA IV administration are reproduced with permission from Krome et al. and discussed within this work [108,109]. As 36 mg/kg was able to deplete the *Wolbachia* more than 95%, the same dose level was chosen for the PK studies. An oral gavage was used for all oral administrations. Blood samples from the tail tip were collected after 5 min, 10 min, 15 min, 30 min, 60 min, 180 min and 480 min. Plasma preparation was performed as described in **Chapter 4.2**.

Table 9. Experimental groups of the PK study in BALB/c mice.

Group	Route	Vehicle	Nominal dose level
1[#]	IV: Solution	Propylene glycol / Kolliphor HS 15 / PBS pH 7.4	36 mg/kg
2[#]	PO: Suspension in water	Povidone	36 mg/kg
3	PO: Suspension in water	Copovidone	36 mg/kg
4[#]	PO: Suspension in PBS pH 7.4	Povidone	36 mg/kg
5	PO: Suspension in PBS pH 7.4	Copovidone	36 mg/kg
6	PO: Suspension in corn oil	Povidone	36 mg/kg
7	PO: Suspension in corn oil	Copovidone	36 mg/kg

[#] Reproduced with permission from Krome et al. [108,109].

4.7.2 Studies for the Species Jird

Since Mongolian gerbils (jirds) represent a relevant CorA efficacy model, PK profiles were determined for this species. The studies were performed at the University Hospital Bonn, Germany, according to the European Union Directive 2010/63/EU and was approved by the State Agency for Nature, Environment, and Consumer Protection North Rhine-Westphalia, Germany, (AZ 81-02.04.2020.A244). Two groups were treated with spray dried CorA-povidone ASD formulation either with 30 mg/kg or 60 mg/kg, following the dose levels of efficacy studies in jirds. Each group comprised of four female animals, housed at the animal facility of the Institute for Medical Microbiology, Immunology and Parasitology at the University Hospital Bonn, Germany. The jirds had free access to food and water throughout the experiment. The formulations were administered as suspension in PBS 7.4 with a dose volume of 3.5 mL/kg. Sampling time points were 5 min, 10 min, 15 min, 45 min, 60 min, 3 h and 6 h. Blood was taken from the vena saphena. Plasma preparation was performed as described in **Chapter 4.2**.

Table 10. Experimental groups of the PK study in jirds.

Group	Route	Vehicle	Nominal dose level
1	PO: Suspension	Povidone	30 mg/kg
2	PO: Suspension	Povidone	60 mg/kg

4.7.3 Studies for the Species Rat

The PK evaluation in rats was conducted at Aurigon Toxicological Research Center Ltd (ATRC, Dunakeszi, Hungary) in compliance with the Directive 210/63/EU and amendments on the approximation of laws, regulations and administrative provisions of the Member states regarding the protection of animals used for experimental and other scientific purposes. For the PK study, 20 female Wistar rats were divided equally into five groups. The first two groups were treated intravenously. Solutions of CorA dissolved in propylene glycol, Kolliphor HS 15 and PBS (pH 7.4) (20:20:60, (V/V/V)) at a concentration of 7.2 mg/mL and a back-up option comprised of PEG 400 and PBS pH 7.4 (60:40, (V/V)) at a concentration of 3.6 mg/mL were freshly prepared before administration. A dose volume of 5 mL/kg with an equivalent dose level of 36 mg/mL (propylene glycol-based solution) and 18 mg/kg (PEG 400 based solution) was used. Blood samples were collected through a pre-implanted central venous catheter after 5 min, 10 min, 20 min, 30 min, 60 min, 2 h, 3 h, 4 h and 8 h. Approx. 0.25 mL blood was collected and centrifuged at 2,000 G at 4 °C for 10 min within 60 min after collection. The supernatant was used for HPLC analysis and quantification of CorA in plasma (**Chapter 4.2**). Three groups were orally treated with a CorA solution (PEG 200) with various dose levels. Two groups were orally treated with either spray-dried CorA-povidone ASD or spray dried CorA-copovidone ASD. The ASD formulations were suspended in PBS 7.4 immediately prior administration. For all oral groups the dose level was 36 mg/kg with a dosing volume of 10 mL/kg. Blood samplings after oral administrations were set at 10 min, 20 min, 30 min, 45 min, 60 min, 2 h, 3 h, 4 h and 8 h to ideally cover the maximum plasma concentration. The handling and processing of blood samples were the same as in the IV group.

Table 11. Experimental groups of the PK study in rats.

Group	Route	Vehicle	Nominal dose level
1a	IV: Solution	Propylene glycol / Kolliphor HS 15 / PBS pH 7.4	36 mg/kg
1b	IV: Solution	PEG 400 / PBS pH 7.4	18 mg/kg
2	PO: Solution	PEG 200	36 mg/kg
3	PO: Suspension in PBS pH 7.4	Povidone	36 mg/kg
4	PO: Suspension in PBS pH 7.4	Copovidone	36 mg/kg
5	PO: Solution	PEG 200	500 mg/kg
6	PO: Solution	PEG 200	1000 mg/kg

4.7.4 Studies for the Species Dog

The PK evaluation in dogs was conducted at Aurigon Toxicological Research Center Ltd (ATRC, Dunakeszi, Hungary) in compliance with the Directive 210/63/EU and amendments on the approximation of laws, regulations and administrative provisions of the Member states regarding the protection of animals used for experimental and other scientific purposes. A total of four beagle dogs were used for the PK study. In contrast to the mouse, jird and rat studies, all treatments were conducted with the same animals and a six-day washout period between every session was kept. An IV administration of CorA solution was performed by using the vehicle propylene glycol, macrogol-15-hydroxystearate and PBS pH 7.4 (20:4:76, (V/V/V)) at a concentration of 3 mg/mL and a dosing volume of 2.5 mL/kg with a corresponding dose level of 75 mg. Blood samples were withdrawn at 5 min, 15 min, 30 min, 45 min, 60 min, 2 h, 4 h, 8 h and 24 h. Approx. 3 mL blood was collected via the vena cephalica antebrachii and centrifuged at 3,000 G at 4 °C for 10 min within 60 min after collection. The supernatant was used for HPLC analysis and quantification of CorA in plasma (**Chapter 4.2**). The remaining study groups received oral formulations comprising CorA-PEG 200 solution, granulated CorA-povidone and CorA-copovidone, each filled in enteric capsules, CorA-povidone and CorA-copovidone tablets and a suspension of mesoporous silica in water. The solution and the suspension were administered via an oral gavage, the capsule and tablets were administered via a disposable plastic feeding tube (B. Braun Levin tube CH18) and disposable plastic syringe

(B. Braun Omnifix 50 mL with catheter tip). The capsules were administered in both fasted and fed state. The other study groups were treated in fasted state. On treatment days, fasted animals (at least 16 h) were treated and food was distributed approx. 2 h after treatment. For groups investigating the fed state, high-fat dog food (crude fat content: approx. 30%) was offered approx. 1 h before the treatment. Approx. 0.5 h later, the remaining food, if any, was taken away. The dose level for the capsules was 75 mg, for tablets 100 mg (two tablets per administration) and for the mesoporous silica suspension 200 and 100 mg/kg, respectively. Blood sampling points were 45 min, 60 min, 1.25 h, 1.5 h, 2 h, 3 h, 4 h, 8 h and 24 h. The handling and processing of blood samples were the same as in the IV group. **Table 12** summarizes the study groups.

Table 12. Experimental groups of the PK study in Beagle dogs.

Group	Route	Vehicle	Nominal dose level	Pentagastrin pre-treatment
1	PO: Solution	PEG 200	75 mg	No
2	PO: Enteric Capsule	Povidone, fasted	75 mg	Yes
3	PO: Enteric Capsule	Copovidone, fasted	75 mg	Yes
4	PO: Enteric Capsule	Povidone, fed	75 mg	Yes
5	PO: Enteric Capsule	Copovidone, fed	75 mg	Yes
6	PO: Suspension	Mesoporous silica, fasted	200 mg/kg	No
7	PO: Suspension	Mesoporous silica, fasted	100 mg/kg	No
8	PO: Sustained release Tablet	Povidone / HPMC, fasted	100 mg	Yes
9	PO: Sustained release Tablet	Povidone / HPMC, fasted	100 mg	Yes
10	IV: Solution	Propylene glycol / Kolliphor HS 15 / PBS pH 7.4	75 mg	No

4.8 Preclinical Toxicology Investigation of CorA

Part of the preclinical investigation of CorA was a toxicologic evaluation. Rats and dogs were chosen as a rodent and a non-rodent species. For both, respective dose levels were derived from preliminary maximum tolerated dose (MTD) studies. The present 7-day

studies represent an exploratory approach guiding the dose finding for the Good Laboratory Practice (GLP) toxicology study. The studies were conducted at the Aurigon Toxicological Research Center Ltd (ATRC, Dunakeszi, Hungary) in compliance with the Directive 210/63/EU and amendments on the approximation of laws, regulations and administrative provisions of the Member states regarding the protection of animals used for experimental and other scientific purposes. Beside toxicological findings, e.g., clinical signs or clinical chemistry parameters, a toxicokinetic evaluation was performed. As toxicological studies require high dose levels, it is important to assess PK in order to connect potential side effects to drug exposure or maximum plasma concentration. Thus, on day 1 of the toxicological study plasma samples were withdrawn for a toxicokinetic evaluation. The study durations were seven treatment days.

4.8.1 Toxicology Study in Rats

The rats (Wistar) were housed in cages with three animals per cage and after catheterization individually. The cages were placed in a humidity and temperature-controlled room with an artificial light/dark cycle of 12 h. Food (rodent diet food) and tab water were delivered ad libitum. A total of 50 animals (25 males and 25 females) were treated within the studies. The animals were divided into three dosing groups (vehicle control, low dose: 250 mg/kg and high dose: 1000 mg/kg), while in the low and high dose groups 10 animals were investigated in terms of toxicology and 8 animals for toxicokinetic, respectively. PEG 200 solution was used as oral toxicology vehicle at concentrations of 50 and 200 mg/mL and a dosing volume of 5 mL/kg. The vehicle control group assessed potential effects caused by the vehicle. Blood samples of the toxicokinetic groups were withdrawn after 15 min, 30 min, 60 min, 2 h, 4 h following an alternating sampling schedule. Each rat was bled four times. Approx. 0.25 mL blood was collected via the lateral tail vein and centrifuged at 2,000 G at 4 °C for 10 min within 60 min after collection. If necessary, samples were temporarily stored in an ice-water bath. The supernatant was used for HPLC analysis and quantification of CorA in plasma.

Viability and mortality were examined twice a day. Once signs of toxicity were noted, animals were isolated and observed more frequently. From the outside perceptible observations were focused on soft feces, coat, posture, breathing and excessive chewing or drinking.

4.8.3 Toxicology Study in Dogs

The dogs (Marshall Beagles) were housed in humidity and temperature-controlled rooms with an artificial light/dark cycle of 12 h. Food (SQC diet for dogs) and tab water (as for human consumption) were offered ad libitum. On treatment days, fasted animals (at least 16 h) were treated and food was distributed approx. 2 h after treatment. A total of 16 dogs (eight males and eight females) were treated within the studies, which were divided into four dosing groups (vehicle control, low-dose: 150 mg/kg, middle-dose: 450 mg/kg and high-dose: 750 mg/kg). Each treatment group was composed of two male and two female animals. The animals were treated with the CorA-silica formulation (**Chapter 4.3.5**), which was suspended immediately before administration in a 1%- NATROSOL® solution. For each group the administration volume was 8 mL/kg and the suspension was administered via an oral gavage. For the vehicle control group, the amount of silica correlated to the high-dose group of 750 mg/kg. This means that the dogs were treated with 750 mg/kg silica, e.g., a 6 kg dog received 4,500 mg silica per administration. At the first day of the toxicology study blood samples were withdrawn after 0.5 h, 1 h, 2 h, 4 h, 6 h, 8 h and 24 h for the toxicokinetic evaluation. Approx. 3 mL blood was collected via the vena cephalica antebrachii and centrifuged at 3,000 G at 4 °C for 10 min within 60 min after collection. If necessary, samples were temporarily stored in an ice-water bath. The supernatant was used for HPLC analysis and quantification of CorA in plasma.

During the treatment days clinical observations were carried out at least once a day with special regard to behavior, skin and coat, urine and fecal excretion, lymph nodes, mucous membranes, eyes, oral cavity and any signs of illness. In addition, body weights and food consumption were recorded daily as an indication of physical impairment.

4.9 *In Silico* PK Predictions of CorA

4.9.1 Input Data Source

Data describing the physicochemical properties and the physiological conditions such as ADMET properties of CorA were obtained from *in vitro* studies and from estimates predicted from the ADMET Predictor software (AP) (version 10.4, Simulations Plus, Inc., Lancaster, CA, USA). For *in silico* predictions, the chemical structure of CorA was built using the incorporated MedChem Designer and integrated to the software. A number of

physicochemical properties of CorA, including molecular weight, pKa, logP and pH dependent solubility have been previously published [108,109].

4.9.2 Physiologically based PK modeling

Plasma concentration-time profiles for CorA formulations were simulated using the PBPK modeling software GastroPlus™ (versions 9.8.3, Simulations Plus, Inc., Lancaster, CA, USA). Data describing the physicochemical properties and the physiology of the investigated species were obtained from *in vitro* studies and from predictions from the AP. Prediction errors (PE) for the PK parameter C_{max} an AUC_{0-inf} were calculated using **Eq. 5** [128].

$$\%PE = \frac{observed\ value - predicted\ value}{observed\ value} \cdot 100 \qquad \textbf{(5)}$$

4.9.2.1 Preclinical Mouse model

First simulations in the preclinical species mouse were based on an immediate-release suspension as the dosage form. In the following, dissolution results were incorporated to the model via Weibull parameters calculated from the monophasic dissolution setup (**Chapter 4.5.3**). The percentage of released dose is described in **Eq. 6** [124].

$$\%Dose\ Released = Max\left(1 - e^{\left(1 - \frac{-(t-T)^b}{A}\right)}\right) \qquad \textbf{(6)}$$

where Max = maximum of released API, T = time lag, b = shape factor of the curve and A = time scale. For PBPK modelling, the observed PK data of oral administration of ASD formulations administered as an aqueous suspension were used from PK studies in mice. The IV data provided the elimination and distribution kinetics of CorA. Fed state was assumed due to the free food access of the mice. A detailed summary of the input parameters is provided in the Results and Discussion part.

4.9.2.2 Physiologically based Biopharmaceutic Model

The physiologically based biopharmaceutic model (PBBM) was built using the physicochemical and biopharmaceutical properties of CorA, measured *in vitro* or predicted *in silico*, combined with data obtained from the literature. Validation of the PBBM based on preclinical *in vivo* data. The obtained cross species model was used for a transfer to human with the aim to predict human PK performance and to estimate the

efficacious dose. As this bottom-up approach displayed a consecutive model building using input parameters resulting from *in vitro, in silico* and *in vivo* experiments, a detailed summary and description of the model is provided in the Results and Discussion part [129].

4.10 Cell Culture Experiments with Regard to the Active Efflux of CorA

Interactions with efflux transporters were studied in collaboration with the working groups of Professor Wiese and Professor Lamprecht. Sahel Vahdati performed the cell culture experiments and was responsible for data curation and visualization.

For the *in vitro* investigation of the interaction of CorA with potential transporter, present in the human gut membrane, P-glycoprotein (P-gp) and the breast cancer resistance protein (BCRP) were investigated. MDCK II parental and the transfected cell lines which overexpress P-gp (MDCK II MDR1) or BCRP (MDCK II BCRP) were used. The cells were a generous gift from Dr. A. Schinkel (The Netherlands Cancer Institute, Amsterdam, The Netherlands). The cells were cultured and kept in Dulbecco's Modified Eagle's Medium enriched with 10% fetal bovine serum, 2 nM L-glutamine, 50 µg/mL streptomycin and 50 U/mL penicillin G. The cells were stored in a humidified incubator at 37 °C exposed with 5% CO_2. After the cells reached a confluence of approximately 90% sub-culturing was performed by detaching the cells by the addition of 0.05% Trypsin and 0.02% EDTA. After centrifugation (4 min at 266 G and 4 °C) the supernatant was removed and the cell pellet was re-suspended in fresh medium. The cells were washed twice with PBS and then counted using a CASY1 model TT equipped with a 150 µm capillary (Schaerfe System GmbH, Reutlingen, Germany).

4.11.1 Investigation of Active Transport via P-GP and BCRP

To identify potential active intestinal transport CorA was exposed to MDCK II parental, MDCK II MDR1 and MDCK II BCRP cells. The amount of accumulated CorA in the single cells was determined. The cells were prepared as described in **Chapter 4.10** and suspended at a final cell density of 250,000 cells/mL together with CorA at different concentrations (0.25, 0.5, 0.75 and 1 µM). Incubation was performed for 1 h at 37 °C and 5% CO_2. After reaching the intra- and extracellular concentration equilibrium, single cell fluorescence was measured on the Red/V channel using a Guava easyCyte 8HT flow

cytometer. Differences in fluorescence intensities of parental and overexpressing cells indicated potential efflux of CorA resulting in different amounts of accumulated CorA. Conversely, similar fluorescence intensities indicated no interaction.

4.11.2 Investigation of the Interaction with the P-gp Inhibitor HOECHST 33342

A potential interaction with a well-known P-gp inhibitor was investigated. Therefore, HOECHST 33342 as a fluorescent substrate of P-gp showing an increase in fluorescent intensity when bound to DNA or embedded in a lipophilic environment like the cell membrane [130]. The effect of CorA on the transport of Hoechst 33342 was investigated using MDCK II MDR1 cells by treating two different CorA concentrations (3.16 and 10 µM) together with varying concentrations of HOECHST 33342 (1, 1.5 and 2 µM). Control experiments were conducted by assessing the transport of HOECHST t 33342 in the absence of CorA. The fluorescence was measured with a POLARstar microplate reader (BMG Labtech, Offenburg, Germany) in constant 1 min intervals up to 60 min, at an excitation/emission of 355/460 nm. The association kinetic of interaction between Hoechst 33342 and P-gp with and without CorA was analyzed using a one-phase association fit (data were analyzed using GraphPad Prism, version 8.0, San Diego, CA, USA).

4.11 Statistics

Mean values, standard deviations (SD) and the median values with interquartile ranges were calculated using Microsoft Excel® (Microsoft Office Professional Plus 2019, Microsoft®, Redmond, WA, USA). GraphPad Prism (Version 8.02; GrapPad Software, Boston, MA, USA) was used for statistical models by applying a one-way analysis of variance (ANOVA) with a significance level of $\alpha = 0.05$.

5. Formulation Development and Characterization of Solid Oral Drug Products of CorA

Antibiotics often lack sufficient oral BA, resulting in low plasma levels and concentrations at the target site below the minimal inhibitory concentration (MIC) that is required to deplete the respective pathogens. However, PO administration is the intended route of administration for CorA in humans as parenteral administrations in the outpatient setting are linked with higher effort for physicians and lower patient compliance, especially in the *Wolbachia*-threatened sub-Saharan regions. Nevertheless, in 2019, 43% (175 projects) of novel antibiotics in the pipeline were formulated for parenteral use and only 10% (41 projects) for oral use [101,131,132]. To develop suitable formulations for the API CorA, a comprehensive analysis and understanding of the factors contributing to CorA absorption and BA, as neat CorA and in different formulations, were, therefore, of utmost importance. Krome et al. already established the ASD formulation principle to be a promising approach to overcome stability, solubility and handling issues of CorA [108,109]. Spray drying was established for manufacturing of the ASDs and enabled first *in vitro* formulation experiments and *in vivo* PD and PK studies. Even though, handling properties of neat CorA were immensely improved, the particles still lack in flowability due to typical small particle sizes resulting from the small-scale spray drying process. For CorA these particles represented intermediates, suitable for preclinical investigations, however, further downstream processes were required to provide appropriate candidates for clinical studies in human and a potential regulatory approval.

Drug release kinetics influence the PK characteristics. While immediate release cause higher and shorter plasma concentrations, a sustained release kinetic aims to decrease C_{max} and prolong the time of therapeutic relevant concentration. Reasons for sustained release include: A short API $t_{1/2}$, the need for maintaining the effective dose at the target site over a period of time or the need to avoid high peak concentrations that may lead to toxic effects. If an effect is attributed to high peak concentrations, an immediate release would be rather beneficial. For CorA it has been assumed that the longer the concentration is kept above the MIC, the more successful the anti-infective effect of CorA. Although, early clinical phase studies focusing on PK and tolerability, establishing a

potentially sustained release formulation might accelerate the future clinical development.

The following work focused on the downstream processes of the spray dried particles to develop candidates for solid oral drug products. Due to limited drug substance amount, processes were implemented using acetaminophen as model API. The goal was to provide both, immediate and sustained release dosage forms as options for initial clinical studies. As tablets and capsules are the most common solid oral drug products, these two options were considered.

5.1 Results and Discussion

5.1.1 Influence of Particle Size Distribution on Processability – Spray Dried Intermediates

After spray drying both ASD intermediates showed small particle sizes resulting in a median (d_{50}) of 12.65 µm for CorA-povidone and 10.83 µm for CorA-copovidone. Comparing both ASD particles, either the d_{50}, as well as, the finest (d_{10}) and coarsest (d_{90}) parts of the distribution were in the same range resulting in a narrow distribution (span of approx. 1). Due to the fine particles the intermediates exhibited poor powder flow, impeding further processing into capsules or direct tablet compression. However, small particle sizes suggest faster dissolution rates caused by increased surfaces [29,30]. These intermediates allowed *in vitro* experiments and *in vivo* oral PK and efficacy studies in mice, jirds and rats. In terms of solid oral drug products, the spray dried products served as starting point for further downstream processes to improve flowability by increasing the particle size which allows the manufacturing of tablets or capsules.

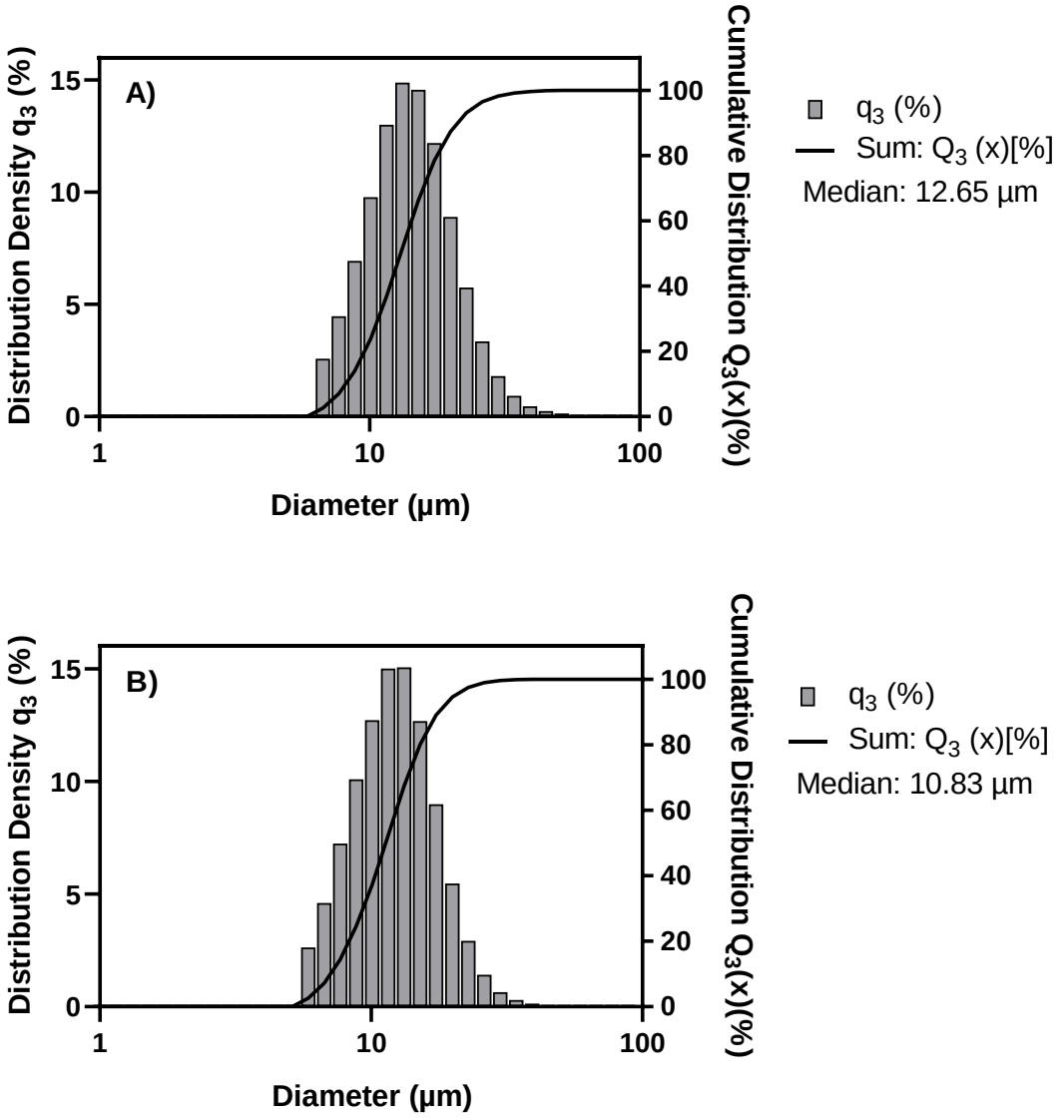

Figure 7. Particle size distribution of the spray dried ASDs. A) CorA-povidone; B) CorA-copovidone.

Table 13. Percentiles (d_{50}, d_{10} and d_{90}) of the spray dried ASDs determined after particle size distribution assessment. A) CorA-povidone; B) CorA-copovidone.

Formulation	d_{50} (µm)	d_{10} (µm)	d_{90} (µm)	Span
CorA-povidone	12.65	7.93	21.03	1.04
CorA-copovidone	10.83	6.84	17.48	0.98

5.1.2 Residual Solvent after the Spray-Drying Process– Gas Chromatography

Ethanol is classified as a solvent with low toxic potential resulting in a ICH concentration limit of 5000 ppm [112]. GC measurements were performed to confirm compliance with this limit and to examine the drying efficiency. After the spray drying process, a subsequent drying step was established (24 h at room temperature under vacuum) to remove residual solvent as far as possible. The measurements demonstrated that both formulations were far below the limit of 5000 ppm showing 244 ppm for CorA-povidone and 178 ppm for CorA-copovidone. Consequently, the spray drying process was able to generate products that fulfil the ICH guidelines and requirements for the final drug product.

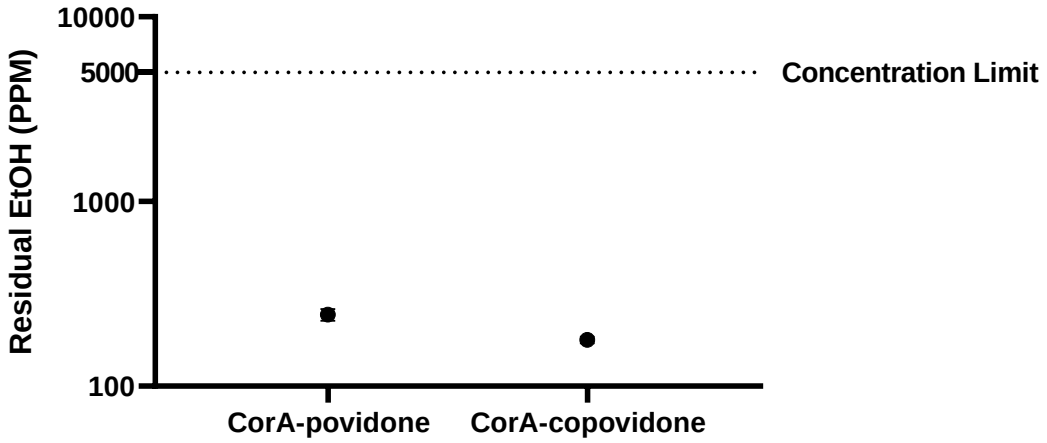

Figure 8. Results of residual solvents determination of the ASDs after spray drying; n=3 (mean ± SD).

5.1.3 Morphology of the Spray-Dried CorA-ASDs - Microscopy

Scanning electron micrographs (SEM) (**Figure 9**) were taken to get insights into particle morphology and to verify the particle sizes of the intermediates measured by laser diffraction. The spray dried CorA-povidone showed different shapes, spherical, as well as, collapsed particles. In contrast, CorA-copovidone showed solely spherical particles. For both, diameters of the measured d_{50} of approx. 10 µm were confirmed, tending to form agglomerates. In general, the particle morphology is able to influence flow characteristics and surface area that is an important factor for the dissolution rate [133,134]. Even though, drug release is expected to be influenced by several parameters the more irregular surface of the CorA-povidone indicated a higher dissolution rate compared to the spherical CorA-copovidone particles. Approx. two-fold higher intrinsic dissolution rates were determined for neat povidone compared to neat copovidone by Chen et al.

(povidone (K30): 15.8 mg/min/cm²; copovidone: 8.1 mg/min/cm²) [135]. Likewise, the faster intrinsic dissolution rate of povidone led to faster dissolution rates of spray dried ASDs comprising the API ketoconazole with a drug load of 20% resulting in 11.8 mg/min/cm² of ketoconazole in a povidone-based ASD and 6.8 mg/min/cm² in a copovidone-based ASD [135]. These results supported the hypotheses made for CorA-ASDs.

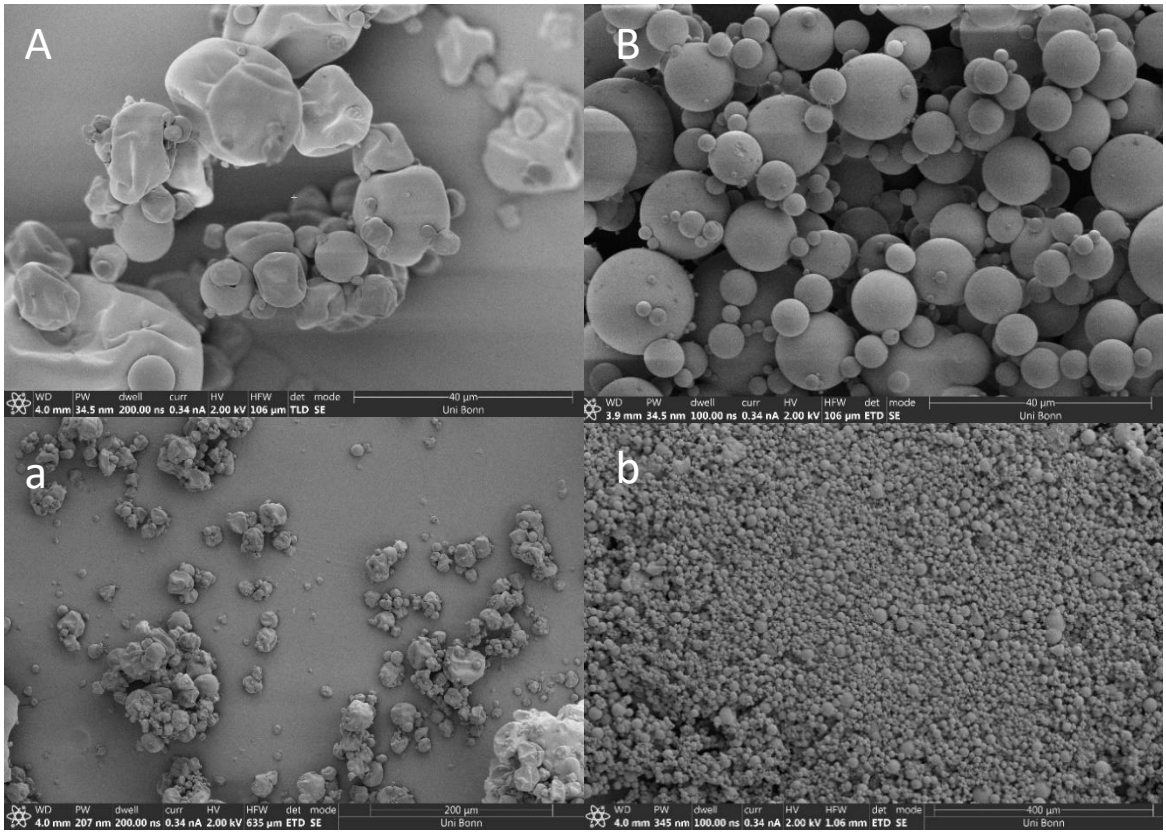

Figure 9. SEM images of spray dried ASD particles. A, a: CorA-povidone; B, b: CorA-copovidone.

5.1.4 Provision of CorA Solid Drug Product Prototypes

Dose estimates are critical challenges during preclinical investigations [136,137]. Body surface conversion tables are established for a first assumption of equivalent dose levels [112]. For CorA, the conversion of an efficacies dose of 30 mg/kg in jirds resulted in an estimated dose of 7.3 mg/kg for the species dog. As dogs were the intended species for an initial PK study for the oral drug products and typically have a body weight up to 10 kg, the targeted absolute dose was set at 75 mg (corresponding to 7.5 mg/kg for 10 kg beagle dog) of CorA. Preliminary studies with acetaminophen as “dummy” drug were performed due to limited availability of CorA drug substance. It was chosen as comparable characteristics to CorA in T_g could be demonstrated (**Figure 10**) and the dissolution

kinetics were not solubility limited. The aim was to set manufacturing parameters without consuming valuable grams of drug substance. Thus, the spray dried dummy-ASD with the polymer povidone was granulated via dry granulation in accordance to the method described in **4.3.2**, classified into sieve fractions and manually filled into HPMC capsules, size 0, until the respective maximum was achieved. **Figure 11** shows dissolution profiles of the different particle sizes and **Table 14** summarizes the maximum quantity fillable in a capsule size 0, dependent on the respective particle size.

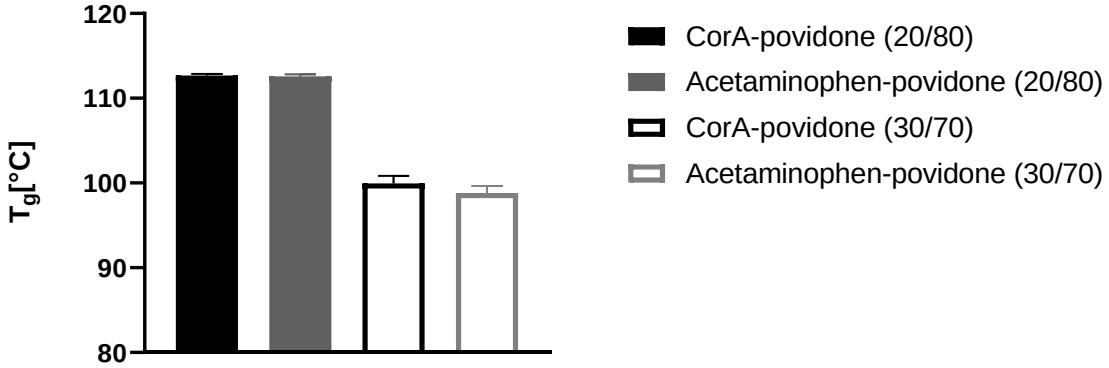

Figure 10. Comparison between the T_gs of spray dried CorA-povidone and acetaminophen-povidone investigating the drug loads 20% and 30%.

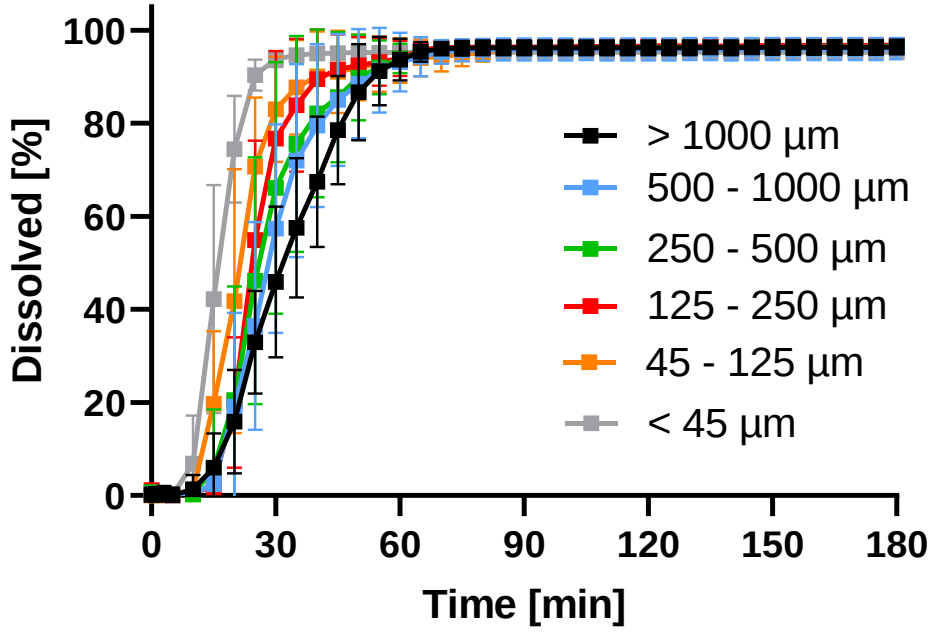

Figure 11. USP II dissolution of different sieve fraction of acetaminophen-povidone ASD in phosphate buffer (0.05 M) pH 6.8; drug load 20%; dissolution volume: 900 mL, paddle speed 75 RPM, 37 °C.

Table 14. Maximum amount of ASD that can be filled into a capsule size 0, dependent on the particle size. The corresponding CorA quantity was calculated based on an ASD drug load of 20%.

Particle size (µm)	Capsule content ± SD (mg)	Corresponding CorA amount ± SD (mg)
x > 1000 µm	429.3 (13.9)	85.9 (2.8)
1000 µm > x > 500 µm	446.3 (11.8)	89.3 (2.4)
500 µm > x >250 µm	449.7 (9.0)	90.0 (1.8)
250 µm > x > 125 µm	411.3 (2.9)	82.3 (0.6)
125 µm > x > 45 µm	288.4 (14.7)	57.7 (2.9)
x < 45µm	217.9 (18.6)	43.6 (3.7)

Particle sizes < 125 µm were not suitable to reach the required dose of 75 mg within one capsule size 0. By exceeding the particle size of 125 µm, the bulk density increased to such an extent that the targeted dose level could be achieved. Moreover, powder flowability is affected by particle properties, such as particle size [138]. In principle, the larger the particle, the better the flow, relevant for tableting processes. Regarding the dissolution rate, the profiles (**Figure 11**) demonstrated that the smaller the particle size the faster the dissolution rate. Consequently, the sieve fraction of 250 µm > x > 125 µm was selected as it showed a fast dissolution and resulted in a high enough bulk density to enable the required absolute dose of 75 mg CorA in one capsule. Moreover, the increase in particle size of the spray dried intermediates led to improved flow properties, which allowed easier manual capsule filling, as well as, the option for a subsequent tableting process. Manual granulation and sieving resulted in a d_{50} of 237.41 µm, a d_{90} of 403.87 µm and a d_{10} of 132.24. Laser diffractometry (**Figure 12**) demonstrated a bimodal distribution with a small fine fraction > 50 µm indicating a successful granulation and sieving process.

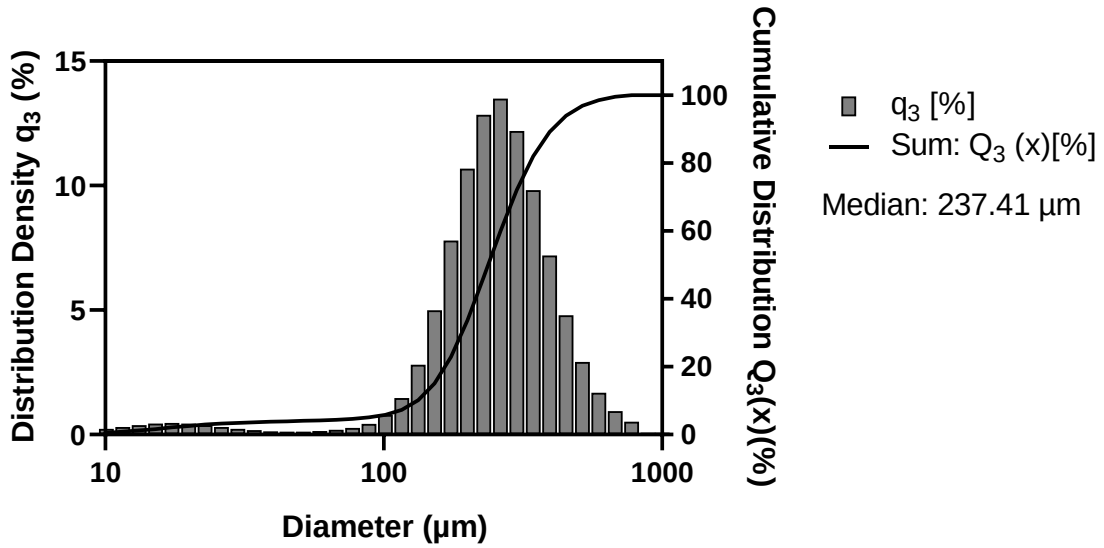

Figure 12. Particle size distribution of the spray dried acetaminophen-povidone ASD of the sieve fraction 125-250 µm.

To verify the results observed with the dummy formulation, capsules were produced comprising CorA-povidone-ASD instead of acetaminophen-ASD. The ASD candidate CorA-povidone was investigated regarding the dissolution performance. To this end, the granulated CorA-ASD was filled into a standard HPMC capsule, as well as, in enteric capsules. The enteric capsules were chosen as an option to eliminate potential acid induced isomerization in the acidic environment present in the stomach. The dissolutions for both capsule types were performed at a constant pH of 6.8 (**Figure 13A**). In addition, for the enteric capsule a setup was performed starting at pH 1 (0.1 N HCl) followed by a pH-shift to pH 6.8 after 30 min by adding McIlvaine buffer concentrate (**Figure 13B**) [83,122].

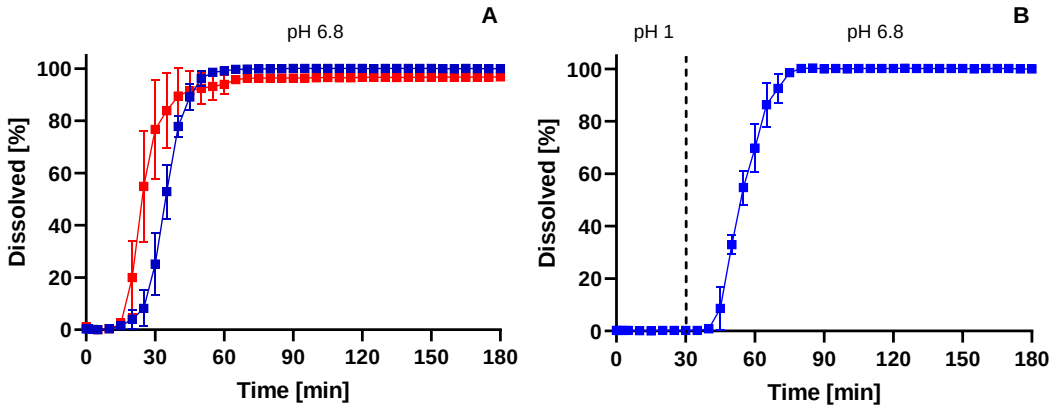

Figure 13. USP II dissolution of capsule formulation of acetaminophen-povidone ASD (■) and enteric capsule formulation of CorA-povidone ASD (■). **A**: Medium: phosphate buffer (0.05 M) pH 6.8; dose: 75 mg; dissolution volume: 500 mL, paddle speed 75 RPM, temperature: 37 °C. **B**: Medium: 0.1 N HCl (0-30 min), citrate-phosphate buffer pH 6.8 (30-180 min); dose: 75 mg; dissolution volume: 500 mL, paddle speed 75 RPM, temperature: 37 °C.

Despite higher solubility of acetaminophen compared to CorA the dissolution kinetics of both ASDs were comparable indicating enhanced dissolution properties for the CorA-ASD (**Figure 13A**). The dissolution experiment with a pH-shift (**Figure 13B**) indicated the same kinetics, delayed by a corresponding lag time. During the first 30 min (pH 1) no CorA was released confirming a successful enteric effect of the capsules. After the pH-shift to pH 6.8 a fast disintegration of the capsule and fast dissolution process of CorA were observed. No increased isomerization was detected using enteric capsules.

By using this “dummy” approach, it was possible to investigate the dissolution properties as well as developing manufacturing parameters for CorA-ASDs. Thus, a rational resource saving development approach was found consuming less than 1 g drug substance.

5.1.5 Selection of a Suitable Sustained Release Approach for Oral Administration of CorA

HPMC based matrix tablets were used as sustained release principle. No further excipients were used to keep the drug load of the tablets as high as possible. Tablet size and geometry were specified as 12x8 mm biconcave with a cup radius of 10.4°, acceptable for administration in dogs. Release profiles were tested in a USP II apparatus at pH 6.8, assuming no solubility limitation, as has been already demonstrated for the capsule formulations. The initial dissolution rate was observed to be similar between CorA-povidone and CorA-copovidone based tablets. During the dissolution experiment (7.5 h)

a constant dissolution rate, following a zero-order kinetic, was obtained for CorA-povidone achieving a C_{max} of 84% (corresponding to 0.084 mg/mL). The initial linear increase of CorA-copovidone decreased after approx. 2 h rather close to a first-order release kinetic. Despite no zero-order kinetics were obtained, a slower dissolution rate compared to capsules indicated its sustained release potential. The difference between the two tablets was the fraction of HPMC in the tablet as the HPMC quantity of CorA-povidone was 20% and for CorA-copovidone 10%. However, the percolation threshold for HPMC is reported to be 20% (w/w) [139]. This means, below this concentration, the system is not likely to form a fully coherent gel layer that is responsible for release control. Due to this failure the drug would be predominantly released by erosion. The lower amount of HPMC for CorA-copovidone was selected, as preliminary studies suggested a too slow dissolution using 20% of HPMC. Thus, the HPMC amount was below the percolation threshold which resulted in the first order dissolution kinetic. Nevertheless, it was possible to extend the dissolution process to 7.5 h. In contrast, the HPMC amount of the CorA-povidone tablet (20%) was high enough to fulfill the percolation threshold confirmed by the observed dissolution profile.

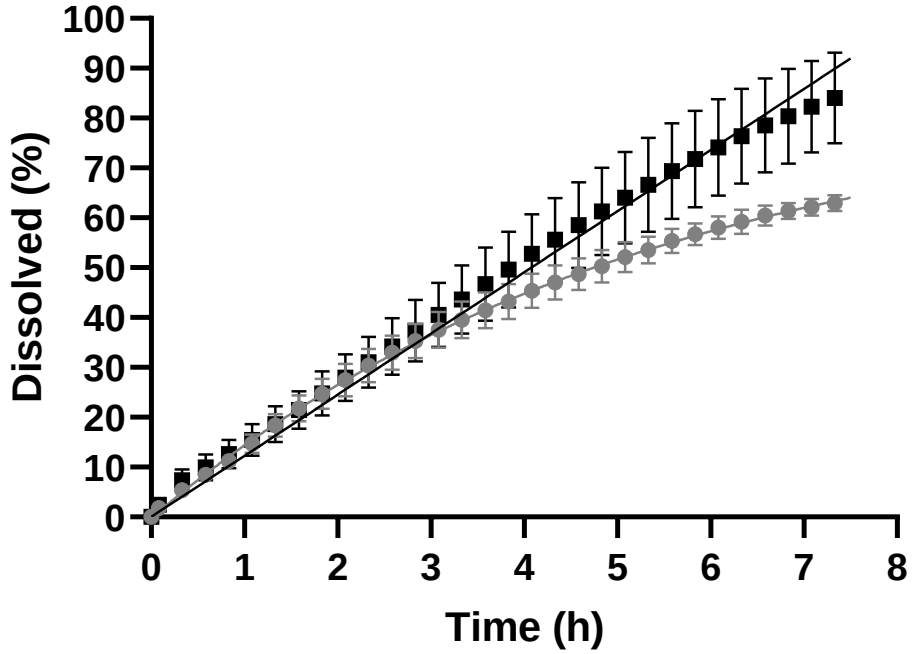

Figure 14. USP II dissolution of CorA-povidone/HPMC (■) and CorA-copovidone/HPMC (■) in phosphate buffer (0.05 M) pH 6.8; drug load: CorA-povidone/HPMC 18%, CorA-copovidone/HPMC 16%; dose: 50 mg, dissolution volume: 500 mL, paddle speed 75 RPM, 37 °C. The black line represents the zero-order kinetic fit for CorA-povidone/HPMC and the grey line represents the first-order kinetic fit for CorA-copovidone/HPMC.

5.1.6 Influence of Intestinal pH and Bile Salts - Biorelevant Solubility of CorA and CorA-ASD Formulations

The pH-dependent solubility of CorA was recently published [108]. Dissolution experiments indicated a solubility improvement by using the ASD formulation principle. To assess the extent of improvement the solubilities of neat CorA and CorA-ASD formulations were investigated in biorelevant media such as FaSSIFV2, FeSSIF-V2, FaSSIF-V2-mouse and FeSSIF-V2-mouse media (**Table 15**). These two setups were chosen to identify potential species-specific differences regarding solubility as different pH-profiles are present in mice and humans. Since no appropriate test media mimicking the gastrointestinal conditions of mice are described in literature, human FaSSIF-V2 and FeSSIF-V2 were adjusted to the reported mouse pH in a fed state similar to the procedure applied by the GastroPlus PBPK software. Sampling points were chosen to determine the initial solubility after 2 min in comparison with the solubility after the small intestinal transit (human: 4 h; mouse: 1 h). In both media representing the human gut conditions

(**Table 15A and B**), the initial dissolved amount of the CorA-ASD formulations (CorA-povidone: 1.09/1.06 mg/mL; CorA-copovidone: 0.96/0.67 mg/mL) were significantly higher (CorA-povidone: $p < 0.0001$; CorA-copovidone: $p < 0.0001$) than those of neat CorA (0.00/0.00 mg/mL) confirming the fast dissolution rate of the ASDs. The low initial value for neat CorA can be explained by the waxy consistency of CorA that leads to a low surface area and therefore, to a slow dissolution rate. No significant difference was detected between the ASD formulations in FaSSIF-V2 ($p = 0.8876$). However, in case of the simulated fed state, CorA-povidone exhibited a significantly higher amount dissolved after 2 min ($p < 0.0001$). Moreover, the ASD formulations achieved high solubility values of CorA-povidone: 1.24/0.94 mg/mL and CorA-copovidone: 1.40/0.93 mg/mL for at least 4 h. Despite at least a 10-fold increase of the solubility compared to the pH-dependent solubility, e.g., 0.091 mg/mL at pH 6.5, the ASDs were able to keep the CorA in solution. The biorelevant solubilities for CorA-ASD formulations were also measured in FaSSIF-V2-mouse and FeSSIF-V2-mouse media (**Table 15C and D**). While for both media the solubility enhancements of the ASD-formulations were demonstrated (CorA-povidone: $p < 0.0001$; CorA-copovidone: $p < 0.0001$) the solubility in FaSSIF-V2-mouse media showed lower values after 2 min (CorA-povidone: 0.11 mg/mL; CorA-copovidone: 0.09 mg/mL) when compared with the FeSSIF-V2-mouse (CorA-povidone: 0.66 mg/mL; CorA-copovidone: 0.45 mg/mL). No dissolved CorA was detected for neat CorA. In FaSSIF-V2-mouse media, a lower concentration for CorA-povidone (0.07 mg/mL) was observed after 1 h, whereas for CorA-copovidone the solubility further increased (0.19 mg/mL). In the FeSSIF-V2-mouse no significant differences were detected after 1 h for either formulation ($p = 0.3080$), indicating no precipitation. For neat CorA, the concentrations after 2 h and 1 h were ≤0.02 mg/mL. Differences between human and mouse media were attributed to the lower pH for the mouse setup. Since the pH conditions in the gastrointestinal tract (GIT) of mice differ drastically from those in humans, the solubilities determined in the mouse setup were used as input parameters for the PBPK modelling of the CorA-ASD formulations in mice.

Interestingly, the biorelevant solubilities of the ASD formulations exceeding the reported pH-dependent solubilities significantly (0.091 µg/mL at pH 6.5). As the solid state of neat CorA is amorphous, the amorphous solubility of CorA-ASDs should not deviate. It was

assumed that the high particle surface area of the spray dried ASD formulations leads to fast dissolving. Lee et al. demonstrated that the dissolution rate is relevant for the extent of supersaturation [60] Moreover, the presence of respective polymer may interact with the dissolved CorA forming liquid colloidal structures [74] and prevent precipitation to amorphous CorA particles for at least 4 h. Further experiments are required to confirm this hypothesis.

Table 15. Solubilities of neat CorA, CorA-povidone and CorA-copovidone ASD formulations over 4 h and 1 h, respectively. A: FaSSIF-V2 medium, pH 6.5; B: FeSSIF-V2, pH 5.8; C: FaSSIF-V2-mouse medium pH 5.2. D: FeSSIF-V2-mouse medium, pH 4.8. n = 3 (mean ± SD).

(A) FaSSIF-V2 pH 6.5 (human)	**Solubility after 2 min (mg/mL)**	**Solubility after 4 h (mg/mL)**
Neat CorA	0.00 (±0.00)	0.25 (±0.06)
CorA-povidone	1.09 (±0.18)	1.24 (±0.04)
CorA-copovidone	0.96 (±0.28)	1.40 (±0.14)
(B) FeSSIF-V2 pH 5.8 (human)	**Solubility after 2 min (mg/mL)**	**Solubility after 4 h (mg/mL)**
Neat CorA	0.00 (±0.00)	0.26 (±0.01)
CorA-povidone	1.06 (±0.02)	0.94 (±0.07)
CorA-copovidone	0.67 (±0.09)	0.93 (±0.05)
(C) FaSSIF-V2-Mouse pH 5.2	**Solubility after 2 min (mg/mL)**	**Solubility after 1 h (mg/mL)**
Neat CorA	0.00 (±0.00)	0.01 (±0.01)
CorA-povidone	0.12 (±0.01)	0.07 (±0.01)
CorA-copovidone	0.09 (±0.01)	0.19 (±0.01)
(D) FeSSIF-V2-Mouse pH 4.8	**Solubility after 2 min (mg/mL)**	**Solubility after 1 h (mg/mL)**
Neat CorA	0.00 (±0.00)	0.02 (±0.01)
CorA-povidone	0.66 (±0.05)	0.54 (±0.01)
CorA-copovidone	0.45 (±0.09)	0.44 (±0.08)

5.2 Summary

The downstream process of the spray dried intermediates was successfully implemented. A resource saving approach for the development of solid oral drug products was established by using acetaminophen as a model drug. Hence, it was possible to provide an enteric capsule formulation and a sustained release tablet formulation as promising prototypes for FIH trials. The spray dried ASDs and the solid oral drug products were planned to be further investigated in preclinical *in vivo* studies and are presented in the following chapters. In addition, differences in biorelevant solubilities were observed indicating a species dependent dissolution process in the respective GITs. Enhanced biorelevant solubilities of the ASD formulations suggested good *in vivo* performances in preclinical species and human.

6. Stability Investigation of Solid Oral Drug Products of CorA

From a regulatory perspective, stability testing of new drug substances and drug products is required for registration and is defined by guidelines [127]. The general aim of this guideline is to shed light on the influence of various factors, such as temperature and humidity and how re-test periods for the shelf life of the drug product must be defined. This should result in appropriate storage conditions to guarantee sufficient physical, chemical, biological and microbiological attributes [127]. The focus of this work was on the physical and chemical stability of a CorA drug product.

The development of a solid oral drug product of CorA is facing the isomerization tendency of CorA. Unfortunately, the efficacy of CorA-isomers was found to be inferior to the parent structure [140]. Even though, no toxic effects were expected regarding CorA isomers, a sufficient and reliable efficacy can only be guaranteed with an appropriate CorA content. According to this, the stability enhanced ASD formulations were investigated in a 12 months stability study. As the enteric capsule formulation is a promising option to be used in a FIH clinical study, these formulations were evaluated regarding CorA content (HPLC-DAD; up to 12 months), physical stability (DSC and Karl-Fischer-titration; up to 6 months) and dissolution performance (USP II and biphasic dissolution; up to 6 months) in order to determine storage conditions required for a sufficient shelf life after manufacturing until the start of a clinical study.

6.1 Results and Discussion

6.1.1 CorA Quantity

In terms of drug substance, batch purity was defined with 90%-95% as the lower acceptance level. The start value of the stability study was set to 100% independent on the batch purity. Previous studies revealed that the isomerization of CorA is favored in presence of oxygen and increased temperatures [108]. Instead of air, nitrogen was used as inert gas for storage. Additionally, desiccant was used to prevent water sorption. By storing the capsules at 5 °C, which represents refrigerator storage, the CorA content remained at 98 ± 4% for CorA-povidone and at 95 ± 5% for CorA-copovidone after 12 months. This indicated a shelf life of at least 12 months (t90% > 12 months) for storage at 5 °C. According to the guideline, the final shelf life will be specified on future real time

data obtained from at least three primary batches of the final drug product [127]. Based on these real time data the shelf life might be prolonged if an extrapolation of the real time data is justified by results of testing under accelerated conditions, goodness of mathematical fit, batch size, etc. [127]. However, increased isomerization predominantly towards CorC was observed at higher temperatures. At 25 °C, the acceptance criteria of 90% was undercut between 6 and 12 months. For CorA-povidone 92 ± 2% and for CorA-copovidone 91 ± 2% were determined after 6 months. A storage up to 12 months further decreased the value to 77 ± 10% for CorA-povidone and 69 ± 6% for CorA-copovidone. Consequently, only 6 months could be guaranteed when the capsules were stored at 25 °C. This tendency continued at 30 °C, as the t90% was not able to reach 6 months (CorA-povidone: 86 ± 3%; CorA-copovidone: 89 ± 1%). At least, after 3 months at 30 °C, values of 97 ± 2% for CorA-povidone and 98 ± 1% for CorA-copovidone could be observed. These results demonstrated that isomerization was catalyzed with increasing temperatures. To guarantee an adequate CorA stability during a potential phase 1 study using the capsule formulation described herein, a storage in refrigerator (5 °C) is recommended. Despite the demonstrated limitations, it has to be outlined that the ASD formulation principle using the polymers povidone and copovidone is a promising approach regarding stability enhancement. Previous studies showed that only 39% of CorA could be detected after 3 months when stored as drug substance under nitrogen at 25 °C. A hypothesis regarding an interaction between CorA and polymer has been proposed [108]. The amid structure, present for both polymers, may interact with the partially positively charged carbocation via Debye forces and therefore, suppress the intramolecular isomerization. Besides, the low T_g of neat CorA (5 °C) indicated molecular mobility at storage temperatures > 5 °C [63]. By increasing the T_g using the polymers povidone and copovidone a reduced molecular mobility, i.e. kinetic stabilization occurred. As CorA-povidone with a T_g of approx. 114 °C showed slightly improved stabilities, especially at 25 and 30 °C compared to CorA-copovidone with a T_g of approx. 82 °C, the kinetic stabilization mechanism is further supported. Providing such stability enhanced formulations was an important milestone during preclinical development. However, the stability of CorA formulations needs to be further improved to simplify supply chains and handling of the drug product for the patient and to enable a successful future market entry.

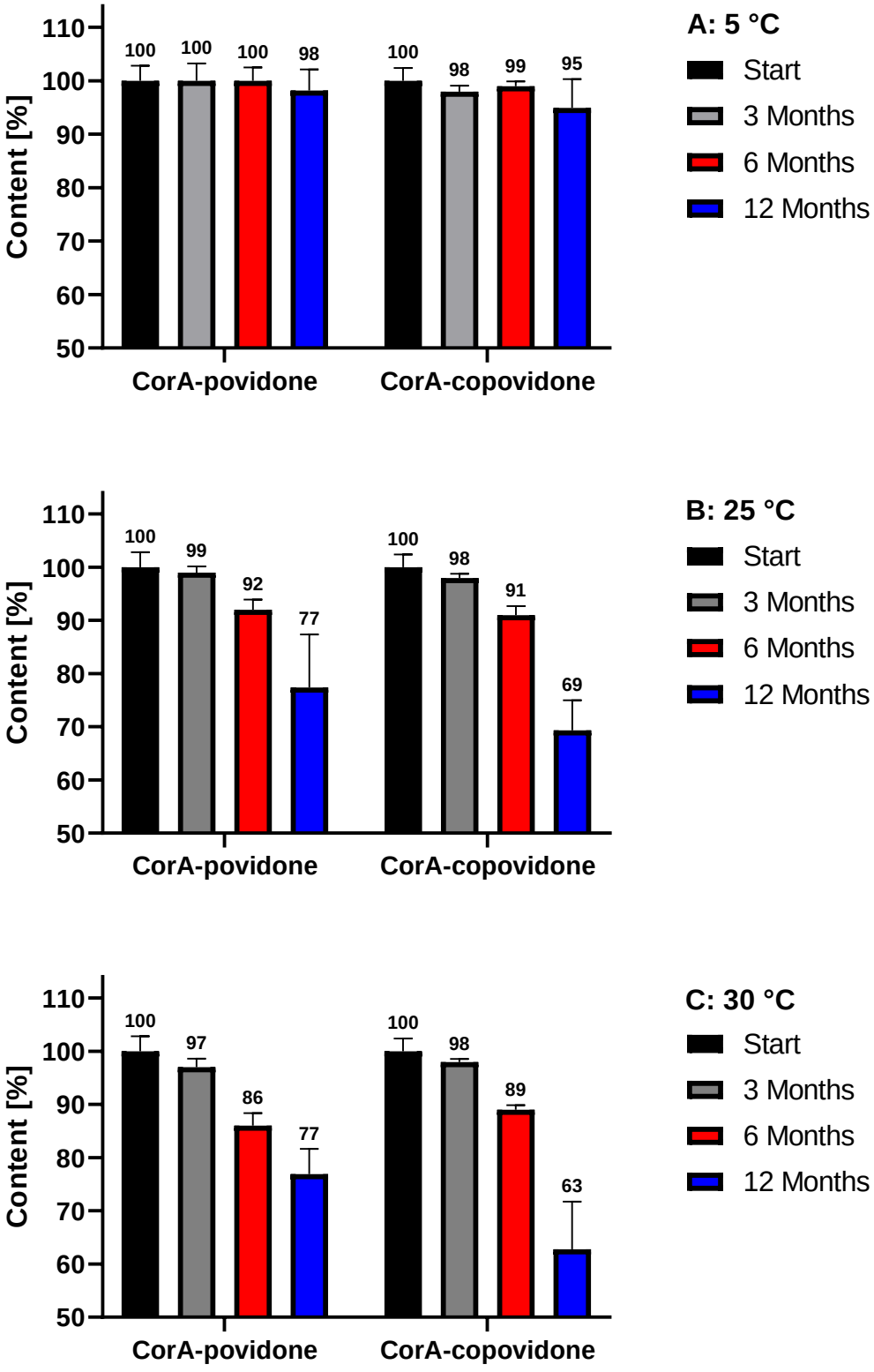

Figure 15. Stability analysis using HPLC-DAD of the capsule formulation CorA-povidone and CorA-copovidone stored in closed Twist Off vials at A: 5 °C, B: 25 °C and C: 30 °C under nitrogen (n=3, mean ± SD).

6.1.2 Phase-Phase Separation During Storage

DSC experiments were performed to examine the T_g of the CorA-ASD formulations. Any changes of the T_g potentially based on phase-phase separations leading to physical instability. Re-crystallinity was excluded a priori due to the permanent amorphous states of the polymers and CorA. No significant differences were observed ($p > 0.9999$) within 6 months of storage independent on storage temperature, indicating a physical stable ASD formulation for both, CorA-povidone and CorA-copovidone. For all DSC measurements, neither additional T_gs nor melting points were detected. In sum, the solid state of both CorA-ASD formulation did not alter, confirming their physical stability.

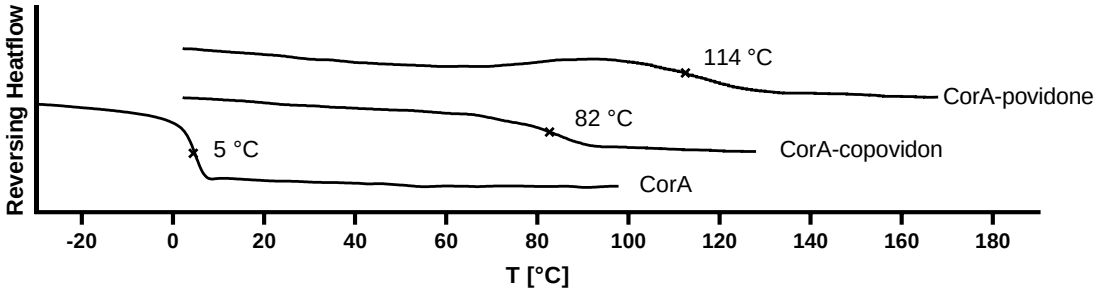

Figure 16. Examples of DSC thermograms of neat CorA (permission to use the data was kindly granted by Krome et al. [108]) and CorA-ASD granules after manufacturing.

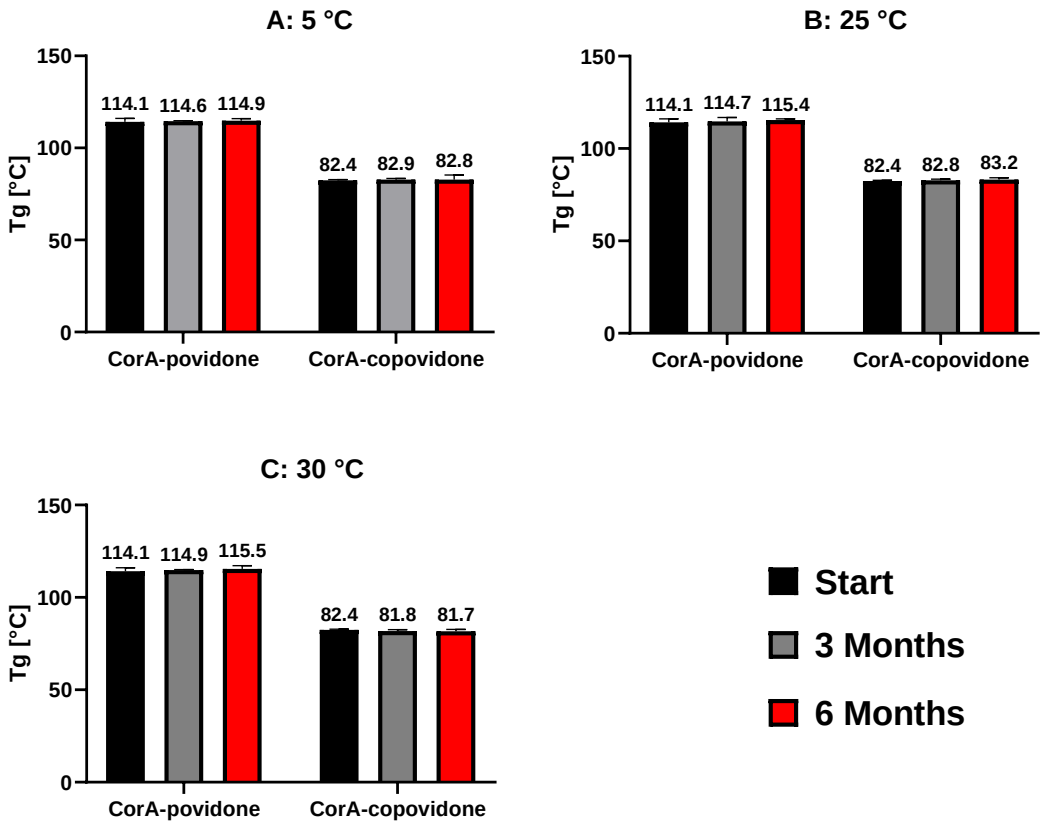

Figure 17. Stability analysis using DSC experiments of the capsule formulation CorA-povidone and CorA-copovidone stored in closed Twist Off vials at A: 5 °C, B: 25 °C and C: 30 °C under nitrogen (n=3, mean ± SD). Approx. 5-7 mg of the capsule contents were withdrawn for DSC analysis.

6.1.3 Water Content

The used polymers tend to have strong (povidone) or moderate (copovidone) hygroscopicity [141]. Furthermore, it is known, that moisture can induce amorphous-amorphous phase separation as moisture might act as a plasticizer. The capsules were stored under nitrogen and desiccant, so that residual moisture was able to be absorbed by the desiccant. As expected, CorA-povidone showed a high-water content of 7.9% after manufacturing, while a lower value of 4.9% for CorA-copovidone was determined. For both ASDs, the water content decreased, pronounced at higher temperatures. Despite no change in solid-states were detected in DSC measurements (**Chapter 6.1.2**), hygroscopicity needs to be considered in manufacturing processes, e.g., by ensuring constant low room humidity conditions and airtight packaging to ensure content uniformity of the final drug products.

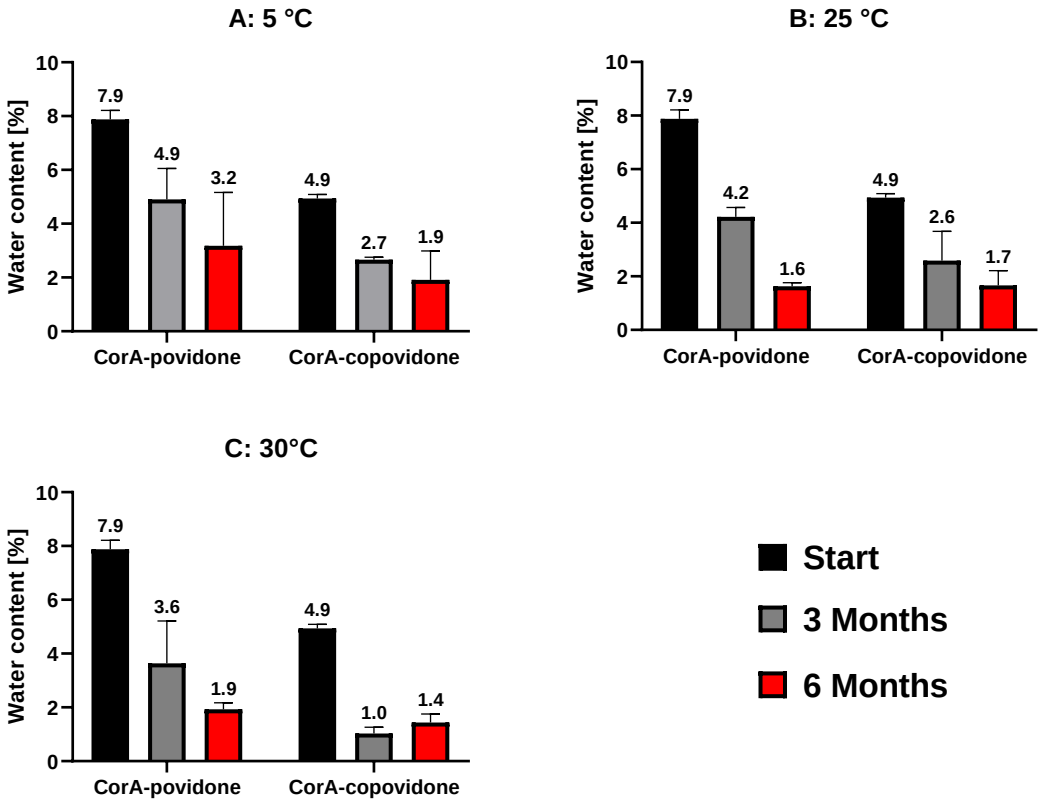

Figure 18. Analysis of the water content using Karl Fischer titration. The capsule formulation CorA-povidone and CorA-copovidone were stored in closed Twist Off vials at A: 5 °C, B: 25 °C and C: 30 °C under nitrogen (n=3, mean ± SD). Approx. 20-30 mg of the capsule contents were withdrawn for Karl Fischer titration.

6.1.4 Influence on Dissolution Performances

6.1.4.1 USP II

The capsules were investigated in a USP II dissolution apparatus at pH 6.8 (500 mL of 0.05 M phosphate buffer). After approx. 15 min both capsules disintegrated followed by a fast dissolution for both formulations. A complete dissolution was achieved for CorA-povidone, corresponding to 0.15 mg/mL, within 60 min. In comparison, CorA-copovidone reached approx. 90% (0.135 mg/mL) after 105 min leading to a slower and slightly lower C_{max} value. As the particle sizes of the granules were comparable after the granulation process, wettability seemed to be a crucial factor for the dissolution rate. Verma and Rudraraju demonstrated increased wetting kinetics and dissolution rates for povidone compared to copovidone [142]. Thus, differences of the ASDs dissolution performances may be caused by the different wetting properties of the polymers [143,144]. The storage at 5 °C, 25 °C and 30 °C for 3 and 6 months did not alter the dissolution rates for both ASD

formulations. Likewise, the maximum dissolved CorA amount was unaltered during the stability study indicating consistent dissolution performances independent of storage temperatures. Overall, a consistent quality of the dissolution performances was demonstrated.

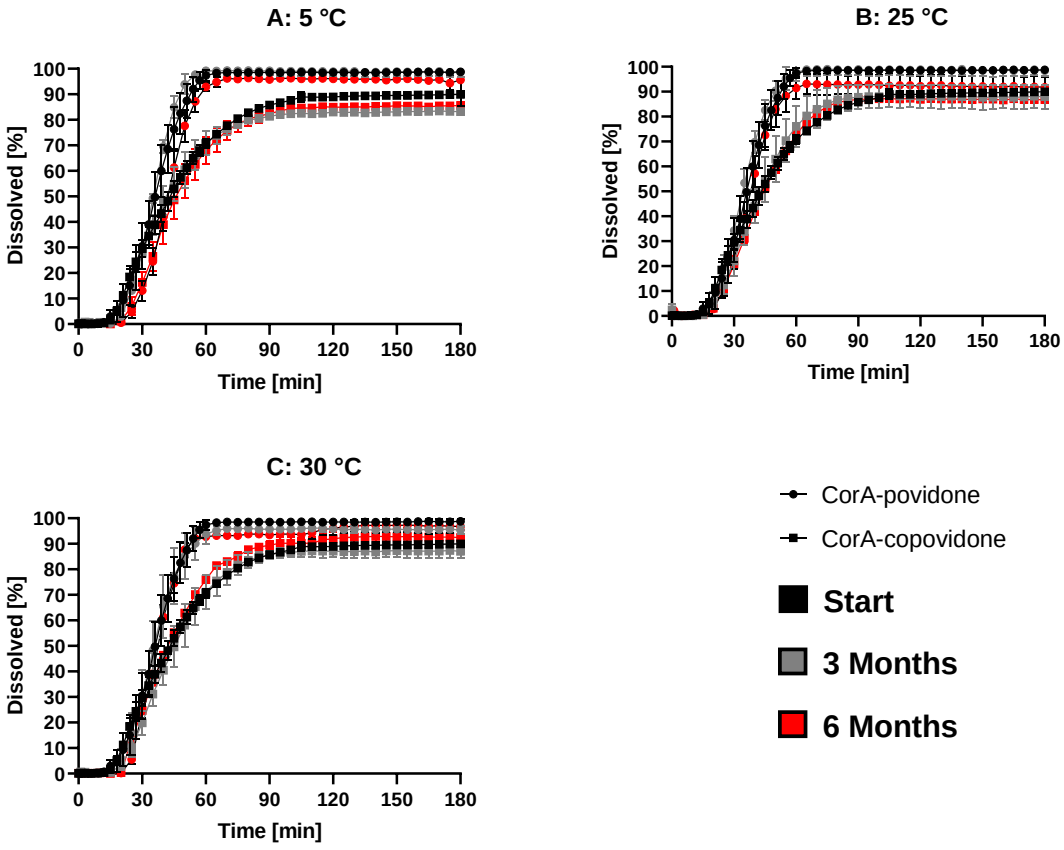

Figure 19. Stability analysis using USP II dissolution of the capsule formulation CorA-povidone and CorA-copovidone stored in closed Twist Off vials at A: 5 °C, B: 25 °C and C: 30 °C under nitrogen (n=3, mean ± SD). Experimental conditions were set at: Dose: 75 mg; Volume: 500 mL 0.05 M phosphate buffer (pH 6.8); Paddle speed: 75 RPM; Temperature: 37 °C; Sinker: Basket.

6.1.4.2 BiPHa+

As an additional assessment, the stability in terms of biorelevant dissolution was investigated using the BiPHa+ apparatus. For this, a total of 50 mg CorA-ASD granulate (corresponding to 10 mg CorA) of the capsule content were withdrawn and tested. Comparing the dissolution during the first 30 min (pH 1) the faster dissolution rate and higher amount of dissolved drug of the CorA-povidone ASD observed in USP II experiments were confirmed in this setup. CorA-povidone reached approx. 50% (0.1 mg/mL), whereas for CorA-copovidone approx. 10% (0.02 mg/mL) were dissolved.

After 30 min the pH was shifted to pH 5.5 accompanied by an increase in dissolved CorA (CorA-povidone: 78%; CorA-copovidone: 39%). The simultaneously added organic phase (1-decanol) initiated the partitioning of the CorA resulting in 73% for CorA-povidone and 59% for CorA-copovidone by the end of the dissolution after 270 min in the absorption phase (1-decanol). These results indicated a better dissolution performance of CorA-povidone and thus, a higher intestinal absorption. Nevertheless, also CorA-copovidone showed good results in terms of biphasic dissolution and displayed a valuable option for future clinical trials.

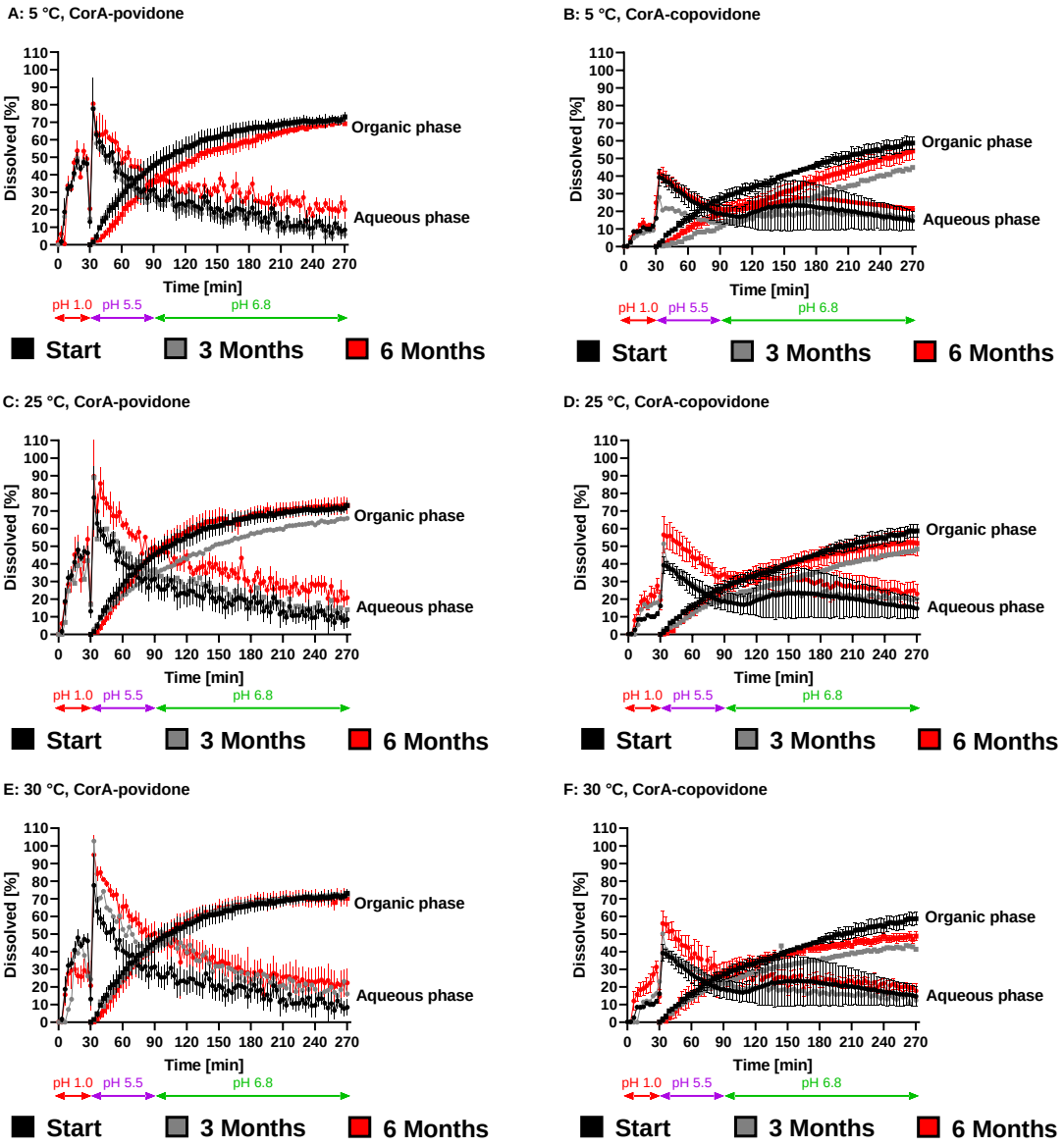

Figure 20. Stability analysis using The BiPHa+-biphasic dissolution. The capsule formulation CorA-povidone (A, C and E) and CorA-copovidone (B, D and F) were stored in closed Twist Off vials at A, B: 5 °C; C, D: 25 °C and E, F: 30 °C under nitrogen (n=3, mean ± SD). A total of 50 mg of the capsule contents were withdrawn for dissolution experiments.

Regarding the stability, slight interexperimental variations were assumed to be independent from storage conditions. In sum, the results did not indicate any physical instability affecting the biphasic dissolution performances. Using the BiPHa+ dissolution setup, a second dissolution approach confirmed that both CorA-ASDs were promising candidates for a stable dissolution performance.

6.2 Summary

The ASD formulation principal, comprising the polymers povidone and copovidone was found to markedly suppress the intramolecular isomerization of CorA. Moreover, the quality of the oral drug product (enteric capsule) was confirmed for at least 6 months at 25 °C. This included the physical state of the ASDs and dissolution properties in a USP II and biorelevant biphasic dissolution setup. Since both polymers exhibit hygroscopic properties, the results suggested manufacturing under dry air environment, as well as, moisture-resistant packaging. Even though, the identified stability enhancement of CorA was a resounding achievement, further optimization is required for the future to enable a successful drug product commercialization. However, for an initial FIH study, the capsule formulations were demonstrated to have adequate stability.

7. *In Vitro* Biorelevant Dissolution

Biorelevant dissolution has been brought into focus in the recent decade to gain the understanding of the *in vivo* relevant relationships regarding dissolution, supersaturation, precipitation, redissolution and absorption. In particular, pH-dependent soluble compounds are potentially affected by the pH-profile present in the GIT. As for most drug candidates the aim is a human application, recent *in vitro* approaches were investigated focusing the human gastrointestinal conditions. However, in preclinical PD and PK evaluations rodent- (e.g., mouse and rat) and non-rodent species (e.g., dog and monkey) are the typically investigated species. Differences in pH-profile, transit time and bile salt composition (**Table 16**) are able to affect dynamic processes like dissolution, supersaturation and precipitation and thus, the absorption and BA. In case of the weak acid CorA, rather acidic conditions, as it can be found in the mouse GIT, were assumed to hamper the dissolution rate and extent. In contrast, higher pH-values in the rat and dog GIT are beneficial regarding the solubility of CorA and a higher and faster dissolution was assumed. However, a lack of appropriate *in vitro* dissolution setups, especially for mice, led to unprecise interpretation of preclinical PK results which could have resulted in over- or underestimations of formulation candidates.

Biorelevant bile salt concentrations of the various species are summarized in detail in the method chapter (**Table 5 - 8**) and the respective concentrations were considered in the biorelevant dissolution assay.

Table 16. Gastrointestinal pH conditions and small intestinal transit times present in the species mouse (fed), rat (fasted), dog (fasted) and human (fasted). The values are based on the information provided by the PBPK modelling software GastroPlus.

Species	pH stomach	Transit time (h) stomach	pH small intestine	Transit time (h) small intestine
Mouse (fed)	3.0	0.32	4.8 - 4.9	0.98
Rat (fasted)	3.9	0.25	5.9 – 6.1	1.81
Dog (fasted)	3.0	0.25	6.2 - 6.7	1.82
Human (fasted)	1.3	0.25	6.0 - 6.9	3.25

The aim of this work was to adjust the established BiPHa+ apparatus to preclinical relevant species to examine the dissolution performances of CorA and CorA-ASDs. The influence on dissolution and absorption characteristics of the species-specific pH-profiles, GIT transit times and bile salt concentrations were investigated.

7.1 Results and Discussion

7.1.1 Biphasic Dissolution Adjusted to Intestinal Mouse Conditions

The dissolution performances of neat CorA, CorA-povidone-ASD and CorA-copovidone-ASD were examined using the biphasic dissolution tool BiPHa+ combined with biorelevant media and a mouse-specific pH-shift. For the species mouse, fed state was assumed due to the free food access of the animals during preclinical investigations. For the CorA-ASD formulations the spray dried intermediates were used, similar to the *in vivo* PK study in BALB/c mice (**Chapter 8.1.1**). Poor dissolution was observed for neat CorA reaching < 1% in the aqueous phase during the first 20 min at pH 3.0, while after the pH-shift to pH 4.8 a maximum of 2% after 80 min was observed (**Figure 21**). Consequently, the partitioning into the organic phase was limited due to the low amount of CorA dissolved in the aqueous phase reaching only 4% partitioning after 80 min, the end of the experiment. By using the ASD formulation approach *in vitro* biphasic dissolution exhibited enhanced dissolution performances. However, differences between the formulations were observed in the stomach compartment at pH 3.0 showing an aqueous concentration for the CorA-povidone dissolution of 76%, which was maintained after the pH shift to pH 4.8. With the addition of the organic phase after 20 min, the partitioning of dissolved CorA started and led to a decreased concentration in the aqueous phase by reaching an equilibrium at approx. 55% within 30 min. In comparison, the aqueous concentration of the CorA-copovidone dissolution resulted in 11% after 20 min and maintained this level until the end of the experiment. As only dissolved API in the aqueous phase was available for partitioning into the organic phase, CorA-povidone reached 34% of partitioned CorA after 80 min whereas for CorA-copovidone only 13% was observed. As the aqueous phases showed constant concentrations, the partitioned amount was continuously replaced by undissolved CorA-ASD. The results clearly demonstrated the dissolution improvements evoked by the ASD formulation principle. Nevertheless, the partitioning of CorA-povidone was 3-fold higher than the partitioning of CorA-copovidone, which was

not to be observed in USP II or BiPHa+ experiments performed under human GIT conditions. This clearly demonstrated, that formulation differences regarding dissolution can already be investigated using this setup in early preclinical phases.

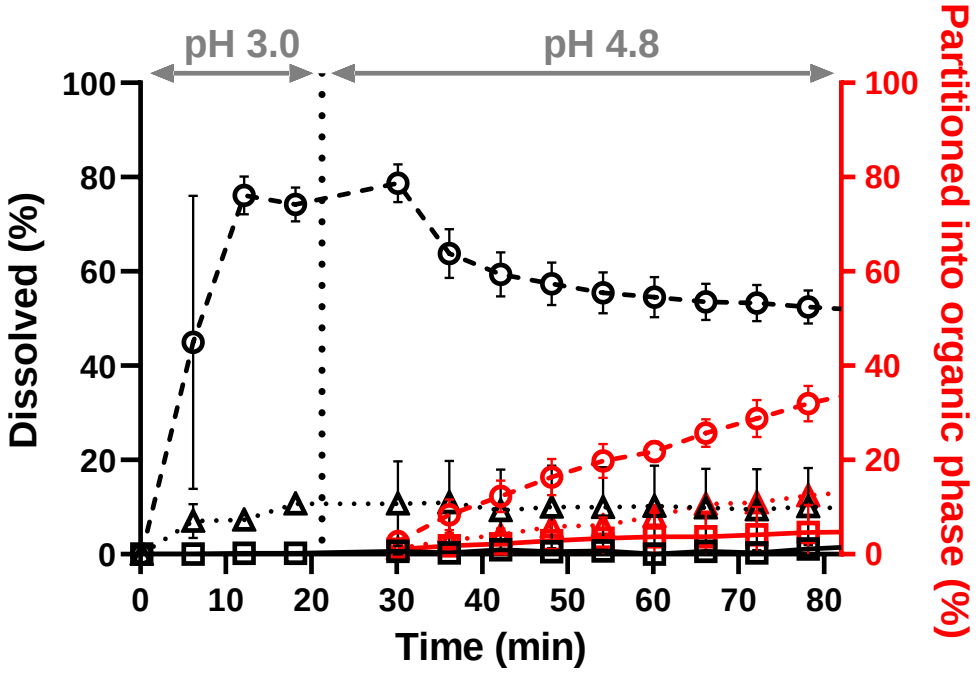

Figure 21. Biphasic dissolution experiment under gastrointestinal conditions in mice; neat CorA (□; solid line), CorA-povidone (○; dashed line) and CorA-copovidone (△; dotted line). n=3 (mean ± SD).

7.1.2 Biphasic Dissolution Adjusted to Intestinal Rat Conditions

For PK evaluations, the species rat has often been used in the past. In contrast to mice, rats are favored, because of its ease of handling, amount of blood and number of time sampling points, as well as, robustness. Moreover, the body weight of rats is low requiring still small amounts of compound, advantageous for early preclinical studies. The spray dried CorA-ASDs were investigated in a PK study in rats (**Chapter 8.1.3**). Accordingly, the biphasic dissolution, tailored to rats, were used to predict the dissolution/absorption performance. The setup based on published media mimicking the conditions observable in the GIT of rats [125]. To provide a partitioning sink, an organic phase was added similar to mouse and human biphasic setup. However, pH-profile, transit times and bile salt concentrations, clearly differed from the setup used for the other species. The first 30 min were performed at pH 2.4 resulting in an aqueous dissolution of 62% for CorA-povidone and 25% for CorA-copovidone (**Figure 22**). Similar to the mouse setup, the dissolution for

CorA-povidone was higher at low pH compared to CorA-copovidone. Nevertheless, the lower pH of 2.4 decreased the dissolved amount for CorA-povidone. In contrast, CorA-copovidone showed higher dissolution compared to the mouse setup. Yet, at pH 2.4 for the first 30 min, CorA-copovidone exhibited a 2-fold increased dissolution compared to the mouse setup. The presence of bile salts in the rat setup might have been responsible for the observed pronounced solubilization and faster dissolution. After 30 min the pH increased to pH 7.5 followed by a concentration increase to 98% for CorA-povidone and 66% for CorA-copovidone. The addition of the organic phase initiated the partitioning of dissolved CorA. Despite different aqueous dissolution profiles, both ASD formulations showed comparable partitioning profiles resulting in 64% after 138 min for both formulations indicating that the partitioning rate has reached a maximum at a certain concentration. Hence, the higher aqueous concentration was not able to further increase the partitioning rate. This indicated that CorA absorption is limited by permeability rather than dissolution. In essence, due to the acidic characteristics of CorA, the conditions in rats were beneficial for the aqueous dissolution in comparison to the low pH present in mouse intestine. In contrast to the mouse results, no differences in the partitioning quantity of the ASD formulations were observed indicating comparable absorption and thus, similar BAs.

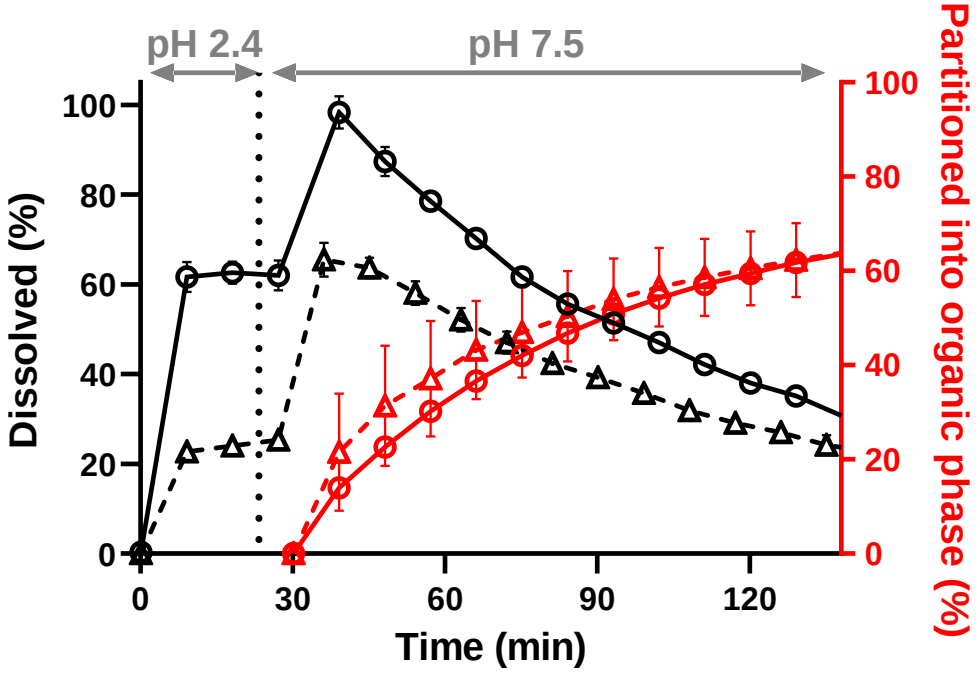

Figure 22. Biphasic dissolution experiment under gastrointestinal conditions in rats; CorA-povidone (○; dashed line) and CorA-copovidone (△; dotted line). n=3 (mean ± SD).

7.1.3 Biphasic Dissolution Adjusted to Intestinal Dog Conditions

A preliminary *in vitro* study was performed investigating the CorA-povidone capsule formulation. For PK trials in dogs, a pretreatment with pentagastrin is well established, that leads to a stomach pH decrease to a value similar to that of humans [145]. This enabled a reproducible pH profile throughout the GIT that mimics the human profile. The first 30 min of the biphasic dissolution started with 50 mL of 0.1 N HCl, corresponding to pH 1. In accordance to the PK study in dogs (**Chapter 8.1.4**), enteric capsules were assessed via *in vitro* dissolution and the investigated formulations were weighed into enteric capsules (size 0). After 30 min the medium was replaced by dog specific biorelevant media using a commercially available biorelevant buffer concentrate (biorelevant.com). The enteric function of the capsule prevented dissolution for the first 30 min. This circumstance allowed a replacement of the dissolution medium. By replacing the medium, which was accompanied by a pH shift to pH 7.5, the disintegration of the capsule started subsequently. Simultaneously, the organic phase was added and covered the aqueous phase. In the aqueous phase the dissolution of CorA-povidone achieved 76%. At the same time, partitioning took place reaching 59% by the end of the experiment. During the same time, the concentration in the aqueous phase decreased to 35%.

Considering, that in both phases together almost the total amount of CorA was dissolved in either the aqueous or the organic phase, the partitioning rate seemed to reach a maximum similar to the rat setup. In comparison to rats, the bile salt concentrations in dogs are lower, however, similar partitioning profiles were observed under consideration of the lag time accompanied by the disintegration of the capsules. This suggested that dissolution and absorption of the CorA-ASDs was dependent on pH rather than on bile salt concentration.

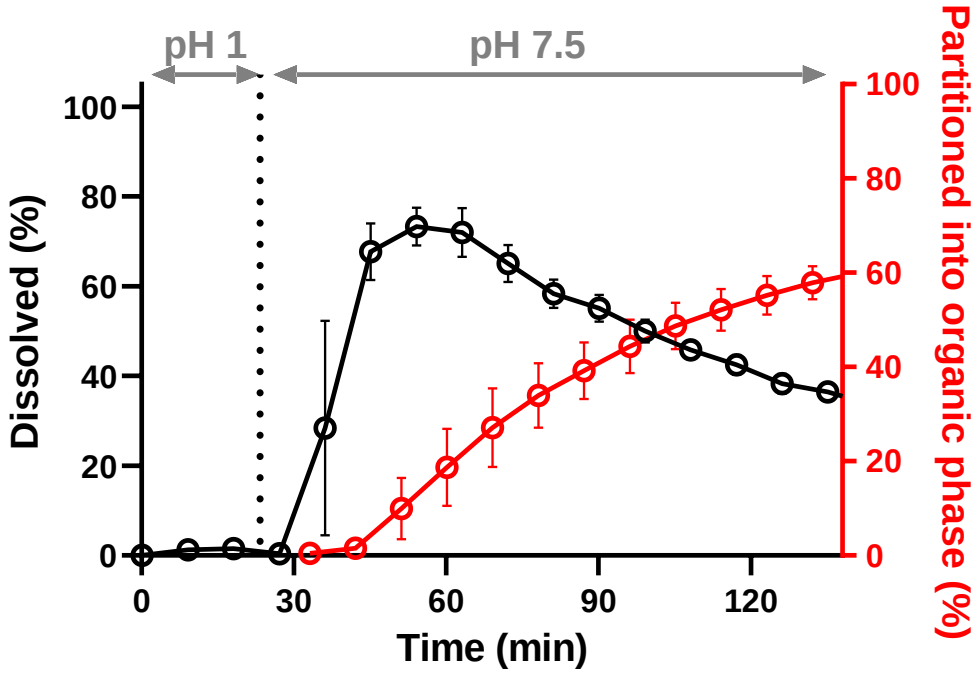

Figure 23. Biphasic dissolution experiment under gastrointestinal conditions in dogs; CorA-povidone (○; dashed line) n=3 (mean ± SD).

7.2 Summary

Selecting promising formulation principles during the preclinical development phase is a great challenge for pharmaceutical scientists. However, the physiology conditions in preclinical species differ in terms of pH-profile, transit times and bile salts. In case of the weak acid CorA, especially the pH markedly influenced drug dissolution and thus, absorption. Providing appropriate *in vitro* dissolutions supported the selection of formulation candidates, as well as, the interpretation of *in vivo* PK results. For CorA, different dissolution performances of the ASD formulations were observed in the mouse biphasic dissolution setup, while for another species, rat, these differences were not

observed. It was assumed that the poorer wettability of CorA-copovidone, especially at low pH values, led to a slower and poorer aqueous dissolution resulting in lower partitioning into the organic phase. These setups revealed, that this effect was more pronounced at the lower pH-values present in mouse GIT. At higher pH (rat and dog small intestine setup: pH 7.5) this effect was observed to have less influence on the aqueous dissolution and finally on the partitioning profiles. Moreover, the determined dissolution data in biorelevant media enabled dissolution as the decisive mechanism governing the oral BA of CorA and CorA formulations to be deduced. Hence, the presented setups demonstrated their preclinical relevance, thus providing a material-saving method to optimize the oral treatment of preclinical species and select promising formulation principles even in early preclinical studies. Future investigations comprising compounds with different physicochemical properties, such as weak bases, need to be investigated to further assess the suitability of the species-specific biphasic setups. By relating the *in vitro* examined results with *in vivo* determined PK results the predictive power regarding the biphasic dissolution can be evaluated and enhance the confidence for the prediction in human. The integration of dissolution data into the PBPK model potentially enable predictions of plasma concentrations (**Chapter 10**).

8. PK Evaluations of CorA Formulations

An important aspect for preclinical investigations is the *in vivo* evaluation to get insights to ADMET properties of the compound and its formulations. A desired PD effect is accompanied with sufficient drug concentration at the target site. Formulation evaluations in different species are crucial to identify the most promising representatives for clinical studies.

The formulation preselection based on *in vitro* experiments, such as dissolution and stability trials [108,109]. The aim of the preclinical *in vivo* studies was to confirm the suitability of the formulation candidates and to get a comprehensive overview of CorA and CorA formulation performances. As CorA exhibited poor solubility, poor handling and isomerization tendency, formulation development took place early in the preclinical phase. Limited drug supply and the fact, that BALB/c mice represented the efficacy model, led to the use of mice for initial PK evaluations of neat CorA and the solid ASD formulations, administered as the spray dried intermediates suspended in water or PBS media. Preliminary *in vitro* studies revealed CorA-povidone and CorA-copovidone to be the most promising candidates in terms of dissolution and stability enhancement [108]. Further PK experiments were performed in jirds, representing a second efficacy model of CorA. Moreover, CorA and spray-dried CorA ASDs were tested in rats, a further rodent PK model with different physiological conditions. Finally, solid oral drug products of CorA (capsules and tablets) were tested in dogs, to evaluate potential candidates for a clinical phase I study. These results were used for a cross-species PBPK-model, which is described in this work in **Chapter 10**. A food effect was investigated first in mice using a high fat suspension medium and later in dogs providing a high caloric dog food, administered prior to the treatment. In addition, the intended toxicological vehicles for the exploratory toxicology studies in rats and dogs were tested in the respective species to determine their PK profile.

8.1 Results and Discussion

The following results are illustrated as median ± IQR. Individual animal profiles and corresponding PK parameters are presented in the **Appendix**.

8.1.1 PK Evaluation of CorA and CorA-ASD Principles in Mice

Plasma profiles after IV administration of neat CorA dissolved in propylene glycol, Kolliphor HS 15 and PBS pH 7.4 (20/20/60; V/V/V), and PO administered neat CorA and CorA-ASD-formulations in BALB/c mice (n=4 per group), suspended in water, and associated PK parameters were generated (**Figure 24** and **Table 17**). The IV administration allowed the calculation of the abs. BA (**Eq. 4**) of PO administrations and yielded 3% for neat CorA, 33% for CorA-povidone and 10% for CorA-copovidone, administered as suspension in water. A later t_{max} was determined for neat CorA (1 h) compared to the ASD formulations (15 min for CorA-povidone and 30 min for CorA-copovidone). Neat CorA exhibited a C_{max} of 0.9 µg/mL, while for CorA-povidone 33.2 µg/mL and for CorA-copovidone 5.0 µg/mL were achieved. The terminal half-life ($t_{1/2}$) for all groups ranged from 2.38 h to 3.73 h indicating a fast elimination. The oral administration of neat CorA showed the lowest plasma concentrations resulting in poor C_{max}, late t_{max} and poor BA. By achieving only 3% of BA, the need for a solubility and dissolution enhancing formulation approach to enable a sufficient therapeutic effect was clearly demonstrated. Both formulations demonstrated their potential to increase the PK profiles accompanied with improved C_{max} and BA. Interestingly, the low t_{max} values indicated a fast dissolution and absorption process. Already after 45 min the elimination dominated, while the absorption rapidly stopped. As a result, the plasma concentrations dropped below 1 µg/mL after 8 h. Recent PD studies indicated that a therapeutic effect would be dependent on a long-term concentration at the target site. The PK profiles revealed that a repeated administration, e.g., three times a day will be beneficial in terms of *in vivo* efficacy. Indeed, differences between both ASD formulations were detected showing an approx. three-fold higher BA for CorA-povidone. These results confirmed the observations obtained during the species adjusted biphasic dissolution, i.e., the pH dependent dissolution seemed to be the rate limiting step for drug absorption in mice. Accordingly, higher BAs were expected by using PBS pH 7.4 as administration medium for the ASD suspensions to create an environment with a higher pH. As the solubility rapidly increases with an increasing pH, it was assumed that this administration further increases the dissolution rate and concentration and thus, the absorption and BA.

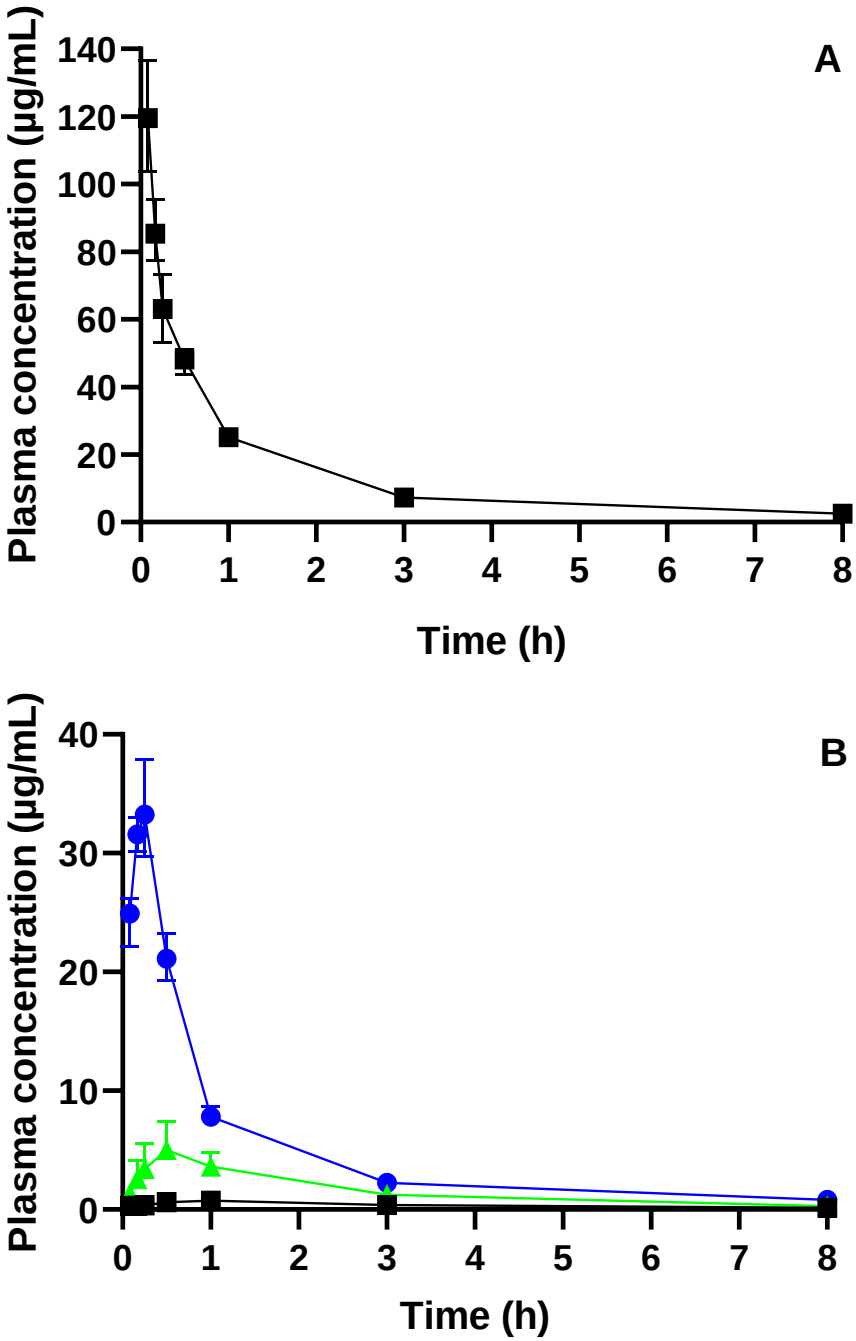

Figure 24. CorA plasma concentration time profiles in BALB/c mice: A: IV administration of a CorA-solution (36 mg/kg) (permission to use the data was kindly granted by Krome et al. [108]); B: PO administration of neat CorA (■), CorA-povidone (●) and CorA-copovidone (▲) (36 mg/kg), administered as aqueous suspension in female BALB/c mice (median ± IQR, n=4 per group).

Table 17. PK parameters of CorA and CorA formulations after IV administration of a CorA-solution (36 mg/kg) and PO administration of the solid neat CorA and the CorA-ASD formulations CorA-povidone and CorA copovidone suspended in water (36 mg/kg) in female BALB/c mice (median ± IQR, n=4 per group).

	$AUC_{0\text{-}inf}$ (µg*h/mL)	**$AUC_{0\text{-}inf}$ per mg/kg dose (µg*h*kg/dose)**	**C_{max} (µg/mL)**	**t_{max} (min)**	**$t_{1/2}$ (h)**	**BA (%)**
Reference of CorA – IV[#]	127.7 (110.2-149.0)	3.5 (3.1-4.1)	119.6 (103.7-136.7)	5*	3.30	100**
Neat CorA	4.5 (3.8-7.4)	0.1 (0.1-0.2)	0.9 (0.6-1.1)	60 (53-90)	3.38	3
CorA-povidone	41.9 (39.6-46.5)	1.2 (1.1-1.3)	33.2 (30.3-37.9)	15 (10-15)	2.38	33
CorA-copovidone	13.4 (11.4-17.4)	0.4 (0.3-0.5)	5.0 (3.0-7.4)	30 (30-38)	3.73	10

* First measured value; ** IV result median set to 100%; # [108].

The assumptions were confirmed as for all administrations (neat CorA and CorA-ASDs) both C_{max} and $AUC_{0\text{-}inf}$ were improved (**Figure 25** and **Table 18**). In addition, the administration in PBS led to an earlier t_{max}, especially for the ASDs, confirming the fast dissolution rate. Overall, BAs were increased approx. two-fold compared to an administration in water. The differences between both ASD formulations were consistent to the water administration as this also demonstrated three-fold improvements in C_{max} and BA. In sum, both ASD formulations improved C_{max} and BA compared to neat CorA, demonstrating promising results for an ASD based solid oral drug product as higher intestinal pH-values are present in the preclinical species rat and dog, as well as, in humans.

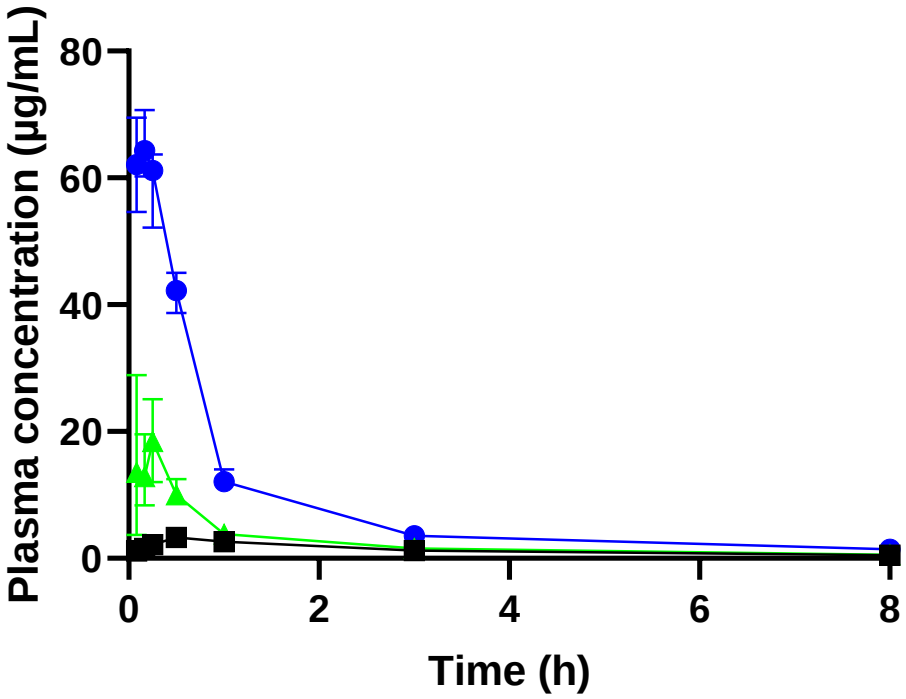

Figure 25. CorA plasma concentration time profiles in BALB/c mice. PO administration of neat CorA (■), CorA-povidone (●) (permission to use the data was kindly granted by Krome et al. [108]) and CorA-copovidone (▲) (36 mg/kg), administered as suspension in PBS pH 7.4 in female BALB/c mice (median ± IQR, n=4 per group).

Table 18. PK parameters of CorA and CorA formulations after PO administration of solid neat CorA and CorA-ASD formulations CorA-povidone and CorA copovidone suspended in PBS pH 7.4 (36 mg/kg) in female BALB/c mice (median ± IQR, n=4 per group). The permission to use the data of CorA-povidone was kindly granted by Krome et al. [108].

	$AUC_{0\text{-}inf}$ (µg*h/mL)	**$AUC_{0\text{-}inf}$ per mg/kg dose (µg*h*kg/dose)**	**C_{max} (µg/mL)**	**t_{max} (min)**	**$t_{1/2}$ (h)**	**BA (%)**
Neat CorA	15.7 (9.8-15.1)	0.4 (0.4-0.5)	3.3 (3.0-3.5)	30 (45-60)	3.98	12.5
CorA-povidone[#]	72.7 (70.4-76.7)	2.0 (2.0-2.1)	65.3 (61.8-70.7)	10 (10-11.25)	3.89	58
CorA-copovidone	24.9 (20.7-31.3)	0.7 (0.6-0.9)	23.7 (20.0-29.8)	10 (5-15)	3.50	20

[108].

The high logP of CorA (5.4) suggests a positive food effect. To assess a potential food effect for CorA, BALB/c mice were treated with CorA-ASDs suspended in corn oil. As no experimental settings are feasible where mice are actively fed with a high caloric meal, corn oil was chosen as suspension medium (**Figure 26 and Table 19**). In comparison to the water-based suspension media, pronouncedly decreased C_{max} values were obtained (CorA-povidone: 8.7 µg/mL and CorA-copovidone: 3.7 µg/mL). A notably prolonged plasma profile was observed resulting in late t_{max} values of 180 min for CorA-povidone and 60 min for CorA-copovidone indicating a prolonged GIT transit. While C_{max} was decreased by the administration in corn oil, the exposures were in a comparable range compared to the suspension administration in water ($AUC_{0\text{-}inf}$: CorA-povidone: 39.8 µg*h/mL; CorA-copovidone: 20.2 µg*h/mL). Thereby, BA of 31% for CorA-povidone and 16% for CorA-copovidone could be achieved. Since neither a positive nor a negative effect could be observed in terms of exposure, CorA was assumed to dissolve, but remained in the fatty oil. The long-lasting plasma profile indicated that CorA was absorbed constantly for at least 3 h caused by prolonged transit and the reservoir function of the fatty oil phase.

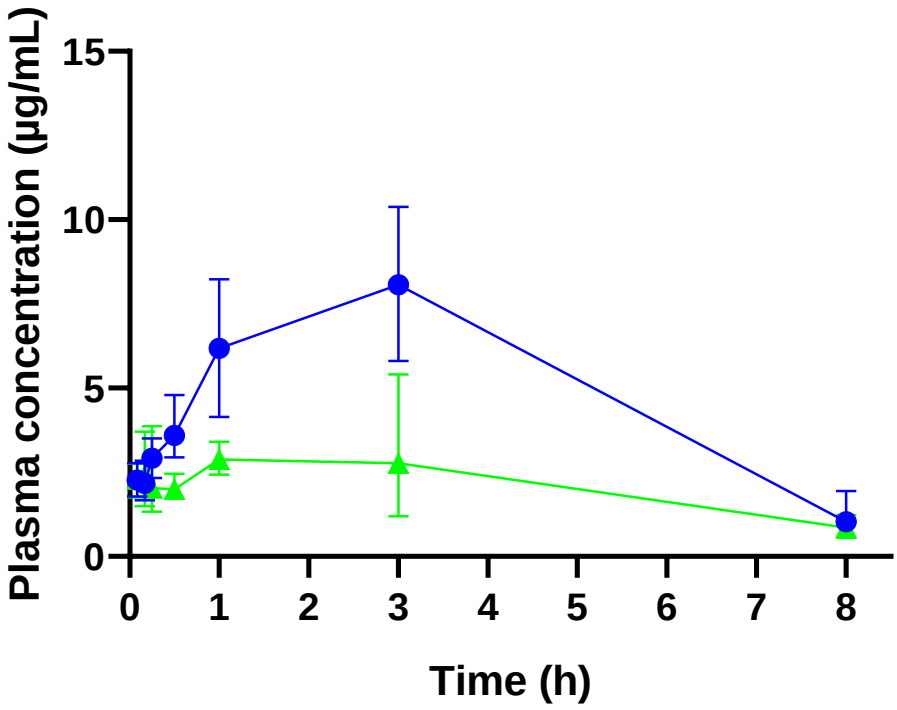

Figure 26. CorA plasma concentration time profiles in BALB/c mice. PO administration of CorA-povidone (●) and CorA-copovidone (▲) (36 mg/kg), administered as suspension in corn oil in female BALB/c mice (median ± IQR, n=4 per group).

Table 19. PK parameters of CorA formulations after PO administration of CorA-ASD formulations CorA-povidone and CorA copovidone suspended in corn oil (36 mg/kg) in female BALB/c mice (median ± IQR, n=4 per group).

	$AUC_{0\text{-}inf}$ (µg*h/mL)	**$AUC_{0\text{-}inf}$ per mg/kg dose (µg*h*kg/dose)**	**C_{max} (µg/mL)**	**t_{max} (min)**	**$t_{1/2}$ (h)**	**BA (%)**
CorA-povidone	39.8 (32.3-57.7)	1.1 (0.9-1.6)	8.7 (7.3-10.4)	180 (150-180)	1.9	31
CorA-copovidone	20.2 (13.2-32.1)	0.6 (0.4-0.9)	3.7 (2.8-5.4)	60 (46.2-180)	2.9	16

8.1.2 PK Evaluation of CorA-povidone at Two Different Dose Levels in Jirds

The *Litomosoides sigmodontis* infection model is established as an efficacy model to investigate drug candidates against filariasis. Mongolian gerbils (jirds) enabled studies focusing on long-term effects of an anti-filarial therapy, e.g., macrofilaricidal activity [100]. Since an oral application is the intended route of administration, CorA-povidone was tested using this efficacy model. The administration medium was PBS pH 7.4 to obtain highest possible concentrations. CorA-copovidone was excluded since data from mice suggested lower exposure and thus a less successful treatment. The PK profiles of two different doses (30 and 60 mg/kg) were examined. For both dose strengths, t_{max} was detected at 30 min. Considering interindividual variability, C_{max} and $AUC_{0\text{-}inf}$ increased in a dose-dependent manner reaching 24.9 µg/mL (C_{max}) and 119.1 µg*h/mL ($AUC_{0\text{-}inf}$) for 30 mg/mL and 66.8 µg/mL (C_{max}) and 278.0 µg*h/mL ($AUC_{0\text{-}inf}$) for 60 mg/mL. Higher dose normalized exposures ($AUC_{0\text{-}inf}$ per mg/kg dose: 30 mg/kg: 4.0; 60 mg/kg: 4.6) compared to mouse ($AUC_{0\text{-}inf}$ per mg/kg dose: 2.0) were observed. In contrast to the PK study in mice, lower C_{max} values were achieved, however, the apparent elimination rate after reaching C_{max} was smaller, suggesting further dissolution and absorption. Overall, using the dissolution and BA enhanced oral formulation CorA-povidone, a successful treatment was observed for the tested doses 30 and 60 mg/mL (PD data not shown). Thus, the oral administration provided a valuable alternative for a long-term efficacy study compared to intraperitoneal administration. At the same time oral administration represents the more relevant application way in terms of clinical trials.

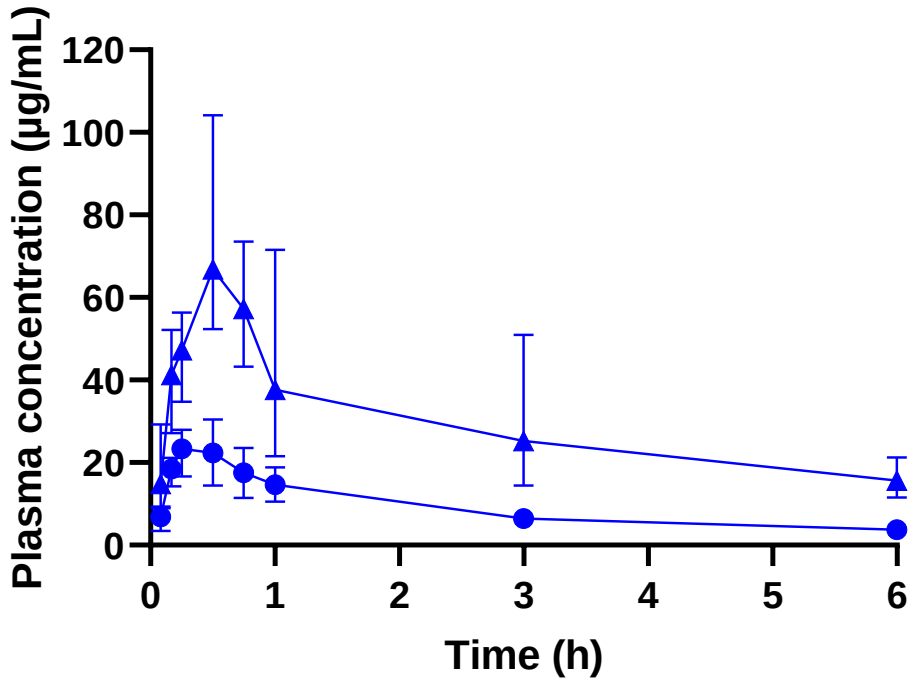

Figure 27. CorA plasma concentration time profiles in Mongolian gerbils (jirds). PO administration of CorA-povidone with the doses 30 mg/kg (●) and 60 mg/kg (▲) administered as suspension in PBS pH 7.4 in female jirds (median ± IQR, n=4 per group).

Table 20. PK parameters after PO administration of CorA-povidone with the doses 30 mg/kg and 60 mg/kg in Mongolian gerbils (jirds) (median ± IQR, n=4 per group).

	$AUC_{0\text{-}inf}$ (µg*h/mL)	**$AUC_{0\text{-}inf}$ per mg/kg dose (µg*h*kg/dose)**	**C_{max} (µg/mL)**	**t_{max} (min)**	**$t_{1/2}$ (h)**	**BA (%)**
30 mg/mL	119.1 (61.2-189.5)	4.0 (2.0-6.3)	24.9 (18.2-30.4)	30 (26.3-30.0)	3.9	n.a.
60 mg/mL	278.0 (202.4-381.9)	4.6 (3.4-6.4)	66.8 (52.4-104.2)	30 (30-30)	3.3	n.a.

8.1.3 Comparison of CorA-Solution and CorA-ASD Formulations after Oral Administration in Rats

The well tolerated IV vehicle propylene glycol, Kolliphor HS 15 and PBS pH 7.4 (20/20/60; V/V/V), successfully tested in mice, caused severe symptoms in Wistar rats, so that the treated rats had to be euthanized for animal welfare reasons. Thereby, an alternative vehicle was established with PEG 400/PBS 7.4 (60/40, V/V). However, due to

solubility limitations, the dose had to be reduced to 18 mg/kg. For BA calculations of the oral treated groups, the exposure was dose normalized. Since poor *in vitro* and *in vivo* performances in mice have been demonstrated for neat CorA, this administration was not performed in this study. Instead, a CorA PEG 200 solution was investigated as it was the intended toxicological vehicle for rats. In addition, an oral solution served as a comparison for ASD formulations as the absence of dissolution process suggests a rapid absorption [146]. The ASD candidates CorA-povidone and CorA-copovidone were administered as suspension in PBS pH 7.4. The $t_{1/2}$ was 3.11 h which was comparable to the value in mice (3.3 h). In general, all oral groups achieved high plasma concentrations with > 60 µg/mL at t_{max} of 90-120 min (**Figure 28**), later than observed in mice. The profiles indicated that absorption still occurred after reaching C_{max}. This led to high exposures for all groups resulting in calculated BAs ≥ 100%. Reasons for these calculated values can be explained by several reasons: The calculation was based on the IV group treated with half the dose and the results potentially suggested a non-dose linearity in this dose range. In addition, the small group size carried a risk for artifacts, which was also reflected in high interindividual variabilities. Even though, the reason for BAs above 100% could not be clearly identified, the data indicated high intestinal dissolution in the case of ASDs and high absorption in general. In contrast to mice, the CorA-copovidone formulation demonstrated higher C_{max} and AUC compared to CorA-povidone accompanied with a later t_{max} for CorA-povidone. However, no significant differences regarding C_{max} and AUC ($p > 0.9$) were observed indicating comparable performances of both ASD formulations. Similar results were obtained when comparing CorA-solution and CorA-ASDs, with no significant differences found ($p > 0.9$). The plasma profile of the CorA-solution suggested a fast absorption of the dissolved CorA until 0.5 h reaching a first plateau. As the dissolved CorA likely exceeded its solubility limit at the acidic stomach pH, precipitation potentially occurred. The second maximum after 2 h can potentially be explained by redissolving of the precipitate by entering the intestinal part with a higher pH. This phenomenon was not identified for the ASD formulations indicating the dissolution rate to be the relevant part for absorption and precipitation was less pronounced. Overall, the rat PK results were promising results regarding the BA of the CorA-ASD formulation candidates and differences among each other were less pronounced as determined in mice

demonstrating species specific performances. Tolerability and sufficient exposure of CorA-PEG 200 were confirmed to be suitable for toxicological studies in rats.

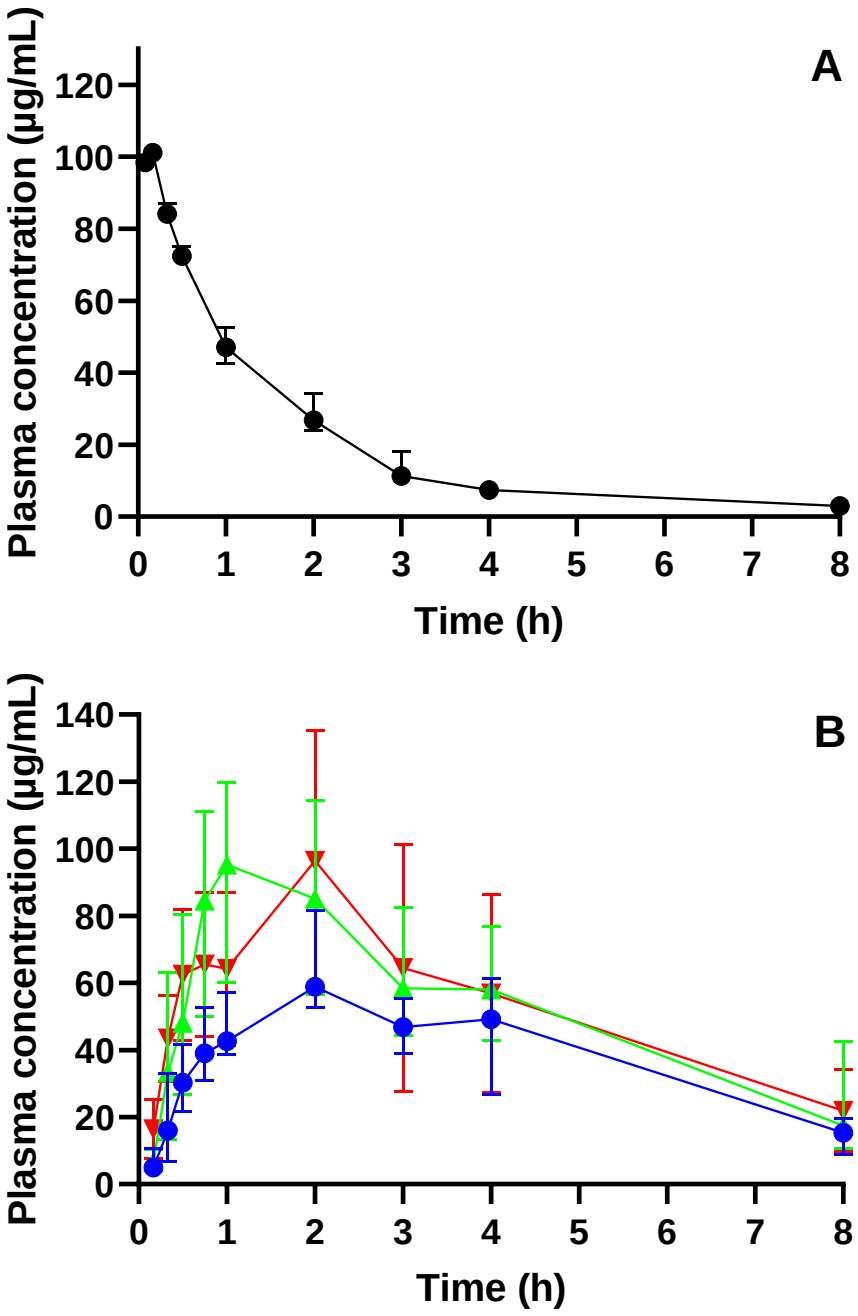

Figure 28. CorA plasma concentration time profiles in Wistar rats. A: IV administration of a CorA-solution (18 mg/kg); B: PO administration of CorA-povidone (●) and CorA-copovidone (▲) (36 mg/kg), administered as suspension in PBS 7.4 and a CorA-PEG 200 solution (▼) (36 mg/kg) in female Wistar rats (median ± IQR, n=4 per group).

Table 21. PK parameters of CorA formulations after IV administration of a CorA-solution (18 mg/kg) and PO administration of CorA-ASD formulations CorA-povidone and CorA copovidone suspended in PBS pH 7.4 (36 mg/kg) and a CorA-PEG 200 solution (36 mg/kg) in female BALB/c mice (median ± IQR, n=4 per group).

	$AUC_{0\text{-}inf}$ (µg*h/mL)	$AUC_{0\text{-}inf}$ per mg/kg dose (µg*h*kg/dose)	C_{max} (µg/mL)	t_{max} (min)	$t_{1/2}$ (h)	BA (%)
Reference of CorA – IV	177.7 (174.2-182.2)	9.9 (9.7-10.1)	102.3 (101.0-102.8)	10 (8.8-10.0)	3.11	100**
CorA-povidone	354.1 (305.6-404.8)	9.8 (8.5-11.2)	61.0 (56.8-69.6)	120 (120-150)	2.44	102
CorA-copovidone	466.1 (422.2-619.8)	13.0 (11.7-17.2)	106.7 (86.1-122.1)	90 (60-150)	2.28	134
CorA-PEG 200 solution	490.4 (409.8-612.8)	13.6 (11.4-17.0)	90.9 (69.4-118.0)	120 (120-120)	2.81	137

** IV result median set to 100%

8.1.4 First PK Assessment of Oral Drug Product Prototypes in Dogs and Potential Toxicology Vehicle

An IV administration allows the determination of the abs. oral BA. Due to tolerability concerns the IV vehicle was adjusted to propylene glycol, Kolliphor HS 15, PBS 7.4 (20/4/76, V/V/V). It was able to provide a solution at a concentration of 3 mg/mL which was administered at an abs. dose of 75 mg (**Figure 29A**). Low variabilities of plasma concentrations and corresponding PK parameters, as well as, good tolerability was observed confirming a successful administration. Groups, treated orally with capsules or tablets, were pre-treated with pentagastrin to induce a decrease of the stomach pH mimicking human conditions. As a delayed release approach, capsules, filled with granulated CorA-ASD were selected. Enteric capsules were used to protect potential acid induced isomerization (**Figure 29B**). Capsules represents a simple approach for the administration of a solid dosage form. The first measured plasma concentration was selected to be 45 min, which was associated to the lag time until the capsules disintegrate.

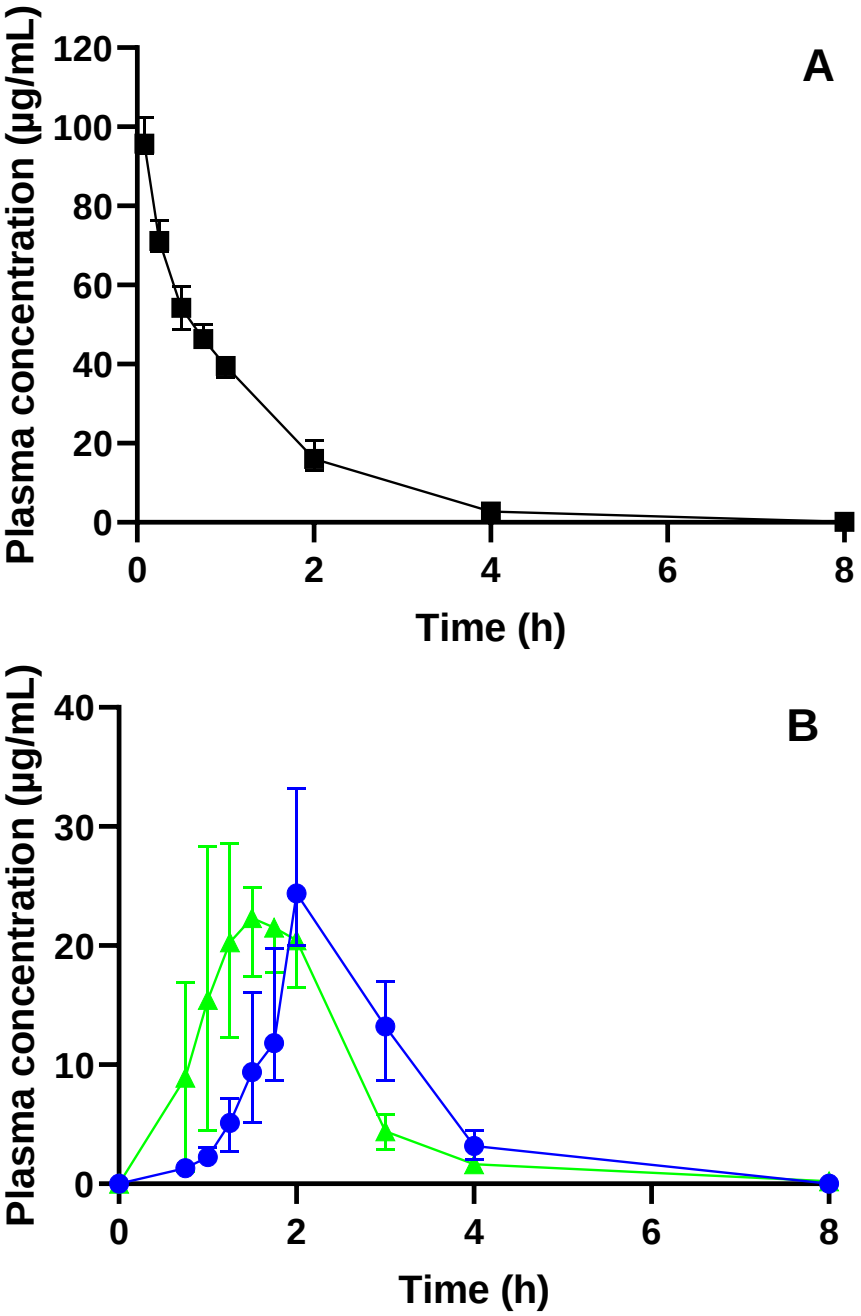

Figure 29. CorA plasma concentration time profiles in fasted Beagle dogs. A: IV administration of a CorA-solution (75 mg); B: PO administration of CorA-povidone (●) and CorA-copovidone (▲) (75 mg), administered as an enteric capsule (median ± IQR, n=4 per group).

Indeed, plasma concentrations were detectable after 45 min indicating a fast disintegration of the capsules followed by fast dissolution and absorption. However, the disintegration of CorA-copovidone was assumed to be slightly faster due to the higher observed plasma levels after 45 min. Both capsules showed comparable C_{max}

(CorA-povidone: 24.4 µg/mL; CorA-copovidone: 22.3 µg/mL) and $AUC_{0\text{-}inf}$ (CorA-povidone: 42.9 µg*h/mL; CorA-copovidone: 51.2 µg*h/mL) (**Table 22**). CorA-copovidone reached C_{max} after 90 min, while for CorA-povidone a t_{max} of 120 min was observed. Afterwards, the plasma levels dropped rapidly for both formulations indicating that the absorption process ended immediately after reaching C_{max}. This could be explained by the short small intestinal transit time of the dogs [147]. In terms of BA (CorA-povidone: 34%; CorA-copovidone: 35%) no clear "frontrunner" could be identified. Furthermore, in HPLC investigations no pronounced isomerization towards CorA' was identified. Thus, both represented promising options as a delayed release formulation for a clinical phase I study.

Table 22. PK parameters of CorA formulations after IV administration of a CorA-solution (75 mg) and PO administration of CorA-ASD enteric capsules comprising CorA-povidone and CorA copovidone granules (75 mg) in fasted Beagle dogs (median ± IQR, n=4 per group).

	$AUC_{0\text{-}inf}$ (µg*h/mL)	**$AUC_{0\text{-}inf}$ per mg/kg dose (µg*h*kg/dose)**	**C_{max} (µg/mL)**	**t_{max} (min)**	**$t_{1/2}$ (h)**	**BA (%)**
Reference of CorA – IV	117.4 (108.2-128.0)	11.4 (9.8-13.9)	95.8 (93.3-102.3)	5 (5-5)	1.00	100**
CorA-povidone	42.9 (35.3-56.2)	3.6 (3.2-4.5)	24.4 (20.0-33.2)	120 (120-120)	0.48	34
CorA-copovidone	51.2 (34.1-61.8)	4.3 (3.6-4.5)	22.3 (19.1-29.0)	90 (71.25-105)	1.35	35

** IV result median set to 100%

Two groups received a high calory meal prior administration of the enteric capsules to investigate a food effect (**Figure 30 and Table 23**). Even though, the high logP (5.4) suggested a positive impact, lower plasma concentrations were determined (C_{max}: CorA-povidone: 8.8 µg/mL; CorA-copovidone: 3.2 µg/mL) resulting in low exposures ($AUC_{0\text{-}inf}$: CorA-povidone: 31.6 µg*h/mL; CorA-copovidone: 24.8 µg*h/mL). Higher t_{max} values were observed with 4 h. In sum, the BAs were decreased to 25% (CorA-povidone) and 14% (CorA-copovidone), indicating that absorption was not positively affected by food intake in dogs. As *in silico* predictions suggested a strong beneficial food effect (**Chapter 10**), the preclinical results should not be overinterpreted, and at least one investigation in a future human study should cover the effects of food intake.

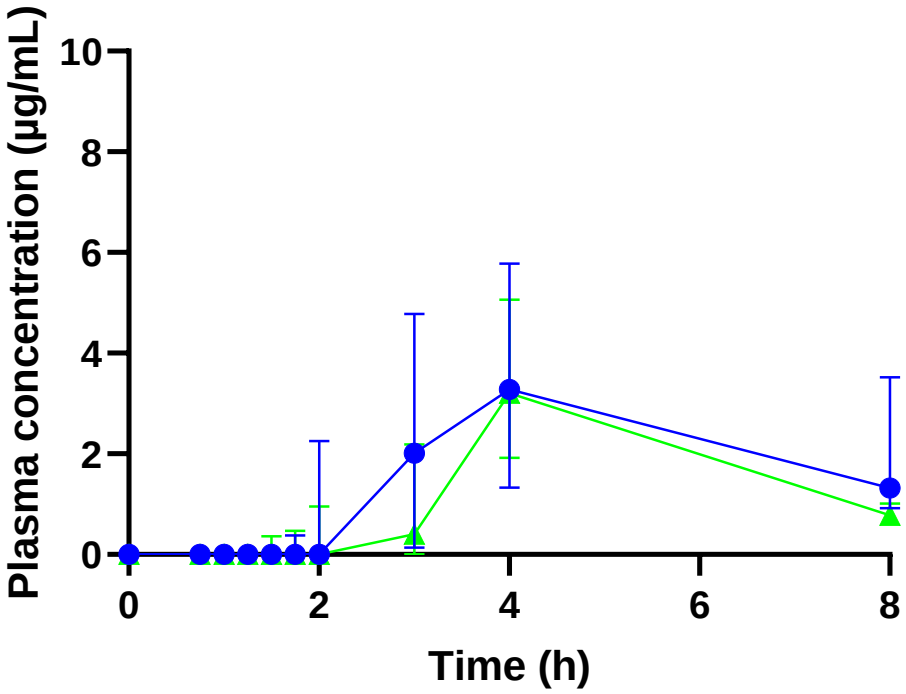

Figure 30. CorA plasma concentration time profiles in fed Beagle dogs. PO administration of CorA-povidone (●) and CorA-copovidone (▲) (75 mg), administered as an enteric capsule (median ± IQR, n=4 per group).

Table 23. PK parameters after PO administration of CorA-ASD enteric capsules comprising CorA-povidone and CorA copovidone granules (75 mg) in fed Beagle dogs (median ± IQR, n=4 per group).

	$AUC_{0\text{-}inf}$ (µg*h/mL)	**$AUC_{0\text{-}inf}$ per mg/kg dose (µg*h*kg/dose)**	**C_{max} (µg/mL)**	**t_{max} (min)**	**$t_{1/2}$ (h)**	**BA (%)**
CorA-povidone	31.6 (23.5-53.2)	2.7 (2.4-3.9)	8.8 (6.9-9.2)	240 (210-300)	8.42	25
CorA-copovidone	24.8 (15.9-29.3)	1.9 (1.3-2.3)	3.2 (2.1-5.1)	240 (240-300)	1.80	14

Beside a delayed release, potential options regarding sustained release formulations were investigated. Therefore, HPMC-based matrix tablets were administered. Even though, *in vitro* dissolution studies (**Chapter 5.1.5**) revealed sustained release profiles of up to 8 h, the plasma concentration time profile of CorA-povidone showed a rather immediate release profile with a specific C_{max} of 40.3 µg/mL after 75 min. Interestingly, the interindividual exposure variability was lower compared to the capsule formulation demonstrating consistent *in vivo* dissolution of the tablets. In case of CorA-copovidone,

the profile tended to follow sustained release kinetics, resulting in a low C_{max} (16.0 µg/mL) after 135 min. The species dog is not an appropriate model for oral sustained release dosage forms. First, the gut length and thus, the intestinal transit times are shorter compared to human [147]. This reduces the absorption window for dissolved drug. Second, the pressures within the GIT are reported to be higher in dogs, which is important for dosage forms based on their structures, such as matrix based tablets [147]. Presumably, the peristaltic forces *in vivo*, induced a faster disintegration for the CorA-povidone tablet and drug release [147]. However, considering the physiological differences and demonstrated *in vitro* sustained release profiles, these results were promising, as BAs were at the same level for CorA-copovidone (36%) and even higher for CorA-povidone (51%) than for the capsules (in the fasted state). In HPLC measurements no pronounced isomerization was detected, although acidic stomach conditions were induced by a pentagastrin pre-treatment. Since *in vitro* dissolution resulted in appropriate sustained release kinetics and adequate BAs were confirmed *in vivo*, sustained release HPMC-based matrix tablets were proven to be valuable principles for controlled release and are worthy to be tested in human clinical studies.

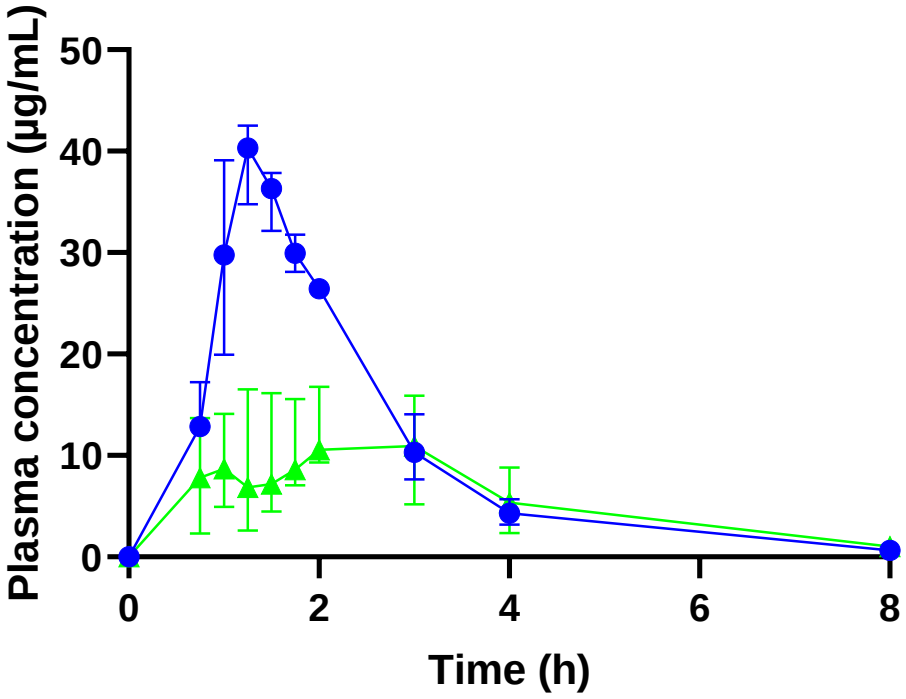

Figure 31. CorA plasma concentration time profiles in fasted Beagle dogs. PO administration of two CorA-povidone/HPMC tablets (●) and two CorA-copovidone/HPMC tablets (▲) (100 mg), (median ± IQR, n=4 per group).

Table 24. PK parameters after PO administration of two CorA-povidone/HPMC tablets and CorA-copovidone/HPMC tablets (100 mg) in fasted Beagle dogs (median ± IQR, n=4 per group).

	$AUC_{0\text{-}inf}$ (µg*h/mL)	**$AUC_{0\text{-}inf}$ per mg/kg dose (µg*h*kg/dose)**	**C_{max} (µg/mL)**	**t_{max} (min)**	**$t_{1/2}$ (h)**	**BA (%)**
CorA-povidone/HPMC	87.8 (83.1-91.3)	5.9 (5.3-7.0)	40.3 (36.4-42.5)	75 (75-82.5)	1.48	51
CorA-copovidone/HPMC	63.9 (56.7-70.6)	4.9 (4.3-5.3)	16.0 (15.7-21.4)	135 (78.75-180)	7.18	36

Prior to a 7-day exploratory toxicology study, the planned vehicle PEG 200, was tested in the PK study. Despite PEG 200 was expected to be well tolerated, discomfort (vomiting observed in three animals) was observed upon administration of a CorA-PEG 200 solution. Likewise, the vehicle without CorA was not tolerated by the dogs. Due to vomiting, plasma sampling was not able to reflect C_{max}, t_{max} and $AUC_{0\text{-}inf}$ correctly and are not reported. Instead, mesoporous silica, administered as an oral suspension in water, was tested within

this PK study to evaluate the potential to be an alternative for toxicological studies (**Figure 32 and Table 25**). The drug load of this formulation was 50%. Higher dose levels (200 and 100 µg/mL) compared to the other study groups were used in accordance to a toxicology study setup. For both, high plasma levels were rapidly achieved, while the lower dose exhibited a C_{max} of 183.1 µg/mL after 1 h. Likewise, for the higher dose 185.4 mg/mL was observed after 1.25 h and further increased up to a C_{max} of 212.1 mg/mL after 3 h. The high concentrations were maintained for approx. 2 h, whereas the plasma concentration dropped after reaching the C_{max} for the lower dose group. A second increase after 1.75 h indicated a continuing drug release and absorption. The fact, that for C_{max} no clear differences were detected between 200 and 100 µg/mL might be solubility and permeability related and thus, the fast and high intestinal absorption was not able to be increased in a dose dependent manner. In contrast, exposure was further increased for the higher dose indicating a prolonged release and absorption process for at least 4 h. Even though, the maximum of dissolvable drug was reached, the undissolved part remained in the silica pores and served as a solubility improved reservoir which was able to replace absorbed drug molecules. At the low-dose, the reservoir function was exhausted more rapidly. In sum, despite high administered doses, high exposures and thus, high BAs were achieved (200 mg/mL: 92%; 100 µg/mL: 59%). Despite ascending dose levels, exposure did not decrease. This fact qualified the mesoporous silica as suitable vehicle for toxicology studies.

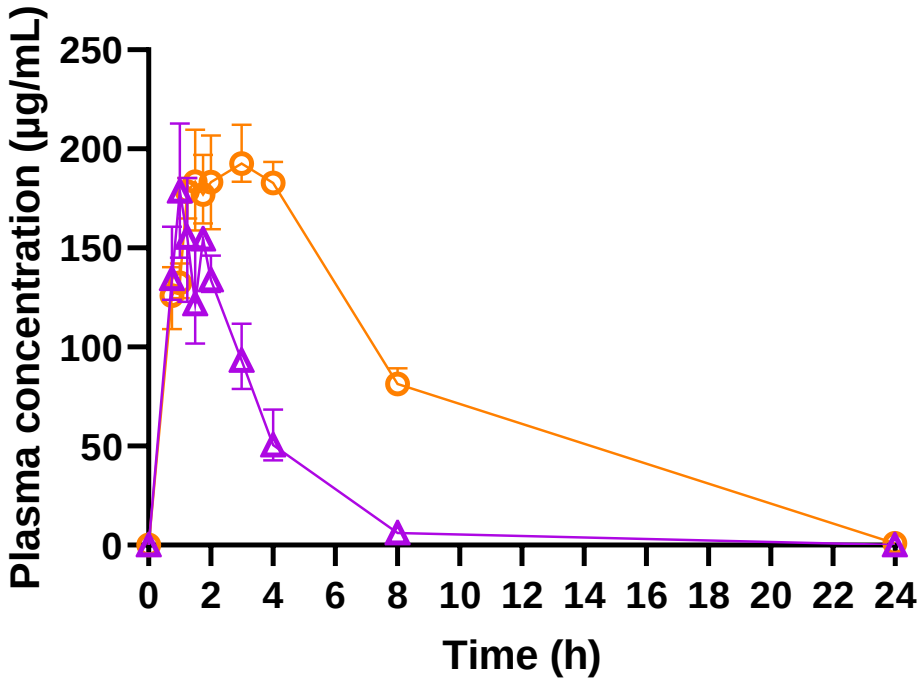

Figure 32. CorA plasma concentration time profiles in fasted Beagle dogs. PO administration of CorA silica with the doses of 200 mg/kg (○) and 100 mg/kg (Δ) (100 mg), (median ± IQR, n=4 per group).

Table 25. PK parameters after PO administration of CorA-silica with the doses 200 mg/kg and 100 mg/kg in fasted Beagle dogs (median ± IQR, n=4 per group).

	$AUC_{0\text{-}inf}$ (µg*h/mL)	**$AUC_{0\text{-}inf}$ per mg/kg dose (µg*h*kg/dose)**	**C_{max} (µg/mL)**	**t_{max} (min)**	**$t_{1/2}$ (h)**	**BA (%)**
CorA-silica 200 mg/kg	1888.8 (1795.8-1989.5)	10.4 (9.9-11.0)	212.2 (202.3-227.6)	135 (90-180)	2.74	92
CorA-silica 100 mg/kg	611.8 (515.9-726.7)	6.7 (5.7-8.0)	183.1 (145.2-219.5)	60 (56.25-71.25)	1.86	59

8.1.5 *In Vitro In Vivo* Relationship

A level C *in vitro-in vivo* relationship was performed by correlating the end points of the organic phase of the mouse biphasic dissolution with the BA of neat CorA and CorA-ASD formulations (**Figure 33**) [148]. The resulting correlation coefficient was 0.9966 demonstrating the good predictability of CorA and CorA formulations of the mouse-specific biphasic dissolution setup.

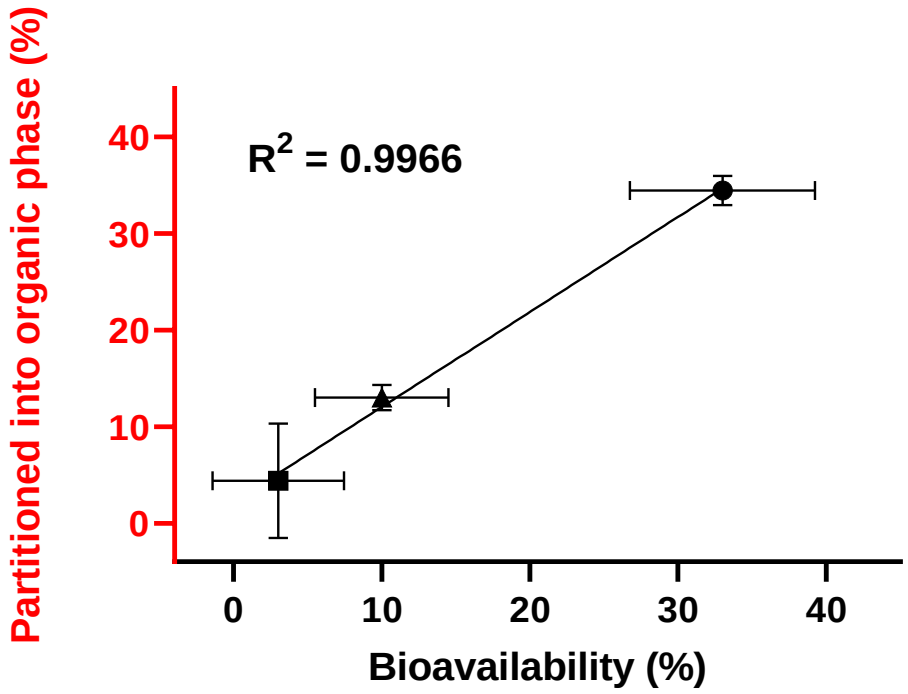

Figure 33. Correlation of *in vitro* fraction partitioned into the organic phase after 80 min, determined by the mouse-specific biphasic dissolution (**Chapter 7.1.1**), and *in vivo* BA of neat CorA (■), CorA-povidone (●) and CorA-copovidone (▲) administered as aqueous suspension in BALB/c mice (**Chapter 8.1.1**).

While mouse dissolution could be successfully correlated to BA values, the BA in rats was underestimated for both ASD formulations. However, the PK studies revealed high interindividual variabilities regarding BA (IQR of 29% and 31%, respectively) resulting in median BAs of > 100%. Even though, this *in vivo* phenomenon could not be clarified so far, several aspects might have favoured this result. The fact that each experimental group comprised only four animals which have not been used for multiple administrations, certainly impaired a comparison between the administration groups. Moreover, for the IV administration the dose had to be reduced from 36 to 18 mg/kg due to solubility limits of CorA in the vehicle, which caused further uncertainty. At this point, the influence of processes like saturation of metabolic processes or enterohepatic circulation, which potentially increased oral BA could not be excluded [149]. Nevertheless, the *in vitro* dissolution setup indicated that both ASD exhibit comparable *in vivo* performances, despite the better aqueous dissolution of CorA-povidone.

The biphasic dog dissolution overestimated the *in vivo* measured median BA. Similar to the rats, the interindividual variability of BA was high (IQR of 26%). Thus, a final cross-

species evaluation of the predictability remains imprecise. As disintegration of the capsule was a relevant factor for time and site of drug absorption it was assumed that this might have caused these high variabilities.

8.2 Summary

The PK characteristics of CorA and CorA formulations were tested in several preclinical species. By using the ASD formulation principle, it was possible to improve *in vivo* BA. The differences between CorA-povidone and CorA-copovidone observed in mice were negligible in rats and dogs. It was found that absorption depended on dissolution, which in turn depended on pH conditions in the GIT. Acidic environment in mice limited drug dissolution and absorption, while higher pH values in rat GIT led to improved BAs. Availabilities of the solid oral drug products (capsule and tablet) were demonstrated in dogs and both approaches represented promising options for clinical phase I trials. Both, IV and PO administrations were valuable inputs for a cross-species PBPK model and are used for the CorA PBPK model, comprehensively described in **Chapter 10**. In addition, vehicles for exploratory toxicology studies were investigated in terms of BA. Both, the PEG 200 solution for rats and the mesoporous silica suspension approach for dogs showed high intestinal absorption and confirmed their suitability.

9. Cell Culture Experiments with Regard to the Active Efflux of CorA

Oral BA can be influenced by interactions with efflux transporters, such as P-gp and BCRP, which are present in the intestinal epithelial membrane [150]. Absorbed drug molecules can be actively transported back into the intestinal lumen reducing the fraction absorbed. Co-administrations with other inhibitors could lead to interactions (e.g., verapamil) that potentially increase the fraction absorbed [151]. Species differences in transporter expression and activity, challenge the translation of data from preclinical species to humans [152]. Instead, *in vitro* cell experiments are able to support the identification of potential transporter compounds and can be integrated into PBPK models to improve predictions for human PK.

As the AP suggested CorA to be a P-gp substrate, the aim was to detect potential interactions, such as active transport with P-gp and BCRP or inhibition of P-gp, to detect possible effects on intestinal absorption. Therefore, CorA was investigated using P-gp or BCRP overexpressing cells to detect, whether CorA is influenced by these transporters. Moreover, potential P-gp inhibition by CorA was tested by the determination of accumulation kinetics of a well-known substrate of P-gp.

9.1 Results and Discussion

9.1.1 Influence of Active Intestinal Transport of CorA via P-gp and BCRP

For substrates of P-gp and BCRP, respectively, the ratio of accumulation of the compound was at least over two-times higher in the parental cells, in comparison with the cells overexpressing these efflux transporters (**Figure 34**). No differences were observed between the accumulated CorA in the different cells, measured as fluorescence intensity, for all tested concentrations (0 – 1.0 µM). In case of a P-gp or BRCP substrate, respectively, the transporters would efflux the compound resulting in lower accumulation. This efflux is pronounced in cells overexpressing these transporters. As this effect was not visible for CorA no active efflux of CorA was expected. Thus, there were no signs of active transport of CorA via P-gp and BCRP influencing the intestinal absorption.

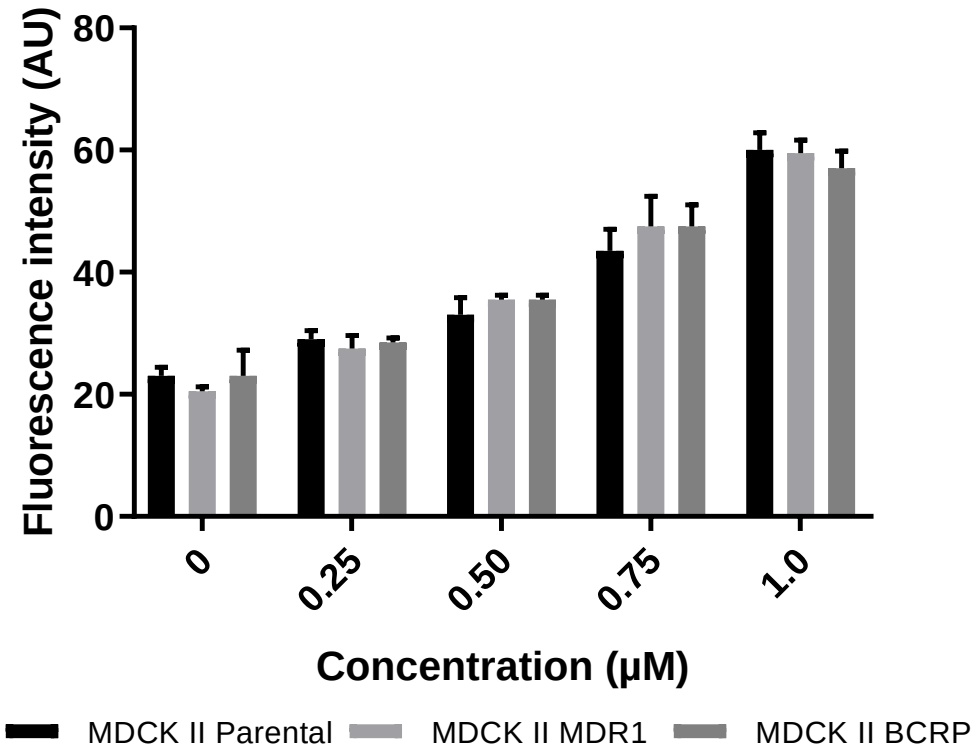

Figure 34. Fluorescence intensities (arbitrary unit; AU) of the cells in the presence of different CorA concentrations (0, 0.25, 0.50, 0.75 and 1.0 µM). The black bars represent the parental cells (MDCK II Parental), the light grey bars represent the cells with an overexpression of P-gp (MDCK II MDR1) and the dark grey bars represent the cells with an overexpression of BCRP (MDCK II BCRP) (mean ± SD, n = 3).

9.1.2 Investigation of the Interaction with P-gp Inhibitors

Hoechst 33342 is a well-known substrate of P-gp interacting with the H-binding site of P-gp (a suspected P-gp substrate binding site on the transporter) [130,153]. Therefore, the accumulation kinetics were investigated in the absence and presence of CorA at concentrations of 3.16 µM and 10 µM) (**Figure 35**). An altered kinetic profile would indicate an inhibition by CorA. For all investigated concentrations of Hoechst 33342, the presence of CorA did not affect the uptake as no change in kinetics was observed. The *k* value (rate constant), as well as, the span (plateau-Y0) showed no changes in the samples without and with CorA. These results confirmed that there is no interaction between CorA and the H-binding site.

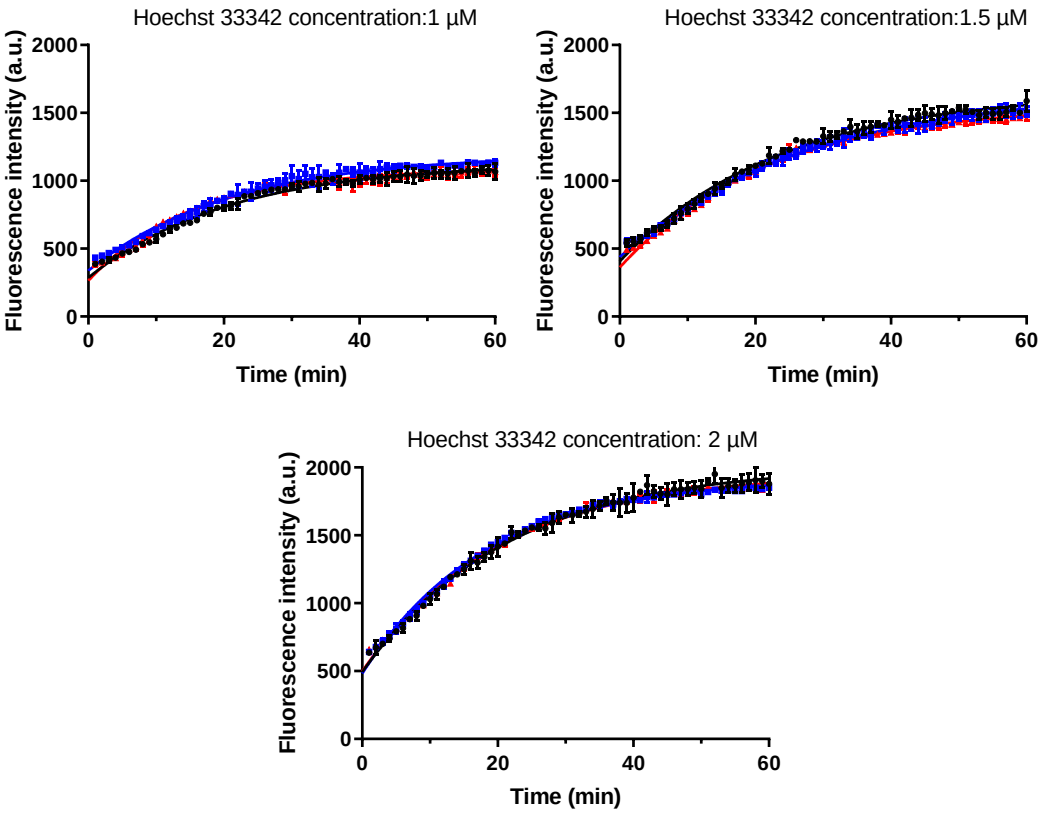

Figure 35. Accumulation kinetics of Hoechst 33342 alone and in the presence of CorA. Three different concentrations of Hoechst 33342 were incubated alone or together with CorA at different concentrations. (●) no CorA, (■) CorA concentration of 3.16 µM and (▲) CorA concentration of 10 µM (mean ± SD, n = 3). Lines were fitted using the one-phase association fit.

9.2 Summary

Despite the *in silico* prediction of CorA presenting a P-gp substrate, *in vitro* cell measurements indicated no influence on intestinal absorption. A further intestinal transporter, BCRP, was similarly excluded as influencing factor. Moreover, CorA was excluded as inhibitor for P-gp substrates of the H-binding site, demonstrated in accumulation assays with the P-gp substrate Hoechst 33342. Accordingly, no intestinal transporter interactions were considered for the PBPK model (**Chapter 10**). Good *in vitro* permeability has been reported for CorA (apparent permeability: $2.0*E^{-5}$ cm/s; measured in Caco-2 cells) and absorption was expected to be not permeability limited. [140].

10. PBPK Modeling in Preclinical Development of CorA

Oral drug absorption is a complex interplay which can be influenced by various factors such as disintegration, dissolution, supersaturation, precipitation, re-dissolution and drug permeability, as well as, parallel food intake [154]. Further physiological relevant factors such as transporters, metabolism in the gut wall and liver may affect subsequent PK performances. Among other things, a PBPK model is able to combine drug and formulation dependent physicochemical properties with physiological relevant conditions to predict PK profiles in plasma and tissues. This *in silico* approach enabled several opportunities of utilization: Prediction of PK behavior in human and preclinical species, drug-drug interaction risk assessment, a better understanding of the ADME profile of drug candidates, influence of food effects, parameter sensitivity analysis and predictions in special populations such as pediatrics, pregnancy and different ethnicities or bioequivalence studies [88,155,156].

Typically, the drug development of an antibiotic is a time consuming process which takes several years from identification to the entry into phase I clinical trials [7]. In contrast, the need for treatment options against NTDs remains high. Limited attention for this diseases makes it all the more important to translate the knowledge gained during preclinical drug development into novel approaches to improve public health [157]. Beside recommendations from regulatory guidelines on the use of state-of-the-art modeling to mitigate the risk for FIH and early clinical trials, PBPK-modeling represents a valuable approach to combine *in vitro* and *in vivo* information to get the most out of clinical trials [158]. Typically, the “top-down” approach uses existing clinical data to characterize potential impact factors on PK [129]. This opportunity is obviously not applicable during preclinical phases. At this stage, the great challenge is to estimate a successful treatment including the required efficacious dose and dose regimen for human administration. However, preclinical data regarding e.g., efficacy, ADMET-profile and animal-PK can be used to build a PBPK-model from the bottom to provide a time- and cost-effective approach for these estimates of human performances. As part of the PBPK-modeling approach, the PBBM strategy focuses on a mechanistic understanding of *in vivo* drug release, taking the formulation impact into account [159]. For CorA, currently under preclinical investigations, this strategy was applied. Thus, a target unbound concentration

was deduced, based on the *in vitro* determined MIC. The enabling oral formulations were used for implementation to the model. Combining these information gives a rational approach to support the following questions of which dose, which formulation and which dose regimen is required to reach the goal of a successful treatment prior initial human studies. Preclinical animal studies allowed extrapolations towards human regarding physiological parameters (e.g., clearance and distribution). To improve the accuracy of a human oral PK prediction, it was crucial to first implement and optimize a sound model for preclinical species [160].

The aim was to build a PBPK model that predicts the PK behavior of CorA and CorA-formulations in the preclinical species mouse, rat and dog. Hence, the goal was to understand physiological parameters such as clearance and distribution of CorA as well as evaluating crucial factors for oral absorption. Data describing the physicochemical properties and the physiology of the investigated species were obtained from *in vitro* studies and from estimates calculated by the AP. At early phases of the preclinic, PK investigations were conducted in mice. *In vitro* biorelevant dissolutions were performed and integrated into the PBPK model to assess the relevance of dissolution on PK. Within preclinical investigations, further species were tested. This enabled a cross-species model for CorA including both IV and PO administrations. The objective of this modeling strategy was to build a PBBM allowing a FIH performance prediction. The PBBM was validated based on the preclinical observed PK profiles in mice, rats and dogs to predict CorA exposure in human. Furthermore, the model was used to predict free drug concentration in tissues following the administration of formulation prototypes to define at which dose and dose regimen the half maximal inhibitory concentration (IC50) of CorA will be achieved and maintained for sufficient time. The IC50 represents the *in vitro* measured concentration that is needed to inhibit the growths of 50% of the *Wolbachia*.

10.1 Results and Discussion

10.1.1 PBPK Model – Mouse

10.1.1.1 Input Parameter

Table 26. Physicochemical, biopharmaceutical and physiological properties to perform PBPK simulations for the species mouse.

Input Parameter	Value/Selection User Defined	Value/Selection Default Settings	Reference
Physicochemical Properties			
Molecular weight (g/mol)	527	527	[108]
pKa	3.6	5.1	[108]
logP	5.4		[108]
Biopharmaceutic Properties			
Caco-2 Papp (cm/s x E10)	2.0		Experimentally given
Dose Volume (mL)	0.2		Experimentally given
pH at reference solubility	1		
Solubility at reference pH (mg/mL)	0.00011		[108]
Mean Precipitation Time (s)	900	900	Default
Biorelevant in vitro solubilities: Solubilization Ratio	$2.40x10^6$ (CorA-povidone) $1.31x10^6$ (CorA-copovidone)	$3.44x10^5$ (CorA-povidone) $3.44x10^5$ (CorA-copovidone)	Experimentally given
Fraction plasma unbound (%)	0.1		Experimentally given
Blood/plasma concentration ratio	0.75	0.75	Predicted by AP
Body weight mouse (kg)	0.02	0.02	Experimentally given
Clearance (L/h)	0.006		Experimentally given
Volume of distribution (L)	0.016		Experimentally given
ACAT™ Model Parameters:			
Gut physiology	Mouse - Physiological - Fed	Mouse - Physiological - Fed	

10.1.1.2 Mouse Monophasic Dissolution

Dissolution profiles of CorA-ASD formulations with a Weibull function fit were generated (**Figure 36**) according to **Chapter 4.5.3**. CorA-povidone showed an initial dissolution of 70% at pH 3.0 meeting an equilibrium at 65% until the end of dissolution (**Table 27**). At pH 3.0 CorA-copovidone achieved 8% of dissolved drug that increased to 16% by the end of the dissolution. Weibull-parameters, obtained by this non-sink *in vitro* dissolution, were determined as input parameter for the mouse PBPK model.

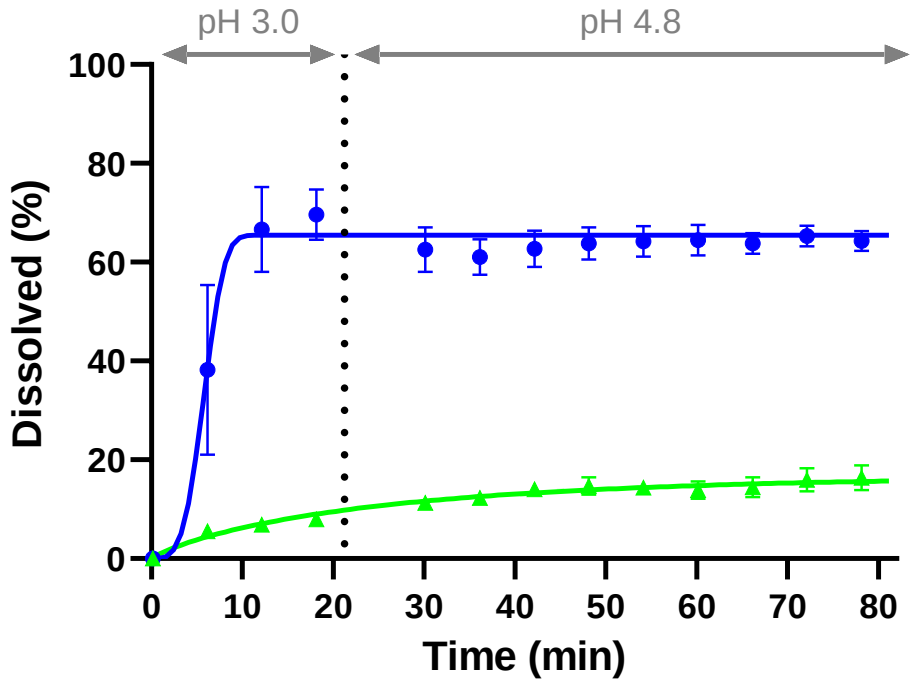

Figure 36. Monophasic dissolution experiment of CorA-povidone (●) and CorA-copovidone (▲) under biorelevant conditions. Lines represent the Weibull fit.

Table 27. Weibull parameters of CorA-povidone and CorA-copovidone, determined using the biorelevant monophasic dissolution setup.

Weibull Parameter	**CorA-povidone**	**CorA-copovidone**
Maximum of released API (%)	65.43	16.78
Time lag (h)	0	0
Shape factor	3.73	0.85
Time scale (h^b)	2×10^{-4}	0.47
R^2	0.92	0.92

The IV data, reported by Krome et al. [108], were used to set the elimination (hepatic clearance) and distribution (volume of distribution) behavior and were modelled to best fit the observed data. Physicochemical and physiological properties were generated by the AP and replaced by *in vitro* results where possible. This status quo represented the starting point for the model for the oral administration of CorA-ASD formulations. In a first step biorelevant solubilities experimentally determined (**Chapter 5.1.6**), were incorporated into the model. **Figure 37A** shows the results of the PBPK modeling for the IV administration of CorA that almost perfectly matched the observed data. The PO administration of CorA-ASD-formulations based on *in vitro* measured solubility, but without the incorporation of *in vitro* dissolution profiles (**Figure 37B**). However, this model was not able to predict the plasma concentrations adequately resulting in a C_{max} underprediction (27.44 µg/mL) for CorA-povidone, while $AUC_{0\text{-}inf}$ (64.64 µg*h/mL) was overpredicted. The prediction for CorA-copovidone led to an overprediction of C_{max} (20.43 µg/mL) and $AUC_{0\text{-}inf}$ (56.60 µg*h/mL). The models were not able to match t_{max} indicating a too slow dissolution process. Moreover, the differences observed *in vivo* were not predicted by the models as biorelevant solubilities of CorA-povidone and CorA-copovidone were too close. Thus, dissolution was assumed to be a relevant factor for the PK of CorA-ASDs. By incorporating the dissolution profiles of the monophasic dissolution, the predictions of the models were improved in terms of C_{max} and $AUC_{0\text{-}inf}$ (**Figure 37C**). For CorA-povidone, PEs were <15% (C_{max}: 1.71%; $AUC_{0\text{-}inf}$: -11.31%) (**Table 28**). For CorA-copovidone C_{max} and $AUC_{0\text{-}inf}$ were slightly overpredicted (C_{max}: -16.20%; $AUC_{0\text{-}inf}$: -12.43%), which were in an acceptable range. In addition, predicted t_{max} matched the observed PK-profiles for both formulations. Consequently, the integration of the measured mouse-specific dissolution parameters enabled PBPK models showing sound predictions for plasma concentrations of CorA-ASD formulations. A PE ≤ 16% in mice was considered to be successful, as predictions in mice are challenging due to difficult oral administration and limited information about mouse physiology. These results deduced that dissolution was the decisive factor for CorA formulation in mice, which was identified as the rate-limiting step for absorption, even though CorA-ASD formulations showed no solubility issues or occurrence of precipitation. Thus, the relevance of species-specific *in vitro* tools was reaffirmed and provided a more comprehensive understanding of the absorption of CorA and CorA-ASD formulations. In sum, combining appropriate *in vitro*

and *in silico* tools can be used as a valuable option for early formulation screening to reduce animal trials and drug substance consumptions.

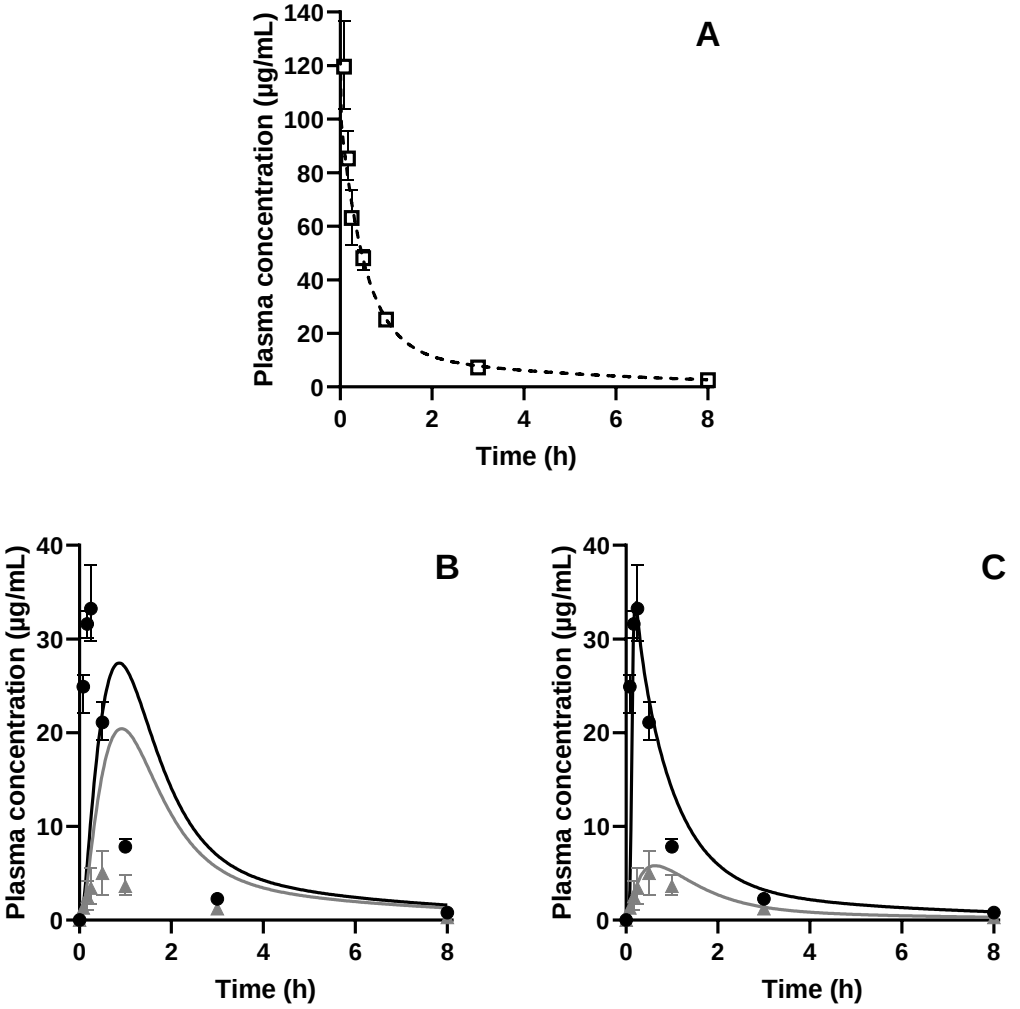

Figure 37. Observed and predicted plasma profiles of CorA in BALB/c mice (n = 4 per group); (**A**): Dashed line represents the prediction of IV administration (**B**): Lines represent the prediction of PO administration of CorA-povidone (black) and CorA-copovidone (grey), based on immediate release; (**C**): Lines represent the prediction of PO administration of CorA-povidone (black) and CorA-copovidone (grey), based on dissolution data; (□) represents observed data following the IV administration, (●) represents observed data following PO administration of CorA-povidone and (▲) represents observed data following PO administration of CorA-copovidone, respectively.

Table 28. Observed and predicted values of C_{max} and $AUC_{0\text{-}inf}$ of CorA-povidone and CorA-copovidone after oral administration.

Parameters	**CorA-povidone**				
	Observed	Predicted (w/o dissolution)	PE (%) (w/o dissolution)	Predicted (w/ dissolution)	PE (%) (w/ dissolution)
C_{max} (µg/mL)	33.24	27.43	21.18	33.80	-1.68
$AUC_{0\text{-}inf}$ (µg*h/mL)	41.83	64.63	-54.51	46.44	-11.02
Parameters	**CorA-copovidone**				
	Observed	Predicted (w/o dissolution)	PE (%) (w/o dissolution)	Predicted (w/ dissolution)	PE (%) (w/ dissolution)
C_{max} (µg/mL)	5.00	20.43	-308.60	5.80	-16.00
$AUC_{0\text{-}inf}$ (µg*h/mL)	13.35	56.60	-323.97	15.00	-12.36

10.1.2 Preclinical PBBM Model

10.1.2.1 Modeling Strategy

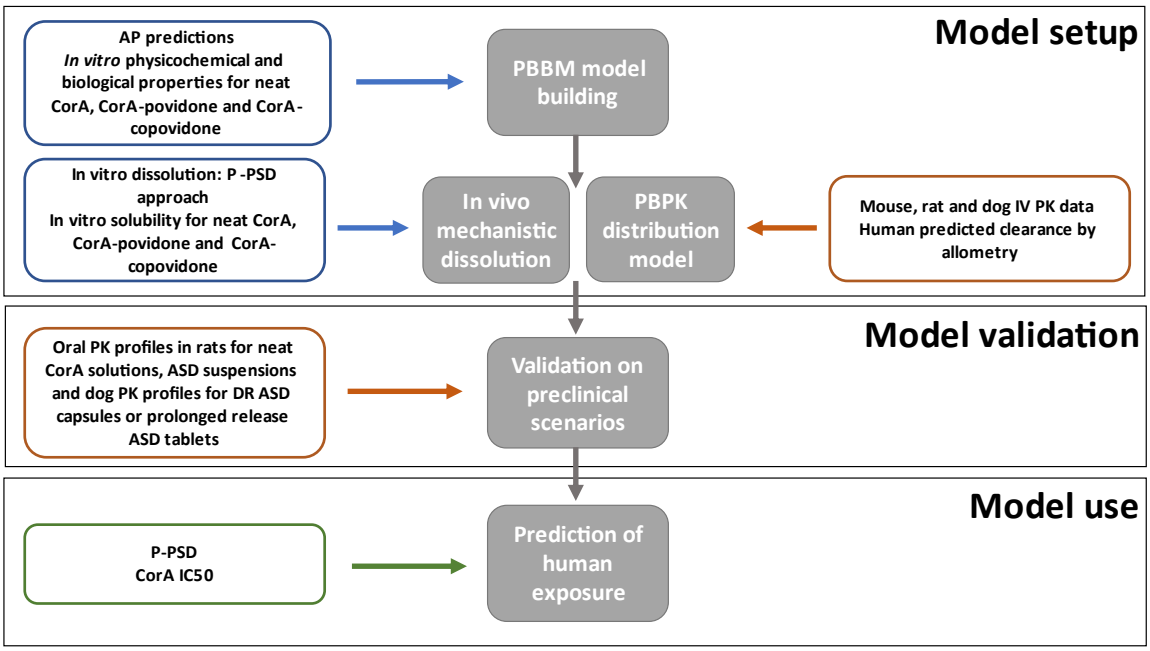

Figure 38. Modeling strategy of PBBM model for human predictions.

The modeling strategy of the built PBBM model is summarized in **Figure 38** and describes a mechanistic procedure for a first prediction of human performance. Physicochemical and biopharmaceutical properties measured either *in vitro* or predicted via the AP were

used as input parameters to generate the base model. Preclinical IV data were used to estimate human metabolic clearance by allometric extrapolation. CYP 2C9 was predicted to be the major enzyme responsible for CorA metabolism. Thus, the *in silico* prediction of Michaelis-Menten constant (Km) for CYP2C9 was integrated to the human model and the corresponding V_{max} was fitted to match the hepatic clearance, predicted from allometry. A PBPK model was applied based on the Lukacova model to calculate plasma partition coefficients. This model is provided by the software. Further models, also provided by the software, were tested, but did not lead to suitable predictions. For the integration of the CorA-ASD dissolutions, the mechanistic P-PSD approach was used as proposed by Pepin et al. [161]. In the next step, the model was validated with PK data of oral administrations in rats and dogs. The P-PSD approach was retained for fitting the observed dissolution for the formulations and to generate a batch specific input to the model. Subsequently the model was applied to predict plasma concentrations following an oral administration of a 100 mg CorA-povidone capsule and tablet, respectively. Moreover, ascending dose levels (100 – 600 mg) were predicted with two administrations per day, bis in die (BID), of the CorA-povidone tablet in fasted and fed state, respectively.

10.1.2.2 Input Parameters

Table 29. Input Parameters used for CorA PBBM model development.

PBPK Parameter	Value CorA	Rationale/Reference(s)
1. Physicochemical and Binding Properties		
Molecular mass (g/mol)	527.66	From structure
Type of drug substance	Drug is amorphous, but its honey like properties (neat CorA) does not allow pharmaceutical processing	
Log P	5.4	Measured [108]
pKa	3.7 (A)	Measured [108]
Precipitation time (s)	Mechanistic model Lindfors Lambda = 1 µm Sigma = 0.022 $J.m^{-2}$	
Intrinsic solubility (mg/mL)	Neat: 1.1E-4 (pH=1) Povidone-ASD: 0.052 (pH=1) Copovidone-ASD: 0.033 (pH=1)	Measured [108]
FaSSIF solubility (mg/mL)	Neat CorA: 0.25 (±0.06) CorA-povidone: 1.24 (±0.04) CorA-copovidone: 1.40 (±0.14)	Measured [162]
Human blood-to-plasma ratio (R_{bp})	0.75 (Mouse/Rat) 0.65 (Dog/Human) 0.003 (Human)	APv10.3
F_u, plasma	0.005 (Rat) 0.013 (Dog) 0.001 (Mouse)	Measured [140]
2. Absorption		
Human effective jejunal permeability (P_{eff}) (×10^{-4} cm/s)	2	Measured [140] See **Chapter 10.1.2.10**
Dissolution model	Johnson	Default, using P-PSD for each batch fitted in 10.3.1.12
3. Distribution		
Method	Full body PBPK, Lukacova method of K_p prediction for all tissues	GastroPlus default approach
4. Metabolism		
CYP2C9 K_m (mg/l)	2.77	APv10.3
PBPK CYP2C9 V_{max} (mg/s/mg-enz)	0.006949	Fitted to an apparent human liver clearance of 2.34 L/h
Gut CYP3A4 V_{max} (mg/s)	0	No gut extraction is anticipated consistently with animal data

10.1.2.3 Solubility vs pH

Due to its vinylogous carboxylic acid structure the solubility of CorA was demonstrated to be highly pH-dependent [108]. Since dissolved CorA itself acts as an acid, the surface pH was assumed to be lower compared to the bulk pH resulting in an altered solubility profile of CorA. This resulted in a pH difference of 2.3 at pH 7.5 between bulk and calculated surface pH. Calculations based on the equations proposed by Pepin et al. [161]. The calculated surface pH was used to estimate surface solubilities for different bulk pH conditions. **Figure 39** depicts the measured bulk solubilities in comparison to the adjusted surface pH.

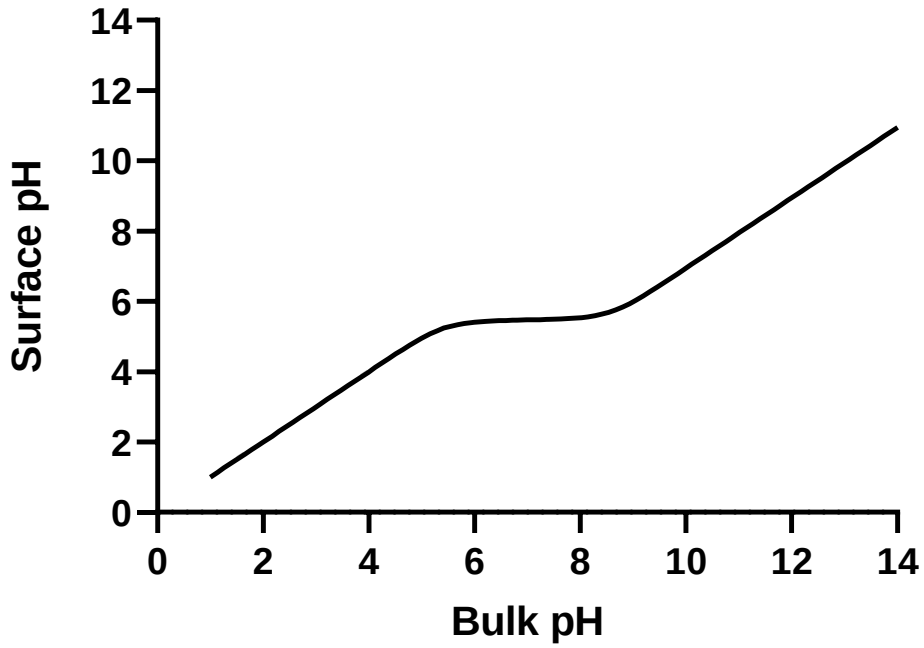

Figure 39. Surface pH vs bulk pH for CorA.

As low intrinsic solubility of CorA was determined (0.11 µg/mL at pH 1) no differences in surface solubility was assumed at pH < 4. Thus, calculated surface solubilities were equal to the measured ones. At pH values close to the pKa an acid base reaction takes place following **Eq. 7** in accordance to the monovalent acidic moiety of CorA.

$$A^{\square} + OH^{-} = A^{-} + H_2O \qquad \textbf{(7)}$$

The molecularly dissolved CorA at the surface likely influence the surface pH and the surface solubility was expected to be lower at pH > the pKa. This led to a solubility profile

plateau between pH 5 and 8. In general, this range is of utmost importance for *in vivo* dissolution as it covers the conditions in animal and human intestine. Therefore, the adjusted solubilities were used as solubility input for the PBBM model.

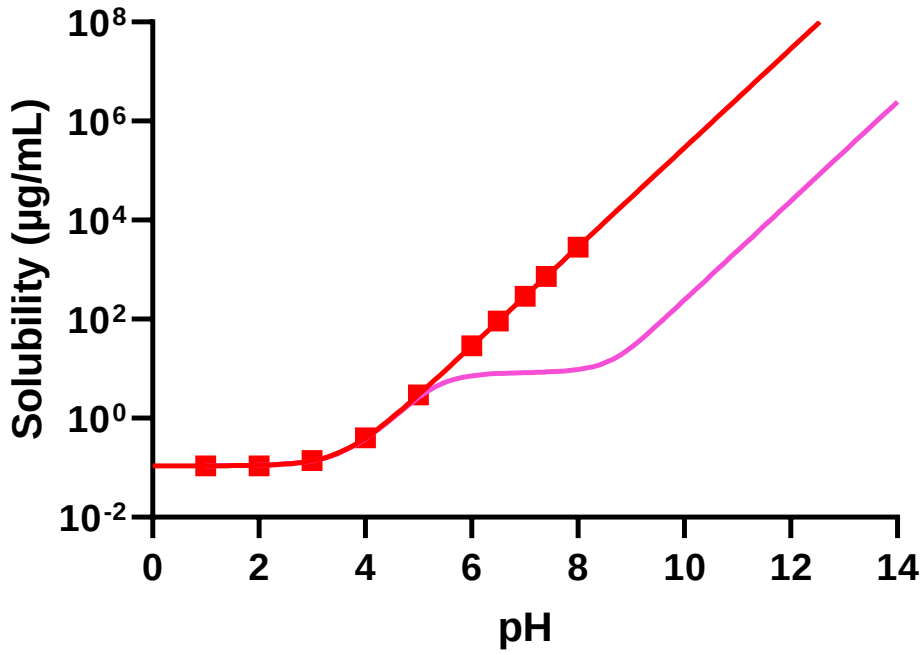

Figure 40. Solubility vs pH of neat CorA. The measured solubilities [108] (■) were used to extrapolate the bulk solubility (-). The pink line represents the calculated surface solubility of CorA (-).

10.1.2.4 LogD vs pH

The logD vs pH profile was reported by Krome et al [108]. For the PBBM model the empirical logD vs pH model was changed and the logP (neutral) – logP (anion) coefficient was adjusted to 4 to match observed data.

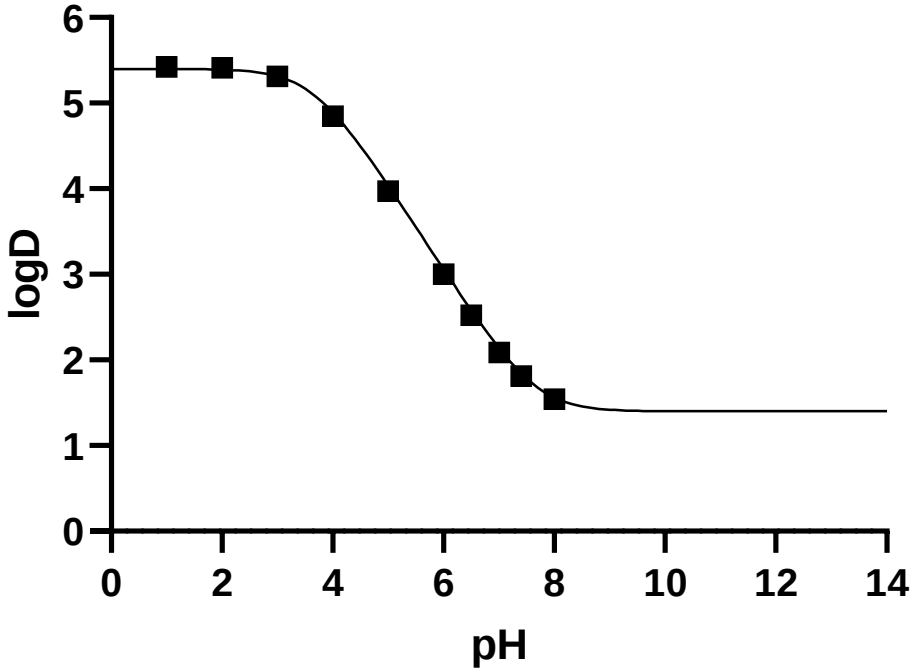

Figure 41. LogD vs pH of CorA. (■) represents the measured logD values and the line the adjusted profile for the PBBM model.

10.1.2.5 Intrinsic Dissolution

The ASD formulation principle was proven to improve solubility and dissolution properties of CorA. Intrinsic solubilities of the spray dried CorA-povidone and CorA-copovidone, respectively were used for the model of the amorphous formulations. **Figure 42** shows a setup to determine precipitation in 0.1 N HCl at pH 1. The first concentration measurement after 5 min was used for the model set at 52 µg/mL for CorA-povidone and 33 µg/mL for CorA- CorA-copovidone. Accordingly, the surface pH solubility profiles were adjusted for CorA-ASD formulations and used for the PBBM and P-PSD approach. The profiles are presented in **Figure 43**.

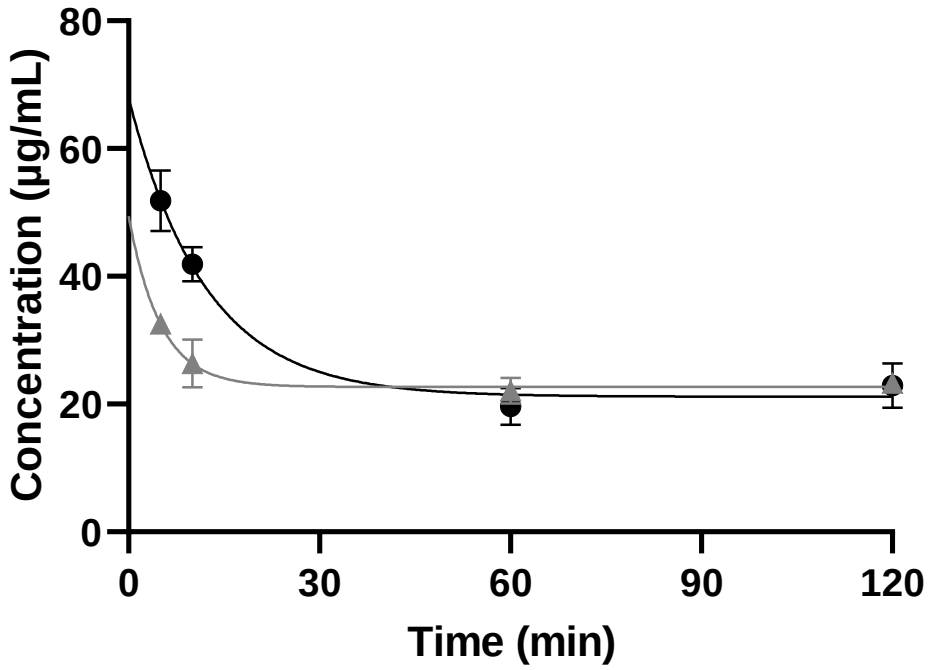

Figure 42. Precipitation of CorA-povidone dispersion (●) and CorA-copovidone dispersion (▲) at pH 1.

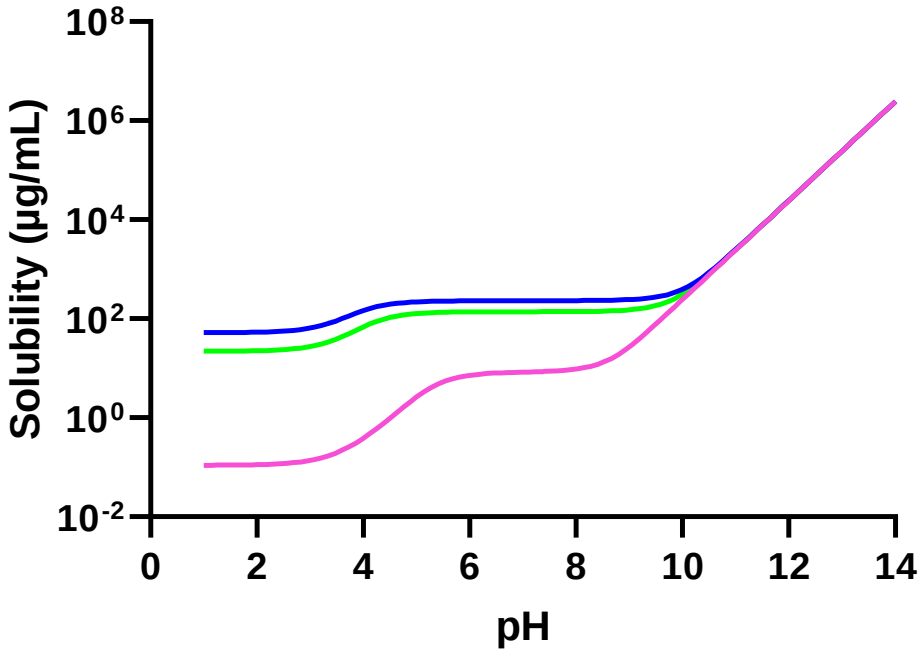

Figure 43. Predicted surface solubility vs pH profile for neat CorA, CorA-copovidone ASD and CorA-povidone ASD at 37°C. The pink line represents the calculated surface solubility of neat CorA (-), the blue line represents the calculated surface solubility of CorA-povidone (-) and the green line represents the calculated surface solubility of CorA-copovidone (-).

10.1.2.6 Effect of Bile Salts

In vivo drug release and the interplay between supersaturation and precipitation may be influenced by the presence of bile salts. The PBBM addresses this effect by using a solubilization ratio factor. This value is obtained by using solubilities in FaSSIF and FeSSIF. The measured solubilities for CorA were used to predict the effect of bile salts for rats (where CorA was administered as a solution). Since the affinity to bile salt micelles is a molecular property, the value for bile salt mediated solubilization ratio was not changed for solid formulations.

Table 30. Input parameters used for CorA bile salt generated solubilization ratio.

	FaSSIF	**FeSSIF**	
pH	6.5	5.8	
Bile Salt Conc (mM)	3	10	
Solubility (mg/mL)	0.25	0.26	
Solubilization Ratio			$1.65\ 10^6$

10.1.2.7 Consideration of Potential Precipitation

Precipitation was observed in the experimental setup at pH 1 (**Figure 42**). An extrapolation yielded in 68 µg/mL for CorA-povidone and 49 µg/mL for CorA-copovidone at time point 0, an infinite time concentration of 21 µg/mL and 23 µg/mL, respectively and a precipitation rate of 0.08299 min^{-1} and 0.1992 min^{-1}. These precipitation rate constants correspond to a precipitation time of 723 s for CorA-povidone and 301 s for CorA-copovidone. A potential precipitation would result in neat CorA with an intrinsic solubility of 0.11 µg/mL at pH 1. In the PBBM, the drug was let to precipitate to this neat form. The effect of precipitation was systematically tested on oral animal PK to assess the impact on PK using a short precipitation time of 200 s.

10.1.2.8 Distribution Model

The volume of distribution is a pharmacological parameter to describe a theoretical relationship between the systemic concentrations and amount of drug in the body [163]. Several distribution models are provided by the PBPK software. In the following, the ability of the default Lukacova model was tested using preclinical IV data in three different

species. This model based on tissue partition coefficients (Kp) which are calculated from tissue composition and fraction unbound in plasma considering drug ionization [164]. For mouse, the predicted profile underestimated the observed data, especially for the later time points. In contrast, the predictions for rat and dog were in sufficient agreement with the observed values. However, the log-scale application of the profiles indicated an under- and overestimation, respectively for the later time points. Thus, the observed deviations were assumed to be rather attributed to clearance. The Lucakova model was expected to provide adequate predictions for the volume of distribution in preclinical animals and was therefore used for estimations of human body distribution.

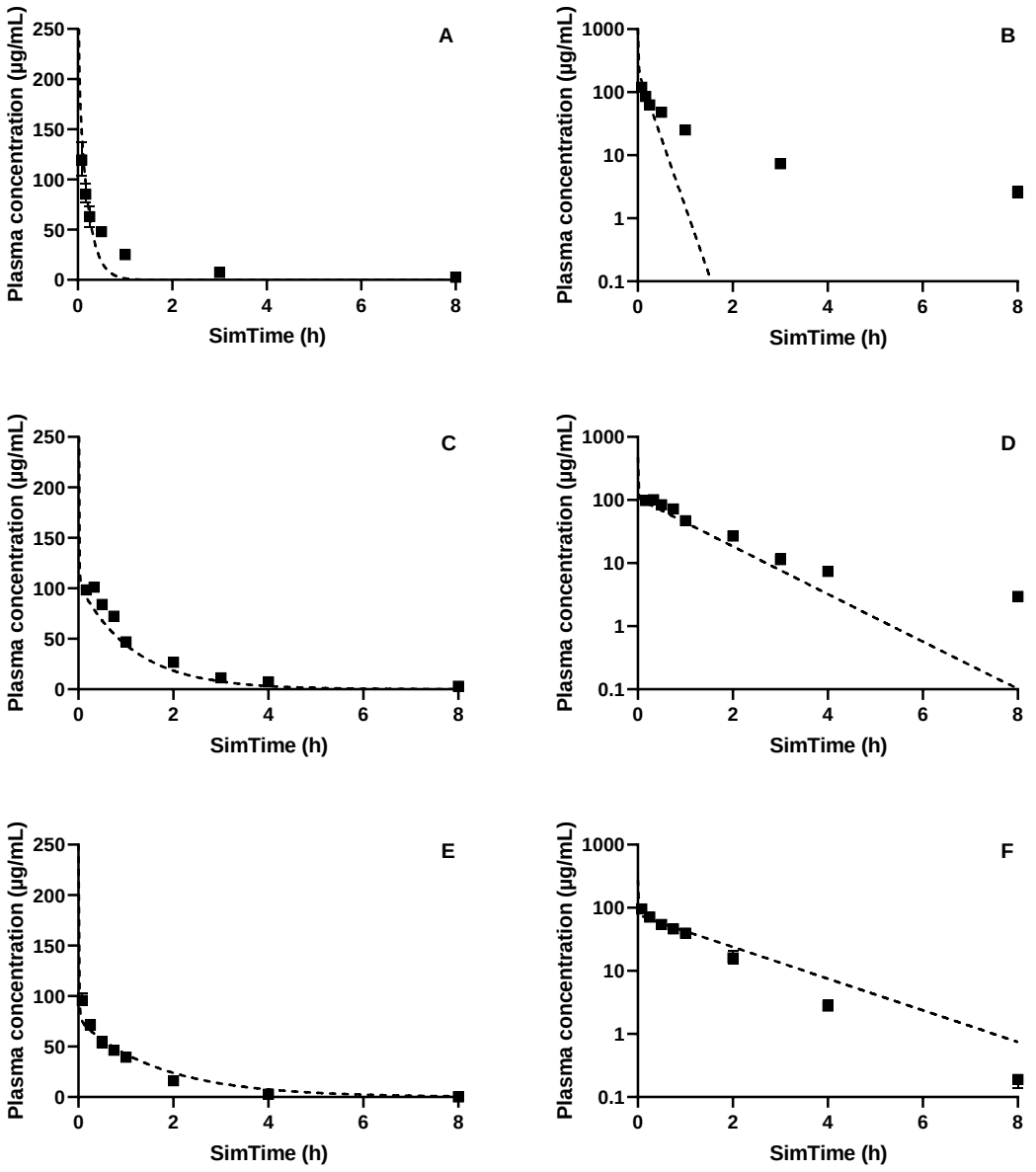

Figure 44. Distribution verification using mouse (A, B), rat (C, D) and dog (E, F) IV-PK profiles. (■) represents the observed plasma concentrations and dotted lines the predictions based on Lucakova model calculations. The left column is depicted in linear scale and the right column in log scale.

10.1.2.9 Clearance Pathways for CorA

The metabolism of CorA was assumed to be mediated by CYP2C9, indicated by the *in silico* prediction of the AP and *in vitro* ADMET profile [140]. Preclinical animal clearance data, obtained from IV data of mouse, rat and dog were fitted to the animals and used to estimate human clearance. Regulatory guidelines suggest the use of allometric scaling as state-of-the-art modeling approach [158].

It allows an estimation of human clearance based on preclinical data and bodyweights. The following **Eq.** was used:

$$Cl = A \cdot BW^b \quad \textbf{(8)}$$

where Cl is the determined or predicted clearance, BW the respective bodyweight and A and b represent the allometric factors. Measured clearance and allometric predictions of the species are presented in **Table 31**.

Table 31. Measured and allometric predicted clearances of CorA in preclinical species and allometric prediction of human clearance.

	BW (kg)	**Measured clearance (L/h)**	**Predicted clearance (L/h)**
Mouse	0.02	0.015	0.015
Rat	0.2	0.026	0.062
Dog	7	0.562	0.563
Human	70		2.342

Allometric parameters A and b were fitted to mouse, rat and dog data and determined to be 0.169 and 0.619, respectively. Extrapolating to human, a clearance of 2.342 L/h was predicted. To integrate the predicted clearance to a full PBPK model, metabolism via CYP2C9 was established. Therefore, a 100 mg IV administration was simulated in a 70 kg human and V_{max} of CYP2C9 was adjusted to match the via allometric scaling estimated clearance. The final values are displayed in **Table 32**.

Table 32. Kinetic Michaelis Menten parameters for CYP2C9 metabolism of CorA.

Enzyme	**Location**	**Data source**	**V_{max} (mg/s)**	**Km (mg/L)**
CYP2C9	PBPK	Microsomes	0.006949	2.77

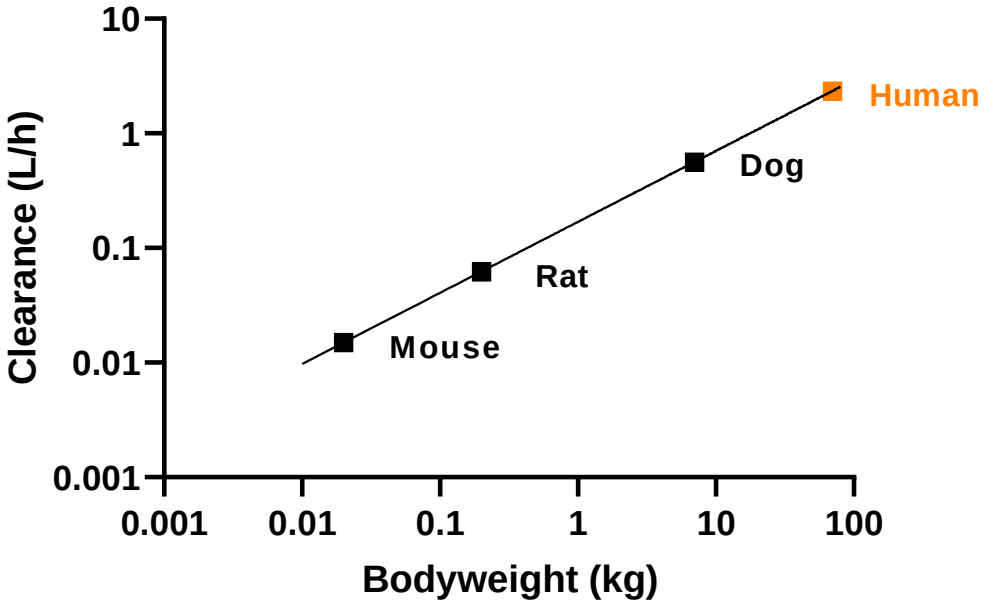

Figure 45. Allometric scaling of preclinical clearances. (■) represents the estimation of human clearance.

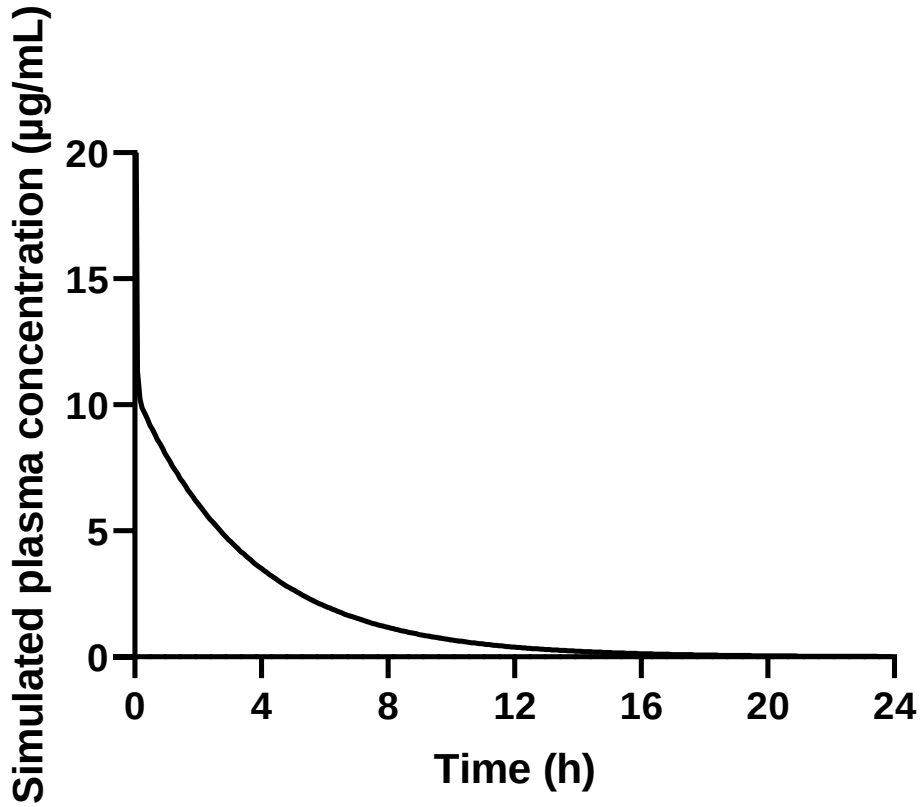

Figure 46. Prediction of 100 mg IV administration in human. V_{max} of CYP2C9 was adjusted to match predicted clearance of 2.342 L/h.

10.1.2.10 Contribution of Transporters to Absorption and Drug Permeability

Permeability of CorA is reported by Ehrens et al. using a Caco-2 cell assay [140]. Apparent apical to basal permeability of CorA ($20 \cdot 10^{-6}$ cm/s) was compared to the permeability of propranolol (29 10^{-6} cm/s). A single point correlation between the observed P_{eff} of propranolol ($2.91 \cdot 10^{-4}$ cm/s) and the observed Caco-2 data was used to predict the CorA human P_{eff} of $2 \cdot 10^{-4}$ cm/s [165]. Despite the prediction of CorA to be a P-gp substrate, *in vitro* experiments (**Chapter 9**) indicated a negligible effect on intestinal absorption.

10.1.2.11 Dosage Forms

Table 33 summarizes the modelled oral dosage forms for each species and administration.

Table 33. Summary of dosage form, dose and formulation used for PBPK model validation.

Species	Dosage form	Dose	Formulation
Mouse	IV - solution	36 mg/kg	Propylene glycol/ Kollliphor HS 15 / PBS pH 7.4 (20/20/60)
Rat	IV - solution	18 mg/kg	PEG 200 / PBS pH 7.4 (60/40)
Dog	IV - solution	75 mg	Propylene glycol/ Kollliphor HS 15 / PBS pH 7.4 (20/4/76)
Rat	Oral solution	36 mg/kg	PEG 200
Rat	Oral suspension	36 mg/kg	Povidone-ASD
Rat	Oral suspension	36 mg/kg	Copovidone-ASD
Dog	Delayed release – Tablet#	75 mg	Enteric capsule – CorA-povidone
Dog	Delayed release – Tablet#	75 mg	Enteric capsule – CorA-copovidone
Dog	Tablet (immediate and controlled release)	100 mg	Tablet – CorA-povidone
Dog	Tablet (immediate and controlled release)	100 mg	Tablet – CorA-copovidone

The delayed release – tablet dosage form was used as a surrogate for the capsule formulations to cover the enteric effect.

10.1.1.12 P-PSD as Dissolution Integration

The P-PSD approach, established by Pepin et al., was used as a mechanistic strategy to integrate dissolution to the PBPK model to allow a model validation in preclinical species and transfer to human [161]. Particle size distributions were manually adjusted to match observed *in vitro* dissolution data and integrated to the model.

Table 34. P-PSD fitting for CorA-formulations.

(A) CorA-povidone capsule	**Radius (µm)**	**%-w/w Distribution**
	23.0	87.8
	116.0	12.2
(B) CorA-copovidone capsule	**Radius (µm)**	**%-w/w Distribution**
	19	81.80
	25	1.40
	91	16.80
(C) CorA-povidone tablet	**Radius (µm)**	**%-w/w Distribution**
	204.7	100
(D) CorA-copovidone tablet	**Radius (µm)**	**%-w/w Distribution**
	150.3	100
(E) CorA-povidone granule	**Radius (µm)**	**%-w/w Distribution**
	2	68.80
	5	31.20
(F) CorA-copovidone granule	**Radius (µm)**	**%-w/w Distribution**
	5	59.99
	10	18.04
	20	21.97

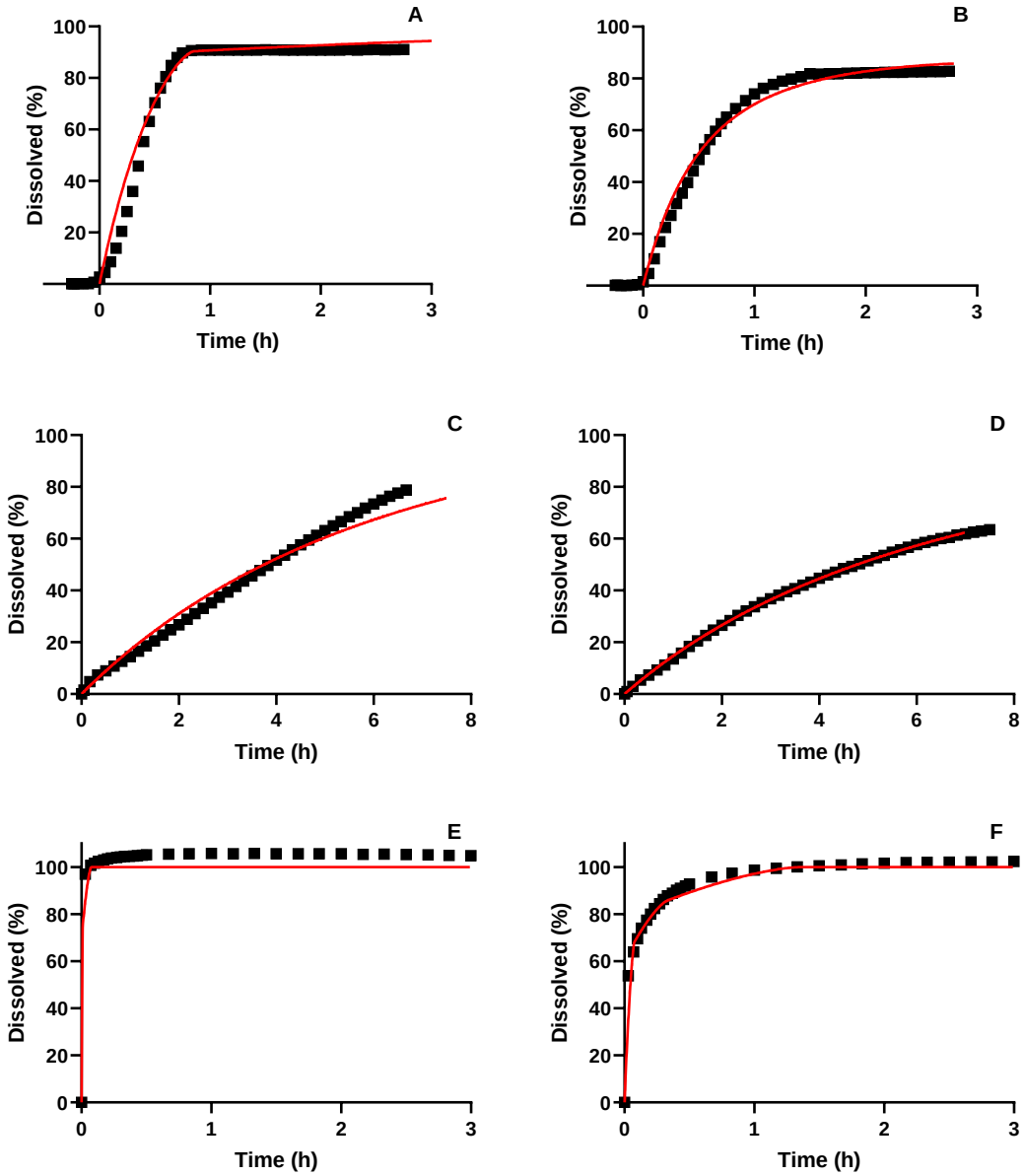

Figure 47. P-PSD fitting for A: 75 mg CorA-povidone DR capsule dissolution in 500 mL at pH 6.8 (solubility of 0.231 mg/mL); B: 75 mg CorA-copovidone DR capsule dissolution in 500 mL at pH 6.8 (solubility of 0.138 mg/mL); C: 50 mg CorA-povidone tablet dissolution in 500 mL at pH 6.8 (solubility of 0.231 mg/mL); D: 50 mg CorA-copovidone tablet dissolution in 500 mL at pH 6.8 (solubility of 0.138 mg/mL); E: 4 mg CorA-povidone granule dissolution in 20 mL FaSSIF (aqueous solubility of 0.231 mg/mL, total solubility = 1.24 mg/mL, radius of micelles = 30 nm); F: 4 mg CorA-copovidone granule dissolution in 20 mL FaSSIF (aqueous solubility = 0.138 mg/mL, total solubility = 1.40 mg/mL, radius of micelles = 30 nm). The red lines represent the predicted dissolution profiles.

10.1.2.13 Modeling Assumptions

For CorA modeling animal and human GIT physiologies in fasted or fed state were applied using the default advanced compartmental absorption and transit (ACAT) models. This

includes factors within the intestinal tract such as rate of dissolution, pH dependence of solubility of drugs, gut metabolism, carrier-mediated transport, secretion of bile salts, regional changes, surface area and influx or efflux transporter if indicated. The default Optimized log D Model SA/V 6.1 was applied to calculate absorption scale factors based on regional absorption models (C1-C4). This model adjusts the absorption scale factors for changes in permeability due to ionization, villi density, and possibly tight junction gap (if paracellular absorption is not treated as a separate process) among the compartments. The coefficients C1-C4 are set to default values, which have been optimized to provide the best fit to observed data for a series of drugs with known human P_{eff}. In parallel, the small intestine and colon luminal volumes were reduced from the default values to 7.5% and 2% volume occupation, respectively, to better reflect the magnetic resonance imaging (MRI) human measurements available in the literature [166–168]. Due to the pH dependent solubility of CorA the lower intestinal volume may influence dissolution and precipitation. Thus, the adjustments created a more physiologically relevant volume of the GI tract.

10.1.2.14 Model Validation

The PBBM was validated based on preclinical data in rats and dogs following oral administration. The following **Figures** (**48-50**) show the predicted PK profiles for CorA.

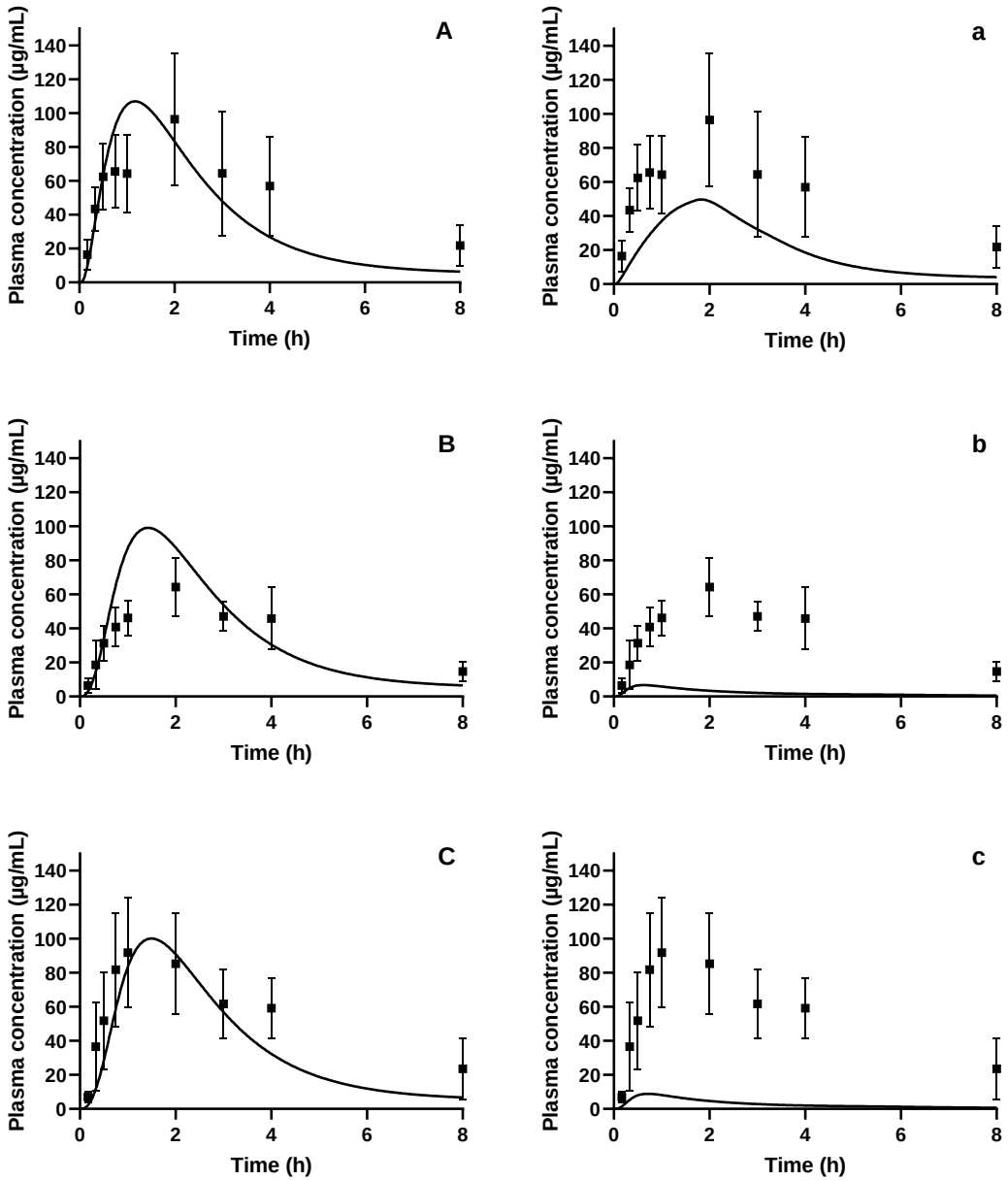

Figure 48. Model validation of (A, a) oral CorA solution (36 mg/kg), (B, b) oral CorA-povidone suspension (36 mg/kg) and (C, c) oral CorA-copovidone suspension (36 mg/kg) in rats without precipitation (capital letter, left panel) or with 200 s precipitation time (lowercase, right panel).

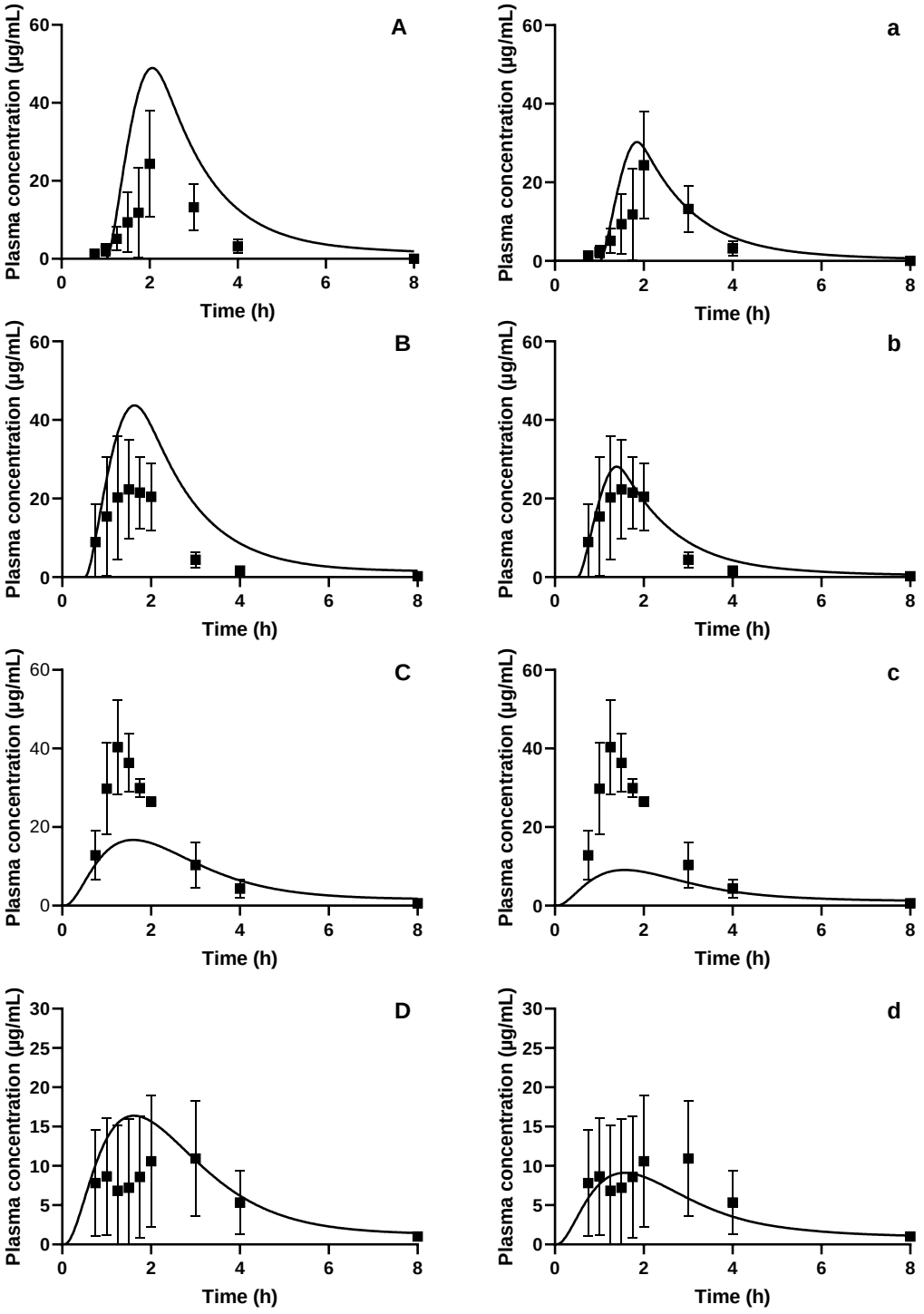

Figure 49. Model validation of (A, a) oral CorA-povidone DR capsules (75 mg), (B, b) oral CorA-copovidone DR capsules (75 mg), (C, c) oral CorA-povidone sustained release tablet (100 mg) and (D, d) oral CorA-copovidone sustained release tablet (100 mg) in dogs without precipitation (capital letter, left panel) or with 200 s precipitation time (lowercase, right panel) based on the P-PSD approach.

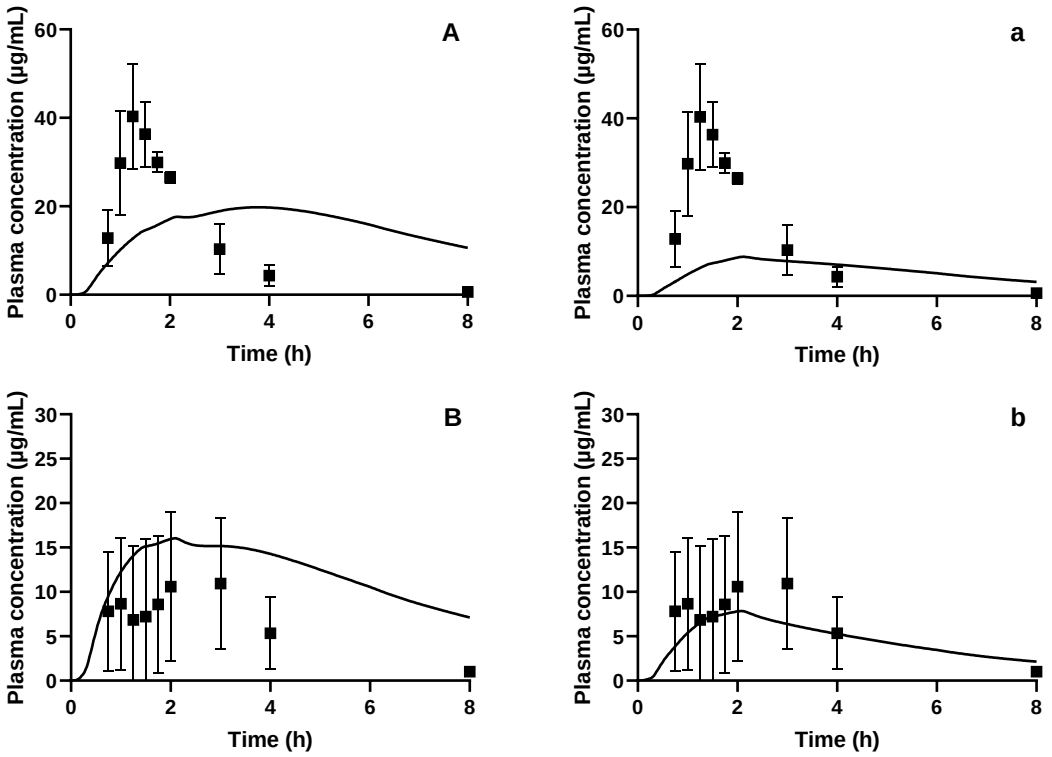

Figure 50. Model validation of (A) oral CorA-povidone sustained release tablet (100 mg) and (B) oral CorA-copovidone sustained release tablet (100 mg) in dogs without precipitation (capital letter, left panel) or with 200 s precipitation time (lowercase, right panel) based on the controlled release approach.

Predicted and observed PK profiles in rats agreed well when precipitation was excluded from the model. The integration of precipitation led to underestimated PK profiles. In contrast, the prediction in dogs were improved when precipitation was assumed by using 200 s as precipitation time. This enabled good predictions with the exception of the 100 mg CorA-povidone tablet. The observed t_{max} was too short to be compatible with the *in vitro* observed time when 50% of CorA were released (approx. 4 h). Consequently, the predicted PK profiles in dog were underestimated. It was assumed that the peristaltic forces *in vivo* have induced a faster disintegration and drug release for this tablet.

Assumptions such as GIT volume reduction (to 7.5% for the small intestine and 2% for the colon) or adjusted surface solubilities were demonstrated to deliver accurate prediction for *in vivo* dissolution. Precipitation was found to be relevant for predictions in dogs, while in rats, the drug seemed to super-saturate without subsequent precipitation. Higher bile salt concentrations in rat GIT may explain the predicted phenomenon. Moreover, the P-PSD approach was proven to allow good predictions, which is promising for human

prediction of drug product performance. This mechanistic approach was more promising compared to the controlled release approach for predictivity of human performance. Predictions using the controlled release function only based on the dissolution profile without considering potential species-related differences. The knowledge gained from this preclinical PBBM was used for the model transfer to human.

10.1.3 Model Application for Human

10.1.3.1 First-in-Human Prediction

The predicted human plasma profiles following a single administration of the enteric capsules or sustained release tablets at a dose level of 100 mg in the fasted state are presented in **Figure 51**. Higher C_{max} values were expected for the capsule formulations (CorA-povidone: 5.94 µg/mL; CorA-copovidone: 5.40 µg/mL) compared to sustained release tablets (CorA-povidone: 2.55 mg/mL; CorA-copovidone: 2.42 µg/mL). In addition, for CorA-povidone the fraction absorbed was 99% for the capsule formulation, whilst it was 84% for the tablet formulation. Slightly lower fraction absorbed were predicted for CorA-copovidone resulting in 96% for the capsule and 72% for the tablet formulation. Despite the decrease of small intestinal and colonic volumes to 7.5% and 2%, respectively, the model predicted no precipitation in human. Depending on dissolution, capsule and tablet PK profiles differed. The capsules were predicted to reach C_{max} after approx. 3-4 h followed by a steeper drop indicating finished absorption processes. The tablet formulation showed later C_{max} after approx. 6 h and longer-lasting PK profiles in accordance to their sustained-release dissolution profiles. Both approaches were predicted to reach therapeutically insufficient concentrations in less than 24 h based on the *in vitro* IC50. A rapid drop of the plasma concentrations was observed when C_{max} was reached, even at higher dosing levels (200, 400, 600 mg) (**Figure 52 and 53**). Therefore, BID administrations of different dose strengths were predicted to evaluate a desired accumulation as in terms of a therapeutic effect, it would be beneficial to keep the plasma concentration as high as possible accompanied with a higher unbound concentration at the targeted tissue site. The CorA-povidone sustained release tablet was chosen for simulations as the accumulation for a BID administration was expected to be superior compared to the capsule formulation. Several dose levels (100-600 mg) and both, fasted and fed state were simulated (**Figure 52 and 53**). Nevertheless, the capsule formulations

also indicated some accumulation regarding BID administration and due to the higher C_{max} this formulation approach remained as option for administration in humans.

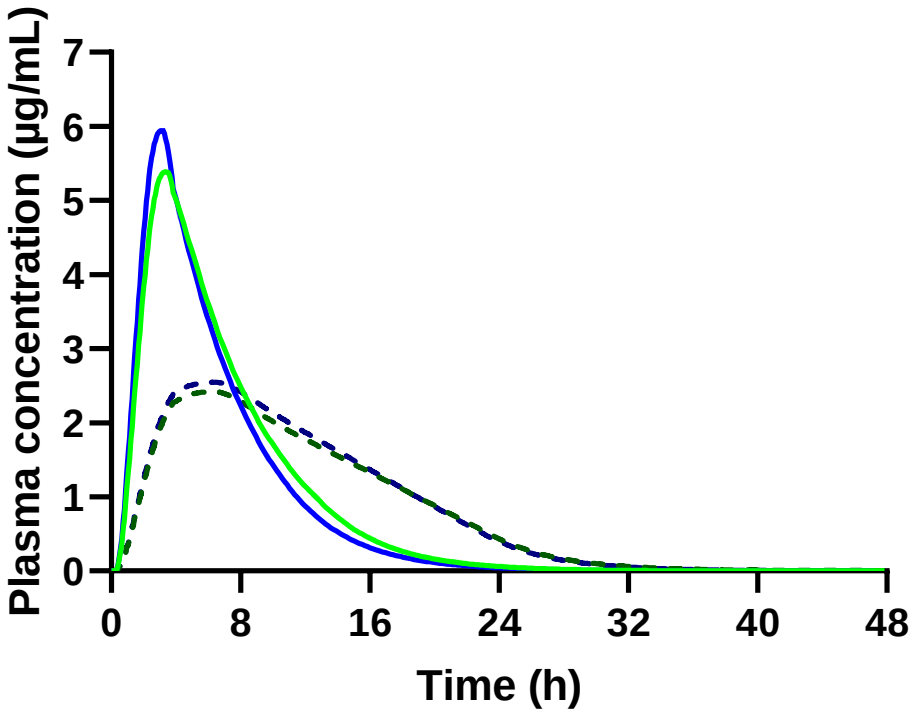

Figure 51. Predicted human plasma PK profile for CorA after 100 mg dosage form administration in the fasted state. The blue lines represent the predictions of CorA-povidone (-) and the green lines represent the predictions of CorA-copovidone (-). The solid lines display the capsule administration and the dotted lines the sustained release tablet administration.

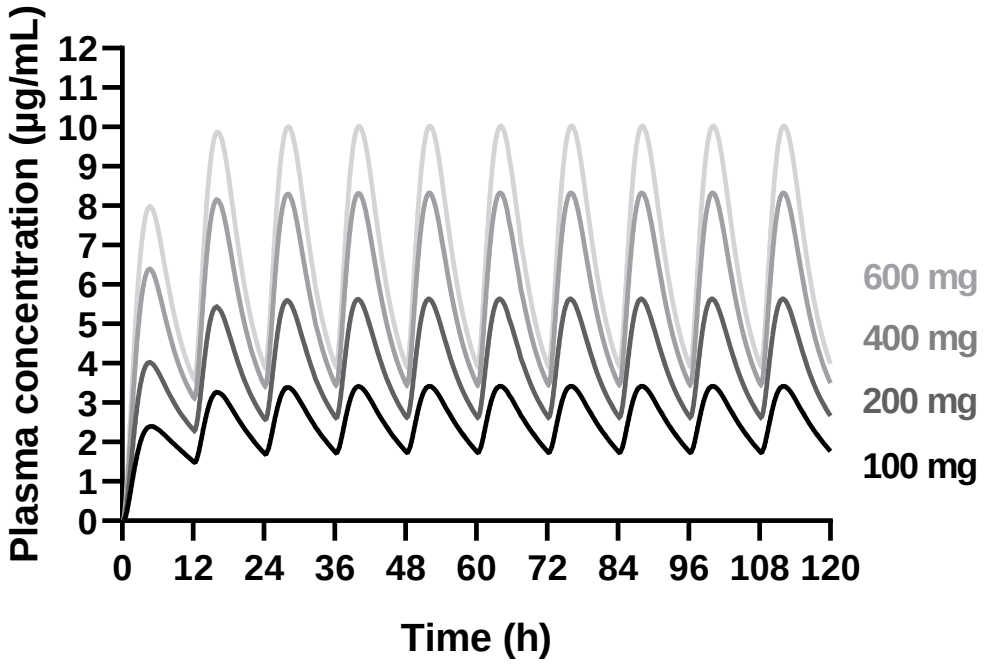

Figure 52. Predicted human plasma PK profile for CorA-povidone tablet after 100 mg to 600 mg BID administration in the fasted state.

For all doses and prandial states the steady state was predicted to be reached after the third administration. In the fasted state C_{max} and fraction absorbed did not increase in a dose dependent manner as higher doses limited *in vivo* dissolution (**Figure 52**). The highest simulated dose, 600 mg, achieved a C_{max} of 10.01 µg/mL and a lowest concentration of 3.93 µg/mL after reaching the steady state. Decisive higher plasma concentrations were predicted when administrations are combined with fed state resulting in a 3.5-fold increase of C_{max} (35.73 µg/mL; 600 mg) (**Figure 53**). The corresponding minimal plasma concentrations after reaching the steady state was 7.15 µg/mL. In contrast to the fasted state, no dose-dependent limitations in terms of C_{max} or fraction absorbed were predicted. Consequently, the fraction absorbed was 100% throughout a broad dosing range, elucidated in **Figure 54**. In contrast, the fraction absorbed in the fasted state markedly decreased with ascencing dose levels.

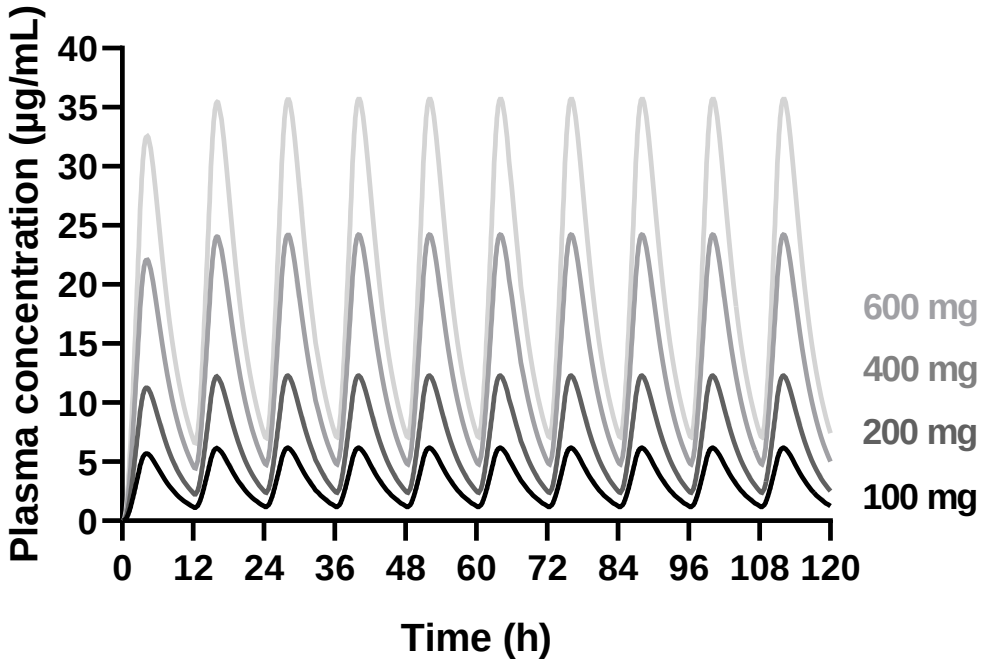

Figure 53. Predicted human plasma PK profile for CorA-povidone tablet after 100 mg to 600 mg BID administration in the fed state.

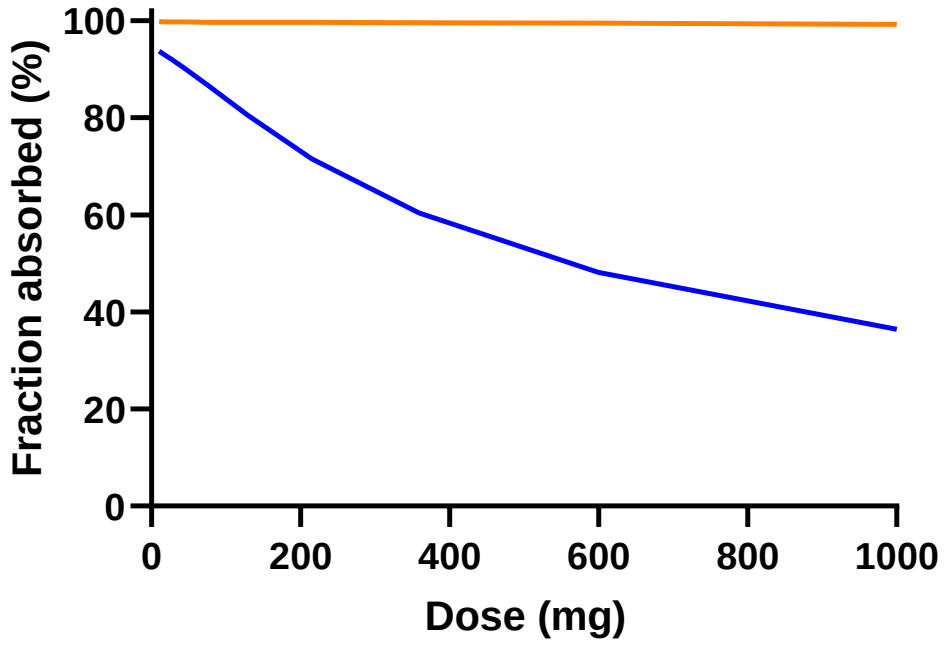

Figure 54. Impact on prandial status (fasted or high fat meal) on fraction CorA absorbed from CorA-povidone tablets. The blue line represents the fasted state and the orange line represents the fed state.

10.1.3.2 Formulation Development Driven by PBBM and Target Exposure to Reach First Time Right Results in Humans

Plasma concentration is an important parameter to evaluate ADMET characteristics. However, a therapeutic success is dependent on the availability at the side of action. Typically, an anti-infective treatment is dependent on the MIC that must be exceeded for a certain time [169]. Ideally, a PK/PD model using well-known standard PD models, e.g. the neutropenic thigh and the neutropenic lung model, defines the target tissue concentration. For CorA such a PK/PD model was successfully established against the pathogen *Staphyloccus aureus* considering the tissue concentration, MIC and reduction in bacterial burden [105]. The *in vivo* model to investigate the efficacy of a CorA treatment against filariasis is more complex and requires more effort. To observe *Wolbachia* depletion a treatment of at least 10 days is required [100]. To date, an in-depth PK/PD model against filariasis comprising relevant tissue concentrations for several dose levels, has not yet been finalized. To this end, as a first approximation, the unbound tissue concentrations were put into proportion to the *in vitro* IC50 of CorA (0.006851 µg/mL). Fasted state simulation revealed that none of the considered dose levels would be able to provide tissue concentrations above IC50 throughout the treatment period. The lower dose levels of 100 and 200 mg were even below the IC50 during the entire simulated treatment. At 400 and 600 mg, the IC50 was exceeded for 5.8 and 7.8 h, respectively. Similar to the enhanced fraction absorbed in fed state, the tissue concentrations of CorA were also increased resulting in up to 6-fold higher concentrations at the highest simulated dose (600 mg) compared with the IC50. Likewise, 400 mg were able to provide sufficient tissue concentrations for almost the entire treatment time. The lower dose at 200 mg, exceeded the IC50 for a certain time, however, an impaired therapeutic effect may occur due to the decrease below the IC50 for approx. 10 h within 24 h. It was predicted that the lowest dose would be below the IC50 for almost the entire time.

Using the IC50 of CorA it was concluded that a 400 mg BID administration of the CorA-povidone tablet formulation in combination with a high fat meal would be successfully reaching tissue exposure levels which would correspond on average, to twice the IC50 as unbound drug concentration.

For a critical interpretation it is important to illuminate the input parameters and their effects on the model. The tissue concentration is highly dependent on plasma protein binding, so changes would immensely affect the outcome of a model. Moreover, the fed state was predicted to be highly beneficial due to the high logP value of CorA. This effect was tested in preclinical species (mouse and dog), but could not be observed contrary to expectation. Especially, for the in dogs tested enteric capsule formulations, no food effect was predicted. However, simulating fed state in preclinical species remained challenging. Therefore, a potential food effect should not be excluded based on animal data and was recommended to be part in an early phase 1 trial. In addition, the deduction of a therapeutic success based on an *in vitro* determined parameter (IC50) limits the predictive power. Nevertheless, it is a helpful approach for a first impression and thus, supporting the dose selection for an initial clinical phase I study. During the remaining preclinical and upcoming clinical investigations, the PBBM model will be further modified and improved once new data become available.

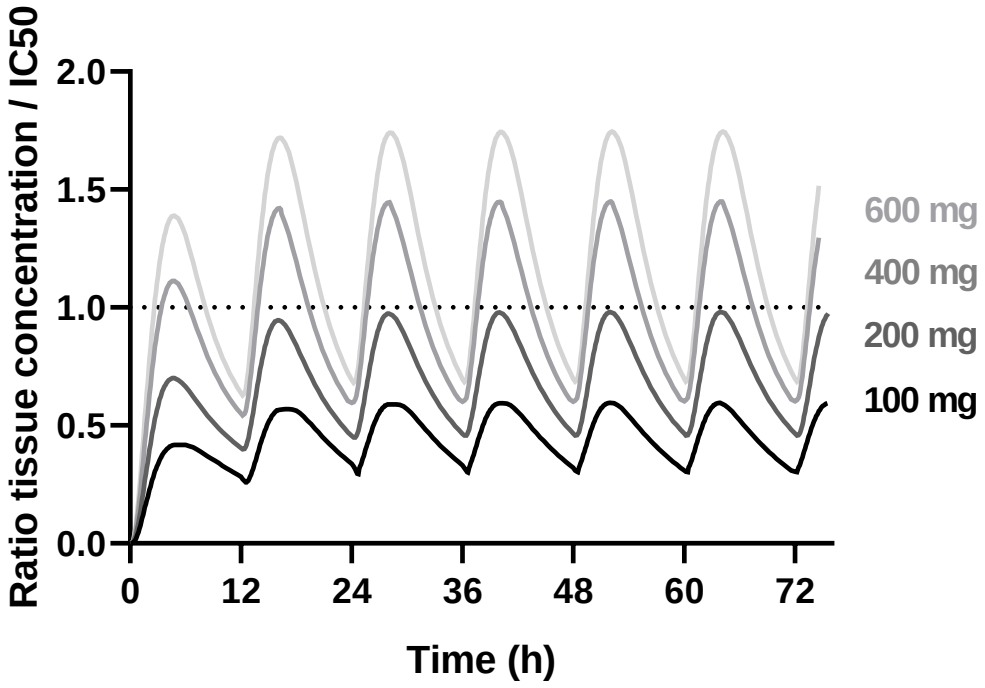

Figure 55. Predicted ratio of human unbound tissue concentration to IC50 over time for CorA after 100 mg to 600 mg BID of CorA-povidone tablet administration in the fasted state.

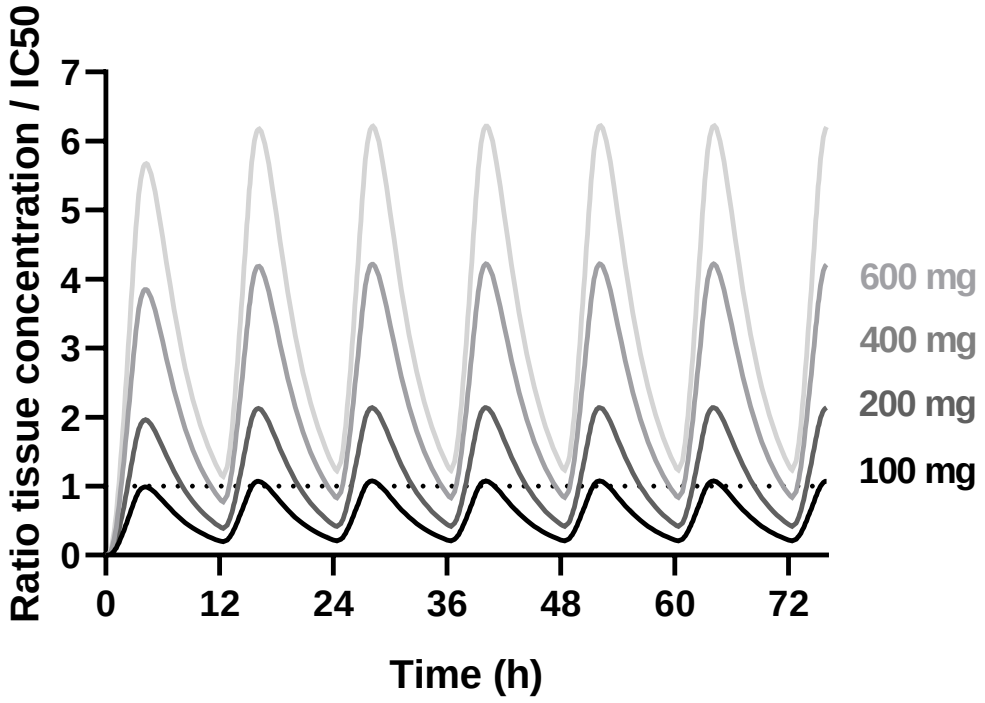

Figure 56. Predicted ratio of human unbound tissue concentration to IC50 over time for CorA after 100 mg to 600 mg BID of CorA-povidone tablet administration in the fed state.

10.4 Summary

First, the *in silico* tool PBPK modeling was used to evaluate the potential of its combination with a preclinical biorelevant dissolution setup. The incorporation of solubility and dissolution into the PBPK model allowed a prediction of plasma concentration in mice, the efficacy model of CorA. These results further confirmed the bio relevance of the mouse-specific *in vitro* dissolution tool. Additionally, the use of physiological parameters measured *in vitro* and predicted *in silico* enabled successful simulations of plasma concentrations in mice, thus increasing confidence in the utility of this simulation approach to forecast the performance in other species.

Moreover, a mechanistic PBBM was developed on the basis of preclinical *in vivo* data in mice, rats and dogs, as well as, *in vitro* dissolution performances of ASD formulations of CorA. Experimental determined IV profiles were used to estimate human clearance and distribution using the established strategies allometry and PBPK modeling. A successful validation based on animal data allowed to translate the model to human performance predictions. A dose of 100 mg (equivalent to 1.4 mg/kg) was simulated, which may serve as the FIH starting dose for initial clinical trials considering preclinical toxicology studies.

Focusing on a potential therapeutic treatment dose, 400 mg BID of the CorA-povidone tablet formulation, administered in combination with a high fat meal was predicted to reach sufficient tissue concentrations. In sum, this *in silico* approach was a rational and helpful tool to combine preclinical *in vivo* data with *in vitro* determined properties of the compound and its formulation to set a first estimate for human PK performance. In addition, the influence on several input factors, such as food effect or plasma protein binding could be estimated. As a model represents a continuously enhancing and altering approach, future preclinical and clinical trials will provide more model confidence regarding required tissue concentrations for a therapeutic success and opportunities in terms of, e.g., potential drug-drug interactions or building of PBPK-PD models to predict effect changes due to dose level, dosage form, and dosing regimen.

11. Preclinical Toxicologic Evaluation of CorA

The purpose of toxicity tests is to characterize the toxicology profile of a compound. These studies are required to ensure a safe entry into human clinical studies [170,171]. This typically includes investigations in different preclinical species, which, however differ in physiologies and thus, in requirements regarding route of administration and type of formulation [17]. As the route of administration should be based on the intended clinical use, the oral administration is often targeted as the most common route in toxicology studies. Especially for poorly soluble drugs, providing an appropriate vehicle covering all requirements is an immense challenge for pharmaceutical scientists. Enabling sufficient exposure is crucial to identify adverse effects in terms of exposure-response relationships in conjunction with establishing a safety window for human administration. For oral administration solutions are the preferred dosage form due to easy handling (e.g. dose escalation) and the elimination of dissolution dependency [17]. However, in contrast to PK and PD studies, a toxicology study may require extremely high dose levels that exceed the therapeutically relevant dose many times over, with the goal of observing adverse effects. If only mild toxic effects will be observed at the starting dose, the dose to be administered may increase to a maximum of 1000 mg/kg body weight in the worst case, as specified in the guideline [170]. This would further limits the assortment of appropriate study vehicles [170]. Ideally, the vehicle should prevent precipitation by providing high solubility in case of solutions or by using a solubility enhancing formulation strategy to improve exposure and thus, enable high BA. Another aspect to be considered represents the tolerability of the respective vehicle, which is in turn dependent on species-specific factors such as route of administration tolerances, concentrations, volumes, dosing regimens and study duration [172]. For example, the commonly used solvent PEG 400 is known to have excellent solubility properties, but exhibit gastrointestinal adverse effects like watery feces or emesis following oral administration in dogs [173]. Although useful excipients are reported and accepted for use in toxicology studies, it is even more important to identify and elaborate alternative strategies to meet the specific requirements of novel compounds.

The objective was to assess mesoporous silica as an alternative vehicle within a seven-day exploratory study in dogs. The investigations included tolerability and PK evaluations for

the vehicle. Therefore, plasma samples were withdrawn at day one to generate toxicokinetic profiles to assess PK parameter at different toxicological dose levels [174]. In addition, a seven- day exploratory study in rats was performed to evaluate the toxicology potential of CorA in a standard rodent species. Within this study the standard PEG 200 vehicle was used. Preliminary studies revealed the MTD and set the dose frame for these seven-day exploratory toxicology studies.

11.1 Results and Discussion

11.1.1 Toxicokinetic Evaluation in Rats

CorA dissolved in PEG 200 was used as oral dosage form. This vehicle was able to achieve sufficient high concentrations to provide the required dose levels and high excipient tolerability. The solution was administered by oral gavage to Wistar rats for seven consecutive days at dose levels of 250 and 1000 mg/kg body weight/day at a dose volume of 5 mL/kg body weight. An increase of the 250 mg/kg dose to 1000 mg/kg resulted in only slight increase of exposure over the first 24 h ($AUC_{0\text{-}24}$: 250 mg/kg: 2986.4 µg*h/mL; 1000 µg/mL: 3875.5 µg*h/mL). No differences regarding C_{max} were observed between the doses, indicating that solubility and absorption rate limits were reached. The absorption process at 1000 mg/kg became even more elongated compared to the 250 mg/kg dose level. Even after 24 h the plasma samples showed high CorA concentration, pronounced for high dose indicating incomplete elimination during 24 h post dose. Due to the unfinished elimination after 24 h, the following repeated administrations were expected to lead to accumulation of CorA. Based on IV administration of the PK study in rats (**Chapter 8.1.3**) BAs of > 100% for 250 mg/kg and 40% for 1000 mg/kg were determined, demonstrating high absorption despite high administered doses. This early exploratory study demonstrated PEG 200 to serve as a suitable tox vehicle in rats, providing sufficient solubility and intestinal absorption even at high doses. For regulatory submission a repeated-dose GLP toxicity is planned to be performed using PEG 200 as toxicology vehicle.

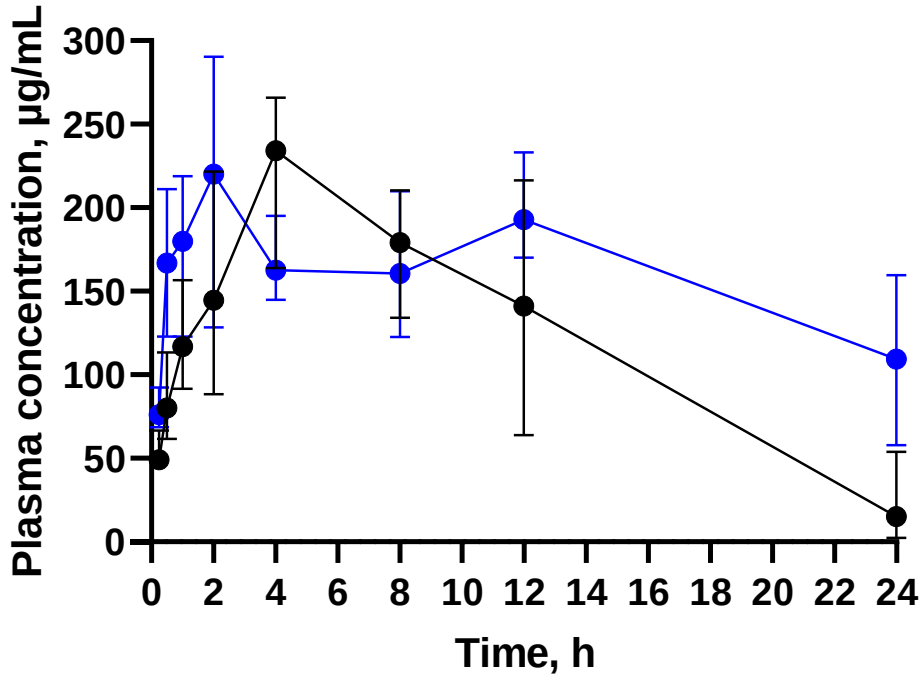

Figure 57. CorA plasma concentration time profiles in Wistar rats. PO administration of CorA-PEG200 solution with the doses of 250 mg/kg (●) and 1000 mg/kg (●), (median ± IQR, n=8 per group; alternating sampling).

Table 35. PK parameters after PO administration of CorA- with the doses 250 mg/kg and 1000 mg/kg in Wistar rats (median, n=8 per group, no IQRs were defined as no individual plasma profiles were performed due to alternating sampling).

	$AUC_{0\text{-}24\ h}$ (µg*h/mL)	$AUC_{0\text{-}24\ h}$ per mg/kg dose (µg*h*kg/dose)	C_{max} (µg/mL)	t_{max} (min)	$t_{1/2}$ (h)	BA (%)
CorA-PEG 200 250 mg/kg	2986.4	11.9	234.0	4	3.73	127
CorA-PEG 200 1000 mg/kg	3875.5	3.9	220.1	2	n.a.	40

11.1.2 Clinical Signs During the Toxicological Study in Rats

No test item related mortality was observed during the study. From day four to seven, excessive drinking and chewing were seen for approx. 30 min after treatment and soft/liquid feces were seen in the test item treated animals. Lower body weight gains and/or food consumptions were recorded in all test item treated dose groups. In the high dose females body weight loss was observed during day one to five. Despite only mild

gastrointestinal disorders, caused by the high molecular weight of PEG 200, it was possible to detect CorA-related severe effects.

11.1.3 Toxicokinetic Evaluation in Dogs

As part of toxicological characterization, preclinical toxicology studies have to be carried out in a non-rodent species. A preliminary study investigated the MTD (data not shown). To this end, a non-GLP seven-day exploratory study was conducted at the doses 150, 450 and 750 mg/kg in dogs [174]. Although PEG 200 has been suggested as an alternative to PEG 400 that causes less GIT disorders, oral administration of PEG 200 to dogs in the PK study (**Chapter 8.1.4**) induced severe vomiting in four beagle dogs, even with pure PEG 200. Hence, a vehicle was needed that have good tolerability, sufficient oral BAs and the ability to apply the targeted high dose of CorA. The poor aqueous solubility of CorA (91.13 µg/mL at pH 6.5) and the required high dose levels (150 mg/kg - 750 mg/kg) excluded many common vehicles for toxicology studies [108]. Alternative non-aqueous solvents that would have suitable solubility, e.g., ethanol (up to 1 g/mL), were not considered due to their own toxicological profile [17]. Simply producing a homogeneous suspension of the drug substance would fail due to the waxy consistency of CorA (T_g of 5 °C) [108]. As no commonly used liquid vehicles were possible to generate a solution, an alternative approach was urgently needed. In terms of solubility and dissolution enhancement enabling formulations like ASDs are commonly used to improve BA. However, high doses would be accompanied with high polymer quantities. Gierke et al. reported that this can result in agglomeration and the formation of pharmacobezoars after several treatment days leading to a fatal obstructive ileus [175]. CorA-ASD formulations, comprised of povidone or copovidone, showed correspondingly promising solubility enhancements. However, the ASDs had a drug load of 20%. This would require a high amount of polymer, especially for the high dose level (600 mg/kg of polymer). The administration using capsules (size 0) would require an impractical number of capsules, approx. 50-100, depending on the individual body weight. Furthermore, providing a homogenous aqueous suspension is challenging due to the water-soluble ASD matrix and poor solubility of CorA. Therefore, an alternative was required to conduct toxicological studies of CorA in dogs.

In recent years, mesoporous silica has been proven to be an easy-to-use powdered intermediate that increases BA of poorly soluble drugs [43,44,46]. In contrast to ASDs, lower risk of pharmacobezoar formation was assumed due to the mineral and inert character of mesoporous silica. In addition, the loading capacity enabled a drug load of 50%, reducing the total amount of administered excipient. The manufacturing process led to the formation of a dry powder that was able to generate a homogeneous suspension. Prior the toxicological assessment of CorA-mesoporous silica, various formulation characteristics were investigated.

The residual ethanol as process solvent was determined after the second drying step to confirm compliance with the limit given by the authorities. **Figure 58** illustrates that the final formulation had an ethanol concentration of 779± 147 ppm for CorA-mesoporous silica, far below the limit of 5000 ppm [176]. Consequently, the drying procedure was able to provide a product that fulfil the ICH guidelines. Key characteristics of the mesoporous silica and the mesoporous silica formulation are summarized in **Table 36**.

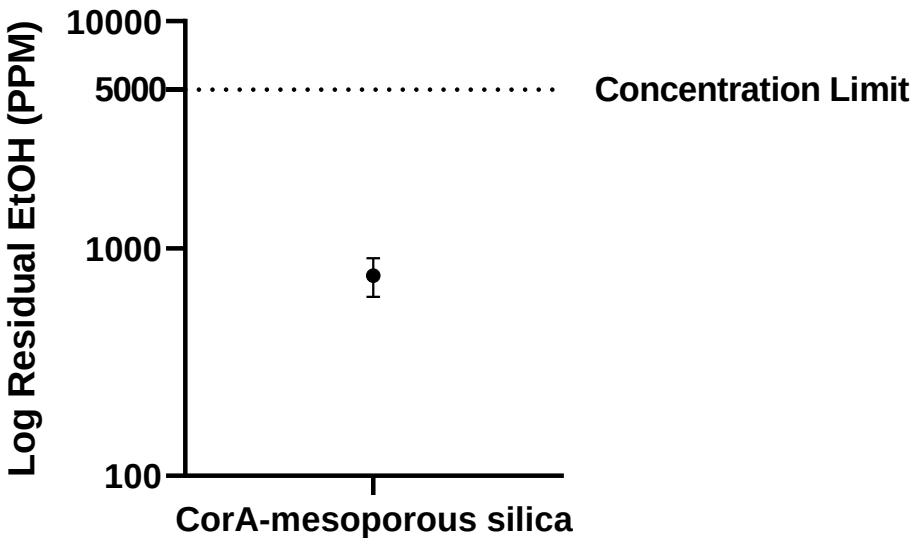

Figure 58. Results of residual solvents determination of the CorA-mesoporous silica formulation after manufacturing; n=3 (mean ± SD).

Table 36. Basic characteristics of Syloid® XDP 3050 and CorA-mesoporous silica formulation.

Parameter	Syloid XDP 3050	CorA-mesoporous silica
Specific surface area (m^2/g)	320 [177]	
Pore size (nm)	22.9 [177]	
Pore volume (mL/g)	1.7 [177]	
Median particle size (µm)	59.42 ± 0.19 [177]	53.8 ± 0.5
Loading efficiency (%)		89 ± 3

The dissolution performance of CorA-silica at pH 6.8 was studied using the mini-scale dissolution apparatus (**Figure 59**). Two target concentrations (0.25 and 0.5 mg/mL) were investigated to observe potential changes in dissolution rate depending on drug concentration. A comparable performance was observed at both doses, with a fast initial drug release reaching 80% (0.25 mg/mL: ± 3%; 0.5 mg/mL: ± 9%) within 30 min. After 180 min, slight differences were detected as 97% ± 2%was observed for the lower dose, while the higher dose reached 93%± 5%. This fast dissolution rate cannot be expected in the toxicological studies, as the doses of CorA exceeded many times those used for the dissolution experiments. However, the profiles indicated faster drug release compared to neat CorA. Thus, this vehicle was expected to be suitable for toxicological investigations in dogs and tested in a seven-days exploratory study.

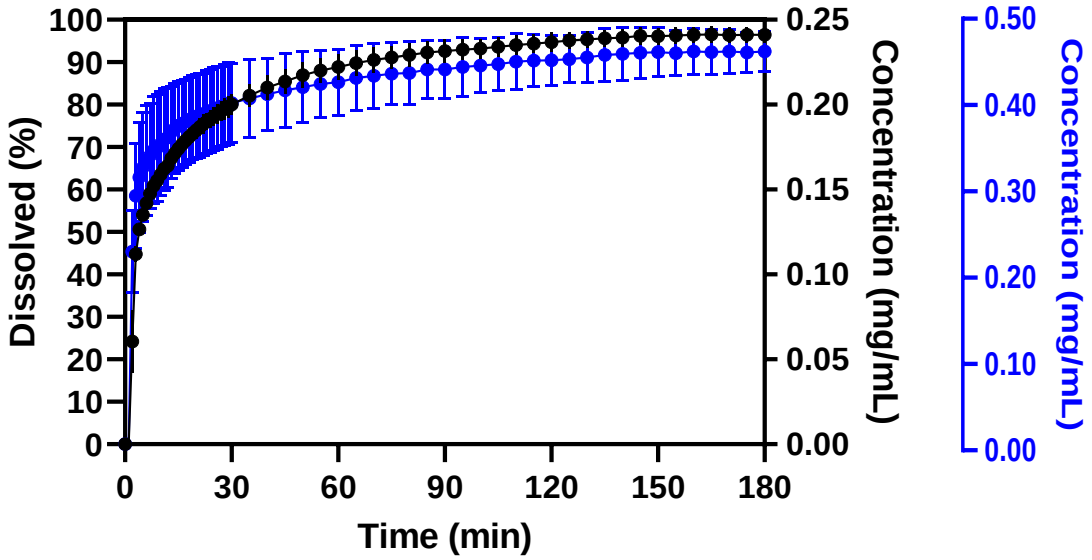

Figure 59. Mini-scale dissolution of the CorA-silica formulation (drug load 50%) (n=3, mean ± SD). Experimental conditions were set at: Dose: 5 mg (●) and 10 mg (●); Volume: 20 mL 0.05 M phosphate buffer (pH 6.8); Paddle speed: 75 RPM; Temperature: 37 °C.

Four groups were treated with ascending dose levels (vehicle-control, 150, 450 and 750 mg/kg), higher than the therapeutic dose, to provoke toxic effects in the time frame of the study and to establish a necessary safety window for FIH clinical trials. The observed C_{max} increased with ascending dose levels (**Figure 60**). For all doses plasma concentrations between 200 and 250 µg/mL were achieved after 1 h indicating fast drug release and absorption. A further increase after 1 h was detected for the middle and high dose. However, no dose linearity was detected leading to minimal differences between the middle and high doses which might be solubility and permeability limited. In particular, intestinal absorption was expected to be saturated by the high amount of CorA. Thus, fast and high intestinal absorption did not increase in a dose-dependent manner. In terms of exposure, pronounced increases were observed with ascending dose levels which additionally suggested a permeation limitation for C_{max} (**Table 37**). For the dose normalized exposures ($AUC_{0\text{-}inf}$ per mg/kg dose) no significant differences were detected between low and middle dose ($p > 0.05$). The plasma concentrations of the middle-dose led to a less steep elimination profile (**Figure 60**), indicating that CorA was still dissolving and absorbed after C_{max} was reached. Similar results were observed for the high-dose,

which, however, resulted in only a slight increase of the $AUC_{0\text{-}inf}$. Consequently, dose normalized exposure ($AUC_{0\text{-}inf}$ per mg/kg dose) for the high-dose decreased below the value of the middle- and low-dose (**Table 37**). It was expected that at the high-dose level intestinal solubility limited further dissolution as CorA was probably not absorbed fast enough resulting in a significant difference between middle and high dose for the dose normalized exposures. BAs were not determined, as the doses of the toxicokinetic study were 12-60-fold higher compared to the performed IV administration (**Chapter 8.1.4**). The t_{max} increased with an ascending dose level (2-4 h indicating a prolonged dissolution and absorption process. By using the mesoporous silica formulation, increased solubility values for CorA, tested in biorelevant media (FaSSIF: 0.835 mg/mL ± 0.002 mg/mL; FeSSIF: 0.615 mg/mL ± 0.031 mg/mL) were examined compared to neat CorA (**Chapter 5.1.6**: FaSSIF: 0.25 mg/mL; FeSSIF: 0.26 mg/mL) [162]. By reaching the solubility maximum, the undissolved part remained in the silica pores and served as a reservoir which is able to replace absorbed drug molecules. For the low dose group t_{max} was reached after 1 h. It was assumed, that the reservoir function was rapidly exhausted resulting in a rapid drop of the plasma concentration. In contrast, the t_{max} in the middle (3 h) and high-dose (4 h) group were increased compared to the low-dose group (**Figure 60**) indicating a longer-lasting reservoir function accompanied with a sufficient concentration gradient. Reservoir functions are already described in the field of ASDs. Hirlak et al. demonstrated that a phase-separated colloidal drug phase is able to serve as a reservoir for already dissolved and absorbed drug molecules, improving the BA of poorly soluble drugs [74].

In sum, the mesoporous silica combined with a 1%-NATROSOL® solution provided a homogenous and stable suspension, overcoming handling issues caused by the waxy consistency of CorA. The low interindividual variability indicated a successful and consistent dose administration. Due to its aqueous insolubility and average particle size of approx. 50 µm, it was assumed that the mesoporous silica is not absorbed in the intestine [178]. This study clearly demonstrated mesoporous silica to be a valuable alternative in cases for which standard vehicles are not applicable. Mesoporous silica was confirmed to not only improve handling, but also increase BA, resulting in high exposures of CorA. If only low doses are required for toxicological investigations, the use of ASDs could present a promising option. In general, the physicochemical characteristics and

physiological potency of each compound need to be considered, such as aqueous solubility, solvent solubility, selection of appropriate polymers for an ASD and required ASD drug load, and toxicological potential to guide the optimal vehicle selection. Even though, mesoporous silica provided the best option for CorA, the use of alternative formulations principles may be beneficial for other compounds. For solutions, which are the ideal approach for toxicology studies, solubility and dissolution may be of different importance for poorly soluble drugs. These drug candidates are usually dissolved in non-aqueous solvents or solubilized with the help of excipients. After oral administration, the dissolved drug may precipitate due to limited solubility in the stomach or intestine [17]. Redissolving of precipitate now determines the intestinal absorption. As a consequence, a solution is not always able to guarantee full absorption during a toxicological study and potential severe effects stay undetected. Thus, the mesoporous silica approach is not necessarily disadvantageous compared to a solution.

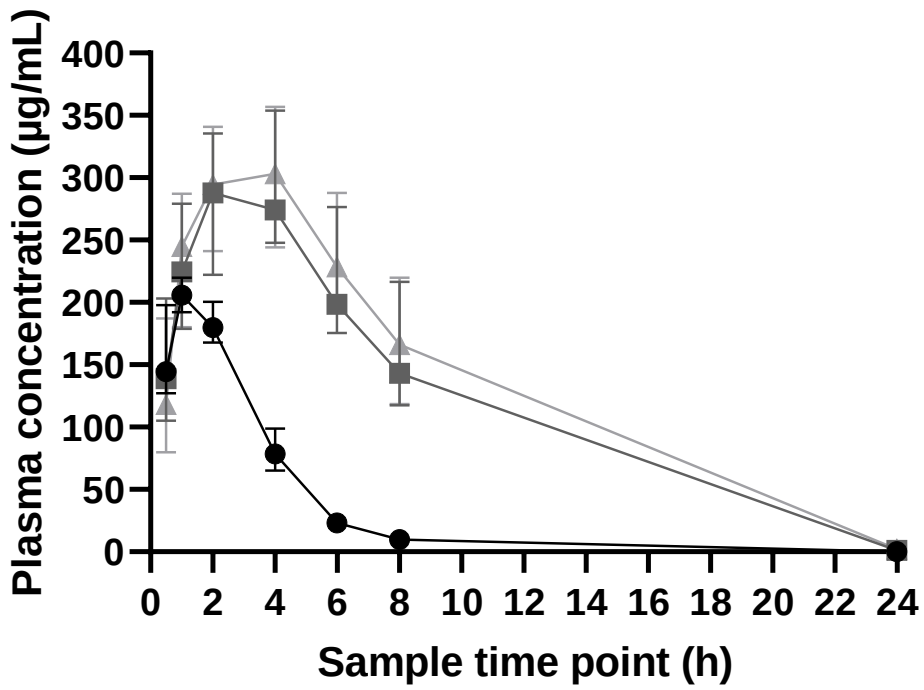

Figure 60. Toxicokinetic profiles of CorA-silica after oral administration in dogs (median ± IQR; n = 4 per group). The dose levels 150 mg/kg (●), 450 mg/kg (■) and 750 mg/kg (▲) were administered as a suspension in 1%-NATROSOL®.

Table 37. Toxicokinetic parameters of CorA-silica after oral administration in dogs (median ± IQR; n = 4 per group).

	$AUC_{0\text{-}inf}$ $\frac{\mu g * h}{mL}$	$AUC_{0\text{-}inf}$ per mg/kg dose $\frac{\mu g * h * kg}{mL * mg}$	C_{max} (µg/mL)	t_{max} (h)
150 mg/kg	814.2 (736.1-869.4)	5.428 (4.91-5.80)	209.36 (202.72-214.40)	1 (1-1.25)
450 mg/kg	2805.3 (2735.38-3201.45)	6.234 (6.08-7.11)	287.79 (248.61-337.93)	3 (2-4)
750 mg/kg	3243.3 (2856.23-3683.58)	4.324 (3.81-4.91)	303.28 (248.74-355.93)	4 (3.5-4)

11.1.4 Clinical Signs During the Toxicological Evaluation in Dogs

As a reference, a control group received unloaded mesoporous silica. The dogs of the control group tolerated the vehicle well and no clinical symptoms were observed. Body weights and food consumption were monitored during the study duration resulting in no irregular body weight alteration of the control group animals and no decreased food consumption. Furthermore, no abnormalities were observed regarding clinical observations, clinical chemistry, histopathology, organ weights, blood pressure, coagulation or electrocardiogram. Thereby, potential dose-dependent adverse effects caused by CorA could be clearly assigned. Consequently, mesoporous silica was suitable to provide a well-tolerated vehicle that enabled high exposure of a poorly soluble drug for a toxicology study in dogs. The dogs tolerated well the administration of CorA at the low (150 mg/kg/day) and the mid dose group (450 mg/kg/day). In the mid dose group, only transient and slight clinical signs (vomiting, thin feces) were observed in low incidence. Minimally to slightly decreased albumin, globulin and total protein concentrations were observed on Day 8 compared to the pre-value. However, the incidence of clinical symptoms was high in the high dose group of both sexes resulting in markedly decreased food consumption and moderate body weight loss was detected in one of the high-dosed females. Slightly decreased albumin, globulin and total protein concentrations were observed on Day 8 compared to the pre-value. Based on the clinical signs, food

consumption and body weight data in the high dose group (750 mg/kg) was regarded to be higher than the MTD.

11.4 Summary

In vivo exploratory toxicological studies were performed in a rodent (rat) and a non-rodent (dog) species. For rats, no CorA related mortality was observed during the study and only mild GIT adverse effects were demonstrated. Likewise, the low and mid dose group in dogs showed good tolerability of CorA resulting in only slight and transient clinical signs, while a high incidence of clinical symptoms was present in the high dose group identifiable by markedly decreased food consumptions, frequent vomiting and moderate body weight loss. Due to the higher dose, plasma concentrations and exposure of the toxicokinetic studies exceeded the values of the performed PK study. Considering the predictions obtained by the PBBM model, the tolerated dose of 450 mg/kg in dogs is approx. 80-fold higher than the expected effective dose in human (400 mg, CorA-povidone tablet) corresponding to a 40-fold increase in exposure. Besides, for the administration of a 100 mg capsule in human approx. 70-fold lower exposure was predicted compared to the mid dose in dogs indicating a broad safety window for human use. Nevertheless, the planned long-term GLP toxicology studies will further increase the confidence of a safe FIH dose. Regarding the used toxicology vehicles, appropriate approaches were identified for rats and dogs demonstrated by good tolerances of the vehicle groups. The toxicokinetic profiles revealed high C_{max} and exposures in comparison to respective PK studies. Thus, PEG 200 was proven to be suitable for rats and mesoporous silica served as a valuable alternative formulation approach for CorA toxicology investigations in dogs. These experiments will guide the study setups and dose selections for the GLP toxicology studies.

12. Summary and Outlook

Corallopyronin A (CorA) is a natural anti-infective compound which is able to deplete *Wolbachia*, endosymbionts of the filarial nematodes. The aim of this PhD project was to support the preclinical development of CorA by investigating and providing suitable formulations to be used in preclinical studies and furthermore for potential human clinical trials. Previous work identified promising formulation principles which served as starting point for further investigations and development. This was required as CorA displays a highly lipophilic character (logP of 5.42) associated with a limited aqueous solubility (0.11 µg/mL at pH 1 and 91 µg/mL at pH 6.5) resulting in poor oral bioavailability and thus, in an insufficient pharmacodynamic effect. Moreover, CorA exhibited isomerization, leading to stability issues of the neat drug substance. Due to the fully amorphous character and low glass transition temperature (T_g of 5 °C), the neat drug substance has a waxy, sticky consistency that impairs processability. Consequently, to overcome these challenges, formulation development took place, which addressed the problems mentioned above. The amorphous solid dispersion (ASD) formulation principle was identified to be the most promising approach for CorA. Thereby, CorA was dissolved in an aqueous soluble polymer which was assumed to enhance dissolution due to maximization of surface area by molecular dispersion, stability due to immobilization of the molecule, as well as, interactions between CorA and the used polymers (Debye forces). Furthermore, this approach enabled a simplified handling due to the formation of a powder. The manufacturing process was carried out using a mini spray dryer (Büchi-290). The polymers povidone (polyvinyl-pyrrolidone) and copovidone (vinylpyrrolidone-vinyl acetate copolymer) have been identified as the most promising polymers using *in vitro* biphasic dissolution and stability studies. A downstream process after spray drying was established via briquetting, milling and sieving. Two different release profiles were developed to be available for clinical trials. The first option was prepared by using enteric capsules to prevent the isomerization of CorA by the acidic stomach conditions. Therefore, the prepared granules were filled into enteric capsules (HPMC-AS) and assessed as a potential drug product via dissolution tests and a stability study. Fast and almost complete release was detected in dissolution experiments for both ASD formulations. Both polymers were able to improve the stability when stored with

desiccant at 5 °C, 25 °C and 30 °C under nitrogen. The dissolution and the physical state were demonstrated to be stable over a period of 6 months with no indication of subsequent alteration. Regarding the CorA-content, increased isomerization was detected with ascending storage temperatures. At 30 °C a content >90% of the starting value could be guaranteed for up to 3 months, while storage at 25 °C was able to keep the CorA amount >90% for up to 6 months. For a longer shelf life, the capsules need to be stored in a refrigerator at 5 °C. At this condition a CorA content of 98% was detected for CorA-povidone and 95% for CorA-copovidone after 12 months. These results showed that the capsules are suitable for an initial phase I clinical study. However, further improvements in terms of stability are required to ensure a sufficient shelf life for a commercial drug product. A second option with an alternative release profile was addressed via a sustained release tablet formulation. Previous efficacy studies indicated that the time above the minimum inhibitory concentration is the driving force for *Wolbachia* depletion. By using the polymer hydroxypropyl methylcellulose in the outer phase of the tablet, a release over 7.5 h was enabled. For both options, delayed release capsule and sustained release tablet, CorA-povidone showed slightly improved dissolution compared to CorA-copovidone. However, both principles and ASDs continued to be part of preclinical investigations.

A further aim of the PhD project was to establish preclinical biorelevant *in vitro* tools for a rational investigation of preclinical formulation candidates. For a pH-dependent soluble drug, the gastrointestinal pH is able to influence the *in vivo* dissolution and thus, absorption and bioavailability. Adjustments, such as pH-profile, bile acids and transit times of the biphasic dissolution BiPHa+ led to species specific predictions regarding the dissolution and absorption of CoA-ASD-formulations. Moreover, these setups provide a material-saving method to optimize the oral availability of CorA in different species and to select well suited formulation principles already in early preclinical studies. Thus, it was possible to predict improved absorption in rats and dogs compared to mice. Differences between CorA-povidone and CorA-copovidone were detected in the mouse setup, while the rat setup displayed comparable profiles. These observations were confirmed by performed pharmacokinetic studies. The determined dissolution data in biorelevant media demonstrated dissolution as the decisive mechanism governing the oral

bioavailability of CorA and CorA formulations to be deduced. For CorA the presented setups confirmed the preclinical relevance, thus providing a material-saving method to optimize the oral treatment for preclinical species and select promising formulation principles already in early preclinical studies. These results also strengthened the predictive power of the biphasic dissolution results for the human setup.

Several pharmacokinetic studies of CorA and CorA-formulations were performed in various preclinical species comprising mouse, jird, rat and dog. Intravenous administrations were available for mouse, rat and dog. In general, the developed CorA-ASD-formulations allowed oral administration and an easy handling of CorA for *in vivo* studies, which was challenging with the neat drug substance. For all investigated species, high bioavailabilities for CorA formulations were observed. Due to limited quantity of drug substance, first trials were conducted in BALB/c mice. Administered as aqueous suspension in phosphate buffered saline pH 7.4, in mice the bioavailability of neat CorA of 11% was increased to 59% for CorA-povidone and to 19% for CorA-copovidone. Poorer performances were observed when administered with water as suspension medium, resulting in bioavailabilities of 3% for neat CorA, 33% for CorA-povidone and 10% for CorA-copovidone reaffirming the pH-dependent dissolution. However, based on the *in vitro* dissolution experiments the superiority of CorA-povidone compared to CorA-copovidone was assumed to be pronounced in mice, but less in other species. The *in vitro* dissolution mimicking the gastrointestinal conditions in rats revealed similar partitioning profiles for both CorA-ASDs. The pharmacokinetic evaluation in rats demonstrated high absorption for both ASDs, administered as oral suspension, resulting in high bioavailabilities. In comparison to an oral administration of a CorA-PEG 200 solution, the performances of the ASDs were not inferior. In particular, the median exposure level of the CorA-copovidone ASD showed similar values compared to the solution. Besides, the solution was identified as a suitable vehicle for toxicological studies in rats providing easy handling and sufficient solubility for CorA. In a pharmacokinetic evaluation in dogs the capsule and tablet prototypes, intended for initial human clinical trials, were investigated, as well as, a potential vehicle for toxicological studies, the CorA-silica formulation. The capsule formulations were able to achieve bioavailabilities of 33% for CorA-povidone and 35% for CorA-copovidone, respectively. The tablets reached 51% (CorA-povidone) and 36% (CorA-

copovidone) for bioavailability. Dogs are not the ideal model to investigate sustained release due to short intestinal transit times, so the release observed *in vitro* over 7.5 h could not be reflected within the pharmacokinetic study. However, tablets showed similar or even higher bioavailabilities compared to capsule formulations and are promising candidates for clinical trials. Despite higher dose levels (100 and 200 mg/kg) the mesoporous silica formulation of CorA was demonstrated to achieve high plasma concentration, exposure and bioavailability (100mg/kg: 59%; 200 mg/kg: 92%). In sum, the results obtained in these studies confirmed the ASD formulation principle as a bioavailability enhancing approach, confirmed in various species and the data were valuable inputs for a cross-species physiologically based pharmacokinetic (PBPK) model. In addition, vehicles for exploratory toxicology studies were investigated in terms of bioavailabilities demonstrating PEG 200 as a suitable solution for rats and mesoporous silica suspension as an alternative approach for dogs, both showing high intestinal absorption.

A PBPK model and physiologically based biopharmaceutic model (PBBM) were developed by integrating the *in vitro* measured and *in silico* predicted physicochemical and physiological characteristics of CorA. By using the biorelevant dissolution data for mice, it was able to predict plasma concentration profiles reaffirming dissolution as the decisive factor for oral bioavailability. Further preclinical *in vivo* data of the species mouse, rat and dog were used to build a cross-species *in silico* model predicting elimination and distribution in human. In addition, the mechanistic P-PSD approach was applied to predict *in vivo* dissolution of the oral drug product. The data for the capsule and tablet formulations were validated using the results of the dog pharmacokinetic study. This approach enabled a rational first-in-human (FIH) prediction. For all drug products the plasma profiles and corresponding pharmacokinetic parameters after a dose of 100 mg were predicted guiding the dose finding in combination with preclinical toxicology studies. Based on the *in vitro* determined half maximal inhibitory concentration (IC50), the efficacious dose was estimated to be 400 mg of the CorA-povidone tablet twice a day in combination with a high fat meal to successfully reach tissue exposure levels which would correspond on average, to twice the IC50 as unbound drug concentration. In contrast, the enteric capsule formulations were not expected to have such an immense positive food

effect as observed in the *in vivo* pharmacokinetic study in dogs. Currently, the deduction of a therpeutic success based on an *in vitro* determined parameter (IC50). However, future preclinical and clinical trials will provide more model confidence regarding required tissue concentrations for a therapeutic success by considering additional pharmacokinetic and pharmacodynamic data. Nevertheless, it is a helpful approach to get a first impression on human performance and thus supporting a rational dose selection for an initial clinical phase I study.

Another part of the preclinical process included seven-days exploratory toxicological studies in rats and dogs. For the toxicological studies in rats, CorA dissolved in polyethylene glycol 200 was found to be a suitable vehicle for offering high solubility properties and good vehicle tolerability. Thus, a dose level of 1000 mg/kg was able to be tested. During the study good tolerability for CorA could be demonstrated and no CorA related mortality was detected. Only mild gastrointestinal adverse effects were observed. Due to frequent vomiting when polyethylene glycol 200 was used for dogs, the vehicle needed to be replaced for this species. Mesoporous silica was identified as a suitable alternative for oral administration offering high loading capacities and good release properties. Moreover, vehicle tolerability was confirmed in a control group that was administered with mesoporous silica for seven consecutive days. The vehicle enabled high dose levels resulting in three dosing groups of 150, 450 and 750 mg/kg, respectively. The low and mid dose groups in dogs showed only slight and transient clinical signs, while a high incidence of clinical symptoms was present in the high dose group showing markedly decreased food consumptions, frequent vomiting and moderate body weight loss. Parallel toxicokinetic studies exhibited that both vehicles, polyethylene glycol and mesoporous silica, were able to provide high plasma concentrations and exposures. These studies will serve as the basis for future long-term good laboratory practice (GLP) toxicology studies required for a safe entry into human clinical trials.

In conclusion, innovative biorelevant dissolution assays for different species were established which in combination with PBPK modeling enabled a resource saving and efficient development and identification of well suitable CorA formulation candidates for clinical studies in human. After the successful completion of all preclinical studies, the developed oral CorA drug products will be examined in a FIH clinical trial, aiming to

provide a novel anti-infective candidate to combat infectious diseases such as neglected tropical diseases (NTD) caused by filarial nematodes.

13. Publications

Parts of this work have been published as peer-reviewed research articles, patents, abstracts, and posters. Text passages and figures of the published work were partly taken as templates and partially quoted directly for this thesis.

Peer-reviewed research papers:

Becker T., Krome A.K., Vahdati S., Schiefer A., Pfarr K., Ehrens A., Aden T., Grosse M., Jansen R., Alt S., Hesterkamp T., Stadler M, Hübner M.P., Kehraus S., König G.M., Hoerauf A., Wagner K.G. "In Vitro–In Vivo Relationship in Mini-Scale—Enabling Formulations of Corallopyronin A". *Pharmaceutics.* 14 (**2022**), doi:10.3390/pharmaceutics14081657.

Becker T., Heitkötter J., Krome A.K., Schiefer A., Pfarr K., Ehrens A., Grosse M., Sandargo B., Stammberger I., Stadler M., Hübner M.P., Kehraus S., Hoerauf A., Wagner K.G. "Mesoporous Silica as an Alternative Vehicle to Overcome Solubility Limitations". *Pharmaceutics*. 16 (**2024**), doi.org/10.3390/pharmaceutics16030386.

Denninger A., Becker T., Westedt U., Wagner K.G. "Advanced In Vivo Prediction by Introducing Biphasic Dissolution Data into PBPK Models". *Pharmaceutics.* 15 (**2023**), doi:10.3390/pharmaceutics15071978.

Rox K., Becker T., Schiefer A., Grosse M., Ehrens A., Jansen R., Aden T., Kehraus S., König G.M., Krome A.K., Hübner M.P., Wagner K.G., Stadler M., Pfarr K., Hoerauf A. "Pharmacokinetics and Pharmacodynamics (PK/PD) of Corallopyronin A against Methicillin-Resistant Staphylococcus Aureus". *Pharmaceutics* 15 (**2022**), doi:10.3390/pharmaceutics15010131.

Ehrens A., Schiefer A., Krome A.K., Becker T., Rox K., Neufeld H., Aden T., Wagner K.G., Müller R., Grosse M., Stadler M., König G.M., Kehraus S., Alt S., Hesterkamp T., Hübner M.P., Pfarr K., Hoerauf A. "Pharmacology and Early ADMET Data of Corallopyronin A, a Natural Product with Macrofilaricidal Anti-Wolbachial Activity in Filarial Nematodes". *Front. Trop. Dis* 3 (**2022**), doi:10.3389/fitd.2022.983107.

Krome A.K., Becker T., Kehraus S., Schiefer A., Gütschow M., Chaverra-Muñoz L., Hüttel S., Jansen R., Stadler M., Ehrens A., Pogorevc D., Müller R., Hübner M.P., Hesterkamp T., Pfarr K., Hoerauf A., Wagner K.G., König G.M. “Corallopyronin A: Antimicrobial Discovery to Preclinical Development“. *Nat. Prod. Rep.* (**2022**), doi:10.1039/D2NP00012A.

López Mármol Á., Denninger A., Touzet A., Dauer K., Becker T., Pöstges F., Pellequer Y., Lamprecht A., Wagner K.G. “The Relevance of Supersaturation and Solubilization in the Gastrointestinal Tract for Oral Bioavailability: An in vitro vs. in vivo Approach”. *International Journal of Pharmaceutics* (**2021**), doi:10.1016/j.ijpharm.2021.120648.

Krome A.K., Becker T., Kehraus S., Schiefer A., Steinebach C., Aden T., Frohberger S.J., Mármol Á.L., Kapote D., Jansen R., Chaverra-Muñoz L., Hübner M.P., Pfarr K., Hesterkamp T., Stadler M., Gütschow M., König G.M., Hoerauf A., Wagner K.G. “Solubility and Stability Enhanced Oral Formulations for the Anti-Infective Corallopyronin A”. *Pharmaceutics* 12 (**2020**), doi:10.3390/pharmaceutics12111105.

Scientific Abstracts and Posters

1. Becker T., Krome A.K., Schiefer A., Pfarr K., Aden T., Hübner M.P., Kehraus S., König G.M., Hoerauf A. and Wagner K.G. „Biorelevant Dissolution and PBPK Modelling to Forecast Oral Absorption – Enabling Formulations for Corallopyronin A". PharmSci360, 16-19 October 2022, Boston, USA. Poster presentation.
2. Becker T., Krome A.K., Schiefer A., Pfarr K., Aden T., Hübner M.P., Kehraus S., König G.M., Hoerauf A. and Wagner K.G. "IVIVR in Mini Scale – Enabling Formulations for Corallopyronin A". 13th Pharmaceutics, Biopharmaceutics and Pharmaceutical Technology World Meeting, 28-31 March 2022, Rotterdam. Poster presentation.
3. Becker T., Krome A.K., Schiefer A., Pfarr K., Aden T., Hübner M.P., Kehraus S., König G.M., Hoerauf A. and Wagner K.G. "Insights from the preclinical development of Corallopyronin A: Formulation evaluations by physiology-based pharmacokinetics and in vivo predictive in vitro tools". 12th Pharmaceutics, Biopharmaceutics and Pharmaceutical Technology World Meeting, 11-14 May 2021, online. Poster presentation.
4. Krome A.K., Becker T., Kehraus S., Schiefer A., Hübner M.P., Pfarr K., Hesterkamp T., König G.M., Hoerauf A. and Wagner K.G. "Bioavailability and Stability Enhanced Solid Oral Formulations of the Anti-Infective Corallopyronin A". Joint Annual Meeting, 01-03 November 2022, Stuttgart. Poster presentation.
5. Krome A.K., Becker T., Vahdati S., Schiefer A., Pfarr K., Aden T., Hübner M.P., Kehraus S., König G.M., Hoerauf A. and Wagner K.G "Evaluating preclinical and enabling formulations for Corallopyronin A". Joint Annual Meeting, 21-23 November 2019, Bad Nauheim. Poster presentation.

Patents

Wagner K.G., Lamprecht A., Krome A.K., Grisic D., Denninger A. and Becker T., Liquisolid Pharmaceutical Formulations and Process for Manufacturing, pending (EP 20 172 440.8).

14. References

1. Lederberg J. Infectious History. *Science* **2000**, *288*, 287-293.
2. Jones, K.E., Patel, N.G., Levy, M.A., Storeygard, A., Balk, D., Gittleman, J.L., Daszak, P. Global Trends in Emerging Infectious Diseases. *Nature* **2008**, *451*, 990–993, doi:10.1038/nature06536.
3. Velavan, T.P., Meyer, C.G. The COVID-19 Epidemic. *Trop Med Int Health* **2020**, *25*, 278–280, doi:10.1111/tmi.13383.
4. Miethke, M., Pieroni, M., Weber, T., Brönstrup, M., Hammann, P., Halby, L., Arimondo, P.B., Glaser, P., Aigle, B., Bode, H.B., et al. Towards the Sustainable Discovery and Development of New Antibiotics. *Nat Rev Chem* **2021**, *5*, 726–749, doi:10.1038/s41570-021-00313-1.
5. AMR-2020-Progress-Report. Available online: https://www.amrindustryalliance.org/wp-content/uploads/2020/01/AMR-2020-Progress-Report.pdf (accessed on 03 December 2023).
6. Matos de Opitz, C.L., Sass, P. Tackling Antimicrobial Resistance by Exploring New Mechanisms of Antibiotic Action. *Future Microbiology* **2020**, *15*, 703–708, doi:10.2217/fmb-2020-0048.
7. Hughes, D., Karlén, A. Discovery and Preclinical Development of New Antibiotics. *Upsala Journal of Medical Sciences* **2014**, *119*, 162–169, doi:10.3109/03009734.2014.896437.
8. Pfarr, K.M., Krome, A.K., Al-Obaidi, I., Batchelor, H., Vaillant, M., Hoerauf, A., Opoku, N.O., Kuesel, A.C. The Pipeline for Drugs for Control and Elimination of Neglected Tropical Diseases: 1. Anti-Infective Drugs for Regulatory Registration. *Parasites Vectors* **2023**, *16*, 82, doi:10.1186/s13071-022-05581-4.
9. Placket B. Why big pharma has abandoned antibiotics. *Nature* **2020**, *586*, 50-52.
10. Towse, A., Hoyle, C.K., Goodall, J., Hirsch, M., Mestre-Ferrandiz, J., Rex, J.H. Time for a Change in How New Antibiotics Are Reimbursed: Development of an Insurance Framework for Funding New Antibiotics Based on a Policy of Risk Mitigation. *Health Policy* **2017**, *121*, 1025–1030, doi:10.1016/j.healthpol.2017.07.011.
11. Mullard, A. Preclinical Antibiotic Pipeline Gets a Pick-Me-Up. *Nat Rev Drug Discov* **2017**, *16*, 741–742, doi:10.1038/nrd.2017.213.
12. Willmann, J.K., van Bruggen, N., Dinkelborg, L.M., Gambhir, S.S. Molecular Imaging in Drug Development. *Nat Rev Drug Discov* **2008**, *7*, 591–607, doi:10.1038/nrd2290.
13. DiMasi, J.A., Feldman, L., Seckler, A., Wilson, A. Trends in Risks Associated With New Drug Development: Success Rates for Investigational Drugs. *Clin Pharmacol Ther* **2010**, *87*, 272–277, doi:10.1038/clpt.2009.295.
14. Maas, J., Kamm, W., Hauck, G. An Integrated Early Formulation Strategy – From Hit Evaluation to Preclinical Candidate Profiling. *European Journal of Pharmaceutics and Biopharmaceutics* **2007**, 10.
15. Chaubal, M.V. Application of Formulation Technologies in Lead Candidate Selection and Optimization. *Drug Discovery Today* **2004**, *9*, 603–609, doi:10.1016/S1359-6446(04)03171-X.

16. Sugawara, M., Kadomura, S., He, X., Takekuma, Y., Kohri, N., Miyazaki, K. The Use of an in Vitro Dissolution and Absorption System to Evaluate Oral Absorption of Two Weak Bases in pH-Independent Controlled-Release Formulations. *European Journal of Pharmaceutical Sciences* **2005**, *26*, 1–8, doi:10.1016/j.ejps.2005.02.017.
17. Neervannan, S. Preclinical Formulations for Discovery and Toxicology: Physicochemical Challenges. *Expert Opinion on Drug Metabolism & Toxicology* **2006**, *2*, 715–731, doi:10.1517/17425255.2.5.715.
18. Steinmetz, K.L., Spack, E.G. The Basics of Preclinical Drug Development for Neurodegenerative Disease Indications. *BMC Neurol* **2009**, *9*, S2, doi:10.1186/1471-2377-9-S1-S2.
19. Amidon G.L., Lennernäs H., Shah V. P., Crison J. R. A Theoretical Basis for a Biopharmaceutic Drug Classfication: The Correlation of in Vitro Drug Product Dissolution and in Vivo Bioavailability. *Pharmaceutical Research* **1995**, *12*.
20. Kawabata, Y., Wada, K., Nakatani, M., Yamada, S., Onoue, S. Formulation Design for Poorly Water-Soluble Drugs Based on Biopharmaceutics Classification System: Basic Approaches and Practical Applications. *International Journal of Pharmaceutics* **2011**, *420*, 1–10, doi:10.1016/j.ijpharm.2011.08.032.
21. Meanwell, N.A. Improving Drug Candidates by Design: A Focus on Physicochemical Properties As a Means of Improving Compound Disposition and Safety. *Chem. Res. Toxicol.* **2011**, *24*, 1420–1456, doi:10.1021/tx200211v.
22. Martinez, M.N., Amidon, G.L. A Mechanistic Approach to Understanding the Factors Affecting Drug Absorption: A Review of Fundamentals. *The Journal of Clinical Pharmacology* **2002**, *42*, 620–643, doi:10.1177/00970002042006005.
23. Aungst, B.J. Optimizing Oral Bioavailability in Drug Discovery: An Overview of Design and Testing Strategies and Formulation Options. *Journal of Pharmaceutical Sciences* **2017**, *106*, 921–929, doi:10.1016/j.xphs.2016.12.002.
24. Hellriegel, E.T., Bjornsson, T.D., Hauck, W.W. Interpatient Variability in Bioavailability Is Related to the Extent of Absorption: Implications for Bioavailability and Bioequivalence Studies. *Clin Pharmacol Ther* **1996**, *60*, 601–607, doi:10.1016/S0009-9236(96)90208-8.
25. Dahan, A., Miller, J.M. The Solubility–Permeability Interplay and Its Implications in Formulation Design and Development for Poorly Soluble Drugs. *AAPS J* **2012**, *14*, 244–251, doi:10.1208/s12248-012-9337-6.
26. Buckley, S.T., Frank, K.J., Fricker, G., Brandl, M. Biopharmaceutical Classification of Poorly Soluble Drugs with Respect to "Enabling Formulations." *European Journal of Pharmaceutical Sciences* **2013**, *50*, 8–16, doi:10.1016/j.ejps.2013.04.002.
27. Singh, A., Worku, Z.A., Van den Mooter, G. Oral Formulation Strategies to Improve Solubility of Poorly Water-Soluble Drugs. *Expert Opinion on Drug Delivery* **2011**, *8*, 1361–1378, doi:10.1517/17425247.2011.606808.
28. Jain, S., Patel, N., Lin, S. Solubility and Dissolution Enhancement Strategies: Current Understanding and Recent Trends. *Drug Development and Industrial Pharmacy* **2015**, *41*, 875–887, doi:10.3109/03639045.2014.971027.
29. Noyes, A.A., Whitney, W.R. The Rate of Solution of Solid Substances in Their Own Solutions. *J. Am. Chem. Soc.* **1897**, *19*, 930–934, doi:10.1021/ja02086a003.
30. Dokoumetzidis, A., Macheras, P. A Century of Dissolution Research: From Noyes and Whitney to the Biopharmaceutics Classification System. *International Journal of Pharmaceutics* **2006**, *321*, 1–11, doi:10.1016/j.ijpharm.2006.07.011.

31. Da Silva, F.L.O., Marques, M.B.D.F., Kato, K.C., Carneiro, G. Nanonization Techniques to Overcome Poor Water-Solubility with Drugs. *Expert Opinion on Drug Discovery* **2020**, *15*, 853–864, doi:10.1080/17460441.2020.1750591.
32. Vogt, M., Kunath, K., Dressman, J.B. Dissolution Enhancement of Fenofibrate by Micronization, Cogrinding and Spray-Drying: Comparison with Commercial Preparations. *European Journal of Pharmaceutics and Biopharmaceutics* **2008**, *68*, 283–288, doi:10.1016/j.ejpb.2007.05.010.
33. Rasenack, N., Müller, B.W. Micron-Size Drug Particles: Common and Novel Micronization Techniques. *Pharmaceutical Development and Technology* **2004**, *9*, 1–13, doi:10.1081/PDT-120027417.
34. Challa, R., Ahuja, A., Ali, J., Khar, R.K. Cyclodextrins in Drug Delivery: An Updated Review. *AAPS PharmSciTech* **2005**, *6*, E329–E357, doi:10.1208/pt060243.
35. Loftsson, T., Jarho, P., Másson, M., Järvinen, T. Cyclodextrins in Drug Delivery. *Expert Opinion on Drug Delivery* **2005**, *2*, 335–351, doi:10.1517/17425247.2.1.335.
36. Stegemann, S., Leveiller, F., Franchi, D., de Jong, H., Lindén, H. When Poor Solubility Becomes an Issue: From Early Stage to Proof of Concept. *European Journal of Pharmaceutical Sciences* **2007**, *31*, 249–261, doi:10.1016/j.ejps.2007.05.110.
37. Sanches, B.M.A., Ferreira, E.I. Is Prodrug Design an Approach to Increase Water Solubility? *International Journal of Pharmaceutics* **2019**, *568*, 118498, doi:10.1016/j.ijpharm.2019.118498.
38. Rodriguez-Aller, M., Guillarme, D., Veuthey, J.-L., Gurny, R. Strategies for Formulating and Delivering Poorly Water-Soluble Drugs. *Journal of Drug Delivery Science and Technology* **2015**, *30*, 342–351, doi:10.1016/j.jddst.2015.05.009.
39. Müllertz, A., Ogbonna, A., Ren, S., Rades, T. New Perspectives on Lipid and Surfactant Based Drug Delivery Systems for Oral Delivery of Poorly Soluble Drugs. *Journal of Pharmacy and Pharmacology* **2010**, *62*, 1622–1636, doi:10.1111/j.2042-7158.2010.01107.x.
40. Mehnert, W., Mäder, K. Solid Lipid Nanoparticles. *Advanced Drug Delivery Reviews* **2012**, *64*, 83–101, doi:10.1016/j.addr.2012.09.021.
41. Talegaonkar, S., Bhattacharyya, A. Potential of Lipid Nanoparticles (SLNs and NLCs) in Enhancing Oral Bioavailability of Drugs with Poor Intestinal Permeability. *AAPS PharmSciTech* **2019**, *20*, 121, doi:10.1208/s12249-019-1337-8.
42. Müller, R.H., Runge, S., Ravelli, V., Mehnert, W., Thünemann, A.F., Souto, E.B. Oral Bioavailability of Cyclosporine: Solid Lipid Nanoparticles (SLN®) versus Drug Nanocrystals. *International Journal of Pharmaceutics* **2006**, *317*, 82–89, doi:10.1016/j.ijpharm.2006.02.045.
43. McCarthy, C.A., Ahern, R.J., Dontireddy, R., Ryan, K.B., Crean, A.M. Mesoporous Silica Formulation Strategies for Drug Dissolution Enhancement: A Review. *Expert Opinion on Drug Delivery* **2016**, *13*, 93–108, doi:10.1517/17425247.2016.1100165.
44. Maleki, A., Kettiger, H., Schoubben, A., Rosenholm, J.M., Ambrogi, V., Hamidi, M. Mesoporous Silica Materials: From Physico-Chemical Properties to Enhanced Dissolution of Poorly Water-Soluble Drugs. *Journal of Controlled Release* **2017**, *262*, 329–347, doi:10.1016/j.jconrel.2017.07.047.
45. Rengarajan, G.T., Enke, D., Steinhart, M., Beiner, M. Stabilization of the Amorphous State of Pharmaceuticals in Nanopores. *J. Mater. Chem.* **2008**, *18*, 2537, doi:10.1039/b804266g.

46. Bukara, K., Schueller, L., Rosier, J., Martens, M.A., Daems, T., Verheyden, L., Eelen, S., Van Speybroeck, M., Libanati, C., Martens, J.A., et al. Ordered Mesoporous Silica to Enhance the Bioavailability of Poorly Water-Soluble Drugs: Proof of Concept in Man. *European Journal of Pharmaceutics and Biopharmaceutics* **2016**, *108*, 220–225, doi:10.1016/j.ejpb.2016.08.020.
47. Shen, S., Ng, W.K., Chia, L., Dong, Y., Tan, R.B.H. Stabilized Amorphous State of Ibuprofen by Co-Spray Drying With Mesoporous SBA-15 to Enhance Dissolution Properties. *Journal of Pharmaceutical Sciences* **2010**, *99*, 1997–2007, doi:10.1002/jps.21967.
48. Vraníková, B., Niederquell, A., Šklubalová, Z., Kuentz, M. Relevance of the Theoretical Critical Pore Radius in Mesoporous Silica for Fast Crystallizing Drugs. *International Journal of Pharmaceutics* **2020**, *591*, 120019, doi:10.1016/j.ijpharm.2020.120019.
49. Pöstges, F., Kayser, K., Stoyanov, E., Wagner, K.G. Boost of Solubility and Supersaturation of Celecoxib via Synergistic Interactions of Methacrylic Acid-Ethyl Acrylate Copolymer (1:1) and Hydroxypropyl Cellulose in Ternary Amorphous Solid Dispersions. *International Journal of Pharmaceutics: X* **2022**, *4*, 100115, doi:10.1016/j.ijpx.2022.100115.
50. López Mármol, Á., Denninger, A., Touzet, A., Dauer, K., Becker, T., Pöstges, F., Pellequer, Y., Lamprecht, A., Wagner, K.G. The Relevance of Supersaturation and Solubilization in the Gastrointestinal Tract for Oral Bioavailability: An in vitro vs. in vivo Approach, International Journal of Pharmaceutics. *International Journal of Pharmaceutics* **2021**, 120648, doi:10.1016/j.ijpharm.2021.120648.
51. Brouwers, J., Brewster, M.E., Augustijns, P. Supersaturating Drug Delivery Systems: The Answer to Solubility-Limited Oral Bioavailability? *Journal of Pharmaceutical Sciences* **2009**, *98*, 2549–2572, doi:10.1002/jps.21650.
52. Sun, W.-J., Aburub, A., Sun, C.C. A Mesoporous Silica Based Platform to Enable Tablet Formulations of Low Dose Drugs by Direct Compression. *International Journal of Pharmaceutics* **2018**, *539*, 184–189, doi:10.1016/j.ijpharm.2018.01.049.
53. Vo, C.L.-N., Park, C., Lee, B.-J. Current Trends and Future Perspectives of Solid Dispersions Containing Poorly Water-Soluble Drugs. *European Journal of Pharmaceutics and Biopharmaceutics* **2013**, *85*, 799–813, doi:10.1016/j.ejpb.2013.09.007.
54. Vasconcelos, T., Sarmento, B., Costa, P. Solid Dispersions as Strategy to Improve Oral Bioavailability of Poor Water Soluble Drugs. *Drug Discovery Today* **2007**, *12*, 1068–1075, doi:10.1016/j.drudis.2007.09.005.
55. Williams, H.D., Trevaskis, N.L., Charman, S.A., Shanker, R.M., Charman, W.N., Pouton, C.W., Porter, C.J.H. Strategies to Address Low Drug Solubility in Discovery and Development. *Pharmacol Rev* **2013**, *65*, 315–499, doi:10.1124/pr.112.005660.
56. Ma, X., Williams, R.O. Characterization of Amorphous Solid Dispersions: An Update. *Journal of Drug Delivery Science and Technology* **2019**, *50*, 113–124, doi:10.1016/j.jddst.2019.01.017.
57. Hancock, B.C., Parks, M. What Is the True Solubility Advantage for Amorphous Pharmaceuticals? What is the True Solubility Advantage for Amorphous Pharmaceuticals? *Pharmaceutical Research* **1999**, *17*, 397-404.

58. Van den Mooter, G. The Use of Amorphous Solid Dispersions: A Formulation Strategy to Overcome Poor Solubility and Dissolution Rate. *Drug Discovery Today: Technologies* **2012**, *9*, e79–e85, doi:10.1016/j.ddtec.2011.10.002.
59. Frank, K.J., Rosenblatt, K.M., Westedt, U., Hölig, P., Rosenberg, J., Mägerlein, M., Fricker, G., Brandl, M. Amorphous Solid Dispersion Enhances Permeation of Poorly Soluble ABT-102: True Supersaturation vs. Apparent Solubility Enhancement. *International Journal of Pharmaceutics* **2012**, *437*, 288–293, doi:10.1016/j.ijpharm.2012.08.014.
60. Sun, D.D., Lee, P.I. Evolution of Supersaturation of Amorphous Pharmaceuticals: The Effect of Rate of Supersaturation Generation. *Mol. Pharmaceutics* **2013**, *10*, 4330–4346, doi:10.1021/mp400439q.
61. Guzmán, H.R., Tawa, M., Zhang, Z., Ratanabanangkoon, P., Shaw, P., Gardner, C.R., Chen, H., Moreau, J., Almarsson, Ö., Remenar, J.F. Combined Use of Crystalline Salt Forms and Precipitation Inhibitors to Improve Oral Absorption of Celecoxib from Solid Oral Formulations. *Journal of Pharmaceutical Sciences* **2007**, *96*, 2686–2702, doi:10.1002/jps.20906.
62. van Drooge, D.J., Hinrichs, W.L.J., Visser, M.R., Frijlink, H.W. Characterization of the Molecular Distribution of Drugs in Glassy Solid Dispersions at the Nano-Meter Scale, Using Differential Scanning Calorimetry and Gravimetric Water Vapour Sorption Techniques. *International Journal of Pharmaceutics* **2006**, *310*, 220–229, doi:10.1016/j.ijpharm.2005.12.007.
63. Hancock, B. C., Shamblin, S. L., Zografi, G. Molecular Mobility of Amorphous Pharmaceutical Solids Below Their Glass Transition Temperatures. *Pharmaceutical Research* **1995**, *12*.
64. Guo, Y., Shalaev, E., Smith, S. Physical Stability of Pharmaceutical Formulations: Solid-State Characterization of Amorphous Dispersions. *TrAC Trends in Analytical Chemistry* **2013**, *49*, 137–144, doi:10.1016/j.trac.2013.06.002.
65. Singh, A., Van den Mooter, G. Spray Drying Formulation of Amorphous Solid Dispersions. *Advanced Drug Delivery Reviews* **2016**, *100*, 27–50, doi:10.1016/j.addr.2015.12.010.
66. Costa, P., Sousa Lobo, J.M. Modeling and Comparison of Dissolution Profiles. *European Journal of Pharmaceutical Sciences* **2001**, *13*, 123–133, doi:10.1016/S0928-0987(01)00095-1.
67. European Medicines Agency. Reflection paper on the dissolution specification for generic solid oral immediate release products with systemic action. **2017**. Online available: https://www.ema.europa.eu/en/documents/scientific-guideline/reflection-paper-dissolution-specification-generic-solid-oral-immediate-release-products-systemic-action-first-version_en.pdf (accessed on 04 February 2024).
68. Shaikh, R., O'Brien, D.P., Croker, D.M., Walker, G.M. The Development of a Pharmaceutical Oral Solid Dosage Forms. In *Computer Aided Chemical Engineering*, Elsevier, 2018, Vol. 41, pp. 27–65 ISBN 978-0-444-63963-9.
69. Gibaldi, M., Feldman, S. Establishment of Sink Conditions in Dissolution Rate Determinations. Theoretical Considerations and Application to Nondisintegrating Dosage Forms. *Journal of Pharmaceutical Sciences* **1967**, *56*, 1238–1242, doi:10.1002/jps.2600561005.

70. Siepmann, J., Siepmann, F. Sink Conditions Do Not Guarantee the Absence of Saturation Effects. *International Journal of Pharmaceutics* **2020**, *577*, 119009, doi:10.1016/j.ijpharm.2019.119009.
71. Phillips, D.J., Pygall, S.R., Cooper, V.B., Mann, J.C. Overcoming Sink Limitations in Dissolution Testing: A Review of Traditional Methods and the Potential Utility of Biphasic Systems. *Journal of Pharmacy and Pharmacology* **2012**, *64*, 1549–1559, doi:10.1111/j.2042-7158.2012.01523.x.
72. Gray, V., Kelly, G., Xia, M., Butler, C., Thomas, S., Mayock, S. The Science of USP 1 and 2 Dissolution: Present Challenges and Future Relevance. *Pharm Res* **2009**, *26*, 1289–1302, doi:10.1007/s11095-008-9822-x.
73. Fotaki, N., Vertzoni, M. Biorelevant Dissolution Methods and Their Applications in In Vitro- In Vivo Correlations for Oral Formulations. *The Open Drug Delivery Journal* **2010**, *4*, 2–13, doi:10.2174/1874126601004020002.
74. Hirlak, O., Dieluweit, S., Merkel, R., Wagner, K.G. Polymer-Mediated Drug Supersaturation – A Spotlight on the Interplay between Phase-Separated Amorphous Drug Colloids and Dissolved Molecules. *Journal of Colloid and Interface Science* **2021**, *603*, 370–379, doi:10.1016/j.jcis.2021.06.089.
75. Carino, S.R., Sperry, D.C., Hawley, M. Relative Bioavailability Estimation of Carbamazepine Crystal Forms Using an Artificial Stomach-Duodenum Model. *Journal of Pharmaceutical Sciences* **2006**, *95*, 116–125, doi:10.1002/jps.20495.
76. Butler, J., Hens, B., Vertzoni, M., Brouwers, J., Berben, P., Dressman, J., Andreas, C.J., Schaefer, K.J., Mann, J., McAllister, M., et al. In Vitro Models for the Prediction of in Vivo Performance of Oral Dosage Forms: Recent Progress from Partnership through the IMI OrBiTo Collaboration. *European Journal of Pharmaceutics and Biopharmaceutics* **2019**, *136*, 70–83, doi:10.1016/j.ejpb.2018.12.010.
77. Kourentas, A., Vertzoni, M., Stavrinoudakis, N., Symillidis, A., Brouwers, J., Augustijns, P., Reppas, C., Symillides, M. An in Vitro Biorelevant Gastrointestinal Transfer (BioGIT) System for Forecasting Concentrations in the Fasted Upper Small Intestine: Design, Implementation, and Evaluation. *European Journal of Pharmaceutical Sciences* **2016**, *82*, 106–114, doi:10.1016/j.ejps.2015.11.012.
78. Alvebratt, C., Keemink, J., Edueng, K., Cheung, O., Strømme, M., Bergström, C.A.S. An in Vitro Dissolution–Digestion–Permeation Assay for the Study of Advanced Drug Delivery Systems. *European Journal of Pharmaceutics and Biopharmaceutics* **2020**, *149*, 21–29, doi:10.1016/j.ejpb.2020.01.010.
79. Berben, P., Brouwers, J., Augustijns, P. Assessment of Passive Intestinal Permeability Using an Artificial Membrane Insert System. *Journal of Pharmaceutical Sciences* **2018**, *107*, 250–256, doi:10.1016/j.xphs.2017.08.002.
80. Eliasen, J.N., Berthelsen, R., Slot, A.L., Müllertz, A. Evaluating Side-by-Side Diffusion Models for Studying Drug Supersaturation in an Absorptive Environment: A Case Example of Fenofibrate and Felodipine. *Journal of Pharmacy and Pharmacology* **2020**, *72*, 371–384, doi:10.1111/jphp.13218.
81. Jørgensen, J.R., Mohr, W., Rischer, M., Sauer, A., Mistry, S., Rades, T., Müllertz, A. In Vitro-in Vivo Relationship for Amorphous Solid Dispersions Using a Double Membrane Dissolution-Permeation Setup. *European Journal of Pharmaceutics and Biopharmaceutics* **2023**, *188*, 26–32, doi:10.1016/j.ejpb.2023.04.026.

82. Pestieau, A., Evrard, B. In Vitro Biphasic Dissolution Tests and Their Suitability for Establishing in Vitro-in Vivo Correlations: A Historical Review. *European Journal of Pharmaceutical Sciences* **2017**, *102*, 203–219, doi:10.1016/j.ejps.2017.03.019.
83. Denninger, A., Westedt, U., Rosenberg, J., Wagner, K.G. A Rational Design of a Biphasic DissolutionSetup—Modelling of Biorelevant Kinetics for a Ritonavir Hot-Melt Extruded Amorphous Solid Dispersion. *Pharmaceutics* **2020**, *12*, 237, doi:10.3390/pharmaceutics12030237.
84. Denninger, A., Westedt, U., Wagner, K.G. Shared IVIVR for Five Commercial Enabling Formulations Using the BiPHa+ Biphasic Dissolution Assay. *Pharmaceutics* **2021**, *13*, 285, doi:10.3390/pharmaceutics13020285.
85. Denninger, A., Becker, T., Westedt, U., Wagner, K.G. Advanced In Vivo Prediction by Introducing Biphasic Dissolution Data into PBPK Models. *Pharmaceutics* **2023**, *15*, 1978, doi.org/10.3390/pharmaceutics15071978.
86. Markopoulos, C., Andreas, C.J., Vertzoni, M., Dressman, J., Reppas, C. In-Vitro Simulation of Luminal Conditions for Evaluation of Performance of Oral Drug Products: Choosing the Appropriate Test Media. *European Journal of Pharmaceutics and Biopharmaceutics* **2015**, *93*, 173–182, doi:10.1016/j.ejpb.2015.03.009.
87. Kostewicz, E.S., Aarons, L., Bergstrand, M., Bolger, M.B., Galetin, A., Hatley, O., Jamei, M., Lloyd, R., Pepin, X., Rostami-Hodjegan, A., et al. PBPK Models for the Prediction of in Vivo Performance of Oral Dosage Forms. *European Journal of Pharmaceutical Sciences* **2014**, *57*, 300–321, doi:10.1016/j.ejps.2013.09.008.
88. Zhuang, X., Lu, C. PBPK Modeling and Simulation in Drug Research and Development. *Acta Pharmaceutica Sinica B* **2016**, *6*, 430–440, doi:10.1016/j.apsb.2016.04.004.
89. Lipka, E., Amidon, G.L. Setting Bioequivalence Requirements for Drug Development Based on Preclinical Data: Optimizing Oral Drug Delivery Systems. *Journal of Controlled Release* **1999**, *62*, 41–49, doi:10.1016/S0168-3659(99)00022-X.
90. Zhao, P., Zhang, L., Grillo, J.A., Liu, Q., Bullock, J.M., Moon, Y.J., Song, P., Brar, S.S., Madabushi, R., Wu, T.C., et al. Applications of Physiologically Based Pharmacokinetic (PBPK) Modeling and Simulation During Regulatory Review. *Clin Pharmacol Ther* **2011**, *89*, 259–267, doi:10.1038/clpt.2010.298.
91. Jamei, M. Recent Advances in Development and Application of Physiologically-Based Pharmacokinetic (PBPK) Models: A Transition from Academic Curiosity to Regulatory Acceptance. *Curr Pharmacol Rep* **2016**, *2*, 161–169, doi:10.1007/s40495-016-0059-9.
92. Hotez, P.J., Fenwick, A., Sachs, S.E. Control of Neglected Tropical Diseases. *n engl j med* **2007**, *357*, 1018-1027, doi: 10.1056/NEJMra064142.
93. World Health Organization Working to Overcome the Global Impact of Neglected Tropical Diseases: First WHO Report on Neglected Tropical Diseases. Trabalhando para superar o impacto global de doenças tropicais negligenciadas: primeiro relatório da OMS sobre doenças tropicais negligenciadas. **2010**. Online available: https://apps.who.int/iris/handle/10665/44440 (accessed April 4, 2023).
94. Cohen, J.P., Silva, L., Cohen, A., Awatin, J., Sturgeon, R. Progress Report on Neglected Tropical Disease Drug Donation Programs. *Clinical Therapeutics* **2016**, *38*, 1193–1204, doi:10.1016/j.clinthera.2016.02.031.

95. Lee, B.Y., Bartsch, S.M., Gorham, K.M. Economic and Financial Evaluation of Neglected Tropical Diseases. In *Advances in Parasitology* **2015**, *87*, 329–417 doi.org/10.1016/bs.apar.2015.01.002 .
96. Basáñez, M.-G., Pion, S.D.S., Churcher, T.S., Breitling, L.P., Little, M.P., Boussinesq, M. River Blindness: A Success Story under Threat? *PLoS Med* **2006**, *3*, e371, doi:10.1371/journal.pmed.0030371.
97. Ottesen, E.A. Lymphatic Filariasis: Treatment, Control and Elimination. In *Advances in Parasitology*, Elsevier, 2006, Vol. 61, pp. 395–441 ISBN 978-0-12-031761-5.
98. Taylor, M.J., Hoerauf, A., Bockarie, M. Lymphatic Filariasis and Onchocerciasis. *The Lancet* **2010**, *376*, 1175–1185, doi:10.1016/S0140-6736(10)60586-7.
99. Schiefer, A., Schmitz, A., Schäberle, T.F., Specht, S., Lämmer, C., Johnston, K.L., Vassylyev, D.G., König, G.M., Hoerauf, A., Pfarr, K. Corallopyronin A Specifically Targets and Depletes Essential Obligate Wolbachia Endobacteria From Filarial Nematodes In Vivo. *The Journal of Infectious Diseases* **2012**, *206*, 249–257, doi:10.1093/infdis/jis341.
100. Schiefer, A., Hübner, M.P., Krome, A., Lämmer, C., Ehrens, A., Aden, T., Koschel, M., Neufeld, H., Chaverra-Muñoz, L., Jansen, R., et al. Corallopyronin A for Short-Course Anti-Wolbachial, Macrofilaricidal Treatment of Filarial Infections. *PLoS Negl Trop Dis* **2020**, *14*, e0008930, doi:10.1371/journal.pntd.0008930.
101. Theuretzbacher, U., Outterson, K., Engel, A., Karlén, A. The Global Preclinical Antibacterial Pipeline. *Nat Rev Microbiol* **2020**, *18*, 275–285, doi:10.1038/s41579-019-0288-0.
102. Krome, A.K., Becker, T., Kehraus, S., Schiefer, A., Gütschow, M., Chaverra-Muñoz, L., Hüttel, S., Jansen, R., Stadler, M., Ehrens, A., et al. Corallopyronin A: Antimicrobial Discovery to Preclinical Development. *Nat. Prod. Rep.* **2022**, 10.1039.D2NP00012A, doi:10.1039/D2NP00012A.
103. Schäberle, T.F., Schmitz, A., Zocher, G., Schiefer, A., Kehraus, S., Neu, E., Roth, M., Vassylyev, D.G., Stehle, T., Bierbaum, G., et al. Insights into Structure–Activity Relationships of Bacterial RNA Polymerase Inhibiting Corallopyronin Derivatives. *J. Nat. Prod.* **2015**, *78*, 2505–2509, doi:10.1021/acs.jnatprod.5b00175.
104. Irschik, H., Jansen, R., Höfle, G., Gerth, K., Reichenbach, H. The Corallopyronins, New Inhibitors of Bacterial RNA Synthesis from Myxobacteria. *J. Antibiot.* **1985**, *38*, 145–152, doi:10.7164/antibiotics.38.145.
105. Rox, K., Becker, T., Schiefer, A., Grosse, M., Ehrens, A., Jansen, R., Aden, T., Kehraus, S., König, G.M., Krome, A.K., et al. Pharmacokinetics and Pharmacodynamics (PK/PD) of Corallopyronin A against Methicillin-Resistant Staphylococcus Aureus. *Pharmaceutics* **2022**, *15*, 131, doi:10.3390/pharmaceutics15010131.
106. Kock, F., Hauptmann, M., Osterloh, A., Schäberle, T.F., Poppert, S., Frickmann, H., Menzel, K.-D., Peschel, G., Pfarr, K., Schiefer, A., et al. Orientia Tsutsugamushi Is Highly Susceptible to the RNA Polymerase Switch Region Inhibitor Corallopyronin A *In Vitro* and *In Vivo*. *Antimicrob Agents Chemother* **2018**, *62*, e01732-17, doi:10.1128/AAC.01732-17.

107. Pogorevc, D., Panter, F., Schillinger, C., Jansen, R., Wenzel, S.C., Müller, R. Production Optimization and Biosynthesis Revision of Corallopyronin A, a Potent Anti-Filarial Antibiotic. *Metabolic Engineering* **2019**, *55*, 201–211, doi:10.1016/j.ymben.2019.07.010.
108. Krome, A.K., Becker, T., Kehraus, S., Schiefer, A., Steinebach, C., Aden, T., Frohberger, S.J., Mármol, Á.L., Kapote, D., Jansen, R., et al. Solubility and Stability Enhanced Oral Formulations for the Anti-Infective Corallopyronin A. *Pharmaceutics* **2020**, *12*, 1105, doi:10.3390/pharmaceutics12111105.
109. Krome, A.K., Dissolution, Solubility, and Stability Enhanced Formulation Strategies for the Novel Anti-infective Corallopyronin A. Doctoral Dissertation, *University of Bonn* **2021**.
110. Kleinebudde, P. Roll Compaction/Dry Granulation: Pharmaceutical Applications. *European Journal of Pharmaceutics and Biopharmaceutics* **2004**, *58*, 317–326, doi:10.1016/j.ejpb.2004.04.014.
111. Michrafy, A., Ringenbacher, D., Tchoreloff, P. Modelling the Compaction Behaviour of Powders: Application to Pharmaceutical Powders. *Powder Technology* **2002**, *127*, 257–266, doi:10.1016/S0032-5910(02)00119-5.
112. U.S. Department of Health and Human Services Food and Drug Administration Center for Drug Evaluation and Research (CDER). Guidance for Industry, Estimating the Maximum Safe Starting Dose in Initial Clinical Trials for Therapeutics in Adult Healthy Volunteers. **2005**. Online available: https://www.fda.gov/regulatory-information/search-fda-guidance-documents/estimating-maximum-safe-starting-dose-initial-clinical-trials-therapeutics-adult-healthy-volunteers (accessed on 03 December 2023).
113. Sutton, S.C. Companion Animal Physiology and Dosage Form Performance. *Advanced Drug Delivery Reviews* **2004**, *56*, 1383–1398, doi:10.1016/j.addr.2004.02.013.
114. Mellaerts, R., Jammaer, J.A.G., Van Speybroeck, M., Chen, H., Humbeeck, J.V., Augustijns, P., Van den Mooter, G., Martens, J.A. Physical State of Poorly Water Soluble Therapeutic Molecules Loaded into SBA-15 Ordered Mesoporous Silica Carriers: A Case Study with Itraconazole and Ibuprofen. *Langmuir* **2008**, *24*, 8651–8659, doi:10.1021/la801161g.
115. GRACE. Technical Data Sheet SYLOID®-XDP Silica-Solution for Liquisolid Formulations. **2020**. Available online: https://grace.com/ products/syloid-silica/ (accessed on 24 February 2024).
116. Ali, S., Kolter, K., Kolliphor® HS 15 - An Enabler for Parenteral and Oral Formulations, *American Pharmaceutical Review* **2019**. Online available: https://www.americanpharmaceuticalreview.com/Featured-Articles/358749-Kolliphor-HS-15-An-Enabler-for-Parenteral-and-Oral-Formulations/ (accessed July 28, 2023).
117. McConnell, E.L., Basit, A.W., Murdan, S. Measurements of Rat and Mouse Gastrointestinal pH, Fluid and Lymphoid Tissue, and Implications for in-Vivo Experiments. *Journal of Pharmacy and Pharmacology* **2008**, *60*, 63–70, doi:10.1211/jpp.60.1.0008.

118. Koziolek, M., Grimm, M., Becker, D., Iordanov, V., Zou, H., Shimizu, J., Wanke, C., Garbacz, G., Weitschies, W. Investigation of pH and Temperature Profiles in the GI Tract of Fasted Human Subjects Using the Intellicap® System. *Journal of Pharmaceutical Sciences* **2015**, *104*, 2855–2863, doi:10.1002/jps.24274.
119. Woting, A., Blaut, M. Small Intestinal Permeability and Gut-Transit Time Determined with Low and High Molecular Weight Fluorescein Isothiocyanate-Dextrans in C3H Mice. *Nutrients* **2018**, *10*, 685, doi:10.3390/nu10060685.
120. Zecevic, D.E., Wagner, K.G. Rational Development of Solid Dispersions via Hot-Melt Extrusion Using Screening, Material Characterization, and Numeric Simulation Tools. *Journal of Pharmaceutical Sciences* **2013**, *102*, 2297–2310, doi:10.1002/jps.23592.
121. DeSesso, J.M., Williams, A.L. Contrasting the Gastrointestinal Tracts of Mammals: Factors That Influence Absorption. *Annual Reports in Medicinal Chemistry* **2008**, *43*, 353–371, doi.org/10.1016/S0065-7743(08)00021-3.
122. McIlvaine, T.C. A Buffer Solution for Colorimetric Comparison. *Journal of Biological Chemistry* **1921**, *49*, 183–186, doi:10.1016/S0021-9258(18)86000-8.
123. Jang, S.-F., Goins, B.A., Phillips, W.T., Santoyo, C., Rice-Ficht, A., McConville, J.T. Size Discrimination in Rat and Mouse Gastric Emptying: Size Discrimination in Gastric Emptying. *Biopharm. Drug Dispos.* **2013**, *34*, 107–124, doi:10.1002/bdd.1828.
124. Langenbucher, F. Letters to the Editor: Linearization of Dissolution Rate Curves by the Weibull Distribution. *Journal of Pharmacy and Pharmacology* **2011**, *24*, 979–981, doi:10.1111/j.2042-7158.1972.tb08930.x.
125. Christfort, J.F., Strindberg, S., Plum, J., Hall-Andersen, J., Janfelt, C., Nielsen, L.H., Müllertz, A. Developing a Predictive in Vitro Dissolution Model Based on Gastrointestinal Fluid Characterisation in Rats. *European Journal of Pharmaceutics and Biopharmaceutics* **2019**, *142*, 307–314, doi:10.1016/j.ejpb.2019.07.007.
126. Arndt, M., Chokshi, H., Tang, K., Parrott, N.J., Reppas, C., Dressman, J.B. Dissolution Media Simulating the Proximal Canine Gastrointestinal Tract in the Fasted State. *European Journal of Pharmaceutics and Biopharmaceutics* **2013**, *84*, 633–641, doi:10.1016/j.ejpb.2013.01.010.
127. European Medicines Agency. Q 1 A (R2) Stability Testing of new Drug Substances and Products. **2003**. Online available: https://www.ema.europa.eu/en/documents/scientific-guideline/ich-q-1-r2-stability-testing-new-drug-substances-products-step-5_en.pdf (accessed on 03 December 2023).
128. European Medicines Agency. Guideline on the pharmacokinetic and clinical evaluation of modified release dosage forms. **2012**. Online available: https://www.ema.europa.eu/en/documents/scientific-guideline/guideline-pharmacokinetic-clinical-evaluation-modified-release-dosage-forms_en.pdf (accessed on 03 December 2023).
129. Lu, T., Fraczkiewicz, G., Salphati, L., Budha, N., Dalziel, G., Smelick, G.S., Morrissey, K.M., Davis, J.D., Jin, J.Y., Ware, J.A. Combining “Bottom-up” and “Top-down” Approaches to Assess the Impact of Food and Gastric pH on Pictilisib (GDC-0941) Pharmacokinetics: Combining “Bottom-up” and “Top-down” Approaches. *CPT Pharmacometrics Syst. Pharmacol.* **2017**, *6*, 747–755, doi:10.1002/psp4.12228.

130. Krapf, M.K., Gallus, J., Vahdati, S., Wiese, M. New Inhibitors of Breast Cancer Resistance Protein (ABCG2) Containing a 2,4-Disubstituted Pyridopyrimidine Scaffold. *J. Med. Chem.* **2018**, *61*, 3389–3408, doi:10.1021/acs.jmedchem.7b01012.
131. Li, H.K., Agweyu, A., English, M., Bejon, P. An Unsupported Preference for Intravenous Antibiotics. *PLoS Med* **2015**, *12*, e1001825, doi:10.1371/journal.pmed.1001825.
132. Shahiwala, A. Formulation Approaches in Enhancement of Patient Compliance to Oral Drug Therapy. *Expert Opinion on Drug Delivery* **2011**, *8*, 1521–1529, doi:10.1517/17425247.2011.628311.
133. Rizi, K., Green, R.J., Donaldson, M., Williams, A.C. Production of pH-Responsive Microparticles by Spray Drying: Investigation of Experimental Parameter Effects on Morphological and Release Properties. *Journal of Pharmaceutical Sciences* **2011**, *100*, 566–579, doi:10.1002/jps.22291.
134. Agrawal, A.M., Dudhedia, M.S., Patel, A.D., Raikes, M.S. Characterization and Performance Assessment of Solid Dispersions Prepared by Hot Melt Extrusion and Spray Drying Process. *International Journal of Pharmaceutics* **2013**, *457*, 71–81, doi:10.1016/j.ijpharm.2013.08.081.
135. Chen, Y., Wang, S., Wang, S., Liu, C., Su, C., Hageman, M., Hussain, M., Haskell, R., Stefanski, K., Qian, F. Initial Drug Dissolution from Amorphous Solid Dispersions Controlled by Polymer Dissolution and Drug-Polymer Interaction. *Pharm Res* **2016**, *33*, 2445–2458, doi:10.1007/s11095-016-1969-2.
136. Nair, A., Morsy, M.A., Jacob, S. Dose Translation between Laboratory Animals and Human in Preclinical and Clinical Phases of Drug Development. *Drug Dev Res* **2018**, *79*, 373–382, doi:10.1002/ddr.21461.
137. Nair, A., Jacob, S. A Simple Practice Guide for Dose Conversion between Animals and Human. *J Basic Clin Pharma* **2016**, *7*, 27, doi:10.4103/0976-0105.177703.
138. Liu, L.X., Marziano, I., Bentham, A.C., Litster, J.D., E.T.White, Howes, T. Effect of Particle Properties on the Flowability of Ibuprofen Powders. *International Journal of Pharmaceutics* **2008**, *362*, 109–117, doi:10.1016/j.ijpharm.2008.06.023.
139. Miranda, A., Millán, M., Caraballo, I. Investigation of the Influence of Particle Size on the Excipient Percolation Thresholds of HPMC Hydrophilic Matrix Tablets. *Journal of Pharmaceutical Sciences* **2007**, *96*, 2746–2756, doi:10.1002/jps.20912.
140. Ehrens, A., Schiefer, A., Krome, A.K., Becker, T., Rox, K., Neufeld, H., Aden, T., Wagner, K.G., Müller, R., Grosse, M., et al. Pharmacology and Early ADMET Data of Corallopyronin A, a Natural Product with Macrofilaricidal Anti-Wolbachial Activity in Filarial Nematodes. *Front. Trop. Dis* **2022**, *3*, 983107, doi:10.3389/fitd.2022.983107.
141. Rumondor, A.C.F., Taylor, L.S. Effect of Polymer Hygroscopicity on the Phase Behavior of Amorphous Solid Dispersions in the Presence of Moisture. *Mol. Pharmaceutics* **2010**, *7*, 477–490, doi:10.1021/mp9002283.
142. Verma, S., Rudraraju, V.S. Wetting Kinetics: An Alternative Approach Towards Understanding the Enhanced Dissolution Rate for Amorphous Solid Dispersion of a Poorly Soluble Drug. *AAPS PharmSciTech* **2015**, *16*, 1079–1090, doi:10.1208/s12249-014-0281-x.

143. Lehmkemper, K., Kyerematen, S.O., Heinzerling, O., Degenhardt, M., Sadowski, G. Long-Term Physical Stability of PVP- and PVPVA-Amorphous Solid Dispersions. *Mol. Pharmaceutics* **2017**, *14*, 157–171, doi:10.1021/acs.molpharmaceut.6b00763.
144. Lu, Y., Tang, N., Lian, R., Qi, J., Wu, W. Understanding the Relationship between Wettability and Dissolution of Solid Dispersion. *International Journal of Pharmaceutics* **2014**, *465*, 25–31, doi:10.1016/j.ijpharm.2014.02.004.
145. Akimoto, M., Nagahata, N., Furuya, A., Fukushima, K., Higuchi, S., Suwa, T. Gastric pH Profiles of Beagle Dogs and Their Use as an Alternative to Human Testing. *European Journal of Pharmaceutics and Biopharmaceutics* **2000,** *49*, 99-102, oi: 10.1016/s0939-6411(99)00070-3.
146. Willems, L., Van Der Geest, R., De Beule, K. Itraconazole Oral Solution and Intravenous Formulations: A Review of Pharmacokinetics and Pharmacodynamics. *J Clin Pharm Ther* **2001**, *26*, 159–169, doi:10.1046/j.1365-2710.2001.00338.x.
147. Koziolek, M., Grimm, M., Bollmann, T., Schäfer, K.J., Blattner, S.M., Lotz, R., Boeck, G., Weitschies, W. Characterization of the GI Transit Conditions in Beagle Dogs with a Telemetric Motility Capsule. *European Journal of Pharmaceutics and Biopharmaceutics* **2019**, *136*, 221–230, doi:10.1016/j.ejpb.2019.01.026.
148. Emami, J. In Vitro - In Vivo Correlation: From Theory to Applications. *J Pharm Pharm* Sci **2006**, *9*, 169-189.
149. Roberts, M.S., Magnusson, B.M., Burczynski, F.J., Weiss, M. Enterohepatic Circulation: Physiological, Pharmacokinetic and Clinical Implications. *Clinical Pharmacokinetics* **2002**, *41*, 751–790, doi:10.2165/00003088-200241100-00005.
150. Murakami, T., Takano, M. Intestinal Efflux Transporters and Drug Absorption. *Expert Opinion on Drug Metabolism & Toxicology* **2008**, *4*, 923–939, doi:10.1517/17425255.4.7.923.
151. Bansal, T., Mishra, G., Jaggi, M., Khar, R.K., Talegaonkar, S. Effect of P-Glycoprotein Inhibitor, Verapamil, on Oral Bioavailability and Pharmacokinetics of Irinotecan in Rats. *European Journal of Pharmaceutical Sciences* **2009**, *36*, 580–590, doi:10.1016/j.ejps.2008.12.005.
152. Chu, X., Bleasby, K., Evers, R. Species Differences in Drug Transporters and Implications for Translating Preclinical Findings to Humans. *Expert Opinion on Drug Metabolism & Toxicology* **2013**, *9*, 237–252, doi:10.1517/17425255.2013.741589.
153. Ferreira, R.J., Ferreira, M.-J.U., Dos Santos, D.J.V.A. Molecular Docking Characterizes Substrate-Binding Sites and Efflux Modulation Mechanisms within P-Glycoprotein. *J. Chem. Inf. Model.* **2013**, *53*, 1747–1760, doi:10.1021/ci400195v.
154. Berlin, M., Ruff, A., Kesisoglou, F., Xu, W., Wang, M.H., Dressman, J.B. Advances and Challenges in PBPK Modeling – Analysis of Factors Contributing to the Oral Absorption of Atazanavir, a Poorly Soluble Weak Base. *European Journal of Pharmaceutics and Biopharmaceutics* **2015**, *93*, 267–280, doi:10.1016/j.ejpb.2015.03.031.
155. Perry, C., Davis, G., Conner, T.M., Zhang, T. Utilization of Physiologically Based Pharmacokinetic Modeling in Clinical Pharmacology and Therapeutics: An Overview. *Curr Pharmacol Rep* **2020**, *6*, 71–84, doi:10.1007/s40495-020-00212-x.

156. Cristofoletti, R., Patel, N., Dressman, J.B. Assessment of Bioequivalence of Weak Base Formulations Under Various Dosing Conditions Using Physiologically Based Pharmacokinetic Simulations in Virtual Populations. Case Examples: Ketoconazole and Posaconazole. *Journal of Pharmaceutical Sciences* **2017**, *106*, 560–569, doi:10.1016/j.xphs.2016.10.008.
157. Woolf, S.H. The Meaning of Translational Research and Why It Matters. *JAMA* **2008**, *299*, doi:10.1001/jama.2007.26.
158. European Medicines Agency. Guideline on strategies to identify and mitigate risks for first-in-human and early clinical trials with investigational medicinal products. **2017** Online available: https://www.ema.europa.eu/en/documents/scientific-guideline/guideline-strategies-identify-mitigate-risks-first-human-early-clinical-trials-investigational_en.pdf (accessed on 03 December 2023).
159. Mitra, A., Suarez-Sharp, S., Pepin, X.J.H., Flanagan, T., Zhao, Y., Kotzagiorgis, E., Parrott, N., Sharan, S., Tistaert, C., Heimbach, T., et al. Applications of Physiologically Based Biopharmaceutics Modeling (PBBM) to Support Drug Product Quality: A Workshop Summary Report. *Journal of Pharmaceutical Sciences* **2021**, *110*, 594–609, doi:10.1016/j.xphs.2020.10.059.
160. Sinha, V.K., Snoeys, J., Osselaer, N.V., Peer, A.V., Mackie, C., Heald, D. From Preclinical to Human - Prediction of Oral Absorption and Drug-Drug Interaction Potential Using Physiologically Based Pharmacokinetic (PBPK) Modeling Approach in an Industrial Setting: A Workflow by Using Case Example: Prediction of Oral Absorption and DDI Using PBPK. *Biopharm. Drug Dispos.* **2012**, *33*, 111–121, doi:10.1002/bdd.1782.
161. Pepin, X.J.H., Sanderson, N.J., Blanazs, A., Grover, S., Ingallinera, T.G., Mann, J.C. Bridging in Vitro Dissolution and in Vivo Exposure for Acalabrutinib. Part I. Mechanistic Modelling of Drug Product Dissolution to Derive a P-PSD for PBPK Model Input. *European Journal of Pharmaceutics and Biopharmaceutics* **2019**, *142*, 421–434, doi:10.1016/j.ejpb.2019.07.014.
162. Becker, T., Krome, A.K., Vahdati, S., Schiefer, A., Pfarr, K., Ehrens, A., Aden, T., Grosse, M., Jansen, R., Alt, S., et al. In Vitro–In Vivo Relationship in Mini-Scale—Enabling Formulations of Corallopyronin A. *Pharmaceutics* **2022**, *14*, 1657, doi.org/10.3390/pharmaceutics14081657.
163. Grover, A., Benet, L.Z. Effects of Drug Transporters on Volume of Distribution. *AAPS J* **2009**, *11*, 250–261, doi:10.1208/s12248-009-9102-7.
164. Rodgers, T., Rowland, M. Physiologically Based Pharmacokinetic Modelling 2: Predicting the Tissue Distribution of Acids, Very Weak Bases, Neutrals and Zwitterions. *Journal of Pharmaceutical Sciences* **2006**, *95*, 1238–1257, doi:10.1002/jps.20502.
165. Lennernäs, H. Intestinal Permeability and Its Relevance for Absorption and Elimination. *Xenobiotica* **2007**, *37*, 1015–1051, doi:10.1080/00498250701704819.
166. Sutton, S.C. Role of Physiological Intestinal Water in Oral Absorption. *AAPS J* **2009**, *11*, 277–285, doi:10.1208/s12248-009-9087-2.
167. Schiller, C., Frohlich, C.-P., Giessmann, T., Siegmund, W., Monnikes, H., Hosten, N., Weitschies, W. Intestinal Fluid Volumes and Transit of Dosage Forms as Assessed by Magnetic Resonance Imaging. *Aliment Pharmacol Ther* **2005**, *22*, 971–979, doi:10.1111/j.1365-2036.2005.02683.x.

168. Mudie, D.M., Murray, K., Hoad, C.L., Pritchard, S.E., Garnett, M.C., Amidon, G.L., Gowland, P.A., Spiller, R.C., Amidon, G.E., Marciani, L. Quantification of Gastrointestinal Liquid Volumes and Distribution Following a 240 mL Dose of Water in the Fasted State. *Mol. Pharmaceutics* **2014**, *11*, 3039–3047, doi:10.1021/mp500210c.
169. Rathi, C., Lee, R.E., Meibohm, B. Translational PK/PD of Anti-Infective Therapeutics. *Drug Discovery Today: Technologies* **2016**, *21–22*, 41–49, doi:10.1016/j.ddtec.2016.08.004.
170. European Medicines Agency. Guideline on Repeated Dose Toxicity. **2007**. Online available: https://www.ema.europa.eu/en/documents/scientific-guideline/guideline-repeated-dose-toxicity-revision-1_en.pdf (accessed on 03 December 2023).
171. S., P. Toxicological Screening. *Journal of Pharmacology and Pharmacotherapeutics* **2011**, *2*, 74–79, doi:10.4103/0976-500X.81895.
172. Gad, S.C., Spainhour, C.B., Shoemake, C., Pallman, D.R.S., Stricker-Krongrad, A., Downing, P.A., Seals, R.E., Eagle, L.A., Polhamus, K., Daly, J. Tolerable Levels of Nonclinical Vehicles and Formulations Used in Studies by Multiple Routes in Multiple Species With Notes on Methods to Improve Utility. *Int J Toxicol* **2016**, *35*, 95–178, doi:10.1177/1091581815622442.
173. Stokes, A.H., Kemp, D.C., Faiola, B., Jordan, H.L., Merrill, C.L., Hailey, J.R., Brown, R.E., Bailey, D.W. Effects of Solutol (Kolliphor) and Cremophor in Polyethylene Glycol 400 Vehicle Formulations in Sprague-Dawley Rats and Beagle Dogs. *Int J Toxicol* **2013**, *32*, 189–197, doi:10.1177/1091581813485452.
174. Becker, T., Heitkötter, J., Krome, A.K., Schiefer, A., Pfarr, K., Ehrens, A., Grosse, M., Sandargo, B., Stammberger, I., Stadler, M., et al. Mesoporous Silica as an Alternative Vehicle to Overcome Solubility Limitations. *Pharmaceutics* **2024**, *16*, 386, doi.org/10.3390/pharmaceutics16030386.
175. Gierke, H., Pfrommer, T., Schäfer, K., Weitschies, W., Nolte, T. Pharmacobezoar Formation From HPMC-AS-Containing Spray-Dried Formulations in Nonclinical Safety Studies in Rats. *Toxicol Pathol* **2022**, *50*, 920–929, doi:10.1177/01926233221145112.
176. European Medicines Agency. ICH Guideline (Q3C (R8) on Impurities: Guideline or Residual Solvents. **2022**. Online available: https://www.ema.europa.eu/en/ich-q3c-r8-residual-solvents-scientific-guideline (accessed on 24February 2024).
177. Vraníková, B., Niederquell, A., Ditzinger, F., Šklubalová, Z., Kuentz, M. Mechanistic Aspects of Drug Loading in Liquisolid Systems with Hydrophilic Lipid-Based Mixtures. *International Journal of Pharmaceutics* **2020**, *578*, 119099, doi:10.1016/j.ijpharm.2020.119099.
178. Kostelanská, K., Prudilová, B.B., Holešová, S., Vlček, J., Vetchý, D., Gajdziok, J. Comparative Study of Powder Carriers Physical and Structural Properties. *Pharmaceutics* **2022**, *14*, 818, doi:10.3390/pharmaceutics14040818.

15. Appendix

A.1 Chapter 8

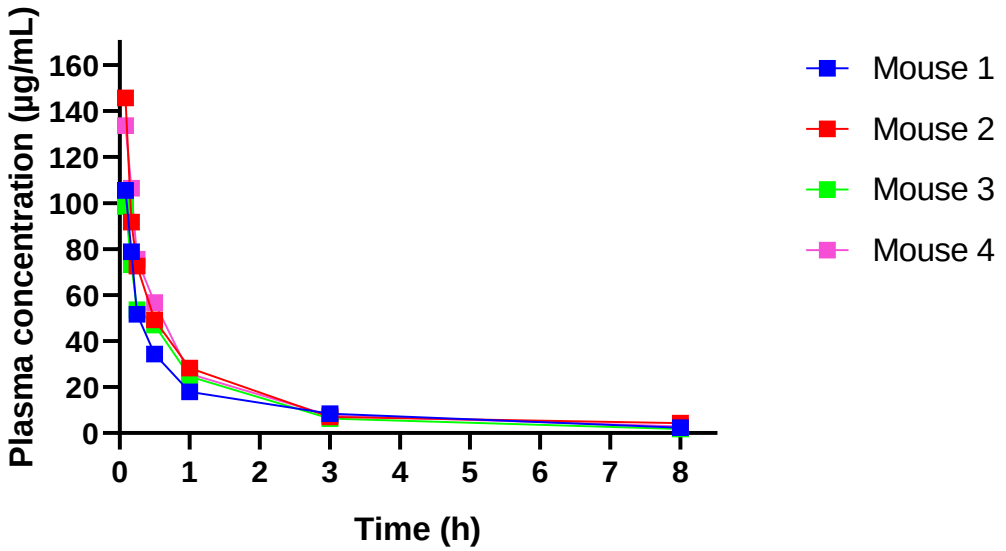

Figure A1. Individual plasma concentration of CorA following IV administration at a dose of 36 mg/kg in BALB/c mice (permission to use the data was kindly granted by Krome et al. [109]).

Table A1. Non-compartmental pharmacokinetic analysis (PKPlus®) of individual animals following IV administration at a dose of 36 mg/kg in BALB/c mice (permission to use the data was kindly granted by Krome et al. [109]).

PK-Parameter		Mouse 1	Mouse 2	Mouse 3	Mouse 4	Median	IQR
t_{max}	min	5	5	5	5	**5**	**0**
C_{max}	µg/mL	105.45	145.72	98.47	133.67	**119.56**	**32.98**
AUC_{0-t}	µg*h/mL	99.70	129.5	103.3	126.3	**114.80**	**24.70**
AUC_{0-inf}	µg*h/mL	108.40	173.20	110.80	140.90	**125.85**	**38.78**
AUC_{0-inf} per mg/kg dose	µg*h*kg/mL*mg	3.01	4.81	3.08	3.91	**3.50**	**1.08**
MRT	h	2.479	5.78	2.135	2.669	**2.574**	**1.054**
Cl	L/h	6.64E-3	4.16E-3	6.50E-3	5.11E-3	**0.006**	**1.66E-3**
$t_{1/2}$	h					**3.30**	
V_{ss}	L	0.016	0.024	0.014	0.014	**0.015**	**0.004**

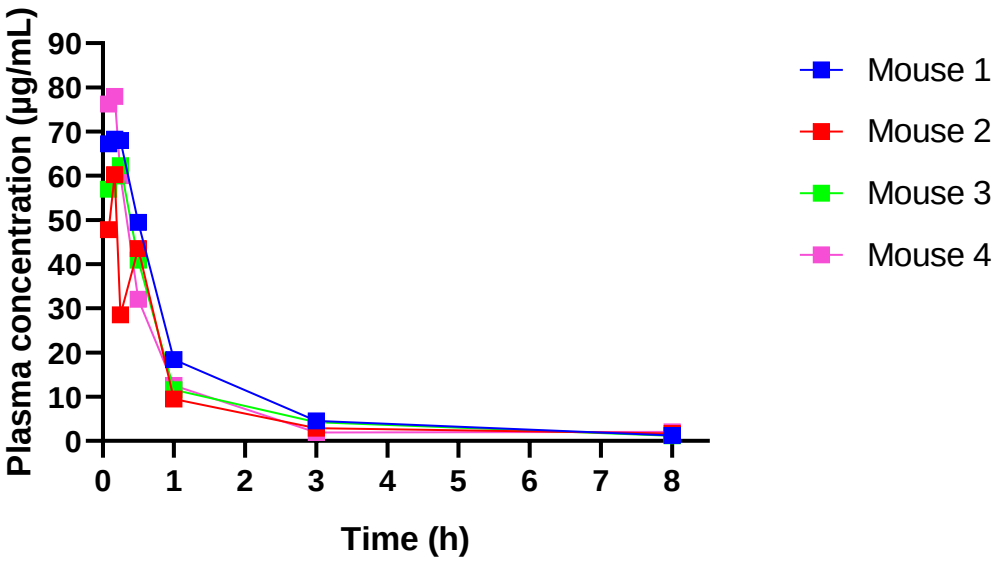

Figure A2. Individual plasma concentration of CorA following oral administration of CorA-povidone as a suspension in PBS pH 7.4 at a dose of 36 mg/kg in BALB/c mice (permission to use the data was kindly granted by Krome et al. [109]).

Table A2. Non-compartmental pharmacokinetic analysis (PKPlus®) of individual animals following oral administration of CorA-povidone administered as a suspension in PBS pH 7.4 at a dose of 36 mg/kg in BALB/c mice (permission to use the data was kindly granted by Krome et al. [109]).

PK-Parameter		Mouse 1	Mouse 2	Mouse 3	Mouse 4	Median	IQR
t_{max}	min	10	10	15	10	**10**	**1.25**
C_{max}	µg/mL	68.26	60.28	62.27	77.98	**65.27**	**8.92**
AUC_{0-t}	µg*h/mL	83.18	56.29	67.78	62.30	**65.04**	**10.83**
AUC_{0-inf}	µg*h/mL	87.67	73.08	72.31	64.47	**72.70**	**6.38**
AUC_{0-inf} per mg/kg dose	µg*h*kg/mL*mg	2.44	2.03	2.01	1.79	**2.02**	**0.18**
MRT	h	1.893	5.272	2.045	1.648	**1.969**	**1.020**

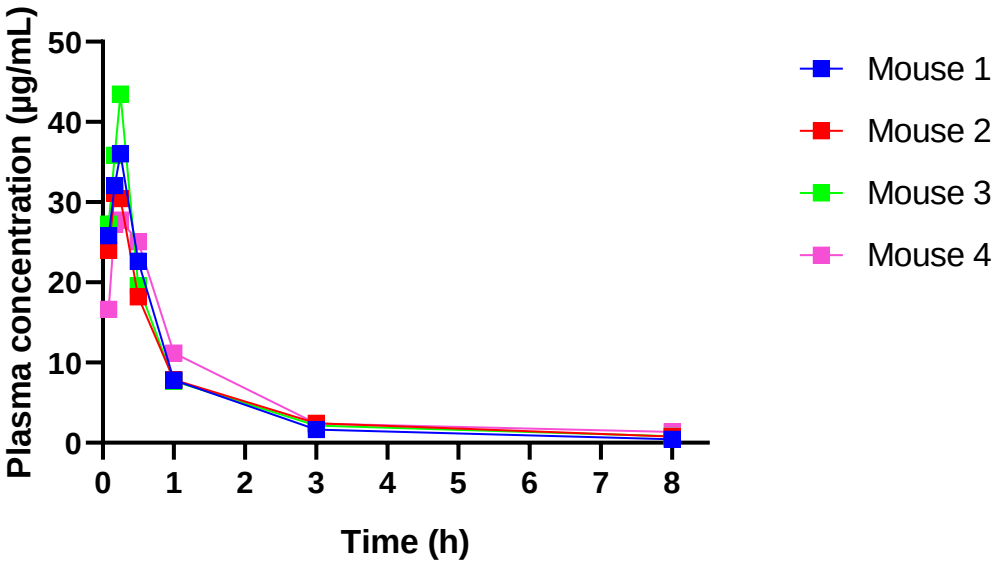

Figure A3. Individual plasma concentration of CorA following oral administration of CorA-povidone as a suspension in water at a dose of 36 mg/kg in BALB/c mice (permission to use the data was kindly granted by Krome et al. [109]).

Table A3. Non-compartmental pharmacokinetic analysis (PKPlus®) of individual animals following oral administration of CorA-povidone administered as a suspension in water at a dose of 36 mg/kg in BALB/c mice (permission to use the data was kindly granted by Krome et al. [109]).

PK-Parameter		Mouse 1	Mouse 2	Mouse 3	Mouse 4	Median	IQR
t_{max}	min	15	10	15	10	**12.5**	**15**
C_{max}	µg/mL	36.04	31.10	43.47	27.75	**33.57**	**36.04**
AUC_{0-t}	µg*h/mL	35.89	36.79	39.03	43.42	**37.91**	**35.89**
AUC_{0-inf}	µg*h/mL	37.43	40.31	43.41	55.57	**41.86**	**37.43**
AUC_{0-inf} per mg/kg dose	µg*h*kg/ mL*mg	1.04	1.12	1.21	1.54	**1.16**	**1.04**
MRT	h	1.596	2.486	2.604	5.009	**2.545**	**1.596**

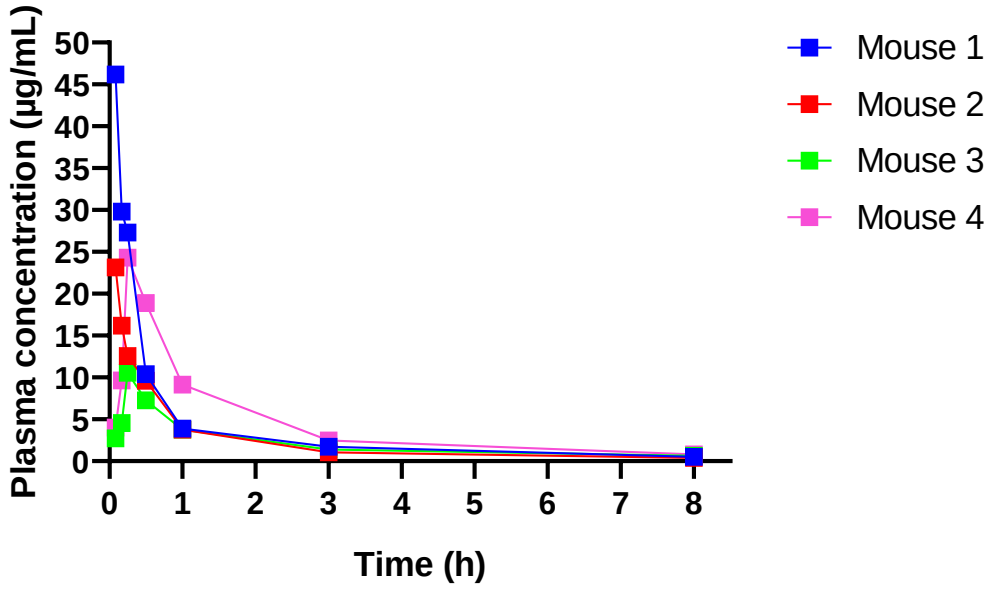

Figure A4. Individual plasma concentration of CorA following oral administration of CorA-copovidone as a suspension in PBS pH 7.4 at a dose of 36 mg/kg in BALB/c mice.

Table A4. Non-compartmental pharmacokinetic analysis (PKPlus®) of individual animals following oral administration of CorA-copovidone administered as a suspension in PBS pH 7.4 at a dose of 36 mg/kg in BALB/c mice.

PK-Parameter		Mouse 1	Mouse 2	Mouse 3	Mouse 4	Median	IQR
t_{max}	min	5	5	15	15	**10.00**	**10.00**
C_{max}	µg/mL	46.17	23.15	10.57	24.33	**23.74**	**9.79**
AUC_{0-t}	µg*h/mL	26.96	18.38	16.37	34.41	**22.67**	**10.95**
AUC_{0-inf}	µg*h/mL	29.06	20.45	20.78	37.93	**24.92**	**10.58**
AUC_{0-inf} per mg/kg dose	µg*h*kg/ mL*mg	0.81	0.57	0.58	1.05	**0.69**	**0.29**
MRT	h	2.147	2.630	4.775	2.688	**2.66**	**0.70**

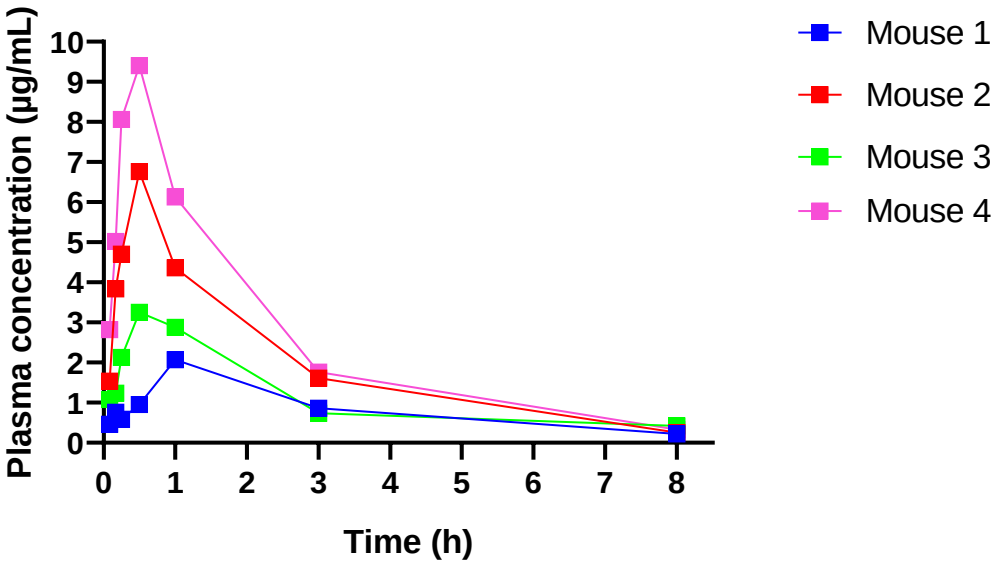

Figure A5. Individual plasma concentration of CorA following oral administration of CorA-copovidone as a suspension in water at a dose of 36 mg/kg in BALB/c mice.

Table A5. Non-compartmental pharmacokinetic analysis (PKPlus®) of individual animals following oral administration of CorA-copovidone administered as a suspension in water at a dose of 36 mg/kg in BALB/c mice.

PK-Parameter		Mouse 1	Mouse 2	Mouse 3	Mouse 4	Median	IQR
t_{max}	min	60	30	30	30	**30**	**7.50**
C_{max}	µg/mL	2.07	6.76	3.25	9.40	**5.01**	**4.47**
AUC_{0-t}	µg*h/mL	6.70	15.48	9.01	20.17	**12.25**	**8.22**
AUC_{0-inf}	µg*h/mL	7.51	16.15	12.71	21.15	**14.43**	**5.99**
AUC_{0-inf} per mg/kg dose	µg*h*kg/ mL*mg	0.21	0.45	0.35	0.59	**0.40**	**0.17**
MRT	h	3.42	2.23	6.52	2.163	**2.83**	**1.98**

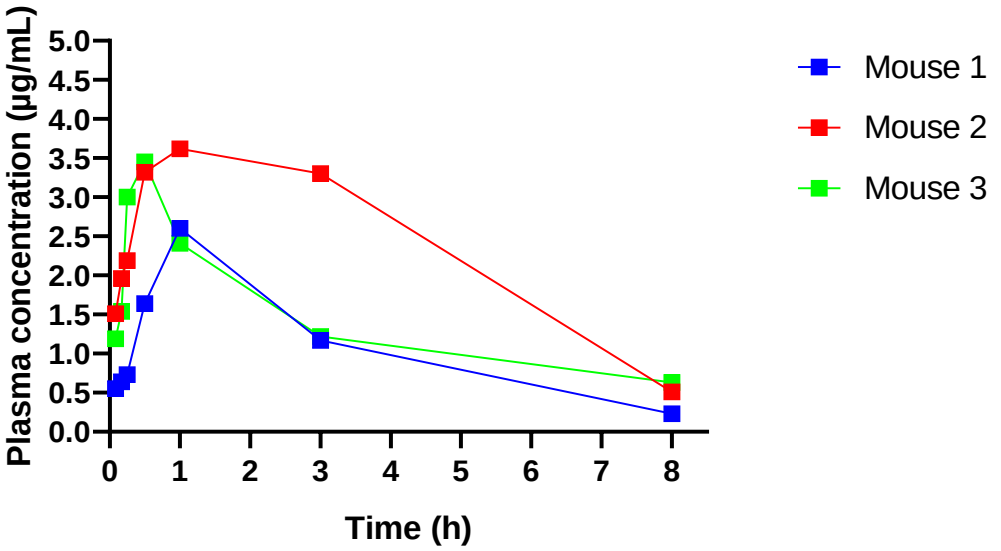

Figure A6. Individual plasma concentration of CorA following oral administration of neat CorA as a suspension in PBS pH 7.4 at a dose of 36 mg/kg in BALB/c mice.

Table A6. Non-compartmental pharmacokinetic analysis (PKPlus®) of individual animals following oral administration of neat CorA administered as a suspension in PBS pH 7.4 at a dose of 36 mg/kg in BALB/c mice.

PK-Parameter		Mouse 1	Mouse 2	Mouse 3	Median	IQR
t_{max}	min	60	60	30	**60**	**15**
C_{max}	µg/mL	2.60	3.62	3.45	**3.45**	**0.51**
AUC_{0-t}	µg*h/mL	8.77	19.26	10.89	**10.89**	**5.25**
AUC_{0-inf}	µg*h/mL	9.47	20.64	15.73	**15.73**	**5.59**
AUC_{0-inf} per mg/kg dose	µg*h*kg/ mL*mg	0.26	0.57	0.44	**0.44**	**0.16**
MRT	h	2.99	3.15	6.68	**3.15**	**1.85**

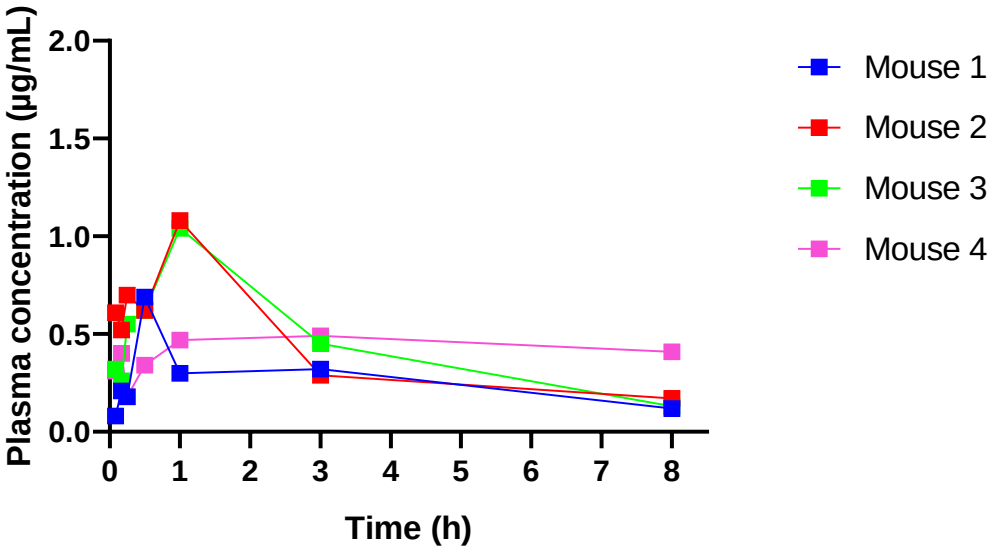

Figure A7. Individual plasma concentration of CorA following oral administration of neat CorA as a suspension in water at a dose of 36 mg/kg in BALB/c mice.

Table A7. Non-compartmental pharmacokinetic analysis (PKPlus®) of individual animals following oral administration of neat CorA administered as a suspension in water at a dose of 36 mg/kg in BALB/c mice.

PK-Parameter		Mouse 1	Mouse 2	Mouse 3	Mouse 4	Median	IQR
t_{max}	min	30	60	60	180	**60**	**37.5**
C_{max}	µg/mL	0.69	1.08	1.04	0.49	**0.865**	**0.41**
AUC_{0-t}	µg*h/mL	2.11	3.23	3.57	3.58	**3.40**	**0.62**
AUC_{0-inf}	µg*h/mL	2.72	4.82	4.10	15.08	**4.46**	**3.63**
AUC_{0-inf} per mg/kg dose	µg*h*kg/ mL*mg	0.08	0.13	0.11	0.42	**0.12**	**0.10**
MRT	h	3.42	2.23	6.52	2.163	**2.83**	**1.98**

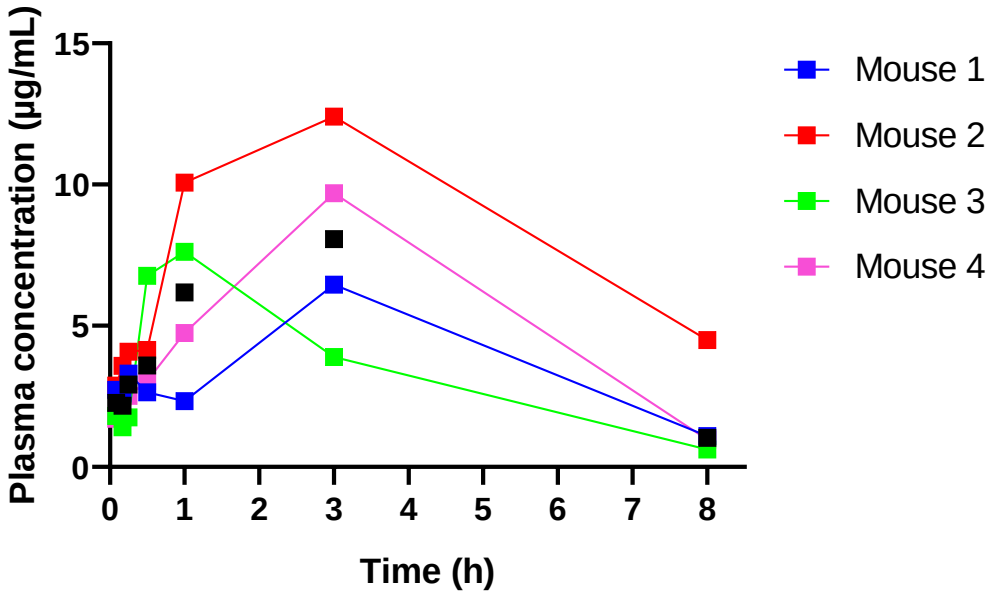

Figure A8. Individual plasma concentration of CorA following oral administration of CorA-povidone as a suspension in corn oil at a dose of 36 mg/kg in BALB/c mice.

Table A8. Non-compartmental pharmacokinetic analysis (PKPlus®) of individual animals following oral administration of CorA-povidone administered as a suspension in corn oil at a dose of 36 mg/kg in BALB/c mice.

PK-Parameter		Mouse 1	Mouse 2	Mouse 3	Mouse 4	Median	IQR
t_{max}	min	180	180	60	180	**180.00**	**30.00**
C_{max}	µg/mL	6.45	12.41	7.62	9.70	**8.66**	**3.05**
AUC_{0-t}	µg*h/mL	30.20	70.02	27.79	44.15	**37.18**	**21.02**
AUC_{0-inf}	µg*h/mL	33.27	92.10	29.48	46.25	**39.76**	**25.39**
AUC_{0-inf} per mg/kg dose	µg*h*kg/mL*mg	0.92	2.56	0.82	1.28	**1.10**	**0.71**
MRT	h	3.796	5.635	2.790	3.228	**3.51**	**1.14**

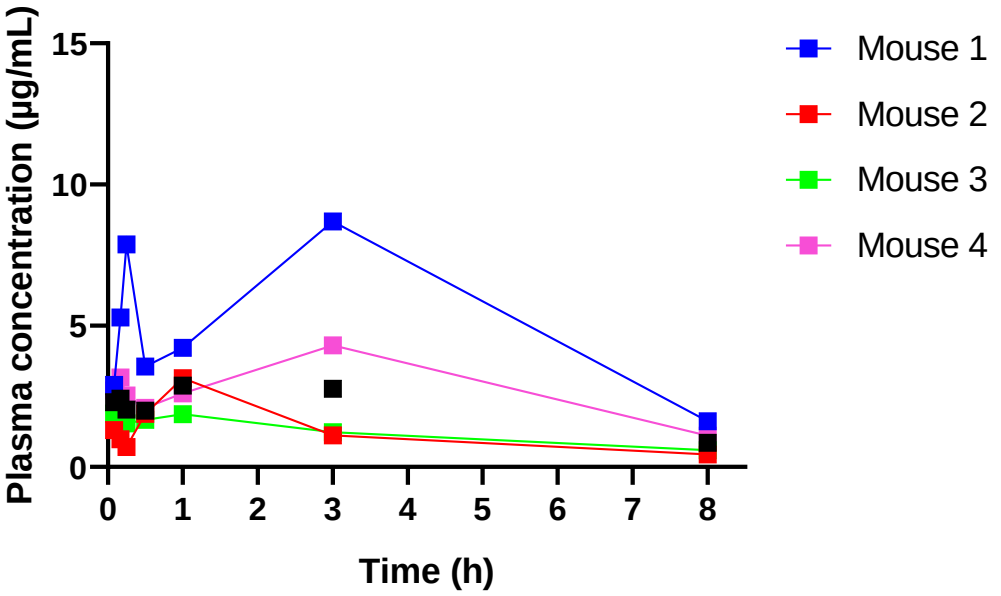

Figure A9. Individual plasma concentration of CorA following oral administration of CorA-copovidone as a suspension in corn oil at a dose of 36 mg/kg in BALB/c mice.

Table A9. Non-compartmental pharmacokinetic analysis (PKPlus®) of individual animals following oral administration of CorA-copovidone administered as a suspension in corn oil at a dose of 36 mg/kg in BALB/c mice.

PK-Parameter		Mouse 1	Mouse 2	Mouse 3	Mouse 4	Median	IQR
t_{max}	min	180	60	5	180	**120.00**	**133.75**
C_{max}	µg/mL	8.70	3.14	1.89	4.31	**3.73**	**2.58**
AUC_{0-t}	µg*h/mL	43.10	9.96	9.32	22.79	**16.38**	**18.07**
AUC_{0-inf}	µg*h/mL	47.91	12.31	13.50	26.82	**20.16**	**18.89**
AUC_{0-inf} per mg/kg dose	µg*h*kg/mL*mg	1.33	0.34	0.38	0.75	**0.57**	**0.53**
MRT	h	3.819	4.574	6.682	4.401	**4.49**	**0.85**

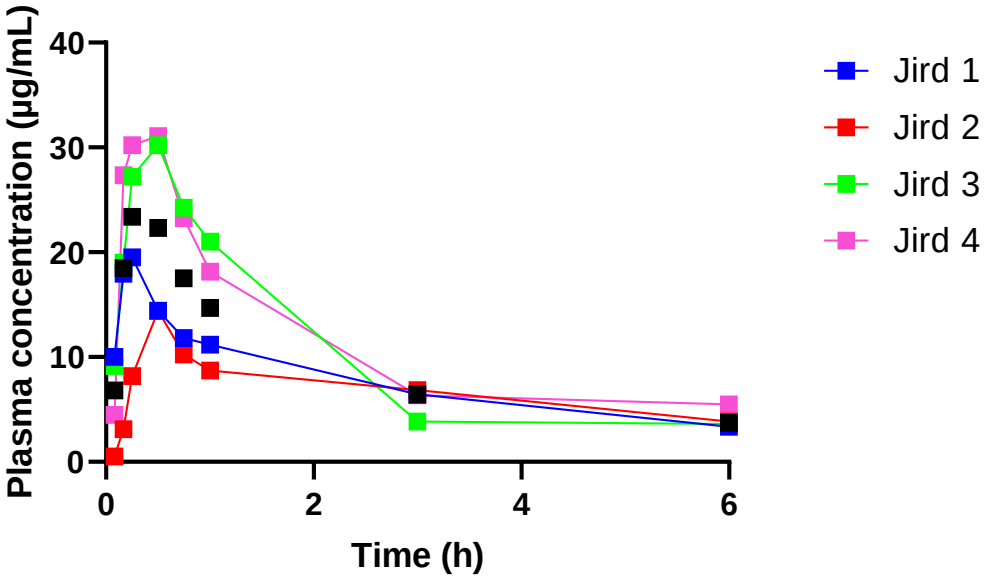

Figure A10. Individual plasma concentration of CorA following oral administration of CorA-povidone as a suspension in PBS pH 7.4 at a dose of 30 mg/kg in Mongolian gerbils (jirds).

Table A10. Non-compartmental pharmacokinetic analysis (PKPlus®) of individual animals following oral administration of CorA-povidone administered as a suspension in corn oil at a dose of 30 mg/kg in Mongolian gerbils (jirds).

PK-Parameter		Jird 1	Jird 2	Jird 3	Jird 4	Median	IQR
t_{max}	min	15	30	30	30	**30**	**3.75**
C_{max}	µg/mL	19.52	14.42	30.21	31.08	**24.87**	**12.18**
AUC_{0-t}	µg*h/mL	45.92	40.50	59.17	65.74	**52.55**	**16.25**
AUC_{0-inf}	µg*h/mL	61.34	60.60	227.4	176.9	**119.12**	**128.37**
AUC_{0-inf} per mg/kg dose	µg*h*kg/mL*mg	2.04	2.02	7.58	5.90	**3.97**	**4.29**
MRT	h	4.234	5.369	39.34	17.26	**11.31**	**17.69**

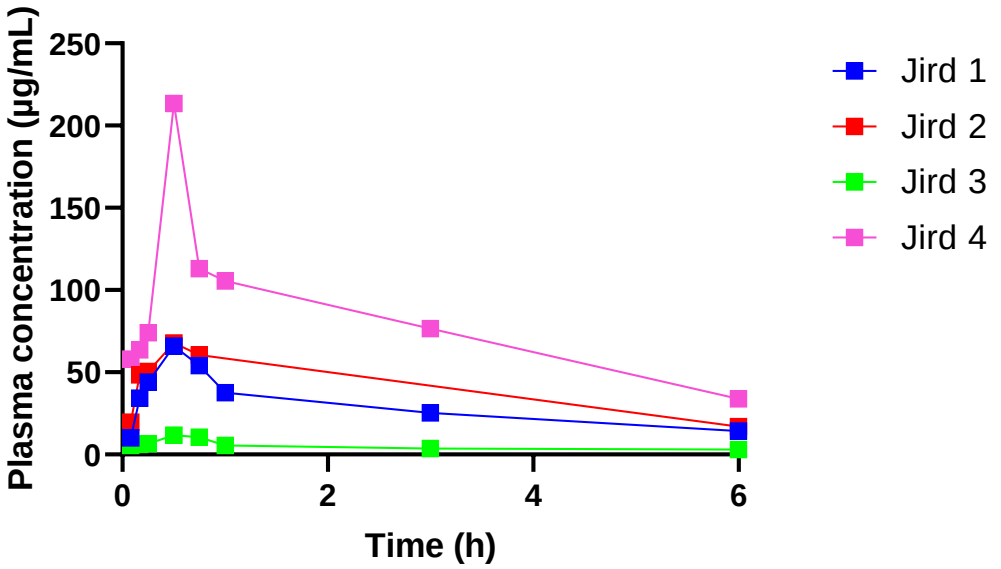

Figure A11. Individual plasma concentration of CorA following oral administration of CorA-povidone as a suspension in PBS pH 7.4 at a dose of 60 mg/kg in Mongolian gerbils (jirds).

Table A11. Non-compartmental pharmacokinetic analysis (PKPlus®) of individual animals following oral administration of CorA-povidone administered as a suspension in corn oil at a dose of 60 mg/kg in Mongolian gerbils (jirds).

PK-Parameter		Jird 1	Jird 2	Jird 3	Jird 4	Median	IQR
t_{max}	min	30	30	30	30	**30**	**0**
C_{max}	µg/mL	65.89	67.75	11.81	213.44	**66.82**	**51.80**
AUC_{0-t}	µg*h/mL	168.0	241.9	27.80	465.1	**205.0**	**164.8**
AUC_{0-inf}	µg*h/mL	243.5	312.5	79.12	590.2	**278**	**179.5**
AUC_{0-inf} per mg/kg dose	µg*h*kg/mL*mg	4.06	5.21	1.32	9.84	**4.64**	**2.99**
MRT	h	5.064	3.586	15.43	3.83	**4.45**	**3.89**

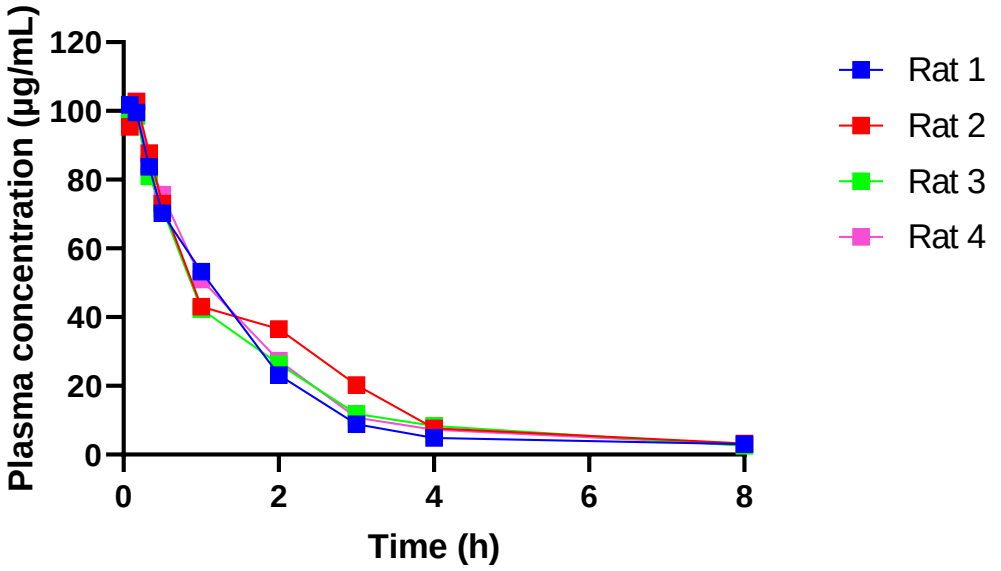

Figure A12. Individual plasma concentration of CorA following IV administration at a dose of 18 mg/kg in Wistar rats.

Table A12. Non-compartmental pharmacokinetic analysis (PKPlus®) of individual animals following IV administration at a dose of 18 mg/kg in Wistar rats.

PK-Parameter		Rat 1	Rat 2	Rat 3	Rat 4	Median	IQR
t_{max}	min	5	10	10	10	**10**	**1.25**
C_{max}	µg/mL	101.8	102.7	98.5	102.9	**102.2**	**1.8**
AUC_{0-t}	µg*h/mL	152.9	178.1	157.9	164.4	**161.15**	**11.175**
AUC0-t per mg/kg dose	µg*h*kg/	8.49	9.89	8.77	9.13	**8.95**	**0.62**
AUC_{0-inf}	µg*h/mL	178.6	193.1	166.7	176.7	**177.7**	**8.0**
AUC_{0-inf} per mg/kg dose	µg*h*kg/ mL*mg	9.92	10.73	9.26	9.82	**9.87**	**0.45**
MRT	h	3.659	2.608	2.179	2.349	**2.4785**	**0.56425**
Cl	L/h	2.50E-02	2.30E-02	2.70E-02	2.50E-02	**0.025**	**0.001**
$t_{1/2}$	h	5.858	3.228	2.36	2.995	**3.1115**	**1.04925**
V_{ss}	L	0.092	0.061	0.059	0.06	**0.0605**	**0.009**

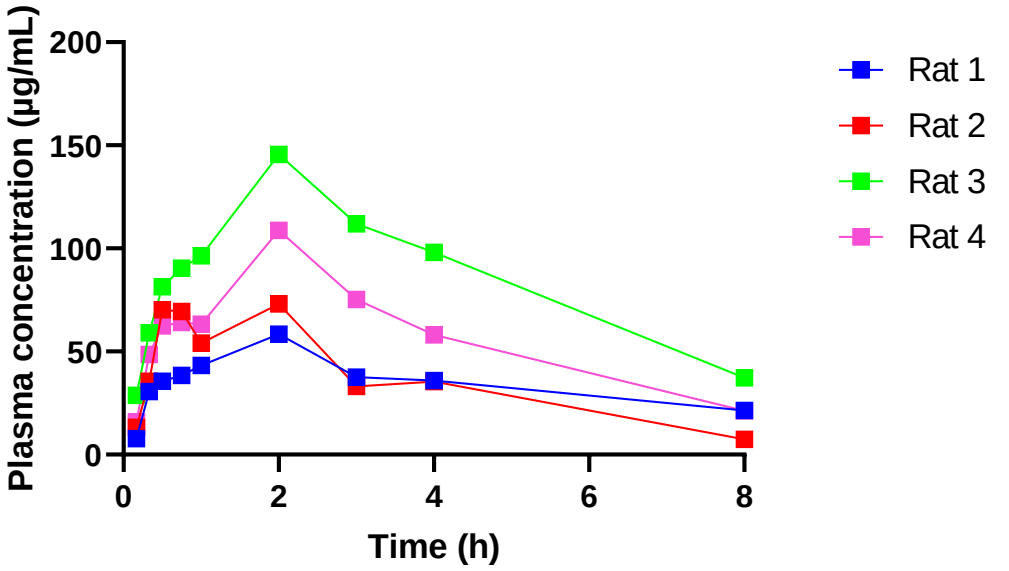

Figure A13. Individual plasma concentration of CorA following oral administration of CorA-PEG 200 solution at a dose of 36 mg/kg Wistar rats.

Table A13. Non-compartmental pharmacokinetic analysis (PKPlus®) of individual animals following oral administration of a CorA-PEG 200 solution at a dose of 36 mg/kg in Wistar rats.

PK-Parameter		Rat 1	Rat 2	Rat 3	Rat 4	Median	IQR
t_{max}	min	120	120	120	120	**120**	**0**
C_{max}	µg/mL	58.44	73.03	145.52	108.78	**90.90**	**48.58**
AUC_{0-t}	µg*h/mL	279.4	283.2	691.6	451	**367.1**	**228.9**
AUC_{0-t} per mg/kg dose	µg*h*kg/mL*mg	7.76	7.87	19.21	12.53	**10.20**	**6.36**
AUC_{0-inf}	µg*h/mL	445.7	302.0	846.2	535.0	**490.4**	**203.0**
AUC_{0-inf} per mg/kg dose	µg*h*kg/mL*mg	12.38	8.39	23.51	14.86	**13.62**	**5.64**
MRT	h	8.059	3.219	4.93	4.541	**4.736**	**1.502**
F	%	87	88	215	140	**137**	**71**

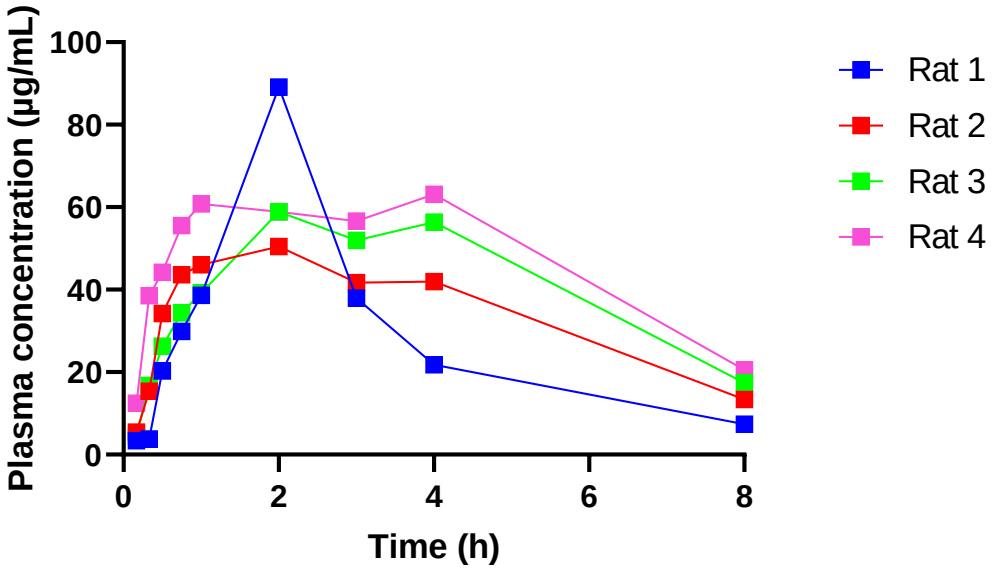

Figure A14. Individual plasma concentration of CorA following oral administration of CorA-povidone as a suspension in PBS pH 7.4 at a dose of 36 mg/kg in Wistar rats.

Table A14. Non-compartmental pharmacokinetic analysis (PKPlus®) of individual animals following oral administration of a CorA-povidone as a suspension in PBS pH 7.4 at a dose of 36 mg/kg in Wistar rats.

PK-Parameter		Rat 1	Rat 2	Rat 3	Rat 4	Median	IQR
t_{max}	min	120	120	120	240	**120**	**30**
C_{max}	µg/mL	89.15	50.48	58.86	63.10	**60.98**	**12.85**
AUC_{0-t}	µg*h/mL	233.3	274.1	328.5	383.8	**301.3**	**78.425**
AUC_{0-t} per mg/kg dose	µg*h*kg/mL*mg	6.48	7.61	9.13	10.66	**8.37**	**2.18**
AUC_{0-inf}	µg*h/mL	260.4	320.7	387.4	456.8	**354.1**	**99.1**
AUC_{0-inf} per mg/kg dose	µg*h*kg/mL*mg	7.23	8.91	10.76	12.69	**9.83**	**2.75**
MRT	h	3.751	4.480	4.698	4.697	**4.589**	**0.400**
F	%	75	92	112	131	**102**	**29**

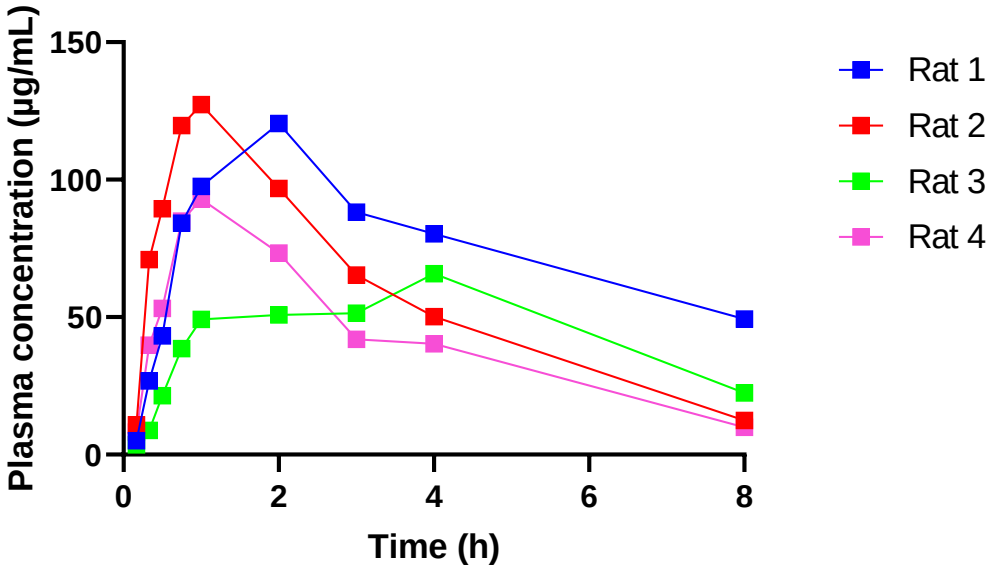

Figure A15. Individual plasma concentration of CorA following oral administration of CorA-copovidone as a suspension in PBS pH 7.4 at a dose of 36 mg/kg in Wistar rats.

Table A15. Non-compartmental pharmacokinetic analysis (PKPlus®) of individual animals following oral administration of a CorA-copovidone as a suspension in PBS pH 7.4 at a dose of 36 mg/kg in Wistar rats.

PK-Parameter		Rat 1	Rat 2	Rat 3	Rat 4	Median	IQR
t_{max}	min	120	60	240	60	**90**	**90**
C_{max}	µg/mL	120.40	127.35	65.83	92.90	**106.65**	**36.00**
AUC_{0-t}	µg*h/mL	604.4	454.4	358.6	334.5	**406.5**	**139.3**
AUC_{0-t} per mg/kg dose	µg*h*kg/mL*mg	16.79	12.62	9.96	9.29	**11.29**	**3.87**
AUC_{0-inf}	µg*h/mL	1008.1	490.3	441.9	363.1	**466.1**	**197.6**
AUC_{0-inf} per mg/kg dose	µg*h*kg/mL*mg	28.00	13.62	12.28	10.09	**12.95**	**5.49**
MRT	h	8.647	3.257	5.182	3.382	**4.282**	**2.698**
F	%	188	141	127	105	**134**	**31**

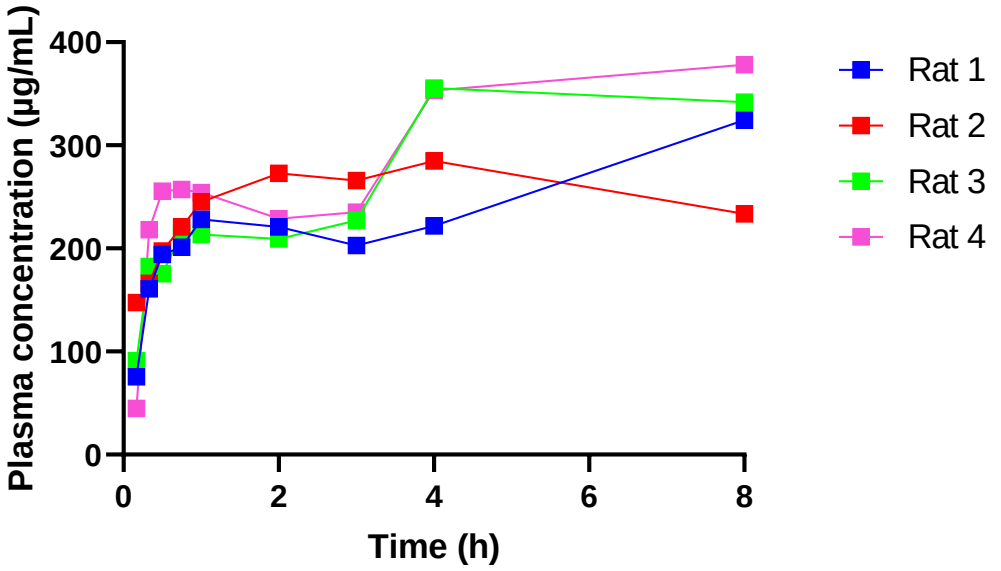

Figure A16. Individual plasma concentration of CorA following oral administration of CorA-PEG 200 solution at a dose of 500 mg/kg Wistar rats.

Table A16. Non-compartmental pharmacokinetic analysis (PKPlus®) of individual animals following oral administration of a CorA-PEG 200 solution at a dose of 500 mg/kg in Wistar rats.

PK-Parameter		Rat 1	Rat 2	Rat 3	Rat 4	Median	IQR
t_{max}	min	480	240	240	480	**360**	**240**
C_{max}	µg/mL	324.61	272.71	355.53	378.08	**340.07**	**49.53**
AUC_{0-t}	µg*h/mL	1900.2	2019.4	2278.3	2423.0	**2148.9**	**324.9**
AUC_{0-t} per mg/kg dose	µg*h*kg/mL*mg	3.80	4.04	4.56	4.85	**4.30**	**0.65**
AUC_{0-inf}	µg*h/mL	1900.2	6724.6	37500.0	2423.0	**4573.8**	**12126.2**
AUC_{0-inf} per mg/kg dose	µg*h*kg/mL*mg	3.80	13.45	75.00	4.85	**9.15**	**24.25**
MRT	h	4.565	20.910	104.400	4.536	**12.738**	**37.225**
F	%	43	45	51	54	**48**	**7**

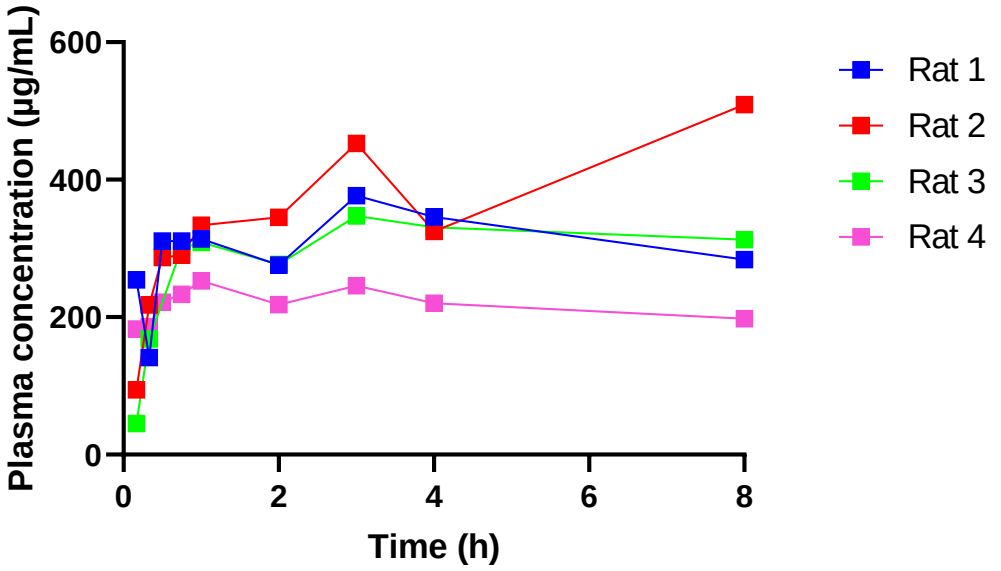

Figure A17. Individual plasma concentration of CorA following oral administration of CorA-PEG 200 solution at a dose of 1000 mg/kg Wistar rats.

Table A17. Non-compartmental pharmacokinetic analysis (PKPlus®) of individual animals following oral administration of a CorA-PEG 200 solution at a dose of 1000 mg/kg in Wistar rats.

PK-Parameter		Rat 1	Rat 2	Rat 3	Rat 4	Median	IQR
t_{max}	min	180	480	180	60	**180**	**105**
C_{max}	µg/mL	376.81	509.09	347.31	252.67	**362.06**	**86.23**
AUC_{0-t}	µg*h/mL	2488.8	3020.4	2426.0	1733.7	**2457.4**	**368.8**
AUC_{0-t} per mg/kg dose	µg*h*kg/mL*mg	2.49	3.02	2.43	1.73	**2.46**	**0.37**
AUC_{0-inf}	µg*h/mL	8243.7	4552.7	25100.0	8983.6	**8613.7**	**5691.8**
AUC_{0-inf} per mg/kg dose	µg*h*kg/mL*mg	8.24	4.55	25.10	8.98	**8.61**	**5.69**
MRT	h	20.950	6.725	73.100	36.820	**28.885**	**28.496**
F	%	28	34	27	19	**28**	**4**

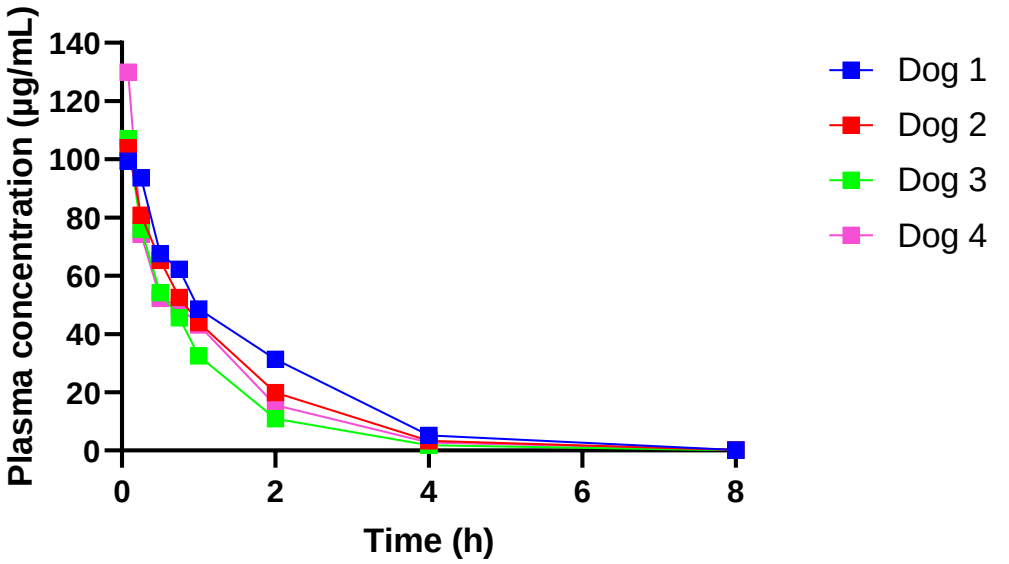

Figure A18. Individual plasma concentration of CorA following IV administration at an abs. dose of 75 mg in Beagle dogs.

Table A18. Non-compartmental pharmacokinetic analysis (PKPlus®) of individual animals following IV administration at an abs. dose of 75 mg in Beagle dogs.

PK-Parameter		Dog 1	Dog 2	Dog 3	Dog 4	Median	IQR
t_{max}	min	5	5	5	5	**5**	**0**
C_{max}	µg/mL	90.2	94.39	97.15	117.96	**95.77**	**9.01**
AUC_{0-t}	µg*h/mL	148.5	121.2	92.11	113.5	**117.35**	**19.87**
AUC_{0-inf}	µg*h/mL	148.5	121.2	92.11	113.5	**117.35**	**19.87**
AUC_{0-inf} per mg/kg dose	µg*h*kg/ mL*mg	18.75	12.28	7.57	10.50	**11.39**	**4.13**
MRT	h	1.402	1.247	0.936	1.19	**1.219**	**0.159**
Cl	L/h	0.88	1.006	n.a.	1.177	**1.006**	**0.149**
$t_{1/2}$	h	0.505	0.619	0.814	0.661	**0.640**	**0.109**
V_{ss}	L	0.708	0.772	0.763	0.786	**0.768**	**0.026**

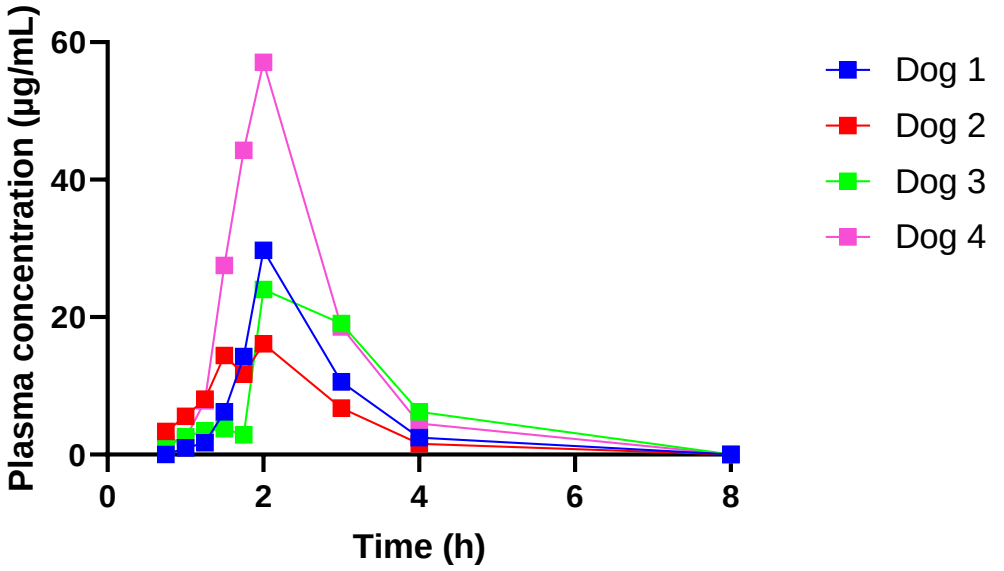

Figure A19. Individual plasma concentration of CorA following oral administration of CorA-povidone at an abs. dose of 75 mg administered as an enteric capsule in fasted Beagle dogs.

Table A19. Non-compartmental pharmacokinetic analysis (PKPlus®) of individual animals following oral administration of CorA-povidone at an abs. dose of 75 mg administered as an enteric capsule in fasted Beagle dogs.

PK-Parameter		Dog 1	Dog 2	Dog 3	Dog 4	Median	IQR
t_{max}	min	120	120	120	120	**120**	**0**
C_{max}	µg/mL	26.97	14.64	21.8	51.82	**24.39**	**13.17**
AUC_{0-t}	µg*h/mL	37.28	29.45	48.56	78.92	**42.92**	**20.83**
AUC_{0-inf}	µg*h/mL	37.28	29.45	48.56	78.92	**42.92**	**20.83**
AUC_{0-inf} per mg/kg dose	µg*h*kg/mL*mg	3.89	2.81	3.35	6.14	**3.62**	**1.23**
MRT	h	2.501	2.219	2.891	2.366	**2.434**	**0.269**
F	%	20.73	22.89	44.25	58.50	**33.57**	**25.46**

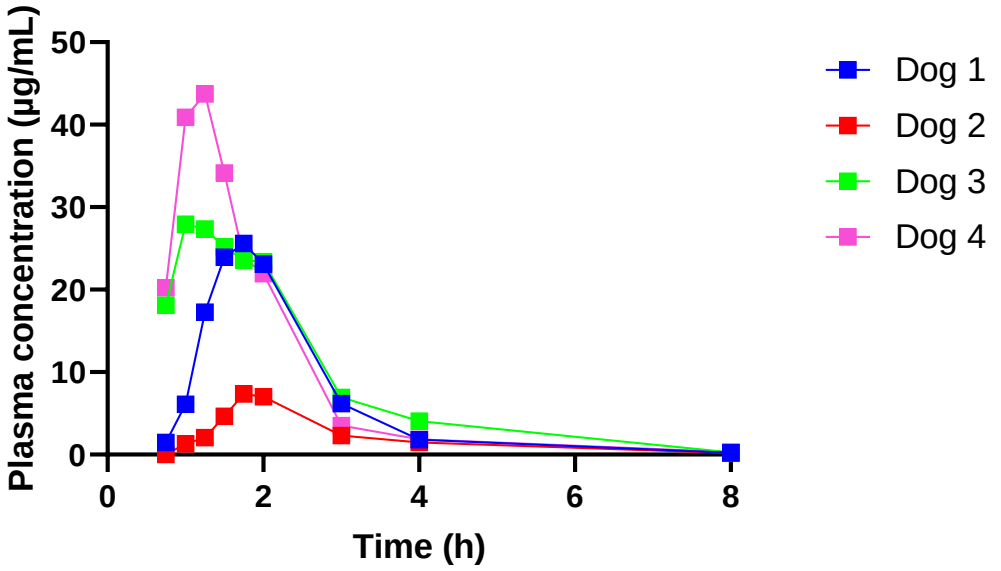

Figure A20. Individual plasma concentration of CorA following oral administration of CorA-copovidone at an abs. dose of 75 mg administered as an enteric capsule in fasted Beagle dogs.

Table A20. Non-compartmental pharmacokinetic analysis (PKPlus®) of individual animals following oral administration of CorA-copovidone at an abs. dose of 75 mg administered as an enteric capsule in fasted Beagle dogs.

PK-Parameter		Dog 1	Dog 2	Dog 3	Dog 4	Median	IQR
t_{max}	min	105	105	60	75	**90**	**33.75**
C_{max}	µg/mL	23.25	6.67	25.37	39.7	**24.31**	**9.85**
AUC_{0-t}	µg*h/mL	40.47	13.27	61.15	61.98	**50.81**	**27.69**
AUC_{0-inf}	µg*h/mL	40.85	13.63	61.48	62.64	**51.17**	**27.73**
AUC_{0-inf} per mg/kg dose	µg*h*kg/ mL*mg	4.32	1.30	4.33	4.88	**4.33**	**0.90**
MRT	h	2.242	2.895	2.074	1.794	**2.158**	**0.401**
F	%	23.03	10.59	57.21	46.43	**34.73**	**29.20**

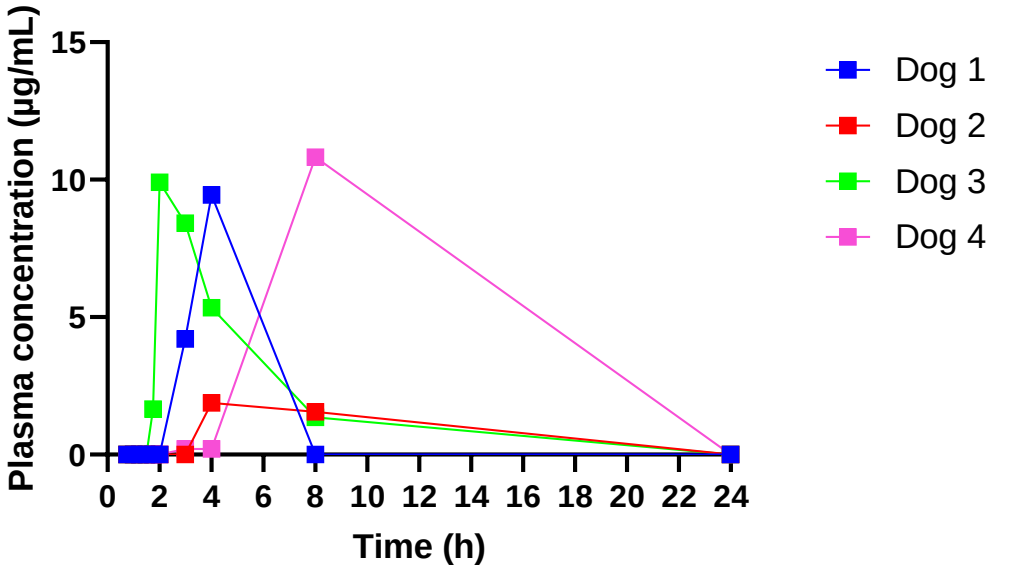

Figure A21. Individual plasma concentration of CorA following oral administration of CorA-povidone at an abs. dose of 75 mg administered as an enteric capsule in fed Beagle dogs.

Table A21. Non-compartmental pharmacokinetic analysis (PKPlus®) of individual animals following oral administration of CorA-povidone at an abs. dose of 75 mg administered as an enteric capsule in fed Beagle dogs.

PK-Parameter		Dog 1	Dog 2	Dog 3	Dog 4	Median	IQR
t_{max}	min	240	240	120	480	**240**	**90**
C_{max}	µg/mL	8.57	1.7	8.99	9.83	**8.78**	**2.35**
AUC_{0-t}	µg*h/mL	25.26	18.35	37.97	98.97	**31.62**	**29.69**
AUC_{0-inf}	µg*h/mL	25.26	18.35	37.97	98.97	**31.62**	**29.69**
AUC_{0-inf} per mg/kg dose	µg*h*kg/ mL*mg	2.63	1.78	2.68	7.70	**2.65**	**1.51**
MRT	h	3.848	7.074	4.765	7.971	**5.920**	**2.763**
F	%	14.04	14.48	35.33	73.36	**24.91**	**30.47**

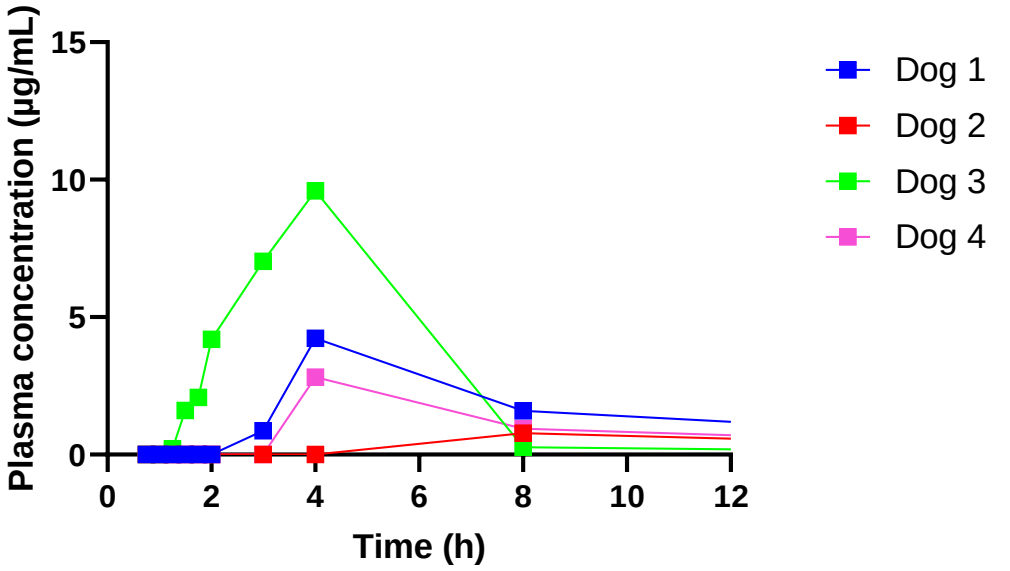

Figure A22. Individual plasma concentration of CorA following oral administration of CorA-copovidone at an abs. dose of 75 mg administered as an enteric capsule in fed Beagle dogs.

Table A22. Non-compartmental pharmacokinetic analysis (PKPlus®) of individual animals following oral administration of CorA-copovidone at an abs. dose of 75 mg administered as an enteric capsule in fed Beagle dogs.

PK-Parameter		Dog 1	Dog 2	Dog 3	Dog 4	Median	IQR
t_{max}	min	240	480	240	240	**240**	**60**
C_{max}	µg/mL	3.85	0.7	8.71	2.56	**3.21**	**2.97**
AUC_{0-t}	µg*h/mL	24.82	7	33.82	21.32	**23.07**	**9.33**
AUC_{0-inf}	µg*h/mL	24.82	7	33.82	n.a.	**24.82**	**13.41**
AUC_{0-inf} per mg/kg dose	µg*h*kg/mL*mg	2.45	0.63	2.21	1.54	**1.87**	**0.96**
MRT	h	6.29	8	3.892	n.a.	**6.290**	**2.054**
F	%	13.06	5.17	29.17	14.62	**13.84**	**7.17**

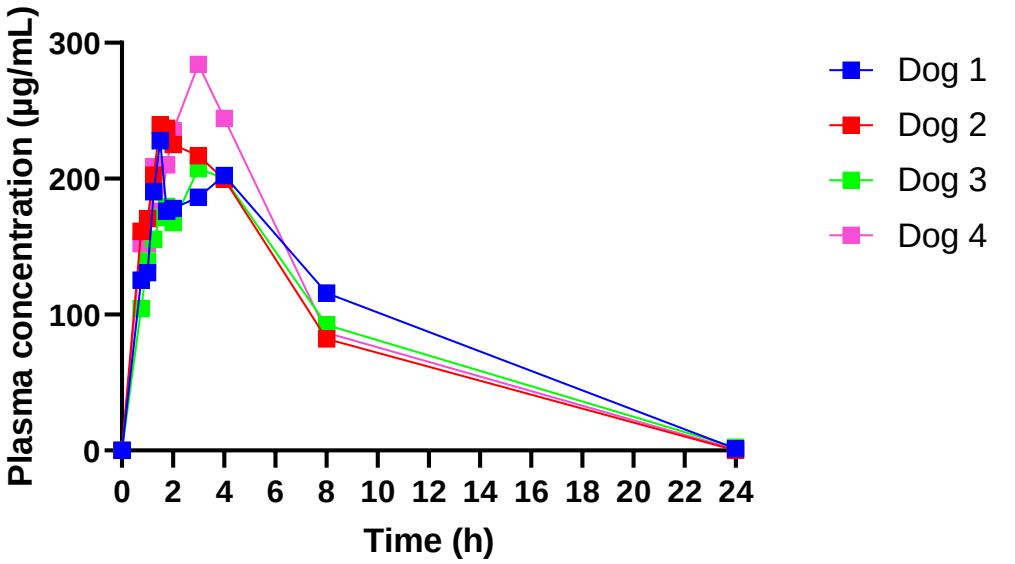

Figure A23. Individual plasma concentration of CorA following oral administration of CorA-silica at a dose of 200 mg/kg administered as a suspension in water in Beagle dogs.

Table A23. Non-compartmental pharmacokinetic analysis (PKPlus®) of individual animals following oral administration of CorA-silica at a dose of 200 mg/kg administered as a suspension in water in Beagle dogs.

PK-Parameter		Dog 1	Dog 2	Dog 3	Dog 4	Median	IQR
t_{max}	min	90	90	180	180	**135**	**90**
C_{max}	µg/mL	206.97	217.48	188.19	257.95	**212.23**	**25.32**
AUC_{0-t}	µg*h/mL	2013.5	1790.6	1788.4	1977.3	**1883.95**	**196.30**
AUC_{0-inf}	µg*h/mL	2017.8	1790.6	1797.5	1980.1	**1888.80**	**193.75**
AUC_{0-inf} per mg/kg dose	µg*h*kg/mL*mg	11.11	9.86	9.90	10.90	**10.40**	**1.07**
MRT	h	5.743	5.003	5.668	5.084	**5.376**	**0.623**
F	%	59.25	80.29	130.68	103.84	**92.07**	**35.52**

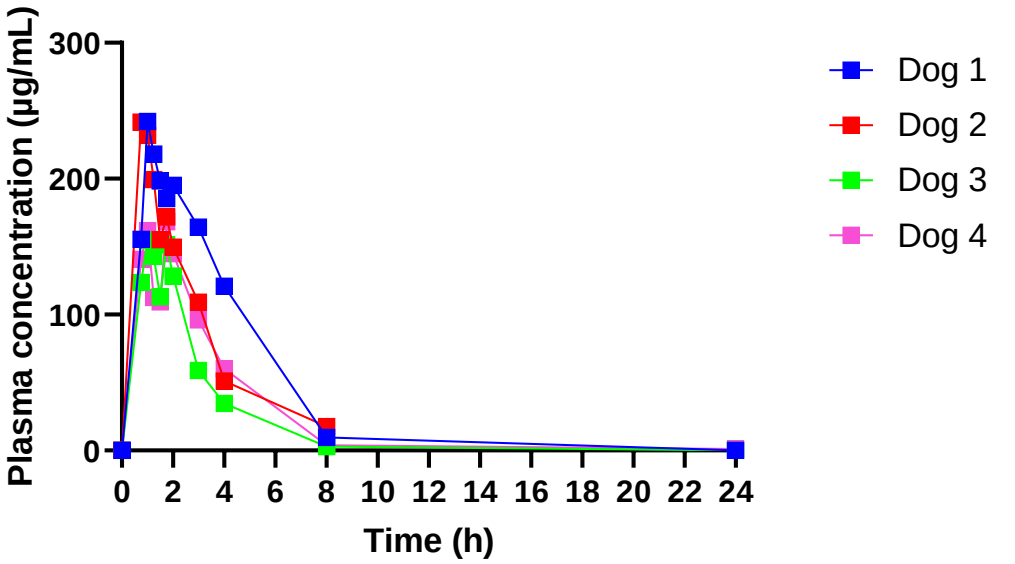

Figure A24. Individual plasma concentration of CorA following oral administration of CorA-silica at a dose of 100 mg/kg administered as a suspension in water in Beagle dogs.

Table A24. Non-compartmental pharmacokinetic analysis (PKPlus®) of individual animals following oral administration of CorA-silica at a dose of 100 mg/kg administered as a suspension in water in Beagle dogs.

PK-Parameter		Dog 1	Dog 2	Dog 3	Dog 4	Median	IQR
t_{max}	min	60	45	60	105	**60**	**15**
C_{max}	µg/mL	219.8	219.45	140.37	146.76	**183.11**	**74.38**
AUC_{0-t}	µg*h/mL	884.9	614.2	414.9	537.9	**576.05**	**174.73**
AUC_{0-inf}	µg*h/mL	884.9	674	414.9	549.5	**611.75**	**210.88**
AUC_{0-inf} per mg/kg dose	µg*h*kg/mL*mg	9.75	7.42	4.57	6.05	**6.74**	**2.32**
MRT	h	3.147	3.269	2.522	3.779	**3.208**	**0.406**
F	%	51.97	60.45	60.33	57.64	**58.98**	**4.14**

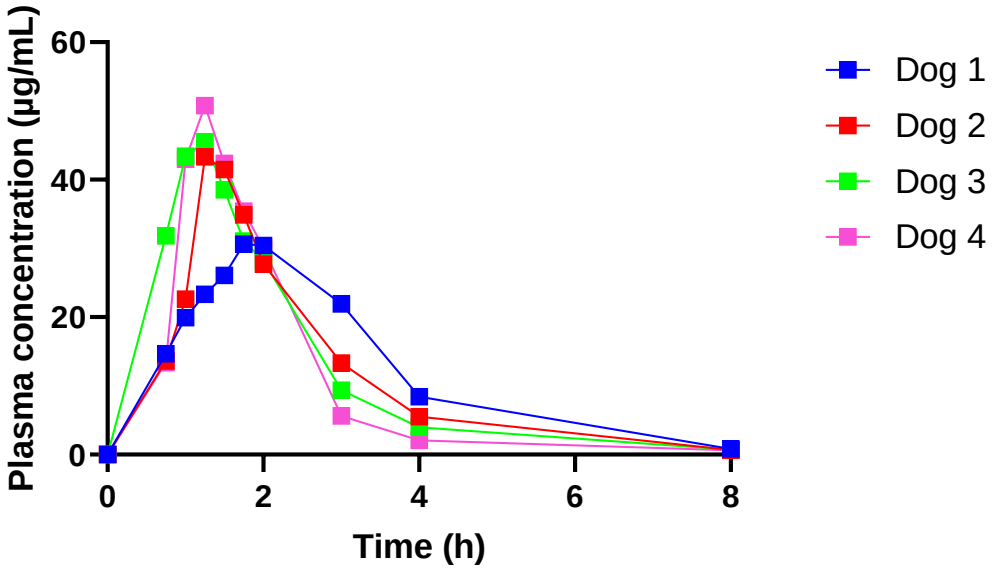

Figure A25. Individual plasma concentration of CorA following oral administration of CorA-povidone/HPMC tablet at an abs. dose of 100 mg in Beagle dogs.

Table A25. Non-compartmental pharmacokinetic analysis (PKPlus®) of individual animals following oral administration of CorA-povidone/HPMC tablet at an abs. dose of 100 mg in Beagle dogs.

PK-Parameter		Dog 1	Dog 2	Dog 3	Dog 4	Median	IQR
t_{max}	min	105	75	75	75	**75**	**7.5**
C_{max}	µg/mL	27.8	39.32	41.34	46.12	**40.33**	**6.10**
AUC_{0-t}	µg*h/mL	93.01	84.98	90.66	77.5	**87.82**	**8.14**
AUC_{0-inf}	µg*h/mL	93.01	84.98	90.66	77.5	**87.82**	**8.14**
AUC_{0-inf} per mg/kg dose	µg*h*kg/ mL*mg	8.60	6.46	5.29	5.12	**5.87**	**1.75**
MRT	h	2.87	2.552	2.275	2.197	**2.414**	**0.376**
F	%	45.88	52.59	69.86	48.77	**50.68**	**8.86**

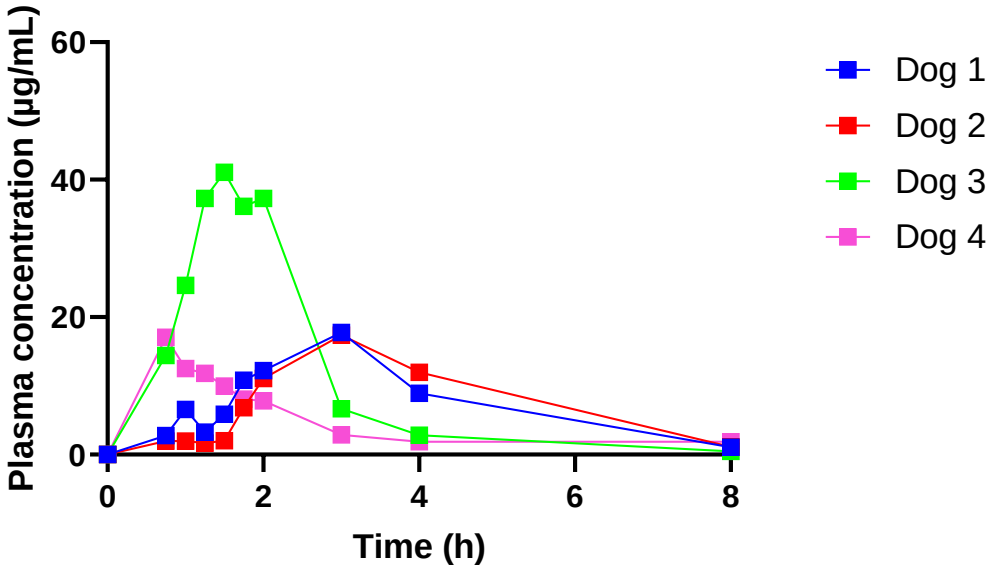

Figure A26. Individual plasma concentration of CorA following oral administration of CorA-copovidone/HPMC tablet at an abs. dose of 100 mg in Beagle dogs.

Table A26. Non-compartmental pharmacokinetic analysis (PKPlus®) of individual animals following oral administration of CorA-copovidone/HPMC tablet at an abs. dose of 100 mg in Beagle dogs.

PK-Parameter		Dog 1	Dog 2	Dog 3	Dog 4	Median	IQR
t_{max}	min	180	180	90	45	**135**	**101.25**
C_{max}	µg/mL	16.14	15.8	37.31	15.5	**15.97**	**5.71**
AUC_{0-t}	µg*h/mL	60.43	65.07	77.37	45.65	**62.75**	**11.41**
AUC_{0-inf}	µg*h/mL	60.43	67.35	80.37	45.65	**63.89**	**13.87**
AUC_{0-inf} per mg/kg dose	µg*h*kg/mL*mg	5.59	5.19	4.69	3.02	**4.94**	**1.02**
MRT	h	3.83	5.594	4.073	4.124	**4.099**	**0.479**
F	%	29.81	42.28	61.94	28.73	**36.05**	**17.65**